Dissertations, Theses, and Masters Projects

Theses, Dissertations, & Master Projects

2002

Coastal zone landscape classification using remote sensing and model development

Kevin R. Slocum
College of William and Mary - Virginia Institute of Marine Science

Follow this and additional works at: https://scholarworks.wm.edu/etd

Part of the Ecology and Evolutionary Biology Commons, Environmental Sciences Commons, Physical and Environmental Geography Commons, and the Remote Sensing Commons

COASTAL ZONE LANDSCAPE CLASSIFICATION USING REMOTE

SENSING AND MODEL DEVELOPMENT

A Dissertation
Presented to
The Faculty of the School of Marine Science
The College of William and Mary in Virginia

In Partial Fulfillment
Of the Requirements for the Degree of
Doctor of Philosophy

by
Kevin R. Slocum
Spring 2002
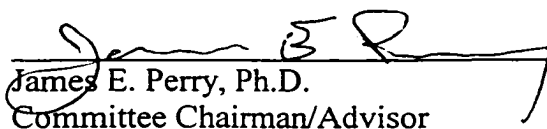
APPROVAL SHEET

This dissertation is submitted in partial fulfillment of

the requirements for the degree of

Doctor of Philosophy

_____
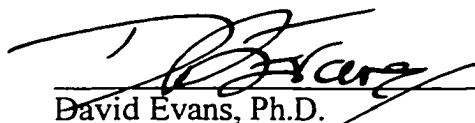
Kevin R. Slocum
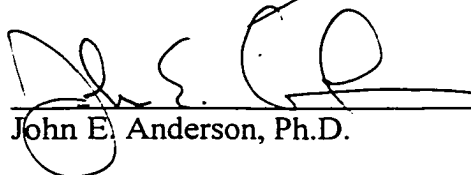
Approved, April 2002

_____

James E. Perry, Ph.D.
Committee Chairman/Advisor

_____
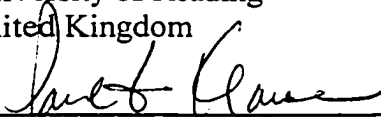
David Evans, Ph.D.

_____

John E. Anderson, Ph.D.

_____

Margaret A. Oliver, Ph.D.
University of Reading
United Kingdom

_____

Paul F. Krause, Ph.D.
U.S. Army Topographic Engineering Center
Alexandria, Virginia

DEDICATION

Thanks Mom and Dad. You taught me early on in life that I if I set my sights on something, I could accomplish it with hard work. Nancy, you had faith in me to pursue this crazy goal of mine, even at my "advanced" age. I don't believe I would have succeeded without your encouragement.

TABLE OF CONTENTS

Page

iv

v

ACKNOWLEDGMENTS

Special thanks to my wife, Nancy, and children, Jessie, Richie, and Danny, for accepting a commuter husband and Daddy for one year. I promise I will not go back to school for post-doctoral work!

I am grateful to you, Dr. Jim Perry, for your advice, your trust, and your friendship. We've both persevered through these last few years. Your flexibility and willingness to take on a leadership role in overseeing this study allowed me to investigate non-traditional VIMS topics, and, as a result, together we have uncovered findings with positive implication to natural resource managers.

Chapters in this manuscript were significantly improved following the individual and collective efforts of my Advisory Committee members. I truly appreciated the even-handed, professional manner in your suggestions and guidance were delivered.

To my professional colleagues, I thank you for the support you provided in the way of funding, time away from work, and assistance of any kind whenever I needed it. Mike, Rob, Joni, and John, thanks especially for your assistance in field-data collection.

To my classmates who worked, studied, shared laughs, and commiserated with me--thanks for the memories. I wish you an early graduation.

Lastly, thank you Lord.

LIST OF TABLES

viii

Chapter 4

Chapter 5

LIST OF FIGURES

x

xi

ABSTRACT

Coastal zone landscape characterization was explained using remote sensing technology and empirical model development. Collectively, six chapters address common issues and concerns faced by resource managers with the monitoring and characterization of landscape conditions within a coastal zone. The opening chapter is a discussion of emergent opportunities for remote sensing as a significant contributing technology to the resource management community. Chapter 2 examines a variety of imagery resolution requirements and training sample selection methods for accurate landscape classification. Imagery with 25nm spectral bandwidths and a 4m square spatial pixel outperformed three other competing combinations of spectral and spatial resolution. These were evaluated by comparing the accuracy of image classification with field-based truth data. Thirteen natural and cultural landscape features were classified. Chapter 3 investigated the capability of high-resolution multi-spectral imagery to characterize *Phragmites australis* stands into high, medium and low biomass classes. Ten *P. australis* sample sites were grouped into these three classes based on image reflectance values and field-based biomass measurements. Similarity of group members showed that reflectance values distinguished rank ordered differences in biomass between various *P. australis* stands. In Chapter 4, correction of an imagery-derived cover map was accomplished by assignment of expert knowledge, integration of that knowledge into a simple spatial model, and subsequent generation of a revised cover map. Step-by-step examples are provided to illustrate this post-classification modeling methodology. A partial prototype selection of expert rules was sufficient to change more than 20 per cent of the originally classified landscape pixels entirely by post-classification. Chapter 5 discusses the development of an empirical model that used vegetation community classes to predict the characteristics: a) soil type, b) soil compaction rate, and c) elevation. Vegetation class distribution proved to be a reliable surrogate for estimating these variables based on field-based statistical scores of association and significance tests. High marsh vegetation grouped together is a statistically significant, reliable predictor of soil compaction rates at depths of 30 and 46cm (12 and 18in), with reliability decreasing at shallower depths of 15, 5, and 0cm (6, 2 and 0in). Analysis of variance tests revealed statistically significant differences between the selectively grouped vegetation community types and decimeter-level changes in elevation data. Lastly, Chapter 6 offers a summary with concluding statements that advocate the use of remote sensing as a resource management tool that should be used more often and for more tasks.

xiv

Coastal Zone Landscape Classification Using Remote Sensing and Model Development

Chapter 1

Introduction

The world's coastal zone is one of the most dynamic areas of the world, with over 440,000 km of shoreline where the processes of the land and sea are brought together (Cooke and Doornkamp, 1990; Krabill *et al*, 2000). Coastal zones do not have well defined boundaries but are considered to be the terrestrial area landward of the land–sea interface that is influenced by the sea. Ahnert (1996) specifically describes this zone as including land influenced by wave action; the near-shore dune zone; and the zone where plant growth is influenced by salty groundwater, salt aerosols, and storms (Ahnert, 1996). Many issues affect coastal and marine resources including: population increase (Cohen *et al*, 1997), heavy metal inputs (Knight and Pasternack, 2000), excess nutrient loadings, over-fishing, input of overheated water from factories, habitat loss, sedimentation, marine and beach debris, oil spills, sea level rise (White and Pickett, 1985; Nicholls *et al*, 1994; Nicholls and Leatherman, 1995), loss of biological diversity, and the introduction of non-indigenous species (Marsh and Dozier, 1981; Smith, 1996; French, 1997). Disturbances along the coast have a profound effect on plant and animal life (Huggett, 1995).

One of the problems we face when setting up management programs for our coastal ecosystems is that they do not recognize artificial political borders (Cooke and Doornkamp, 1990). Strategies to protect coastal ecosystems, therefore, have proven politically and physically difficult to implement (Turner and Schubel, 1994). Fortunately, technological advances are providing application tools to complement the needs and objectives of disparate organizations faced with the difficult process of rendering informed decisions designed to effect long-term sustainability of our coastal habitat. These technology tools include: a) software models (Lam *et al*, 1998 {environmental monitoring}; Quattrochi *et al*, 2001

{thermal urban landscapes}; Sanders and Tabuchi, 2001 {flood risk assessments}; b) geographic information systems (Jansen *et al,* 1990); and c) remote sensing (Harris and Ventura, 1995; Jensen, 1996; Cihlar *et al,* 2000a; Steele, 2000). These technologies are available and ready for inclusion into a resource manager's tool-box irregardless of their political or organizational affiliation. Resource managers should closely evaluate the present capabilities, and limitations, of each of these technologies, with special attention given to the use of these tools for the generation of the geospatial data needed in support of GIS and ecological modeling (Wessman *et al,* 1998).

Long-term studies of varied environments and the monitoring of competing influences of nature and man are critical for decision-makers to have information enabling them to make informed judgments (Cooke and Doornkamp, 1990; Cihlar *et al,* 2000b; Slater and Brown, 2000). The term "landscape", as defined by Lyle (1999), is considered to be an ecosystem comprised of biotic and abiotic element interaction, flow of energy and materials, and land resource inventory. A complementary description of landscape as defined by Huggett (1995) is the land surface and its associated terrestrial habitats mapped at medium scales. Remote sensing has been used for landscape characterization (identifying and describing by cover type), monitoring changes (presence or absence) and assessing the effect of the change on the quality of the landscape in environmentally sensitive areas (Slater and Brown, 2000).

A land resource inventory is a necessary beginning for environmental planning or resource management decision-making (Lyle, 1999). Remote sensing provides a fast,

accurate, affordable means to acquire such land resource data (Redfern and Williams, 1996). This land resource data is crucial to assist in determining the functioning of terrestrial ecosystems (Cihlar *et al,* 2000b). Much of this needed data has yet to be acquired. For example, United States land resource data (specifically, Anderson level II data) is only about 60% complete for all land resource cover classes (Yang *et al,* 2001; Vogelmann *et al,* 2001). Additional data will need to be acquired to fill in the missing 40%, and updated data sets of the present 60% coverage will be routinely required from a growing user community expectation for current land cover data for monitoring purposes (Vogelmann, *et al,* 2001).

Landscape researchers and policy makers require data at different spatial scales and resolution (Gulinck *et al,* 2000). Ecologists study environmental problems that require understanding across many scales, from an individual organism to large landscape mosaics (Huggett, 1995). Some scientists feel that land cover will tend to exhibit spatial patterns when determined, at least partially, by landform or climate (Steele, 2000). All environments are continuous in spatial structure, yet we can only sample a finite number of sites (Webster and Oliver, 2001). Cihlar *et al* (2000a) attempted to capture total landscape variability by use of high-resolution imagery sample plots (in lieu of ground plots) strategically sampled across a large-area coarser resolution image scene. Processes and patterns of variation important at one spatial scale might be unimportant at another, as the relative importance of variables might change as the scale changes (Meentemeyer and Box, 1987). Further understanding of various scales of importance, such as local or regional, can be enhanced by the geostatistical analysis of remotely sensed data. For example, a variogram can identify different scales of variation present. Factorial kriging can be used to filter these variations

(Oliver et al, 2000). Understanding regional patterns of ecosystem properties will be important if we are to monitor ecosystem change effectively due to land use and climate change.

Bridging the gap between landscape policy and remote sensing is needed because there is a divergence in central goals, vocabularies and methods (Gulinck *et al*, 2000). Remote sensing offers a powerful tool for landscape cover and distribution mapping, landscape metrics, and assessment of temporal change (Gulinck *et al*, 2000). It should be driven by scientific hypothesis and any future modeling should account for a remote sensing and landscape process model merge (Wessman *et al*, 1998). To date, integration of remote sensing into landscape ecology research and applications has been relatively scarce (Gulinck *et al*, 2000). Ecological models should be designed to use direct or derived variables from remote sensing (Wessman et al, 1998). Landscape criteria or indicators for which remote sensing input would be considered very useful were determined to be: land cover diversity, degree of urbanization, degree of greenness, quantity of open water, size and form of biotopes, spatial arrangement of biotopes, vegetation vitality and disturbances, and land use change (Gulinck *et al*, 2000). Remote sensing input to measuring biodiversity was interestingly evaluated to be of very limited input (Gulinck *et al*, 2000). Overall, remote sensing provides the best tool available for looking at large areas of the earth's surface to analyze, map and monitor ecosystem patterns and processes (Gould, 2000).

Multi-spectral remote sensing acquires visible (blue, green and red), reflected-infrared (IR), and thermal IR regions of the electromagnetic spectrum. Reflected and emitted

radiation are collected and made ready for future processing and analysis (Avery and Berlin, 1992). To detect a landscape feature, the spatial resolution of the sensor should be less than half the size of the feature to be measured (Jensen, 1996). High spatial ground detection resolution (GDR) might not increase the ability to detect and classify smaller features because of the concomitant decrease in class spectral separability resulting from increased interclass variability (Hay *et al*, 1996). Features that were too small or were imperceptible to the detection capabilities of sensors such as SPOT XS and panchromatic (20 and 10m spatial pixels) or Landsat Thematic Mapper (30m spatial pixels) may soon be identified by emerging high-resolution commercial sensors with 4 and 1m spatial resolution (Aplin *et al*, 1997; Lillesand and Keifer, 1994).

A program to address the integration of ecology-based models with GIS and remote sensing at the National Center for Geographic Information and Analysis was started a decade ago (Ehlers, 1995). However, remote sensing has only recently been embraced by the resource management community. Ehlers (1995) cited over-zealous promotion of remote sensing as a solution, restrictions on data use, and lack of attention to user needs as reasons. Based on recent proliferation of literature on the application of remote sensing to environmental issues, this attitude seems to be changing (Redfern and Williams, 1996; Phinn *et al*, 1999; Kenward, 2000; Hill *et al*, 2001; Judge *et al*, 2001).

Coastal zone environments may best be examined from two perspectives: 1) a ground, field-based investigation, and 2) from a remote distance (Turner, 1994) with remotely sensed imagery offering a synoptic top-down view. Field investigations provide

detailed levels of information that are unattainable from remote image source. This information supplements remote sensing by providing validation points for image classifications and by serving as training sample points from which supervised image classifications may occur. Remote sensing can simplify field sampling because it can be used to delineate spatial and temporal patterns in the landscape that can be used to optimize a sampling design (Wessman *et al*, 1998).

Phinn *et al* (2000) described a successful framework for selecting optimal data sets and image processing techniques at three coastal environment study sites by combining remote sensing and landscape ecology concepts. The critical question their work raised was how does one choose from the vast collection of emerging sensors and processing methods (Phinn *et al*, 2000)? Chapter 2 of this manuscript has attempted to answer this question, at least in part. Phinn *et al* (2000) predict an increase in the number of potential users of remotely sensed data due to the increase in sensors (approximately 10 available as of year 2000 with spatial resolutions between 5m and 1km) and increased GIS and image analysis software packages. The integration of remote sensing and GIS technologies has also proved especially useful (Zhenkui *et al*, 2001).

The overall purpose of this collection of studies was to show how coastal zone landscape can be characterized using remote sensing and empirical model development to the betterment of the resource management community. The following chapters discuss the application of remote sensing in a progressive sequence that can be used by resource managers.

Chapter 2 examines resolution requirements of imagery for accurate landscape classification. Results from this work provide a basis to select appropriate remote sensing imagery to suit a coastal area land cover inventory. The chapter also provides insight into the expected classification capability of emergent commercial satellite systems. High-spatial resolution imagery used in this study responds to requirements of clientele in exploitation of improved sensor imagery (Aplin *et al*, 1997). Chapter 3 investigates the capability of imagery to provide information beyond simply land cover classification by remotely assessing biomass differences in stands of *Phragmites australis*, measured by a high-resolution multi-spectral imagery source. *Phragmites australis* is monitored by resource managers because of its propensity to out-compete other native and threatened plant species (Marks *et al*, 1994; Pyke *et al*, 1999). Chapter 4 describes a post-classification technique that introduces expert knowledge into the imagery-derived map classification process. A landscape cover classification map compiled from imagery was visually assessed for blunders based on ecological knowledge of the area. This information was used to parameterize a spatial model of the environment. Deterministic rules are well suited to areas with well-defined boundaries between land cover types (Harris and Ventura, 1995) and, as suggested by Hutchison (1982), are easily developed. Step-by-step examples are provided to encourage acceptance of this post-classification modeling methodology. Chapter 5 discusses the development of empirical models that utilize vegetation class to predict a) soil type, b) soil compaction rate, and c) decimeter-level elevation range. In the absence of a direct remote sensing method for measuring soil conditions, and elevation where the surface is concealed by vegetation, the vegetation itself was used a surrogate to estimate these indirect landscape variables. Collectively, chapters 2 to 5 address the common issues and concerns a

resource manager faces with the monitoring and characterization of landscape conditions within a coastal zone. Lastly, chapter 6 summarizes the findings and provides recommendations for future implementation of remote sensing to support landscape characterization.

References

Ahnert, F., 1996. Chapter 23-The littoral system, <u>Introduction to Geomorphology</u>, John Wiley and Sons, Inc., New York, 286-316.

Aplin, P., Atkinson, P.M., Curran, P.J., 1997. Fine spatial resolution satellite sensors for the next decade. *International Journal of Remote Sensing,* 18 (18): 3873-3881.

Atkinson, P.M., Foody, G.M., Curran, P.J., and Boyd, D.S., 2000. Assessing the ground data requirements for regional scale remote sensing of tropical forest biophysical properties. *International Journal of Remote Sensing,* 21 (13&14):2571-2587.

Avery, T.E., and Berlin, G.L., 1992. Chapter 6- Electro-Optical Scanners. <u>Fundamentals of Remote Sensing and Airphoto Interpretation</u>, 5th ed., Macmillan Publishing Co., New York.

Cihlar, J., Latifovic, R., Chen, J., Beaubien, J., and Li, Z., 2000a. Selecting representative high resolution sample images for land cover studies. Part 1: Methodology, *Remote Sensing of Environment,* 71:26-42.

Cihlar, J., Latifovic,R., Chen, J., Beaubien, J., Li, Z., and Magnussen, S., 2000b. Selecting representative high-resolution sample images for land cover studies. Part 2: Application to estimating land cover composition, *Remote Sensing of Environment*, 72(2):127-138.

Cohen, J.E., Small, C., Mellinger, A., Gallup, J., Sachs, J., 1997. Estimates of coastal populations, letter to *Science*, 278 (5341), 1211-1212.

Congalton, R.G., 1991. A review of assessing the accuracy of classifications of remotely sensed data. *Remote Sensing of Environment*, 37:35-46.

Cooke, R.U., and Doornkamp, J.C., 1990. Geomorphology in Environmental Management-A New Introduction, 2nd ed., Clarendon Press, Oxford.

Ehlers, M., 1995. Integrating remote sensing and GIS for environmental monitoring and modeling: where are we?, *Geo Info Systems*, 5 (7): 36-43.

French, P.W., 1997. Coastal and Estuarine Management, Routledge, New York.

Gould, W., 2000. Remote Sensing of vegetation plant species richness and regional biodiversity hotspots. *Ecological Applications* 10 (6): 1861-1870.

Gulinck, H., Dufourmont, H., Coppin, P., Hermy, M. 2000. Landscape research, landscape policy, and earth observation. *International Journal of Remote Sensing*, 21 (13&14): 2541-2554.

Harris, P.M., and Ventura, S.J., 1995. The integration of geographic data with remotely sensed imagery to improve classification in an urban area. *Photogrammetric Engineering and Remote Sensing*, 61: 993-998.

Hay, G.J., Niemann, K.O., and McLean, G.F., 1996. An object-specific image texture analysis of high-resolution forest imagery. *Remote Sensing of Environment*, 55: 108-122.

Hill, J.M., Graham,L.A., and Henry, R.J., 2001. Wide-area topographic mapping and applications using airborne Light Detection and Ranging (LIDAR) technology. *Photogrammetric Engineering & Remote Sensing*, 6 (8): 908-914.

Huggett, R.J., 1995. Geoecology-An Evolutionary Approach, Routledge, New York.

Hutchinson, C.F., 1982. Techniques for combining Landsat and ancillary data for digital classification improvement. *Photogrammetric Engineering and Remote Sensing*, 48 (1):123-130.

Janssen, L.L.F., Jaarsma, M.N., and van der Linden, E.T.M., 1990. Integrating topographic data with remote sensing for land-cover classification. *Photogrammetric Engineering and Remote Sensing,* 56 (1): 1503-1506.

Jensen, J.R., 1996. Introductory Digital Image Processing, Prentice-Hall, New Jersey.

Judge, E.K., and Overton, M.F., 2001. Remote sensing of barrier island morphology: evaluation of photogrammetry-derived digital terrain models. *Journal of Coastal Research*, 17 (1): 207-220.

Kenward, T., Lettenmaier, D.P., Wood, E.F., and Fielding, E., 2000. Effects of digital elevation model accuracy on hydrologic predictions. *Remote Sensing of Environment*, 74 (3): 432-444.

Knight, M.A. and Pasternack, G.B., 2000. Sources , input pathways, and distributions fo Fe, Cu, and Zn in a Chesapeake Bay tidal freshwater marsh. *Environmental Geology*, 39 (12): 1359-1371.

Krabill, W.B., Wright, C.W., Swift, R.N., Frederick, E.B., Manizade, S.S., Yunger, J.K., Martin, C.F., Sonnta, J.G., Duffy, M., Hulslander, W., and Brock, J.C., 2000. Airborne laser mapping of Assateague national seashore beach. *Photogrammetric Engineering and Remote Sensing*, 66 (1) 65-71.

1-13

Lam, N.S., Quattrochi, D., Qiu, H-L., Zhao, W., 1998. Environmental assessment and monitoring with image characterization and modeling system using multiscale remote sensing data. *Applied Geographic Studies*, 2 (2): 77-93.

Light Detection and Ranging (LIDAR)- Krabill, W.B., Wright, C.W., Swift, R.N., Frederick, E.B., Manizade, S.S., Yunger, J.K., Martin, C.F., Sonnta, J.G., Duffy, M., Hulslander, W., and Brock, J.C., 2000. Airborne laser mapping of Assateague national seashore beach. *Photogrammetric Engineering & Remote Sensing*, 66 (1) : 65-71.

Lillesand, T.M., and Keifer, R.W., 1994. Remote Sensing and Image Interpretation, 3rd ed., Chichester: John Wiley and Sons, Ltd.

Lyle, J.T., 1999. Design for Human Ecosystems, Island Press, New York.

Marks, M., Lapin, B., and Randall, J., 1994. *Phragmites australis (P. communis)*: Threats, management, and monitoring. *Natural Areas Journal*, 14: 285-294.

Marsh, W.M., and Dozier, J., 1981. Landscape: An Introduction to Physical Geography, Addison-Wesley Publishing Company, Inc., Boston, MA.

Meentemeyer, V, and Box, E.O., 1987. Scale effects in landscape studies. In Landscape Heterogeneity and Disturbance, edited by M.G. Turner, Springer, New York, 15-36.

Nicholls, R.J., and Leatherman, S.P., 1995. Chapter 14- Sea-level rise and coastal

management. In Geomorphology and Land Management in a Changing Environment,

ed. by D.F.M. McGregor and D.A. Thompson, John Wiley and Sons, Inc., New York,

229-244.

Nicholls, R.J., Leatherman, S.P., Dennis, K.C., and Volonte, C.R., 1994. Impacts and

responses to sea-level rise: Qualitative and quantitative assessments. *Journal of*

Coastal Research, Special Issue 14, 26-43.

Ogden, J.C., Case Study, Chapter 10- Southern California Natural Community Conservation

Planning- Science as the Crossroads of Management and Policy. In Bioregional

Assessments- Science as the Crossroads of Management and Policy, edited by K. N.

Johnson and others, Island Press, Washington, D.C., 231-247.

Ogden, J.C., Case Study, Chapter 8- Everglades- South Florida Assessments. In Bioregional

Assessments- Science as the Crossroads of Management and Policy, edited by K. N.

Johnson and others, Island Press, Washington, D.C., 169-186.

Oliver, M.A., Webster, R., and Slocum, K., 2000. Filtering SPOT

imagery by kriging analysis. *International Journal of Remote Sensing*, 21

(4): 735-752.

Phinn, S.R., Stown, D.A., van Mouwerik, D., 1999. Remotely sensed estimates of vegetation structural characteristics in restored wetlands, Southern California. *Photogrammetric Engineering and Remote Sensing*, 65 (4): 485-493.

Phinn, S.R., Menges, C., Hill, G.J.E., and Stanford, M., 2000. Optimizing remotely sensed solution for monitoring, modeling, and managing coastal environments. *Remote Sensing of Environment*, 73 (2):117-132.

Pyke, C.R., and Havens, K.J., 1999. Distribution of the invasive reed *Phragmites australis* relative to sediment depth in a created wetland. *Wetlands*, 19 (1): 283-287.

Quattrochi, D.A., Luvall, J.C., Rickman, D.L., Estes, M.G., Laymon, C.A., and Howell, B.F., 2001. A decision support information system for urban landscape management using thermal infrared data. *Photogrammetric Engineering & Remote Sensing*, 66 (10): 1195-1207.

Redfern, H., and Williams, R.G., 1996. Remote sensing--latest developments and users. *Chartered Institution of Water and Environmental Management*, 10 (6): 423-428.

Sanders, R. and Tabuchi, S., 2001. Decision support system for flood risk analysis for the river Thames, United Kingdom. *Photogrammetric Engineering & Remote Sensing*, 66 (10): 1185-1193.

Silberhorn, G., 1999. <u>Common Plants of the Mid-Atlantic Coast: A Field Guide</u>. 3rd ed., Johns Hopkins University Press, Baltimore.

Slater, J., and Brown, R., 2000. Changing landscapes: monitoring environmentally sensitive area using satellite imagery. *International Journal of Remote Sensing*, 21 (13&14): 2753-2767.

Smith, R.L., 1996. <u>Ecology and Field Biology</u>, 5th ed., Harper Collins, New York.

Steele, B.M., 2000. Combining multiple classifiers: an application using spatial and remotely sensed information for land cover type mapping. *Remote Sensing of Environment*, (74 (3): 545-556.

Turner, R.E., 1994. Chapter 7- Landscapes and the Coastal Zone, in Environmental Science in the Coastal Zone: Issues for Further Research, Proceedings of a retreat at J. Erik Jonsson Woods Hole Center, Woods Hole, Massachusetts, June 25 - 26, 1992, edited by National Research Council, National Academy Press, Washington, D.C., 85-105.

Turner, R.E., and Schubel, J.R., 1994. Chapter 11- Research and Development Funding for Coastal Science and Management in the United States, in Environmental Science in the Coastal Zone: Issues for Further Research, Proceedings of a retreat at J. Erik Jonsson Woods Hole Center, Woods Hole, Massachusetts, June 25 - 26, 1992, edited. by National Research Council, National Academy Press, Washington, D.C., 155-164.

Vogelmann, J.E., Howard, S.M., Yang, L., Larson, C.R., Wylie, B.K., and van Driel, N., 2001. Completion of the 1990s national land cover data set for the conterminous United States from Landsat Thematic Mapper data and ancillary data sources. *Photogrammetric Engineering and Remote Sensing*, 67 (6): 650-662.

Webster, R., and Oliver, M.A., 2001. Geostatistics for Environmental Scientists, John Wiley and Sons, Ltd., New York.

Wessman, C.A.,, Cramer, W., Gurney, R.J., Martin, P.H., Mauser, W., Nemani, R., Paruelo, J.M., Penuelas, J., Prince, S.D., Running, S.W., and Waring, R.H., 1998. Chapter 5- Group report: remote sensing perspectives and insights for study of complex landscapes. In Integrating Hydrology, Ecosystem Dynamics, and Biogeochemistry in Complex Landscapes, edited by J.D. Tenhunen and P. Kabat, John Wiley and Sons, New York, 89-103.

Wheatley, J.M., Wilson, J.P., Redmond, R.L., Zhenkui, M., DiBenedetto, J., 2000. Chapter 15- Automated land cover mapping using Landsat Thematic Mapper images and topographic attributes. In Terrain Analysis- Principles and Applications, edited by. J.P. Wilson and J.C. Gallant, John Wiley and Sons, Inc., New York, 245-266.

White, P.S., and Pickett, S.T.A., 1985. Natural disturbance and patch dynamics: an introduction, In The Ecology of Natural Disturbance and Patch Disturbance, Academic Press, Orlando, Florida, 3-13.

Yang, L., Stehman, S.V., Smith, J.H., Wickman, J.D., 2001. Thematic accuracy of MLRC land cover over the eastern United States. *Remote Sensing of Environment*, 76 (3): 418-422.

Zhenkui, M., Hart, M.M., and Redmond, R.L., 2001. Mapping vegetation across large geographic areas: integration of remote sensing and GIS to classify multisource data. *Photogrammetric Engineering and Remote Sensing*, 67 (3): 295-307.

Chapter 1 to Chapter 2 Transition

A need for remote sensing as a critical technology to support landscape management was described in chapter 1. Chapter 2 will evaluate the accuracy of emerging high spatial resolution image source, given 70- and 25-nanometer spectral bandwidths, for classifying landscape cover characteristics. Broad community-level vegetation types were mapped and ground-truthed for accuracy using one of four combinations of spectral and spatial resolution. High-resolution satellite and airborne imagery poses the question to potential users: Is this the preferable source material to use for classification? While the selection of an image source depends on a user's need for particular cover classes, the next chapter illustrates classification differences that occur in the mapping of identical features using variable spectral and spatial resolution image data.

Chapter 2

Accuracy of Coastal Landscape Classification Based Upon Varied
Imagery Spectral Bandwidth, Pixel Resolution, and Training Sample
Selection Method

Abstract

Four multi-spectral imagery combinations (25nm/1m, 25nm/4m, 70nm/1m, 70nm/4m), each employing 6 distinct training sample methods for a total of 24 total combinations, were processed to compile 24 classification map products containing thirteen land cover features over a coastal study site at Fort Story, Virginia, USA. Eight themes comprised natural features (oak and American holly forest, mixed forest, loblolly forest, maintained grass, beach grass, ocean, sand, clay soil) and 5 themes comprised cultural (man-made) features (asphalt, concrete, gray shingle roof building, brown shingle roof building, and shoreline rip-rap). Each of the 24 classifications was segmented into 3 groups: a) all landscape features, b) natural landscape features, and c) cultural landscape features, creating a total of 72 landscape classifications. Final classifications were tested by ground-truth points, error matrices, and scores for Kappa and overall accuracy. Accuracy results were based on the contributions of a) spectral bandwidth and b) spatial resolution, c) combined spectral and spatial contribution, and d) training sample methods to classification accuracy. Spectral bandwidth 25nm was better for "natural and cultural", and "cultural" features. Pixel resolution was significantly different for the classification of "natural" features, where 4m pixels outperformed 1m pixels. The combination of 25nm spectral and 4m spatial resulted in higher Kappa scores than other combinations, however, the only statistically

significant differences occurred between accuracy scores achieved from 25nm/4m imagery and 70nm/1m imagery in the classification of natural and cultural, and natural features. Training sample methods that defined larger numbers of training sample pixels for the classification of landscape features resulted in more accurate classification maps. Accordingly, differences in methods of training sample selection were significant, as determined by the differences in overall accuracies attained by the different sampling techniques.

Introduction

Landscape data acquired through imagery can represent inherent landscape variability (Wessman *et al*, 1998; Oliver et al, 2000), especially when data are spatially dependent as are most natural features (Webster, 1985). Accordingly, as Webster and others have stated from the geostatistical disciplines (see for example Burgess *et al*, 1981; Webster and Oliver, 2001), field data acquired by a classic random sampling design may not exhibit the data independence condition required for follow-on statistical analysis. Classical statistical sampling methods may not be adequate to capture true spatial scales (Webster and Oliver, 2001). Sampling designs based on inherent spatial variability in a remote sensing scene would help minimize difficulties that arise from a classical random-based field sampling (Wang *et al*, 2001). Field samples should be acquired to support the training and testing of the coincident imagery (Congalton and Green, 1999), and the imagery resolution should directly support the level of land-use land-cover (LULC) classification desired by the user (Phinn *et al*, 2000). For example, Jensen (1996) references the four-tiered U.S. Geological

Survey (USGS) land classification system and pertinent image sources needed to provide such information. Greater detail at larger map scales requires lower altitude imagery, with the implication that higher spatial resolution would solve a user need for finer detail at multiple scales (Aplin *et al*, 1997). Predictions of spectral characterization difficulties from emerging high-resolution imagery sources originated from several sources (see Lillesand and Keifer, 1994; Aplin *et al*, 1997).

Multi-spectral imagery is acquired by satellite or airborne systems with different spectral bandwidths and spatial pixel resolutions. Choices of type of imagery are growing with the advent of each new system that is launched and users must choose the best types to suit their intended needs. There is also a wide choice of methods for processing image data (Civco, 1998). Cihlar *et al* (2000) described their solution for selecting high-resolution imagery sample sites from large area coarse resolution imagery. Knowledge of land cover distribution over large areas is increasingly important for scientific and policy purposes and is a key input for land use and management decisions (Cooke and Doornkamp, 1990; Cihlar *et al*, 2000a). Most imagery users are interested in maximizing the accuracy of the classified land cover types and this desire may lead to a spatial aggregation of pixels (Vogelmann *et al*, 2001). However, many land managers are interested in Anderson Level III type classifications, or species level vegetation. Accuracies reported by Skidmore and Turner (1988) for this level of mapping have been low with the best scores between 65 and 75 per cent for Thematic Mapper resolution imagery. When mapping natural environmental features it is probable that uncertainty in class cover assignment will lead to errors (Zhang and Stuart, 2001).

The objective of this study was to compare variable multi-spectral imagery bandwidth and pixel resolutions, as well as variable training sample selection methods, and statistically assess the results of landscape classification generated from the numerous combinations of resolutions and sample methods to determine if certain combinations were more accurate than others. Questions such as: "What source(s) of imagery are best in terms of bandwidths and pixel size to minimize inevitable error in landscape classification of both natural and man-made features?" and "Which training sample method works best for achieving the highest optimal solution for accuracy?" were addressed. Identification of preferred bandwidth and pixel sizes would assist in future development of sensor capability and in the selection of appropriate image data from multiple commercial vendors. Determination of preferred training sample method(s) based upon unique imagery bandwidth and pixel size should improve landscape classification accuracy. The level of landscape features to be classified was pre-determined to be Anderson Level II, with land cover types represented as sub-divisions of larger land cover types (e.g., forest land represented at Level I is depicted as deciduous, evergreen, and mixed at Level II), and the classification level formed the basis for all analyses, assessments, and recommendations. A different level of landscape detail might have altered the results.

Null hypotheses tested at the 95% confidence level were:

a) H_{01}-accuracy results generated for 70nm and 25nm spectral bandwidth imagery derived landscape classifications would be equivalent;

b) H_{02}-accuracy results generated for 1m and 4m spatial pixel size imagery derived landscape classifications would be equivalent;

c) H_{03}-accuracy results generated for 70nm/4m, 70nm/1m, 25nm/4m, and 25nm/1m resolution imagery derived landscape classifications would be equivalent; and

d) H_{04}-accuracy results generated for 6 varied training sample method derived landscape classifications would be equivalent.

We evaluated various combinations of 4-channel multispectral airborne imagery similar in bandwidth and pixel size to the emerging high resolution IKONOS satellite imagery. Image classification accuracy was assessed by field sample plots, an approach endorsed by Milne and Cohen (1999). A combination of two spectral bandwidths, two pixel sizes, and six training sampling methods were evaluated with the accuracy of classifications discussed in sequence by: a) spectral bandwidth contribution, b) spatial pixel size contribution, and c) a combination of both bandwidth and pixel size. For each evaluation, accuracy was individually addressed against (i) *all* landscape features, (ii) *natural* landscape features only, and (iii) *cultural* landscape features only. Evaluation of spectral and spatial resolution analysis was followed by an evaluation of training sample methods, once again individually addressed against (i) *all* landscape features, (ii) *natural* features only, and (iii) *cultural* features only. A recommendation for bandwidth, pixel size and training sample method was provided based on desired landscape features as reference for future coastal landscape classification in similar geomorphology.

Methods

Study site

Fort Story, Virginia, USA, is a small joint services military installation situated along the coast at the intersection of the Chesapeake Bay and Atlantic Ocean (Figure 1). This prominent cape location provides a safe harbor for endangered flora and fauna and is an example of tenuous competing coastal land uses. Fort Story is a mixed land-use land-cover installation. The study site selected was approximately 400 by 500 meters in size and contained all landscape classes found at the Fort except forested wetlands (sand, maintained grass, clay soil, loblolly pine forest, hardwood forest, mixed forest, beach grass, ocean, asphalt pavement, rip-rap shoreline, concrete pavement, and variable roofing material). The area is heavily influenced by anthropogenic activity. Complexity of cultural and natural features found at this site provided a suitable challenge for comparing variable combinations of spectral bandwidth, spatial pixel size, and training sample method combinations. Land resource issues that demand accurate landscape classification include beach erosion, inadvertent vegetation removal, soil compaction, introduction of non-native species, threatened species survival, and preservation of forested wetlands.

Imagery Acquisition

Four-channel multi-spectral imagery was acquired over the coastal study site of Fort Story, Virginia, on the cloud-free morning of 15 October 1999. Two flights were flown to acquire imagery collected through cameras equipped with 70 and then 25nm band interference filters. Band centers for each flight were 450nm (blue), 550nm (green), 650nm

(red), and 780 (near infra-red, NIR). Flight one occurred between 0826 and 0840 hours using

70nm filters that closely emulated conventional satellite bandwidths. Spatial ground

detection resolution (GDR) was approximately 1m. The second flight was between 0947 and

1005 hours equipped with custom 25nm band-pass filters. Band centers and GDR were

identical to the earlier flight. Four-meter spatial resolution flights were not acquired

separately. Rather, to minimize change in both environmental conditions and future geo-

registration issues, the 25 and 70nm 1m pixel images were spatially degraded to a resolution

of 4m using a mean degradation filter available within ERDAS Imagine software (ERDAS

Inc., 1999). Average reflectance of sixteen 1m pixels adequately represented the spectral

response that would have been returned had corresponding 4m pixels been initially acquired.

One-meter imagery was geometrically tied-down to a U.S. Geological Survey digital ortho-

photo quad (DOQ) prior to the creation of the 4m image scenes. The 25nm and 70nm

imagery over the study sites was registered with control point root mean square error of

approximately 1m. Each of the four images covered identical size and area over Fort Story.

The four scenes available for classification and comparison were:

1. 1m spatial with 70nm spectral

2. 1m spatial with 25nm spectral

3. 4m spatial with 70nm spectral

4. 4m spatial with 25nm spectral

Five hundred and twenty-three sampling locations were randomly assigned to the

imagery study area. Appendix 1 is a listing of 250 geographic locations that were classified

in the field; the remaining 273 sampling locations were easily photo identified by an analyst with total awareness of all landscape conditions within the small study plot. Each sample location was field-classified into one of 13 possible landscape categories. Precise Lightweight Global Positioning System (PLGR) was used for real-time field positioning at an accuracy of 10m horizontal. In addition, an extensive assemblage of photo identifiable cultural features existed within the study area and facilitated visual field navigation to the sample locations. If a field sampling location was at the edge of two landscape features and there was a risk of misclassification because of horizontal accuracy limitations, the field plot was re-positioned away from the edge and wholly into a single feature class. A radial sampling plot distance of 5m was used during classification. Loblolly pine dominated the forest overstory in one stand, with suppressed hardwoods and understory shrubs. Seventy-five additional training sample points were randomly acquired for use in training sample generation and made available for image processing. Training and testing locations were selected from the 1m spatial / 25nm spectral data and applied to each of the other three geo-registered spatial image sets. Natural landscape classes identified for classification from each image set were common U.S. Geological Survey Land Use/Land Cover Classification System data themes (Jensen, 1996). Cultural landscape themes selected reflected a research interest in disparate road surface and roofing material, as well as interest in remotely mapping the sustainability of rip-rap (boulder-lined) shoreline protection. Landscape features classified for this study were:

Natural Features

1. Sand

2. Maintained Grass

3. Soil (clay)

4. Loblolly pine dominated maritime forest

5. Live oak and American holly dominated maritime forest

6. Mixed Forest (pine and hardwood)

7. Beach grass

8. Ocean

Cultural Features

9. Asphalt

10. Rip-Rap (extensive boulders along ocean shoreline)

11. Concrete

12. Gray Shingle Roof Building

13. Brown Shingle Roof Building

Spectral training set data were acquired for all four image combinations for each of the thirteen terrain classes. Minor changes in reflectance values between the 70 and 25nm imagery can be primarily attributable to a sun angle change from 0826 to 0947 hours, the respective starting times for the 70 and 25nm flights. Although radiometric corrections were individually completed for the 70 and 25nm image data, radiometric correction to adjust one

image set to match the other was not attempted. The 25nm imagery was the beneficiary of slightly shorter shadows and higher radiant energy over the study site, attributable to a higher sun angle. The degree to which this sun angle difference may have independently influenced (negatively or positively) final classification accuracy is unknown. Seven transformed divergence scores measured between-class separability for 25nm imagery that were less than 1950, while only five scores less than 1950 were computed for between-class separability for the 70nm imagery, despite the 70nm image's longer shadows from lower sun angle.

Training sample selection methods chosen for evaluation were choices that would be available to imagery analysts using commercial image processing packages for remotely sensed image classification. Training samples ranged from the simplest, most objective methods, to the most difficult and subjective methods, generally providing the greatest amount of representative class information. "Seed grow" is a method available within ERDAS Imagine that searches surrounding pixels at a user defined euclidean distance from the identified point (seed-pixel) and selects all similar pixels to add to the training sample set (ERDAS, 1999). Identical geographic locations were used for all point methods. Polygon training samples were screen digitized by an image analyst surrounding all previously chosen point locations. Training methods investigated were:

1. Point method

2. Point with 2-euclidean distance seed grow.

3. Point with 5-euclidean distance seed grow

4. Point with 15-euclidean distance seed grow

5. Point with 25-euclidean distance seed grow

6. Polygon method

Each training sample method returns a training sample set of pixels that may be tested for separability, one class from the other. With greater separability of training samples representing the landscape feature classes, there is greater chance for accurate classification of the imagery into correct feature classes. The technique for testing this separability was to use a transformed divergence measurement as described by Jensen (1996). Both the mean and covariance of the training sample class statistics are used in divergence to identify classes of optimum separability and classes that overlap. Transformed divergence exponentially adjusts the between-class scores and reports values on a scale between 0 and 2000, with 2000 indicating excellent between-class separation (Jensen, 1996).

Comparative Assessment

Accuracy of each image-derived landscape classification was determined by comparing the field truth points to the mapped landscape themes (Congalton and Green, 1998). Landscape classes for each image were computed using each of the 6 identical training sample methods, by a maximum likelihood classification algorithm that utilizes covariance of pixel signatures in the final class selection. Maximum likelihood was selected over the less computational algorithms (minimum distance or parallelpiped) because it provides a more rigorous technique that can capture pixel level probability information useful for follow-on research into inclusion of *a posteriori* pixel probabilities and their propogational effect on decision software models. A total of 24 landscape classification

maps (6 training methods * 4 spectral / spatial combinations = 24 maps) were created for accuracy assessment. Error matrices were generated in table format to determine accuracy levels and to assess statistical significance of the results.

Kappa statistics (Cohen, 1960; Verbyla, 1995; Congalton & Green, 1999) were computed to test for agreement between landscape conditions expected (defined by reference ground truth points) and those that were found (landscape classification maps). The result of Kappa analysis is the KHAT statistic (Cohen, 1960). The range of values is similar to Pearson's r correlations where values can range from -1.0 to +1.0, and 0.00 represents no agreement whatsoever. Positive KHAT scores are expected because remotely sensed classifications and reference data should be positively correlated (Congalton and Green, 1999) (see equation 1). Applying a scale imposed by Landis and Koch (1977), high Kappa scores were considered as 0.80 or greater, moderate scores between 0.40 and 0.80, and low scores were less than 0.40.

In the following equations, let k denote categories of remotely sensed classification; let $p_{ii}=$ proportion of samples classified into category i found in the ith row; let $p_{i+}=$ proportion of samples classified into category i ($i = 1, 2,...., k$) found in the jth column, and $p_{+i}=$ proportion of samples in the reference classification and category j ($j=1,2,..., k$) found in the ith row.

Where
$$p_o = \sum_{i=1}^{k} p_{ii}$$

equals the actual agreement between reference data and classification (or overall

accuracy) , and

$$p_c = \sum_{i=1}^{k} p_{i+} p_{+j}$$

equals the chance agreement between reference data and classification, and

$$Kappa = \frac{p_o - p_c}{1 - p_c} \tag{1}$$

Z-test statistics were then computed for each Kappa score to test that agreement

between the remotely sensed classification and the reference ground data was better than

random chance, at the 95% confidence level (see equation 2).

$$Z = Kappa \ / \ Sqrt \ (Kappa \ variance) \tag{2}$$

For a detailed description on computing the square root of Kappa variance, refer to

Congalton and Green (1999), where large sample variances were computed for overall Kappa

scores using the Delta method. Statistical differences between the Kappa accuracy results in

the landscape classifications were assessed by comparison of best Kappa scores within a

landscape category against all other Kappa scores, testing at the 95% confidence (see

equation 3). Null hypothesis is rejected if the z-score computed from equation 3 is greater

than 1.96. The rationale for this test is that future imagery will likely appear in the form of

one of these four possible image combinations and, if given a choice of the four

combinations, which selection is the best? The best Kappa score, and all others considered

statistically the same, determined image combinations with the highest classification

accuracy. All image combinations with similarly high Kappa scores were also compared

later, testing ANOVA for respective overall accuracy scores to determine if these scores were

statistically different.

$$|Kappa1 - Kappa2| \ / \ Sqrt (Kappa1 \ variance + \ Kappa2 \ variance) \qquad (3)$$

Kappa scores for each landscape classification were grouped into four respective

spectral –spatial imagery combinations: 25nm/1m, 25nm/4m, 70nm/1m, and 70nm/4m

image combinations. These four groups were then subdivided into the six training sample

methods selected for image processing. The rationale for this test was that high-resolution

image data could negate conventionally recommended methods for training sample selection

and subsequent classification processing. Accordingly, Kappa scores from identical image

combinations were compared to each other using equation 3 above to test for statistical

differences in the training sample methods. Similarly high Kappa scores were also compared

by their respective overall accuracy scores. All accuracy scores within 3% of the highest

overall accuracy score were assessed as representing training sample methods that would be

most effective for the respective spectral-spatial imagery combination.

In addition to Kappa scores, overall accuracy percentages were generated for each of

the landscape classification maps. Analysis of variance (ANOVA) testing (StatSoft, 1995)

was applied to determine if accuracy scores derived from the 24 spectral – spatial combinations were statistically different from one another at the 95% confidence. Overall accuracy scores were grouped into logical classes (spectral, spatial, spectral and spatial) and variances among the respective groups compared for similarity by traditional ANOVA testing. Criteria for use of ANOVA were met (normal distribution, randomness of data (total data population is tested in this case), and data independence, tested by the error terms of the variates) (Sokal and Rohlf, 1995). ANOVA F-statistics were examined to determine if spectral groups (25 and 70nm images), spatial groups (1 and 4m pixels), and combined spectral-spatial groups were statistically different from one another. Overall accuracy scores were determined for each of the classifications by dividing the trace, or sum of correct measurements in each error matrix leading diagonal, by the sum of the total in each row (or column) (Congalton and Green, 1999).

Accuracy scores were not high for any landscape classifications. While an increase in accuracy classification might have been achieved with continued image processing, no attempt was made to improve the accuracy of any initial classification score, in the belief that this would introduce considerable individual bias into the experiment. By avoiding the temptation to improve the accuracy scores, all results for this test were achieved by the same methods and could be compared on an "equal footing".

Results

Divergence scores less than or equal to 1950 for any classification cover pair are identified in Table 1 for each spectral – spatial imagery combination. All other pairs have a

score between 1951 and 2000. Low transformed divergence scores consistently improve when pixel size increases from 1m to 4m (e.g., Loblolly pine / unmaintained grass; Loblolly pine / hardwood forest). Similarly, whenever pixel sizes are the same, several divergence scores improved when changing from a 70nm to 25nm bandwidth (e.g., Loblolly pine / unmaintained grass; hardwood forest / unmaintained grass). Variability may be the result of pixel size, spectral bandwidth, or both.

All imagery combinations have been reclassed into spectral, spatial, and spectral-spatial groupings for comparison and evaluation. For the spectral component, Kappa and overall accuracy scores for 25 nm spectral images are classed separately from 70nm spectral imagery.

Table 2a (all features) shows Kappa scores separated into 25 and 70nm spectral bandwidth groups. The spectral results from the 25nm imagery provide greater overall accuracy. The top 25nm result (25nm/4m/seed15) compared to the top 70nm result (70nm/4m/seed25) showed no statistical difference. All remaining 70nm combinations were statistically different from the best 25 nm outcome. The narrower bandwidths provided five possible image combination/training sample solutions that were equally effective, while the wider 70nm bandwidth provided one solution. Kappa results suggest that the 25nm bandwidth did a better job at classification of natural and cultural features over the Fort Story study area. Table 2b shows natural features with Kappa scores separated into 25 and 70nm spectral groups. There are no statistical differences with any of the spectra-spatial-training sample combinations as reported by these Kappa results. Table 2c shows cultural features,

with Kappa scores separated into 25 and 70nm spectral bandwidth groups. The spectral results suggest the 25nm imagery provides greater classification accuracy. The top 25nm result (25nm/4m/polygon) is statistically similar to the top three 70nm results but different from the remaining nine combinations of 70nm images. The narrower 25nm bandwidth provided seven possible image combination/training sample solutions that were equally effective, while the wider 70nm bandwidth provided only three effective solutions. Kappa results suggest that the 25nm bandwidth did a better job at classification of "cultural" features over the Fort Story study area as the top four 25nm scores are higher than the top score for 70nm imagery.

Table 3 shows overall accuracy scores separated into 25 and 70nm spectral bandwidth groups, identified by classification of natural and cultural, natural, and cultural features. Grouping of scores by spectral bandwidth enabled analysis of variance (ANOVA) tests to compare the accuracy scores from the two groups (Table 4). There were no statistical differences in overall accuracy results for all, natural or cultural features when every training sample method was applied. However, with the removal of training sample methods "point" and "seed grow 2" eliminated because of consistently poor performance, ANOVA results for "natural and cultural" and "cultural" features showed statistical differences between the spectral groups at the 95% confidence level. Figures 2a-c (natural and cultural, natural, cultural) show the overall accuracy of each image combination by spectral bandwidth group, shown in decreasing order of accuracy. The plots illustrate 25nm data achieved higher classification accuracy for natural and cultural, natural, and cultural feature types. 70nm scores averaged about 5% less accurate than the 25nm scores. ANOVA results affirmed the

Kappa findings; the narrowness of the 25nm bandwidth has had a statistically significant positive effect on all and cultural feature discrimination and classification. Natural features alone were not statistically affected by the differences in spectral bandwidth, with a recorded p-value = 0.20. The original null hypothesis (H_{01}-accuracy results generated for 70nm and 25nm spectral bandwidth imagery derived landscape classifications would be equivalent at the 95% confidence level) was accepted for natural landscape features and rejected for all and cultural landscape features.

For the spatial comparison, Kappa and overall accuracy scores for 1m pixel imagery are classed separately from 4m pixel sizes. Table 5a (natural and cultural features) shows Kappa scores separated into 1 and 4m pixel sizes. The top Kappa score is from a 4m spatial image (25nm/4m/seed15). There is no statistical difference with this score and the top two scores from the 1m imagery, as indicated by a pairwise test statistic of 1.44, but all other 1m imagery scores are different. The top four finishing 4m imagery are all very similar (test statistics 0.00 to 0.58 with 1.96 as the defining critical threshold). The coarser pixel size provided four possible image combination/training sample solutions that were equally effective, while the finer 1m spatial imagery provided only two effective solutions. Kappa results show that the 4m spatial imagery did a better job at classification of "all" features over the Fort Story study area. Table 5b shows natural features with Kappa scores separated into 1 and 4m pixel groups. There are no statistical differences with any of the spectra-spatial-training sample combinations as reported by these Kappa results. Neither 1m nor 4m performed better. Table 5c shows cultural features with Kappa scores separated into 1 and 4m spatial pixel groups. The top three Kappa scores are from a 4m spatial image. There is

original null hypothesis (H_{02}-accuracy results generated for 1m and 4m spatial pixel size imagery derived landscape classifications would be equivalent at the 95% confidence level) was accepted for natural and cultural, and cultural, landscape features, and rejected for natural features.

Lower resolution 4m pixels were better at capturing the overall feature reflectance signature and minimizing the variability in the training sample signatures. A more detailed evaluation of the accuracy achieved in classification of the eight individual natural landscape feature themes was completed from a user's (categorical row accuracy from the accuracy matrix) and producer's (categorical column accuracy from the accuracy matrix) standpoint, using the seed grow-15 training sample selection method results. User's accuracy was higher for all themes when 4m data were used as opposed to 1m data. Sand was the single exception to this finding, with higher scores achieved from the 1m spatial imagery. Producer's accuracy results suggested that either 4 or 1m spatial resolution was acceptable; it really depended on the feature. Sand, ocean and maintained grass each scored higher with 1m data. Each of the three forest features responded better to the 4m data. Shadows, understory, and within canopy differences that might otherwise cause confusion with a small 1m pixel were minimized by the larger spatial pixel. Earlier unpublished findings by the author at an alternative study site corroborate this finding of improved accuracy in forest classification from 4m data as compared to 1m data.

Cultural features were adequately classified by 4m imagery. Visually, the degraded 4m imagery does not represent man-made features with their inherent angular forms as neatly

as the 1m imagery. It was not appealing to observe buildings as amorphous blobs when once they were cleanly defined rectangles. However, this did not adversely affect the accuracy. It was encouraging to note that cultural features classified by 4m data were not reported to be statistically different from cultural features classed by 1m data. Despite the favorable classification achieved by the 4m data, from the standpoint of map output and end-user appeal, it is unlikely that the 1m imagery would be dismissed, if available, in favor of 4m data. The 4m derived landscape classifications did not look as good for portraying of cultural features.

After evaluating the contribution of the spectral and spatial properties of imagery independently, the two components were evaluated together to determine their contribution on the accuracy of feature classifications. As before, both Kappa and overall accuracy scores for 25nm/1m, 25nm/4m, 70nm/1m, and 70nm/4m were classed separately. Table 8a (natural and cultural features) shows Kappa scores separated into 25nm/1m, 25nm/4m, 70nm/1m, and 70nm4m classes. The Kappa results from the 25nm/4m imagery suggest greater classification accuracy is achieved from this combination than from any other combination of spectral - spatial imagery, as top scores are from 25nm/4m/seed15 and 25nm/4m/polygon imagery. While there is no statistical difference between these top scores and the Kappa scores for 25nm/1m (pairwise comparison = 1.44) and 70nm/4m imagery (pairwise comparison = 0.58), with 1.96 as the critical threshold, the scores for the 25nm/4m imagery are clearly highest. No scores from 70nm/1m imagery are statistically close. Table 8b (natural features), shows Kappa scores separated into 25nm/1m, 25nm/4m, 70nm/1m, and 70nm4m classes. There is no statistical difference with any spectra-spatial-training sample

combination as reported by these Kappa results. Top scores, although not by much, come

from the 25nm/4m and 70nm/4 imagery combinations. Table 8c is for cultural features, and

shows Kappa scores separated into 25nm/1m, 25nm/4m, 70nm/1m, and 70nm4m classes.

The top three Kappa scores are all from the 25nm/4m/polygon imagery, although there is no

statistical difference with top score (Kappa = 0.77) and any of the other spectral-spatial

combination top finishing scores. Each combination has at least one training sample method

combination that was statistically equivalent. The 25nm/1m combination reported 4 scores

that were statistically equivalent although each of these scores is lower than the top three

25nm/4m scores. These top three Kappa scores corroborate earlier findings for spectral

bandwidth alone that suggested 25nm spectral bandwidth was better, as well as the earlier

findings for spatial pixel size suggesting that 4m spatial pixel sizes were better. Kappa

results suggests that the 25nm/4m imagery did a better job at classification of "cultural"

features over the Fort Story study area because the top three scores are attained with this

resolution combination .

Table 9a to c (natural and cultural, natural, cultural) represent overall accuracy scores

separated into 25nm/1m, 25nm/4m, 70nm/1m, and 70nm/4m groups. Grouping of overall

accuracy scores by combined spectral and spatial group enabled analysis of variance

(ANOVA) tests to compare the scores between the two groups. Table 10 initially lists

selected ANOVA results comparing 25nm/4m (spectral – spatial combination achieving the

highest overall accuracy score) against 70nm/1m and 4m (the lowest scores), revealing no

statistical differences for natural and cultural, natural or cultural features. Training sample

methods "point" and "seed grow 2" were ultimately eliminated because of consistently poor

performance. ANOVA results that excluded accuracy scores from these two training sample methods, comparing the 25nm/4m against all other imagery combinations, showed statistically significant differences in overall accuracy classification scores with 70nm/1m imagery for natural and cultural, and natural landscape features. There was no statistical difference for the cultural features. Image combination 25nm/1m was almost significantly different from 25nm/4m imagery. Figures 4a-c (natural and cultural, natural, cultural) depict the overall accuracy of each combination of spectral - spatial imagery, shown in decreasing order of accuracy. Image combination 25nm/4m consistently showed the highest overall accuracy scores for training sample methods used to classify natural and cultural, natural, and cultural features. The earlier null hypothesis (H_{03}-accuracy results generated for 70nm/4m, 70nm/1m, 25nm/4m, and 25nm/1m resolution imagery derived landscape classifications would be equivalent at the 95% confidence level) was accepted for all combinations of image resolution except 70nm/1m, which reported a statistically significant difference with the top scores achieved from the 25nm/4m imagery for the classification of natural and cultural features, and natural features; consequently, the null hypothesis was rejected for equivalency of 25nm/4m and 70nm/1m classifications.

Table 11 summarizes the overall Kappa performance of the 24 possible spectral - spatial combinations, taking into consideration the performance of all training sample methods evaluated. The place order (first, second, third, or fourth) was determined by rank ordering all Kappa scores and assigning a rank of 1 to the highest Kappa score and 24 to the lowest Kappa score. Lowest total cumulative rank order position for all training sample methods within each spectral – spatial combination determined the placement of each

spectral-spatial combination into first, second, third, or fourth place. The best training sample finish for each spectral- spatial combination is also reported and is supporting evidence to the place ordering finishes. Combination 25nm/4m was the best overall combination of imagery achieving first place finishes in all possible categories. Conversely, combination 70nm/1m was the worst overall, consistently finishing last for all possible categories. This poor performing combination should closely represent 1m IKONOS panchromatic imagery after HSI transformation by its coincident ~70nm/4m multi-spectral image channels.

Tables 12a-c (natural and cultural, natural, cultural) list Kappa scores subdivided within the table into each of the 6-training sample methods. All scores were pairwise statistically compared to the top scores. In Table 12a (natural and cultural features), top scores were achieved from the seed grow-15 and polygon training sample method, both from 25nm/4m imagery. It is evident from this table that seed grow-5, seed grow-2, and point methods are not close to achieving the highest accuracy scores. Kappa scores derived from each training sample method were determined and compared in a pairwise manner against all other Kappa scores from the identical method. In Table 12b (natural features), curiously enough, top scores were achieved from the seed grow-25, polygon, seed grow-2, and point training sample methods, from the 25nm/4m and 70nm/1m imagery. Pairwise comparison of the top Kappa scores indicated no statistical difference in training sample methods for the classification of natural features. In Table 12c (cultural features), top scores were achieved from the seed grow-25 and polygon training sample methods, once again originating from the

25nm/4m imagery. It is evident from this table that seed grow-2 and point methods are not close to achieving the highest accuracy scores.

Table 13a list the overall accuracy scores, grouped by six training sample methods, as identified for the classification of natural and cultural features. These groups of values were used for an ANOVA test to determine if training sample methods contributed to statistically different overall accuracy scores. Table 13b is the ANOVA results listing the training sample methods that reported statistically different accuracy scores. Consistently, the seed grow-15, seed grow-25, and polygon training sample methods were statistically better than the point, seed grow-2, and seed-grow-5 methods for classification of natural and cultural features. Point method was the poorest performer, followed by seed grow-2 and seed grow-5. These findings strongly suggest that there were insufficient pixels to represent the feature classifications.

Table 14a lists the overall accuracy scores, grouped by six training sample methods, as identified for the classification of natural features. These groups of values were used for an ANOVA test to determine if training sample methods contributed to statistically different overall accuracy scores. Table 14b gives the ANOVA results listing the training sample methods that reported statistically different accuracy scores. Consistently, the seed grow-15, seed grow-25, and polygon training sample methods were statistically better than the point and seed grow-2 methods for classification of natural and cultural features. Point method was again the poorest performer, followed by seed grow-2. These findings strongly suggest that there were insufficient pixels to represent the natural feature classifications.

Table 15a lists the overall accuracy scores, grouped by six training sample methods, as identified for the classification of cultural features. These groups of values were used for an ANOVA test to determine if training sample methods contributed to statistically different overall accuracy scores. Table 15b gives the ANOVA results listing the training sample methods that reported statistically different accuracy scores. Consistently, the seed grow-15, seed grow-25, and polygon training sample methods were statistically better than the point and seed grow-2 methods for classification of natural and cultural features. Point method was again the poorest performer, followed by seed grow-2. These findings strongly suggest that there were insufficient pixels to represent the cultural feature classifications.

For natural and cultural, natural, and cultural landscape feature classification alike, only seed grow-15, seed grow-25, and heads-up polygon digitizing were accepted as viable methods for achieving highest accuracy scores. Point and seed grow-2 training sample collection methods produced statistically unacceptable classification results. Seed grow-5 method was also not effective for the classification of natural and cultural features. Figures 5a-c (all, natural, cultural) depict the overall accuracy derived from the different sampling methods with the four imagery combinations. Polygon, seed grow-15 and seed grow-25 methods are always plotted with higher overall accuracy (%) than point, seed grow-2 and seed grow-5 training sample methods. The null hypothesis (H_{04}-accuracy results generated for each of the 6 varied training sample method derived landscape classifications would be equivalent at the 95% confidence level) was therefore rejected for point, seed grow-2, and

seed grow-5 training sample methods and accepted for the seed grow-15, seed grow-25 and polygon methods.

A total of seventy-two error matrices were generated for assessing the accuracy of the landscape classifications (24 combinations evaluated against all (i) natural and cultural landscape features, (ii) natural landscape features, and (iii) cultural landscape features). These tables are given in Appendices 2-73 (Accuracy Assessments) and are summarized in accuracy assessment Tables 8a to c (Kappa scores) and Tables 9a to c (overall accuracy scores). Figures 6a-c (all, natural, cultural) graphically depict Kappa scores determined from accuracy assessments of image classifications for natural and cultural, natural, and cultural features.

Discussion

Four-meter multispectral, 1m panchromatic, satellite imagery is still a newly available image combination with the IKONOS satellite originating the collection and dissemination of this data resolution since 1999. No investigation by prior researchers into detailed accuracy assessments of high-resolution imagery such as IKONOS for classification of land cover characteristics was found in the literature. Dare and Fraser (2001) documented a non-scientific visible comparison of standard IKONOS 4m multispectral imagery against a panchromatic fused image set that imitated 1m spatial accuracy over a coincident South African urban fringe area. The 1m imagery clearly showed individual small buildings, paths, and tracks not identifiable from the 4m image. Also, the panchromatic-multispectral fusion appeared to highlight differences in soil and vegetation conditions not visible in the

standard 4m multispectral image. Moore (2000) examined coastal mapping techniques in cartography, photogrammetry, and GIS and cited recommendations appear to support the application of 1 and 4m spatial imagery. Conversely, there are ample documented reviews of the accuracy of landscape resource inventories derived from what would now be considered moderate spatial resolution 30m Landsat Thematic Mapper (Skidmore and Turner, 1988; Vogelmann *et al*, 2001, Yang *et al*, 2001). From these reviews, Anderson Level II land cover classes derived from Thematic Mapper were accurate about 65-75% of the time, leaving little hope for mapping at Anderson Level III, or vegetation species-level, to be sufficiently accurate to meet users needs. Data derived from Landsat Thematic Mapper is adequate for regional and national scale investigations while local scale investigations will require data sources of higher resolution (Vogelmann *et al*, 2001).

Some scientists have suggested attempts to map at the species level could be replaced by the remote inventorying of canopy structural measurements such as Leaf Area Index (LAI) (Wessman *et al*, 1998). Supplementary information such as LAI may indeed suffice for particular regional scale projects but metrics such as these should not be considered as replacements for species level land cover mapping as this level of mapping may yet be achievable at user acceptable accuracies. Species level vegetation mapping could be quite inferential as to the evolving state of an ecosystem (see chapter 5 in this dissertation, as well as citations by Walker *et al*, 1989; Hayden *et al*, 1995; Shao *et al*, 1998; Slater and Brown, 2000). Walker *et al* (1989) discussed the catena relationship of terrain, soils, and vegetation in an Alaskan scenario; Hayden *et al* (1995) addressed geomorphologic controls on vegetation that directly related to hydrogeochemical processes; Shao *et al* (1998) suggested

that shoreline adjustments and proportion, and relative location of woody vegetation are dynamically linked processes; and Slater and Brown used remote sensing derived vegetation changes to monitor ecological sensitivity areas in England. Chapter 5 of this dissertation also demonstrates that species level vegetation mapping is crucial for establishing ecological relationships between vegetation, soil properties and elevation. High spatial resolution imagery, or narrow spectral bandwidth imagery, or some combination therefore, will provide the and acceptable remote image source for species level discrimination and classification.

Spectral bandwidth and spatial pixel size were evaluated to see if one variable or the other was dominant in determining accuracy. For all final evaluations, the decision to remove results derived from the minimalist point and seed grow-2 training samples was based on their consistently dismal accuracy performance for all tests and the expectation that representation of true class variability was not achieved by these small training sets (Wang *et al*, 2001). Spectral bandwidth was a significant contributor to the accurate classification of cultural features and all landscape features combined, but it was not significant in the classification of natural features alone. With increasing spatial resolution and subsequent increasing spectral variability within classes (Hay *et al*, 1996; Aplin *et al*, 1997), it was anticipated that the narrower bandwidth spectral imagery (25nm) would outperform the wider bandwidth imagery (70nm) regardless of landscape feature type. Aplin *et al* (1997) explained that within-class variability that is too large may cause spectral overlap in landscape cover classes. The original null hypothesis (H_{o1}- accuracy results generated from landscape classifications derived from 70 and 25nm spectral bandwidth imagery would be equivalent) was accepted for natural landscape features. In comparing pairs of 1 and 4m

spatial imagery, this finding indicated that 25nm bandwidths were not small enough to change the within class spectral variability found from 70nm bandwidths. A review of the transformed divergence matrices for 25 and 70nm bandwidths imagery training sample data confirmed that there was little additional separability for the natural landscape classes attributable to narrowing the spectral resolution. Transformed divergence is a suggested test for the exploratory analysis of selecting appropriate image bands to maximize intra class variance (Phinn *et al*, 2000). A comparative test against imagery acquired with narrower bandwidths (10nm) currently available on hyperspectral sensors platforms could result in a review of this hypothesis.

Spatial pixel size accuracy results were at first surprising. Evaluation of imagery from airborne 1 and 4m spatial pixels was expected to reveal higher cultural feature accuracy from 1m data. However, the original null hypothesis (H_{o2}-accuracy results generated for 1 and 4m spatial pixel size imagery derived landscape classifications would be equivalent) was accepted for all and cultural landscape features, but rejected for natural features. The stratified random ground plot sampling design did not purposefully locate plots at cultural feature edges where the opportunity for finer evaluation in cultural feature accuracy might have been pursued. A re-evaluation of the spatial contribution of pixel size to cultural feature accuracy would warrant a collection of plots at edges near cultural feature edges. From a solely visual standpoint, the 1m imagery was superior to the 4m imagery in cultural information display, affirming comparative comments made by Dare and Fraser (2001) about 1 and 4m image data. Regarding the differences in accuracy of natural features attributable to pixel size differences, a clear and consistent separation of the overall accuracy scores was

evidenced with 4m data always outperforming the 1m data by an average of approximately 5

percent. This finding does support the predictions of Lillesand and Keifer (1994) and Aplin

et al (1997), and the implicit suggestion of Arnold *et al* (2000) that spatial resolution at too

fine a scale could actually impact the within class variability to a point where accuracy was

affected. The present IKONOS imagery with 4m multispectral spatial accuracy and a 1m

panchromatic band appears to have captured the preferred spatial dimensionality based on

these tests.

Phinn *et al* (2000) were also interested in optimizing spatial resolution, and suggested

minimizing class variance for all landscape cover classes. The spatial resolution range

recommended was between 240 and 480 meters, suggesting that certain land covers perform

better for particular spatial resolutions. Results from this paper agree with Phinn *et al*

(2000), where cultural and natural landscape features were separately evaluated and found to

respond differently to variable pixel size. Individual landscape features found within the

natural and cultural categories clearly responded differently to variable pixel size. This

information could prove useful in the future and is therefore recoverable within the

Appendices for accuracy assessments.

Imagery collected commercially combines spectral and spatial resolution. Imagery

users are given latitude only to choose the spectral–spatial resolution combination with which

they wish to work. Selection may come from either satellite or airborne imagery services.

The airborne multispectral sensing systems will probably be limited by cost to using

commercially available 25nm bandpass interference filters, or the more standard 70nm

bandpass filters. An inquiry by the author to vendors of bandpass filters revealed a cost-prohibitive increase in custom ground bandpass filters. Resolution at 1 and 4m is available now from airborne and satellite. Accordingly, the earlier null hypothesis (H_{03}-accuracy results generated for 70nm/4m, 70nm/1m, 25nm/4m, and 25nm/1m resolution imagery derived landscape classifications would be equivalent) represented a reasonable comparison of imagery choices for today's user of high-resolution imagery. With the elimination of the point and seed grow-2 training sample methods, there was an acceptance of the null hypothesis that cultural landscape feature classifications would be equivalent regardless of image combination, and a partial rejection of the hypothesis for image combination equivalency in class accuracy for all and natural landscape feature classifications. This rejection was the result of statistically significant differences for all and natural landscape features comparing 25nm/4m against 70nm/1m imagery.

How does this relate to image sensors available for today? IKONOS, used here as an example of a baseline high-resolution commercial satellite sensor, is generally a 70nm/4m (spectral) sensor. Bandwidths vary a little depending on image channel, but the 70nm width is a reasonable approximation. This combination of 70nm/4m was not statistically different from the 25nm/1m combination tested in this study. Increasing 1m panchromatic spatial accuracy with an HSI transform does visibly improve the product (Dare and Fischer, 2001) but it may not improve the landscape class accuracy. High-resolution 25nm/1m is representative of the sensing capability of airborne acquisition systems. In fact, resolution fidelity greater than 1m are easily obtained. However, an absence of any statistical differences in accuracy for the 1 and 4m spatial 25nm imagery raises a question about the

usefulness of 1m imagery for landscape class characterization at the Anderson II level. Four-meter spatial resolution guarantees fewer frames of imagery necessary to cover a study area and increases the possibility for coverage of a larger study area on the ground. For every single 4m ground detection spatial resolution pixel acquired, sixteen 1m pixels are needed for the higher resolution.

Several training sample methods were tested with regard to their impact on classification accuracy. The point and seed grow-2 were poor performers in all conditions. Sampling should be representative of the variability in the class (Magurran, 1988) and these training sample methods clearly under-represented class variability. Polygon training methods, if collected as advised by Jensen (1996), should attempt to capture the variability of the landscape to be classified. Significant environmental factors can control signature extension and Jensen (1996) recommends identification of these variables. This recommendation may not be easily achievable. There will always be subjectivity in the outlining of training sample class polygons as applied by different imagery analysts. Accuracy of landscape classifications depends critically on the size and quality of the training set and class clusters that overlap in spectral feature space will result in misleading classifications (Hubert-Moy *et al*, 2001). It follows then that an objective, replicable method of training sample selection would be preferred. This is precisely what the seed grow technique accomplishes using a predetermined starting point with known class (perhaps by field-based GPS classification). This technique allows the starting point "seed" to grow algorithmically out to a user defined euclidean distance. Only pixels that are statistically similar in multivariate feature space and within a user-defined distance threshold are included

in the final training sample. This technique was successful in this study and is recommended for follow-on work.

Conclusion

Four multi-spectral imagery combinations (25nm/1m, 25nm/4m, 70nm/1m, 70nm/4m), each image combination employing 6 distinct training sample methods for a total of 24 combinations, were processed with remote sensing software to compile 24 map classification products containing thirteen unique land cover landscape themes over a mixed land cover coastal study site. There were a total of 8 natural features (oak and American holly forest, mixed forest, loblolly forest, maintained grass, beach grass, ocean, sand, clay soil) and 5 cultural man-made features (asphalt, concrete, gray shingle roof building, brown shingle roof building, and shoreline rip rap). Each of the 24 map classifications were further sub-divided into 3 groups: a) all landscape features, b) natural landscape features, and c) cultural landscape features, in essence creating a new total of 72 landscape classifications. Accuracy of each of the 72 classifications was tested with field data, with scores for Kappa, users, producers, and overall accuracy reported.

Bandwidth, pixel size, both bandwidth and pixel size, and training sample methods were evaluated and compared for each of the three landscape segmented classification groups (all, natural, and cultural). In terms of spectral bandwidth performance, landscape classifications compiled from sensors with 70nm bandwidth image channels were outperformed by imagery from sensors with 25nm bandwidths. "All" and "cultural" landscape classification groups were statistically different for 70nm and 25nm accuracy

results; "Natural" landscape group showed equivalent accuracy results between 70 and 25nm bandwidth imagery. Pixel size influenced "natural" landscape feature classifications, where 4m pixel imagery generated classifications that were better and statistically different than the 1m pixel imagery. There was no statistical difference for cultural or all features. Analysis of combined bandwidth and pixel size showed that 25nm imagery with 4m spatial resolution received the highest Kappa scores for all features, natural features, and cultural features. Statistically, however, only classifications from image combination 25nm/4m and 70nm/1m were different for natural and cultural features (p-value = 0.04) and natural features (p-value = 0.02). Finally, training sample method selection did affect the classification accuracy for the studied imagery. Sample methods that selected the fewest pixels as training samples were the least effective. These ineffective methods were: point, seed grow-2, and seed grow-5 methods. Effective and statistically equivalent methods were: polygon, seed grow-15, and seed grow-25.

In all cases, 70nm bandwidth with 1m spatial resolution received the lowest Kappa scores representing classification accuracy. The 1m spatial pixels showed evidence of being too small. A 4m pixel contains the equivalent of sixteen 1m pixels and, accordingly, represents the average of the 16 reflectance values. The benefit of averaging pixels achieved by using the 4m pixels was especially evident for the classification of natural features.

Alternative imagery choices to the 25nm/4m imagery were statistically acceptable, but produced slightly lower overall accuracy scores. If all landscape themes incorporating both cultural and natural features were to be classified, a 70nm/4m image scene provided a

reasonable alternative data set. For natural landscape themes, the recommended alternative image combination was again 70nm/4m imagery. For cultural landscape theme classification, the recommended alternative image combination was 25nm/1m imagery. Training sample methods that failed to achieve comparably accurate classification results were approaches that minimized the number of sample pixels selected. Point, seed grow-2, and seed grow-5, were dismissed as unacceptable training sample methods; seed-15, seed-25, and heads-up polygon digitizing were each retained as acceptable solutions. The seed grow training sample method was the most objective and replicable.

In conclusion, results of this study have several implications for resource management.

- First, selection of an imagery source may directly affect the accuracy of any derived land cover classification maps. An understanding of the influence of both spectral and spatial resolution components of an image should assist a manager in selection of an image source.

- Second, the narrower bandwidths used in this study are presently available only from airborne multispectral imagery and not satellite multispectral imagery. Accurate classification of all (natural and cultural features) and cultural features alone was best achieved from the narrower 25nm narrower bandwidth imagery.

- Third, imagery with pixels that are 1m in size, or even smaller, may be too small for general land cover type mapping. Accuracy of 1m and 4m cover maps were statistically different for the classification of natural features, with 4m imagery returning higher

scores. Four-meter pixel imagery can be created from 1m pixel imagery by degrading the higher resolution down to a coarser resolution.

• Fourth, the joint contribution of spectral and spatial resolution was evaluated for four image combinations. The results of their respective landscape cover classifications were generally not statistically different at the 95% confidence level. There was a statistical difference between the 25nm/4m imagery and the 70nm/1m imagery in the classification accuracy of all natural and cultural features, and natural features alone. The 25nm/4m imagery consistently received the highest Kappa scores for all features, natural features, and cultural features.

• Fifth, generation of a cover classification map from an image source using supervised image processing techniques demands the creation of a training sample set. An effective number of training pixels were acquired using the seed grow-15, seed grow-25, and polygon techniques. Ineffective sampling methods were the point, seed grow-2 and seed grow-5 techniques.

• Lastly, training sample methods selected will result in varying classification accuracy. Transformed divergence scores provide immediate feedback on the training sample selection process and the ability to adequately separate landscape features into distinct classes. Imagery can be classified twice using different training sample methods, if necessary for features to be spectrally classed more effectively using an alternative method.

A mapping scenario of multi-scale remote sensing imagery resolution might assist in accurately classifying a variety of different landscape types. Coops and Waring (2001)

considered multi-resolution sources for evaluating forest growth capacity, with Thematic Mapper providing the high-resolution information and coarser resolution providing the regional scale coverage. At the higher resolutions of imagery (1 and 4m), it is equally possible that 1m data could be acquired as sample transects designed to supplement (and train) the complete study acquisition of the 4m imagery. A future recommendation is to compare high-resolution spectral-spatial imagery with coarser resolution imagery in the classification of species-level landscape mapping. Species delineation of grass from common reed has been demonstrated (Slocum *et al*, unpublished work) using 25nm/1m imagery but results were not compared from image sources such as SPOT or Landsat. While this present study has not suggested definitively that higher spectral and spatial resolution are necessary for broad category landscape cover mapping, it is anticipated that mapping of plant species-level classifications will benefit from the higher resolution imagery. Identification and classification of natural resources at a species level would increase scientific understanding of ecosystems and biodiversity. To manage an environment intelligently, one must know as much about that environment as possible. Narrow bandwidth, high spatial resolution imagery is a likely source for harnessing that intelligence.

References

Aplin, P., Atkinson, P.M., Curran, P.J., 1997. Fine spatial resolution satellite sensors for the next decade. *International Journal of Remote Sensing*, 18 (18): 3873-3881.

Arnold, C.L., Civco, D.L., Prisloe, M.P., Hurd, J.D., and Stocker, J.W., 2000. Remote sensing-enhanced outreach education as a decision support system for local land-use officials. *Photogrammetric Engineering & Remote Sensing*, 66 (10): 1251-1260.

Atkinson, P.M., Fody, G.M., Curran, P.J., and Boyd, D.S., 2000. Assessing the ground data requirements for regional scale remote sensing of tropical forest biophysical properties. *International Journal of Remote Sensing*, 21 (13&14):2571-2587.

Avery, T.E., and Berlin, G.L., 1992. Fundamentals of Remote Sensing and Airphoto Interpretation, 5th ed., Macmillan Publishing Company, New York.

Burgess, T.M., Webster, R. and McBratney, A.B., 1981. Optimal interpolation and isarithmic mapping of soil properties: sampling strategy. *Journal and Soil Science*, 35: 641-654.

Cihlar, J., Latifovic, R., Chen, J., Beaubien, J., and Li, Z., 2000. Selecting representative high resolution sample images for land cover studies. Part 1: Methodology, *Remote Sensing of Environment*, 71:26-42.

Cihlar, J., Latifovic,R., Chen, J., Beaubien, J., Li, Z., and Magnussen, S., 2000(a). Selecting representative high resolution sample images for land cover studies. Part 2: Application to estimating land cover composition. *Remote Sensing of Environment*, 72(2):127-138.

Civco, D.L., 1998. Software review- executive summary. *Photogrammetric Engineering & Remote Sensing*, 64 (9): 879-883.

Cohen, J., 1960. A coefficient of agreement of nominal scales. *Educational and Psychological Measurement* (20) 1:37-46.

Congalton, R.G., and Green, K., 1999. Assessing the Accuracy of Remotely Sensed Data: Principles and Practices, Lewis Publishers, Washington, D.C.

Cooke, R.U., and Doornkamp, J.C., 1990. Geomorphology in Environmental Management- A New Introduction, 2nd ed., Clarendon Press, Oxford.

Coops, N.C., and Waring, R.H., 2001. The use of multiscale remote sensing imagery to derive regional estimates of forest growth capacity using 3-PGS. *Remote Sensing of Environment*, 75 (3): 324-34.

ERDAS, Inc, 1999. ERDAS Imagine image processing software, Image Analysis Module.

Hayden, B., Dueser, R., Callahan, J., and Shugart, H., 1991. Long-term research at the

Virginia Coast Reserve. *Bioscience*, 41 (5): 310-318.

Hubert-Moy, L., Cotonnec, A., Le Du, L., Chardin, A., and Perez, P., 2001. A comparison of

parametric classification procedures of remotely sensed data applied on different

landscape units. *Remote Sensing of Environment*, 75 (2): 174-187.

Hudson, W. D. and Ramm, C.W., 1987. Correct formulation of the kappa coefficient of

agreement. *Photogrammetric Engineering and Remote Sensing*, (53) 4: 266-267.

Jensen, J.R., 1996. Introductory Digital Image Processing: A Remote Sensing Perspective,

2nd ed., Prentice Hall, Inc., New Jersey.

Landis, J., and Koch, G., 1977. The measurement of observer agreement for categorical data.

Biometrics, 33: 159-174.

Lillesand, T.M., and Keifer, R.W., 1994. Remote Sensing and Image Interpretation, 3rd ed.,

Chichester: John Wiley and Sons, Ltd.

Moore, L.J., 2000. Shoreline mapping techniques. *Journal of Coastal Research*, 16 (1):

111-124.

Phinn, S.R., Menges, C., Hill, G.J.E., and Stanford, M., 2000. Optimizing remotely sensed solution for monitoring, modeling, and managing coastal environments. *Remote Sensing of Environment*, 73(2):117-132.

Magurran, A.E., 1988. Chapter 3- Sampling. In Ecological Diversity and Its Measurement, Princeton University Press, New Jersey, 47-59.

Oliver, M.A., Webster, R., and Slocum, K., 2000. Filtering SPOT imagery by kriging analysis. *International Journal of Remote Sensing*, 21:735-752.

Skidmore, A.K., and Turner, B.J., 1988. Forest mapping accuracies are improved using supervised nonparametric classifier with SPOT data. *Photogrammetric Engineering and Remote Sensing*, 54: 1415-1421.

Slocum, K., Fischer, R., Campbell, M, and Wakefield, G., unpublished work. Spectral differentiation between *Spartina* grasses and common reed species in a barrier island site.

Slayter, J., and Brown, R., 2000. Changing landscapes: monitoring environmentally sensitive area using satellite imagery. *International Journal of Remote Sensing*, 21 (13&14): 2753-2767.

Space Imaging, Inc., 1996. Provider of IKONOS 4meter multispectral imagery.

Stat Soft, Inc., 1995. Statistica statistical software, General Linear Model.

Verbyla, D.L., 1995. Satellite Remote Sensing, Lewis Publishers, New York.

Vogelmann, J.E., Howard, S.M., Yang, L., Larson, C.R., Wylie, B.K., and van Driel, N.,

2001. Completion of the 1990s national land cover data set for the conterminous

United States from Landsat Thematic Mapper data and ancillary data sources.

Photogrammetric Engineering & Remote Sensing, 67 (6): 650-662.

Walker, E.P., Binnian, E., Evans, B.M., Lederer, N.D., Nordstrand, E., and Webber, P.J.,

1989. Terrain, vegetation, and landscape ecology of the R4D research site, Brooks

Range Foothills, Alaska. *Holarctic Ecology*, 12: 238-261.

Wang, G., Gertner, G., Xiangyun, X., Wente, S., and Anderson, A.B., 2001. Appropriate

plot size and spatial resolution for mapping multiple vegetation types.

Photogrammetric Engineering & Remote Sensing, 67 (5): 575-584.

Webster, R.,1985. Quantitative spatial analysis of soil in the field. *Advances in Soil Science*,

3: 1-70.

Webster, R., and Oliver, M.A., 2001. Geostatistics for Environmental Scientists, John Wiley

and Sons, New York.

Wessman, C.A., Cramer, W., Gurney, R.J., Martin, P.H., Mauser, W., Nemani, R., Paruelo, J.M., Penuelas, J., Prince, S.D., Running, S.W., and Waring, R.H., 1998. Chapter 5-Group report: remote sensing perspectives and insights for study of complex landscapes. In <u>Integrating Hydrology, Ecosystem Dynamics, and Biogeochemistry in Complex Landscapes</u>, edited by J.D. Tenhunen and P. Kabat, John Wiley and Sons, New York, 89-103.

Wheatley, J.M., Wilson, J.P., Redmond, R.L., Zhenkui, M., DiBenedetto, J., 2000. Chapter 15-Automated land cover mapping using Landsat Thematic Mapper images and topographic attributes. In <u>Terrain Analysis- Principles and Applications</u>, edited J.P. Wilson and J.C. Gallant, John Wiley and Sons, Inc., New York, 245-266.

Yang, L., Stehman, S.V., Smith, J.H., Wickman, J.D., 2001. Thematic accuracy of MLRC land cover over the eastern United States. *Remote Sensing of Environment*, 76 (3): 418-422.

Table 1. Within-class variability that is too large may cause spectral overlap in landscape cover classes. Variability may be the result of pixel size, spectral bandwidth, or both. Transformed divergence scores ("Divergence Score") less than or equal to 1950 for any classification cover pair ("Cover Pair") are identified for each spectral – spatial imagery combination ("Image Combination"). All other pairs have a score between 1951 and 2000.

Image Combination	Cover Pair	Divergence Score
25nm/1m	Sand / Concrete	1825
25nm/1m	Large stone asphalt / ocean	1934
25nm/1m	Grey shingle roof / concrete	1861
25nm/1m	Loblolly pine / hardwood forest	316
25nm/1m	Loblolly pine / unmaintained grass	1927
25nm/1m	Hardwood forest / unmaintained grass	1945
25nm/4m	Loblolly pine / hardwood forest	465
70nm/1m	Loblolly pine / hardwood forest	347
70nm/1m	Loblolly pine / unmaintained grass	1782
70nm/1m	Hardwood forest / unmaintained grass	1931
70nm/4m	Loblolly pine / hardwood forest	619
70nm/4m	Loblolly pine / unmaintained grass	1942

Table 2a. Kappa scores, grouped by spectral bandwidths 25 and 70nm, reported for classification accuracy of natural AND cultural features. Kappa scores from the 25nm imagery indicate greater accuracy. "Pairwise comparison to top score" results represent a statistical comparison of Kappa scores from each "Spectral Combination" compared to the Top Score. This comparison determines if scores are significantly similar with the Top score at the 95% confidence level. Scores that are statistically similar (between 0.00 and 1.96) are marked by a double asterisk (**). The top 25nm result (25-4-seed15) compared to the top 70nm result (70-4-seed25) showed no statistical difference. All remaining 70nm combinations were statistically different from the best 25 nm outcome. Spectral combination variables represent bandwidth in nanometers-pixel size in meters- and training sample methodology.

Natural and Cultural Features

Spectral Combination	Kappa Score	Pairwise comparison to the top score
25-4-seed15	0.57	Top score
25-4-polygon	0.57	0.00**
25-4-seed25	0.56	0.29**
25-1-polygon	0.52	1.44**
25-1-seed25	0.52	1.44**
25-1-seed15	0.5	2.02
25-1-seed5	0.47	2.89
25-4-seed5	0.44	3.75
25-1-seed2	0.42	4.33
25-4-seed2	0.38	5.73
25-4-point	0.32	7.54
25-1-point	0.30	8.14
70-4-seed25	0.55	0.58**
70-4-polygon	0.49	2.31
70-4-seed15	0.49	2.31
70-1-polygon	0.47	2.89
70-1-seed15	0.47	2.89
70-1-seed25	0.45	3.46
70-4-seed5	0.42	4.52
70-1-seed5	0.39	5.43
70-4-seed2	0.36	6.33
70-1-seed2	0.35	6.63
70-4-point	0.29	8.44
70-1-point	0.27	9.05

Table 2b. Kappa scores, grouped by spectral bandwidths 25 and 70nm, reported for classification accuracy of "natural" features. "Pairwise comparison to top score" results represent a statistical comparison of Kappa scores from each "Spectral Combination" compared to the Top Score. This comparison determines if scores are significantly similar with the Top score at the 95% confidence level. Scores that are statistically similar (between 0.00 and 1.96) are marked by a double asterisk (**). There are no statistical differences with any of the "Spectral combinations" as reported by these Kappa results. Spectral combinations are grouped by narrow 25nm bandwidth and wider 70nm bandwidths. Spectral combination variables represent bandwidth in nanometers-pixel size in meters- and training sample methodology.

Natural Features

Spectral Combination	Kappa Score	Pairwise comparison to top score
25-4-seed2	0.40	Top Score
25-4-seed25	0.40	Top Score
25-4-polygon	0.39	0.24**
25-4-seed15	0.39	0.24**
70-4-polygon	0.39	0.24**
70-4-seed15	0.39	0.24**
70-4-seed25	0.39	0.24**
25-4-point	0.38	0.49**
25-4-seed5	0.38	0.47**
70-4-seed2	0.38	0.50**
70-4-seed5	0.37	0.73**
70-4-point	0.35	1.21**
70-1-point	0.40	0.00**
70-1-polygon	0.40	0.00**
70-1-seed2	0.40	0.00**
25-1-polygon	0.39	0.24**
25-1-seed15	0.39	0.24**
25-1-seed25	0.39	0.24**
70-1-seed25	0.39	0.24**
70-1-seed5	0.39	0.24**
25-1-seed2	0.38	0.47**
25-1-seed5	0.38	0.49**
70-1-seed15	0.38	0.47**
25-1-point	0.37	0.73**

Table 2c. Kappa scores, grouped by spectral bandwidths 25 and 70nm, reported for classification accuracy of "cultural" features. "Pairwise comparison to top score" results represent a statistical comparison of Kappa scores from each "Spectral Combination" compared to the Top Score. This comparison determines if scores are significantly similar with the Top score at the 95% confidence level. Scores that are statistically similar (between 0.00 and 1.96) are marked by a double asterisk (**). The spectral results suggest the 25nm imagery provides greater classification accuracy. The top 25nm result (25-4-polygon) is statistically similar to the top three 70nm result but different from the remaining nine combinations of 70nm images. The narrower 25nm bandwidth provided seven possible image combination/training sample solutions that were equally effective. Spectral combination variables represent bandwidth in nanometers-pixel size in meters- and training sample methodology.

Cultural Features

Spectral combination	Kappa Score	Pairwise comparison to top score
25-4-polygon	0.77	Top score
25-4-seed15	0.76	0.13**
25-4-seed25	0.72	0.60**
25-1-seed25	0.71	0.72**
25-1-polygon	0.68	1.16**
25-1-seed5	0.64	1.58**
25-1-seed15	0.63	1.67**
25-4-seed5	0.44	3.69
25-4-seed2	0.4	4.52
25-1-seed2	0.36	5.38
25-1-point	0.3	6.65
25-4-point	0.27	7.07
70-4-seed15	0.70	0.84**
70-1-seed15	0.63	1.67**
70-4-seed25	0.61	1.91**
70-4-polygon	0.51	2.90
70-1-seed5	0.49	3.35
70-1-seed25	0.48	3.24
70-1-polygon	0.46	5.24
70-4-seed2	0.33	5.83
70-4-seed5	0.32	6.07
70-1-seed2	0.32	5.46
70-1-point	0.25	6.67
70-4-point	0.17	10.60

Table 3. Overall accuracy assessment results, grouped by spectral bandwidths 25 and 70nm, reported for classification accuracy of natural and cultural, natural, and cultural features. Training Sample Method variables represent pixel size in meters- and training sample method.

Training Sample Method	Natural and Cultural		Natural		Cultural	
	25nm	70nm	25nm	70nm	25nm	70nm
1m/point	37.70	35.00	45.40	36.40	44.00	50.00
1m/polygon	57.60	52.60	59.70	57.30	77.90	64.40
1m/seed15	55.83	52.96	58.73	55.17	73.68	75.00
1m/seed2	48.76	41.87	54.67	45.07	52.08	53.76
1m/seed25	57.74	51.05	58.68	54.88	80.61	65.56
1m/seed5	53.35	45.32	54.62	47.45	75.00	64.52
4m/point	39.20	37.70	45.30	47.90	46.00	27.60
4m/polygon	61.80	54.50	64.00	62.00	84.40	63.40
4m/seed15	61.95	55.64	65.36	58.82	84.88	80.26
4m/seed2	44.83	43.40	49.33	50.13	55.56	45.56
4m/seed25	60.54	60.42	63.35	64.92	81.32	74.73
4m/seed5	50.86	48.95	58.01	58.18	63.22	43.33

Table 4. Analysis of variance (ANOVA) results, comparing overall classification accuracy scores grouped by spectral bandwidths 25- and 70nm (found in Table 3), reported for natural AND cultural, natural and cultural features. A 95% confidence interval was used to compute the F-critical value. F-statistics less than the F-critical value, or p-values greater than 0.05, were not significantly different, suggesting bandwidth did not make a statistical difference. Statistical differences in overall accuracy scores were observed for both natural and cultural features and cultural features after the point and seed-grow-2 training sample methods were removed from the sample testing. These statistically significant values are marked by double asterisks (**). Degrees of freedom are noted by d.f.

Features Classified	F-statistic	F-critical	p-value	d.f.
NATURAL and CULTURAL	1.65	4.3	0.21	23
NATURAL	1.13	4.3	0.3	23
CULTURAL	2.17	4.3	0.15	23
Minus "point" and "seed grow 2"				
NATURAL AND CUTURAL	5.03**	4.6	0.042**	15
NATURAL	1.75	4.6	0.21	15
CULTURAL	5.71**	4.6	0.031**	15

Table 5a. Kappa scores, grouped by *spatial* pixel sizes 1m and 4m, as reported for classification accuracy of natural and cultural features. "Pairwise comparison to top score" results represent a statistical comparison of Kappa scores from each "Spatial Combination" compared to the Top Score. This comparison determines if scores are significantly similar with the Top score at the 95% confidence level. Scores that are statistically similar (between 0.00 and 1.96) are marked by a double asterisk (**). The top Kappa score is from a 4m spatial image (25nm/4m-seed15). There is no statistical difference with the top two finishing 1m imagery, as indicated by a test statistic of 1.44, but all others are different. Kappa results suggest that the 4m spatial imagery did a better job at classification of "all" features over the Fort Story study area. Spatial combinations variables represent bandwidth in nanometers- pixel size in meters- and training sample methodology.

Natural and Cultural

Spatial Combination	Kappa Score	Pairwise comparison to top score
25-4-seed15	0.57	Top Score
25-4-polygon	0.57	Top Score
25-4-seed25	0.56	0.29**
70-4-seed25	0.55	0.58**
70-4-polygon	0.49	2.31
70-4-seed15	0.49	2.31
25-4-seed5	0.44	3.75
70-4-seed5	0.42	4.52
25-4-seed2	0.38	5.73
70-4-seed2	0.36	6.33
25-4-point	0.32	7.54
70-4-point	0.29	8.44
25-1-polygon	0.52	1.44**
25-1-seed25	0.52	1.44**
25-1-seed15	0.5	2.02
25-1-seed5	0.47	2.89
70-1-polygon	0.47	2.89
70-1-seed15	0.47	2.89
70-1-seed25	0.45	3.46
25-1-seed2	0.42	4.33
70-1-seed5	0.39	5.43
70-1-seed2	0.35	6.63
25-1-point	0.30	8.14
70-1-point	0.27	9.05

Table 5b. Kappa scores, grouped by *spatial* pixel sizes 1m and 4m, as reported for classification accuracy of natural features. "Pairwise comparison to top score" results represent a statistical comparison of Kappa scores from each "Spatial Combination" compared to the Top Score. This comparison determines if scores are significantly similar with the Top score at the 95% confidence level. Scores that are statistically similar (between 0.00 and 1.96) are marked by a double asterisk (**). The top Kappa scores are from 4m and 1m spatial images. There is no statistical difference with any of the possible spatial combinations of imagery as reported by these Kappa results. Spatial combinations variables represent bandwidth in nanometers-pixel size in meters- and training sample methodology.

Natural Features

Spatial Combination	Kappa	Pairwise comparison to top score
25-4-seed2	0.40	Top Score
25-4-seed25	0.40	Top Score
25-4-polygon	0.39	0.24**
25-4-seed15	0.39	0.24**
70-4-polygon	0.39	0.24**
70-4-seed15	0.39	0.24**
70-4-seed25	0.39	0.24**
25-4-point	0.38	0.49**
25-4-seed5	0.38	0.47**
70-4-seed2	0.38	0.50**
70-4-seed5	0.37	0.73**
70-4-point	0.35	1.21**
70-1-point	0.40	Top Score
70-1-polygon	0.40	Top Score
70-1-seed2	0.40	Top Score
25-1-polygon	0.39	0.24**
25-1-seed15	0.39	0.24**
25-1-seed25	0.39	0.24**
70-1-seed25	0.39	0.24**
70-1-seed5	0.39	0.24**
25-1-seed2	0.38	0.47**
25-1-seed5	0.38	0.49**
70-1-seed15	0.38	0.47**
25-1-point	0.37	0.73**

Table 5c. Kappa scores, grouped by *spatial* pixel sizes 1m and 4m, as reported for classification accuracy of "cultural" features. "Pairwise comparison to top score" results represent a statistical comparison of Kappa scores from each "Spatial Combination" compared to the Top Score. This comparison determines if scores are significantly similar with the Top score at the 95% confidence level. Scores that are statistically similar (between 0.00 and 1.96) are marked by a double asterisk (**). The top Kappa scores is from a 4m spatial image (25nm/4m-polygon training sample method). There is no statistical difference with the top five finishing 1m imagery as indicated by a test statistic of 1.67. The top four finishing 4m imagery are all statistically similar (test statistics 0.00 to 0.84 with 1.96 as the defining critical threshold). Kappa results suggest that the 4m spatial imagery did a better job at classification of "natural" features over the Fort Story study area. Spatial combinations variables represent bandwidth in nanometers-pixel size in meters- and training sample methodology.

Cultural Features

Spatial combination	Kappa	Pairwise comparison to top score
25-4-polygon	0.77	Top Score
25-4-seed15	0.76	0.13**
25-4-seed25	0.72	0.60**
70-4-seed15	0.70	0.84**
70-4-seed25	0.61	1.91
70-4-polygon	0.51	2.91
25-4-seed5	0.44	3.69
25-4-seed2	0.40	4.52
70-4-seed2	0.33	5.83
70-4-seed5	0.32	6.07
25-4-point	0.27	7.07
70-4-point	0.17	10.61
25-1-seed25	0.71	0.72**
25-1-polygon	0.68	1.16**
25-1-seed5	0.64	1.59**
25-1-seed15	0.63	1.67**
70-1-seed15	0.63	1.67**
70-1-seed5	0.49	3.35
70-1-seed25	0.48	3.24
70-1-polygon	0.46	5.24
25-1-seed2	0.36	5.38
70-1-seed2	0.32	5.46
25-1-point	0.30	6.65
70-1-point	0.25	6.71

Table 6. Overall accuracy assessment results, grouped by *spatial* pixel sizes 1m and 4m, as reported for natural and cultural, natural, and cultural features.

Training Sample Method	Natural and Cultural		Natural		Cultural	
	1m	4m	1m	4m	1m	4m
25nm/point	37.70	39.20	45.4	45.3	44.0	46.0
25nm/polygon	57.60	61.80	59.7	64.0	77.9	84.4
25nm/seed15	55.83	61.95	58.73	65.36	73.68	84.88
25nm/seed2	48.76	44.83	54.67	49.33	52.08	55.56
25nm/seed25	57.74	60.54	58.68	63.35	80.61	81.32
25nm/seed5	53.35	50.86	54.62	58.01	75	63.22
70nm/point	35.00	37.70	36.4	47.9	50.0	27.6
70nm/polygon	52.60	54.50	57.3	62.0	64.4	63.4
70nm/seed15	52.96	55.64	55.17	58.82	75	80.26
70nm/seed2	41.87	43.40	45.07	50.13	53.76	45.56
70nm/seed25	51.05	60.42	54.88	64.92	65.56	74.73

Table 7. Analysis of variance (ANOVA) results, comparing overall accuracy scores grouped by spatial pixel sizes 1- and 4m (found in Table 6), reported for classification of natural and cultural, natural and cultural features. A 95% confidence interval was used to compute the F-critical value. F-statistics less than the F-critical value, or p-values greater than 0.05, were not significantly different, suggesting pixel size did not make a statistical difference. Statistical differences in overall accuracy scores were observed for natural features after the point and seed-grow-2 training sample methods were removed from the sample testing. Statistically significant values are noted by double asterisks (**). Degrees of freedom are noted by d.f.

Features Classified	F-stat	F-critical	p-value	d.f.
Natural and Cultural	0.55	4.3	0.47	23
NATURAL	2.82	4.3	0.11	23
CULTURAL	0.11	4.3	0.74	23
Minus "point" and "seed grow 2" training methods				
Natural and Cultural	2.35	4.6	0.15	15
NATURAL	11.73**	4.6	0.004**	15
CULTURAL	0.0006	4.6	0.98	15

Table 8a. Kappa scores, grouped by spectral - spatial combination, reported for classification accuracy of natural and cultural features. "Pairwise comparison to top score" results represent a statistical comparison of Kappa scores from each "Spatial Combination" compared to the Top Score. This comparison determines if scores are significantly similar with the Top score at the 95% confidence level. Scores that are statistically similar (between 0.00 and 1.96) are marked by a double asterisk (**). Spectral – spatial combination variables identify the sample image bandwidth (25nm or 70nm), pixel size (1m or 4m), and training samples method. The top Kappa scores are from 25nm/4m- seed15 and 25nm/4m-polygon imagery. No scores from 70nm/1m imagery are statistically close to these scores. Spectral - spatial combination variables represent bandwidth in nanometers-pixel size in meters- and training sample methodology.

Natural and Cultural Features

Spectral - Spatial Combination	Kappa Score	Pairwise comparison to top score
25-1-seed25	0.52	1.44**
25-1-polygon	0.52	1.44**
25-1-seed15	0.5	2.02
25-1-seed5	0.47	2.89
25-1-seed2	0.42	4.33
25-1-point	0.30	8.14
25-4-seed15	0.57	Top Score
25-4-polygon	0.57	Top Score
25-4-seed25	0.56	0.29*
25-4-seed5	0.44	3.75
25-4-seed2	0.38	5.73
25-4-point	0.32	7.54
70-1-seed15	0.47	2.89
70-1-polygon	0.47	2.89
70-1-seed25	0.45	3.46
70-1-seed5	0.39	5.43
70-1-seed2	0.35	6.63
70-1-point	0.27	9.05
70-4-seed25	0.55	0.58**
70-4-seed15	0.49	2.31
70-4-polygon	0.49	2.31
70-4-seed5	0.42	4.52
70-4-seed2	0.36	6.33
70-4-point	0.29	8.44

Table 8b. Kappa scores, grouped by spectral - spatial combination, reported for "natural" features. "Pairwise comparison to top score" results represent a statistical comparison of Kappa scores from each "Spatial Combination" compared to the Top Score. This comparison determines if scores are significantly similar with the Top score at the 95% confidence level. Scores that are statistically similar (between 0.00 and 1.96) are marked by a double asterisk (**). There is no statistical difference with any spectra-spatial-training sample combination as reported by these Kappa results. Top scores, although not by much, come from the 25nm/4m and 70nm/4 imagery combinations. Spectral - spatial combination variables represent bandwidth in nanometers-pixel size in meters- and training sample methodology.

Natural Features

Spectral - Spatial Combination	Kappa Score	Pairwise comparison to top score
25-1-point	0.37	0.73**
25-1-polygon	0.39	0.24**
25-1-seed15	0.39	0.24**
25-1-seed2	0.38	0.47**
25-1-seed25	0.39	0.24**
25-1-seed5	0.38	0.49**
25-4-point	0.38	0.49**
25-4-polygon	0.39	0.24**
25-4-seed15	0.39	0.24**
25-4-seed2	0.40	Top Score
25-4-seed25	0.40	Top Score
25-4-seed5	0.38	0.47**
70-1-point	0.40	Top Score
70-1-polygon	0.40	Top Score
70-1-seed15	0.38	0.47**
70-1-seed2	0.40	Top Score
70-1-seed25	0.39	0.24**
70-1-seed5	0.39	0.24**
70-4-point	0.35	1.21**
70-4-polygon	0.39	0.24**
70-4-seed15	0.39	0.24**
70-4-seed2	0.38	0.50**
70-4-seed25	0.39	0.24**
70-4-seed5	0.37	0.73**

Table 8c. Kappa score results, grouped by spectral - spatial combination, as reported for "cultural" features. "Pairwise comparison to top score" results represent a statistical comparison of Kappa scores from each "Spatial Combination" compared to the Top Score. This comparison determines if scores are significantly similar with the Top score at the 95% confidence level. Scores that are statistically similar (between 0.00 and 1.96) are marked by a double asterisk (**). The top Kappa score is from the 25nm-4m-polygon imagery. Each spectral – spatial combination has at least one training sample method combination that is statistically equivalent to the top score. The 25nm/1m combination reported 4 scores that were statistically equivalent although each of these scores is lower than the top three 25nm/4m scores. Spectral - spatial combination variables represent bandwidth in nanometers, pixel size in meters, and training sample methodology.

Cultural Features

Spectral – Spatial combination	Kappa Score	Pairwise comparison to top score
25-1-seed25	0.71	0.72**
25-1-polygon	0.68	1.16**
25-1-seed5	0.64	1.59**
25-1-seed15	0.63	1.67**
25-1-seed2	0.36	5.38
25-1-point	0.3	6.65
25-4-polygon	0.77	Top Score
25-4-seed15	0.76	0.13**
25-4-seed25	0.72	0.60**
25-4-seed5	0.44	3.69
25-4-seed2	0.4	4.52
25-4-point	0.27	7.07
70-1-seed15	0.63	1.67**
70-1-seed5	0.49	3.35
70-1-seed25	0.48	3.24
70-1-polygon	0.46	5.24
70-1-seed2	0.32	5.46
70-1-point	0.25	6.71
70-4-seed15	0.70	0.84**
70-4-seed25	0.61	1.91
70-4-polygon	0.51	2.91
70-4-seed2	0.33	5.83
70-4-seed5	0.32	6.07
70-4-point	0.17	10.61

Tables 9a-c. Overall accuracy assessment scores, grouped by spectral – spatial image combination, as reported for (a) natural and cultural features, (b) natural features, and (c) cultural features.

(9a) Natural and cultural features

Training Sample Method	25nm/1m	25nm/4m	70nm/1m	70nm/4m
Point	37.70	39.20	35.00	37.70
Polygon	57.60	61.80	52.60	54.50
Seed-15	55.83	61.95	52.96	55.64
Seed-2	48.76	44.83	41.87	43.40
Seed-25	57.74	60.54	51.05	60.42
Seed-5	53.35	50.86	45.32	48.95

(9b) Natural features

Training Sample Method	25nm/1m	25nm/4m	70nm/1m	70nm/4m
Point	45.40	45.30	36.40	47.90
Polygon	59.70	64.00	57.30	62.00
Seed-15	58.73	65.36	55.17	58.82
Seed-2	54.67	49.33	45.07	50.13
Seed-25	58.68	63.35	54.88	64.92
Seed-5	54.62	58.01	47.45	58.18

(9c) Cultural features

Training Sample Method	25nm/1m	25nm/4m	70nm/1m	70nm/4m
Point	44.00	46.00	50.00	27.60
Polygon	77.90	84.40	64.40	63.40
Seed-15	73.68	84.88	75.00	80.26
Seed-2	52.08	55.56	53.76	45.56
Seed-25	80.61	81.32	65.56	74.73
Seed-5	75.00	63.22	64.52	43.33

Table 10. Analysis of variance (ANOVA) results, comparing overall accuracy scores, grouped by a spectral and spatial combination (found in Table 9a-c), reported for classification of natural and cultural, natural and cultural features. A 95% confidence interval was used to compute the F-critical value. F-statistics less than the F-critical value, or p-values greater than 0.05, were not significantly different, suggesting pixel size did not make a statistical difference. Statistical differences in overall accuracy scores were observed for natural and cultural, and natural features, after the point and seed-grow-2 training sample methods were removed from the sample testing. These statistically significant values are marked by double asterisks (**). The differences were between image combination 25nm/4m and 70nm/1m in both cases. Degrees of freedom are denoted by d.f.

Feature Classified	Combination	F-stat	F-critical	p-value	d.f.
Natural and Cultural	25nm/4m & 70nm/1m	1.86	4.96	0.20	11
NATURAL	25nm/4m & 70nm/1m	2.99	4.96	0.11	11
CULTURAL	25nm/4m & 70nm/4m	1.56	4.96	0.24	11
Minus "point" and "seed grow 2 training					
Natural and Cultural	25nm/4m & 70nm/1m	6.75**	5.99	0.04**	7
Natural and Cultural	25nm/4m & 70nm/4m	1.21	5.99	0.31	7
Natural and Cultural	25nm/4m & 25nm/1m	0.87	5.99	0.39	7
NATURAL	25nm/4m & 70nm/1m	11.15**	5.99	0.02**	7
NATURAL	25nm/4m & 70nm/4m	0.58	5.99	0.48	7
NATURAL	25nm/4m & 25nm/1m	5.82	5.99	0.05	7
CULTURAL	25nm/4m & 70nm/1m	3.73	5.99	0.10	7
CULTURAL	25nm/4m & 70nm/4m	1.82	5.99	0.22	7
CULTURAL	25nm/4m & 25nm/1m	0.10	5.99	0.77	7

Table 11. Summary of overall Kappa ranking, grouped by spectral – spatial combination, reported for natural and cultural, natural, and cultural features. The place order (first, second, third, or fourth) was determined by rank ordering all Kappa scores and assigning a rank of 1 to the highest Kappa score and 24 to the lowest Kappa score. Lowest cumulative total within each spectral – spatial combination determined the placement (first, second, third, or fourth place). The best training sample finish for each spectral- spatial combination is also reported as "top position" and is supporting evidence to the place ordering finishes. Combination 25nm/4m was consistently first in place and position for all possible feature classifications. Conversely, combination 70nm/1m was consistently last for all "place" finishes.

Spectral – Spatial Combination	Natural & cultural features	Natural & cultural features	Natural features	Natural features	Cultural features	Cultural features	Overall Performance
	Place	Top Position	Place	Top Position	Place	Top Position	
25nm/1m	3rd	5th	3rd	6th	2nd	4th	
25nm/4m	1st	1st	1st	1st	1st	1st	BEST
70nm/1m	4th	11th	4th	12th	4th	8th	WORST
70nm/4m	2nd	4th	2nd	2nd	3rd	5th	

Table 12a- Kappa scores for 6 types of training sample methods are presented. These scores were computed from a classification of both natural and cultural features. "Kappa Z-score to top score" results represent a statistical pairwise comparison of Kappa scores from each training sample method to the Top Score(s). This comparison determines if the scores are significantly similar at the 95% confidence level. Scores that are statistically similar (between 0.00 and 1.96 in the Kappa Z-score-to-top-score) are marked by a double asterisk (**). Scores marked with asterisks were attained from training sample methods that would provide the most accuracte classification(s) from the particular image combination selected (25nm/1m, 25nm/4m, 70nm/1m, and 70nm/4m).

Natural and Cultural Features

Training Sample Method	Kappa Score 25nm 1m	Pair-wise to top score	Kappa Score 25nm 4m	Pair - wise to top score	Kappa Score 70nm 1m	Pair-wise to top score	Kappa Score 70nm 4m	Pair-wise to top score
Polygon Method	0.52**	1.44	0.57**	Top Score	0.47	2.89	0.49	2.31
Seed Grow-25 Method	0.52**	1.44	0.56**	0.29	0.45	3.46	0.55**	0.58
Seed Grow-15 Method	0.50	2.02	0.57**	Top Score	0.47	2.89	0.49	2.31
Seed Grow-5 Method	0.47	2.89	0.44	3.75	0.39	5.43	0.42	4.52
Seed Grow-2 Method	0.42	4.33	0.38	5.73	0.35	6.63	0.36	6.33
Point Method	0.30	8.14	0.32	7.54	0.27	9.05	0.29	8.44

Table 12b- Kappa scores for 6 types of training sample methods are presented. These scores were computed from a classification of natural features. "Kappa Z-score to top score" results represent a statistical pairwise comparison of Kappa scores from each training sample method to the Top Score(s). This comparison determines if the scores are significantly similar at the 95% confidence level. Scores that are statistically similar (between 0.00 and 1.96 in the Pairwise-to-top-score) are marked by a double asterisk (**). Scores marked with asterisks were attained from training sample methods that would provide the most accurate classification(s) from the particular image combination selected (25nm/1m, 25nm/4m, 70nm/1m, and 70nm/4m).

Natural Features

Training Sample Method	Kappa Score 25nm 1m	Pair-wise to top score	Kappa Score 25nm 4m	Pair-wise to top score	Kappa Score 70nm 1m	Pair-wise to top score	Kappa Score 70nm 4m	Pair-wise to top score
Polygon Method	0.39**	0.24	0.39**	0.24	0.40**	Top Score	0.39**	0.24
Seed Grow-25 Method	0.39**	0.24	0.40**	Top Score	0.39**	0.24	0.39**	0.24
Seed Grow-15 Method	0.39**	0.24	0.39**	0.24	0.38**	0.47	0.39**	0.24
Seed Grow-5 Method	0.38**	0.47	0.38**	0.47	0.39**	0.24	0.37**	0.70
Seed Grow-2 Method	0.38**	0.47	0.40**	Top Score	0.40**	Top Score	0.38**	0.47
Point Method	0.37**	0.70	0.38**	0.47	0.40**	Top Score	0.35**	1.18

Table 12c- Kappa scores for 6 types of training sample methods are presented. These scores were computed from a classification of cultural features. "Kappa Z-score to top score" results represent a statistical pairwise comparison of Kappa scores from each training sample method to the Top Score(s). This comparison determines if the scores are significantly similar at the 95% confidence level. Scores that are statistically similar (between 0.00 and 1.96 in the Pairwise-to-top-score) are marked by a double asterisk (**). Scores marked with asterisks were attained from training sample methods that would provide the most accurate classification(s) from the particular image combination selected (25nm/1m, 25nm/4m, 70nm/1m, and 70nm/4m).

Cultural Features

Training Sample Method	Kappa Score 25nm 1m	Pair-wise to top score	Kappa Score 25nm 4m	Pair-wise to top score	Kappa Score 70nm 1m	Pair-wise to top score	Kappa Score 70nm 4m	Pair-wise to top score
Polygon Method	0.68**	1.03	0.76**	Top Score	0.46	5.07	0.51	2.80
Seed Grow-25 Method	0.71**	0.60	0.72**	0.48	0.48	3.13	0.61**	1.79
Seed Grow-15 Method	0.63**	1.55	0.76**	Top Score	0.63**	1.55	0.70**	0.72
Seed Grow-5 Method	0.64**	1.47	0.44	3.58	0.49	3.23	0.32	5.93
Seed Grow-2 Method	0.36	5.25	0.40	4.40	0.32	5.34	0.33	5.70
Point Method	0.30	6.51	0.27	6.93	0.25	6.58	0.17	10.43

Table 13a. Overall accuracy scores grouped by six training sample methods, reported for the classification of natural and cultural features.

Natural and Cultural Features

Spectral – Spatial Combination	Polygon	Seed Grow-25	Seed Grow-15	Seed Grow-5	Seed Grow-2	Point
25/1	57.60	57.74	61.95	53.35	48.76	37.70
25/4	61.80	60.54	55.83	50.86	44.83	39.20
70/1	52.60	51.05	52.96	45.32	41.87	35.00
70/4	54.50	60.42	55.64	48.95	43.40	37.70

Table 13b. Analysis of variance (ANOVA) of overall accuracy scores, grouped by training sample methods, as determined from the classification of natural and cultural features (found in Table 13a). A 95% confidence interval was used to compute the F-critical value. F-statistics less than the F-critical value, or p-values greater than 0.05, were not significantly different, suggesting pixel size did not make a statistical difference. Statistical differences in overall accuracy scores were observed between seed grow 5, seed grow 2 and point training sample methods and training sample methods: polygon, seed grow 25, and seed grow 15. All statistically significant values are noted in the table below. Degrees of freedom are denoted by d.f.

Natural and Cultural Features

Training Sample Pair ANOVA	F-Stat	p-Value	d.f.
Polygon and Point	78.89	0.0001	1,6
Polygon and Seed Grow-2	23.02	0.003	1,6
Polygon and Seed Grow-5	7.62	0.0328	1,6
Seed Grow-25 and Point	32.95	0.0012	1,6
Seed Grow-25 and Seed Grow-2	13.45	0.0105	1,6
Seed Grow-25 and Seed Grow-5	6.58	0.0426	1,6
Seed Grow-15 and Point	85.39	0.0000	1,6
Seed Grow-15 and Seed Grow-2	24.33	0.0026	1,6
Seed Grow-15 and Seed Grow-5	7.86	0.0310	1,6

Table 14a. Overall accuracy scores grouped by six training sample methods, reported for the classification of natural features.

Natural Features

Spectral – Spatial Combination	Polygon	Seed Grow-25	Seed Grow-15	Seed Grow-5	Seed Grow-2	Point
25/1	59.70	58.68	58.73	54.62	54.67	45.40
25/4	64.00	63.35	65.36	58.01	49.33	45.30
70/1	57.30	54.88	55.17	47.45	45.07	36.40
70/4	64.92	62.00	58.82	58.18	50.13	47.90

Table 14b. Analysis of variance (ANOVA) of overall accuracy scores, grouped by training sample methods, as determined from the classification of natural features (found in Table 14a). A 95% confidence interval was used to compute the F-critical value. F-statistics less than the F-critical value, or p-values greater than 0.05, were not significantly different, suggesting pixel size did not make a statistical difference. Statistical differences in overall accuracy scores were observed between seed grow 2 and point training sample methods and training sample methods: polygon, seed grow 25, and seed grow 15. All statistically significant values are noted in the table below. Degrees of freedom are denoted by d.f.

Natural Features

Training Sample Pair ANOVA	F-Stat	p-Value	d.f.
Polygon and Point	32.75	0.0047	1,6
Polygon and Seed Grow-2	19.20	0.0012	1,6
Seed Grow-25 and Point	25.69	0.0023	1,6
Seed Grow-25 and Seed Grow-2	13.24	0.0108	1,6
Seed Grow-15 and Point	22.87	0.0031	1,6
Seed Grow-15 and Seed Grow-2	11.27	0.0153	1,6

Table 15a. Overall accuracy scores grouped by six training sample methods, reported for the classification of natural features.

Cultural Features

Spectral – Spatial Combination	Polygon	Seed Grow-25	Seed Grow-15	Seed Grow-5	Seed Grow-2	Point
25/1	77.90	80.61	73.68	75.00	52.08	44.00
25/4	84.40	81.32	84.88	63.22	55.56	46.00
70/1	64.40	65.56	75.00	64.52	53.76	50.00
70/4	63.40	74.73	80.26	43.33	45.56	27.60

Table 15b. Analysis of variance (ANOVA) of overall accuracy scores, grouped by training sample methods, as determined from the classification of cultural features (found in Table 15a). A 95% confidence interval was used to compute the F-critical value. F-statistics less than the F-critical value, or p-values greater than 0.05, were not significantly different, suggesting pixel size did not make a statistical difference. Statistical differences in overall accuracy scores were observed between seed grow 2 and point training sample methods and training sample methods: polygon, seed grow 25, and seed grow 15. All statistically significant values are noted in the table below. Degrees of freedom are denoted by d.f.

Cultural Features

Training Sample Pair ANOVA	F-Stat	p-Value	d.f.
Polygon and Point	18.44	0.0051	1,6
Polygon and Seed Grow-2	13.78	0.0010	1,6
Seed Grow-25 and Point	30.16	0.0015	1,6
Seed Grow-25 and Seed Grow-2	31.46	0.0014	1,6
Seed Grow-15 and Point	43.27	0.0006	1,6
Seed Grow-15 and Seed Grow-2	62.85	0.0002	1,6

Figure 1. Study site map of Fort Story, Virginia, USA, a small joint services military installation situated along the coast at the intersection of the Chesapeake Bay and Atlantic Ocean. This prominent cape location provides a safe harbor for endangered flora and fauna and is an example of tenuous competing coastal land uses. Fort Story is a mixed land-use land-cover installation. The study site selected was approximately 400 by 500 meters in size and contained all landscape classes found at the fort except forested wetlands (sand, maintained grass, clay soil, loblolly pine forest, hardwood forest, mixed forest, beach grass, ocean, asphalt pavement, rip rap shoreline, concrete pavement, and variable roofing material). Complexity of cultural and natural features found at this site provided a suitable challenge for comparing variable combinations of spectral bandwidth, spatial pixel size, and training sample method combinations.

Fort Story, Virginia, USA

0 10mi
10km

King And Queen
Courthouse
(30)

Kilmarnock
White Stone

Onley
Accomac

Melfa
Painter

Saluda

West Point (33)
Deltaville
Belle Haven
Exmore

(214) 220
Cressitt
Ark
(3)
Gwynn

Nassawadox

(60) 227

Gloucester

64

288

White Marsh

Eastville

199

Gloucester Point
Yorktown

Cape Charles

Claremont

(10) Surry

Poquoson

Kiptopeke

256

Rushmere

262

13

(31) Newport News

Hampton

Wakefield
Isle Of Wight

258

273

Zuni

Norfolk

(616)

Portsmouth

Virginia Beach

Sedley
Windsor

337

6/8

2
(44)

Suffolk

Chesapeake

Carrsville

(58) (58)

168

Study Site

Fort Story

nhaven Colony

Broad Bay Colony

Shore Dr

(60)

North Vir

Corapeake
Como Gates

Moyock
Knotts Island

Winton Gatesville

South Mills
Shawboro
Currituck
Barco
Corolla

Ahoskie

Elizabeth City

(17)

Shiloh
Poplar Branch

Powellsville
Colerain
Hertford
Weeksville
Jarvisburg

Valhalla

(158)
Southern Shores

Figures 2a-c. Line plots depicting overall accuracy of each image combination by spectral

bandwidth 70nm or 25 nm, reported for (a) all terrain features (natural and cultural), (b)

natural features, and (c) cultural features. Imagery combinations plotted along the x-axis

represent 6 training sample methods tested for 1m and 6 training sample methods tested for

4m images, totaling 12 images. Overall accuracy scores (%) for classification were sorted

and plotted from highest to lowest to illustrate score differences attributable to spectral

bandwidth contribution.

SPECTRAL- Natural and Cultural

Legend: 25-NM, 70-NM

(a)

X-axis: Imagery combinations (1 to 12)
Y-axis: Overall accuracy (%) (30 to 65)

(b)

SPECTRAL- Natural

SPECTRAL-Cultural

(c)

Legend: 25-nm, 70-nm

X-axis: Imagery Combinations (1–12)

Y-axis: Overall accuracy (%) (20–90)
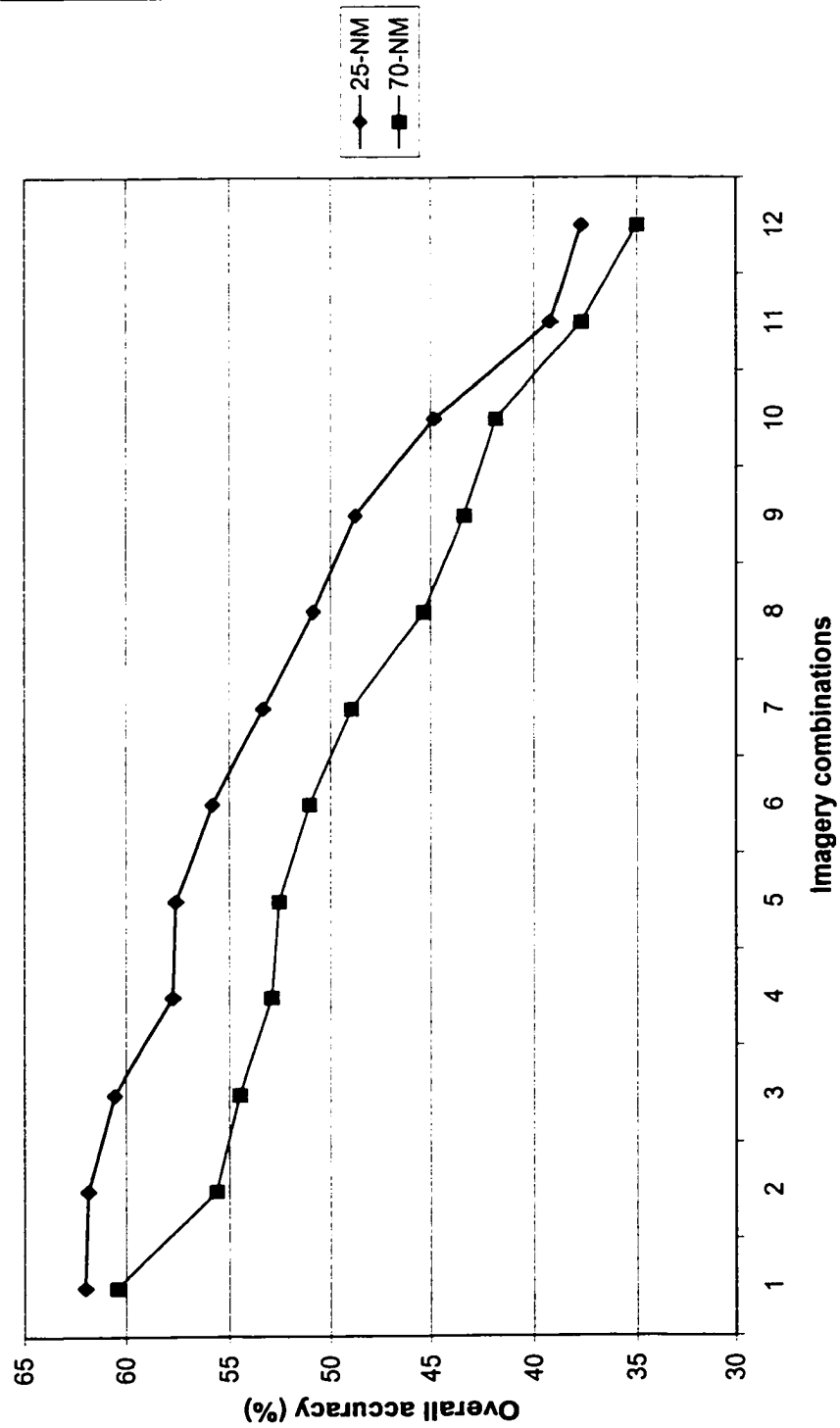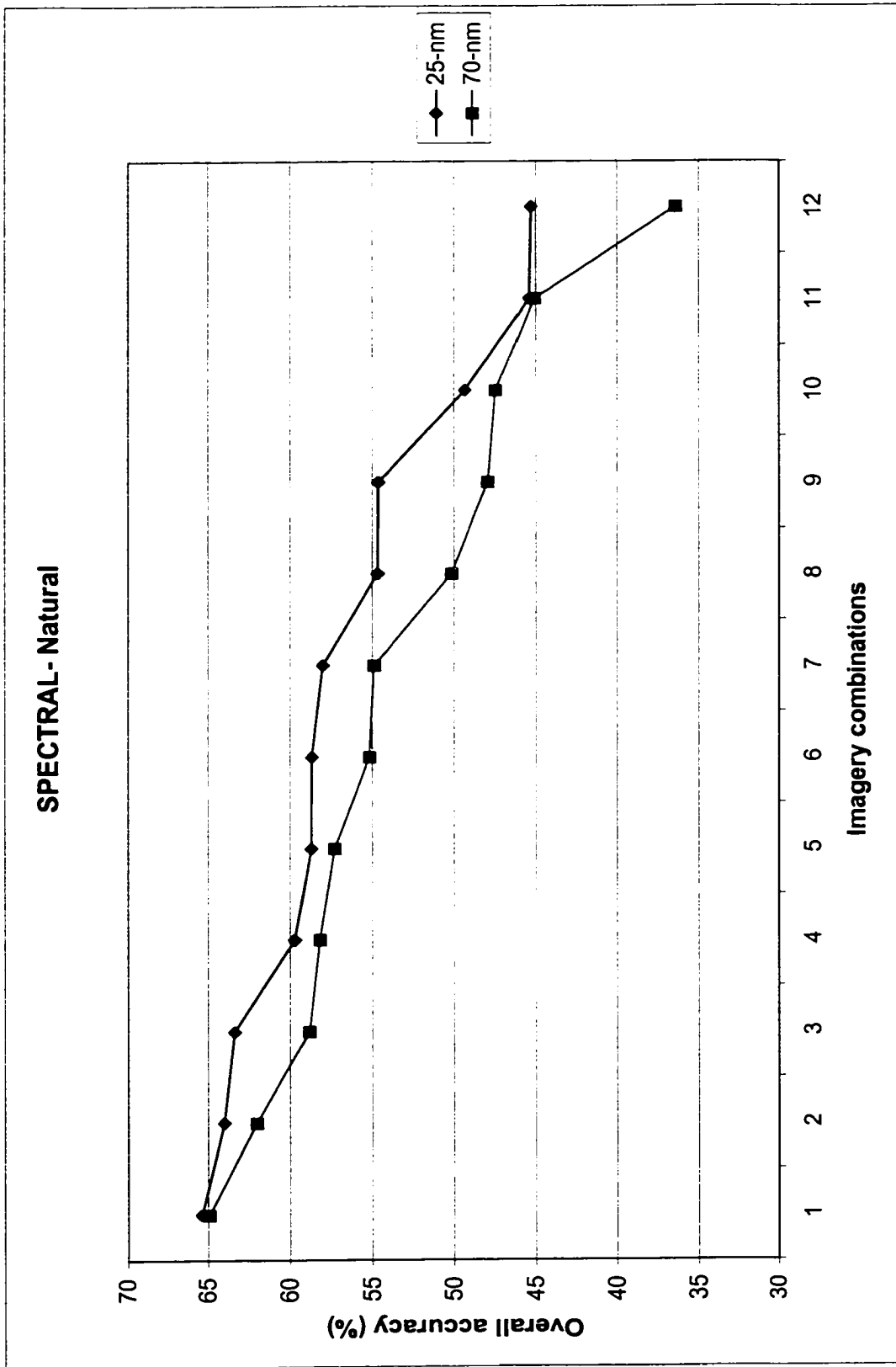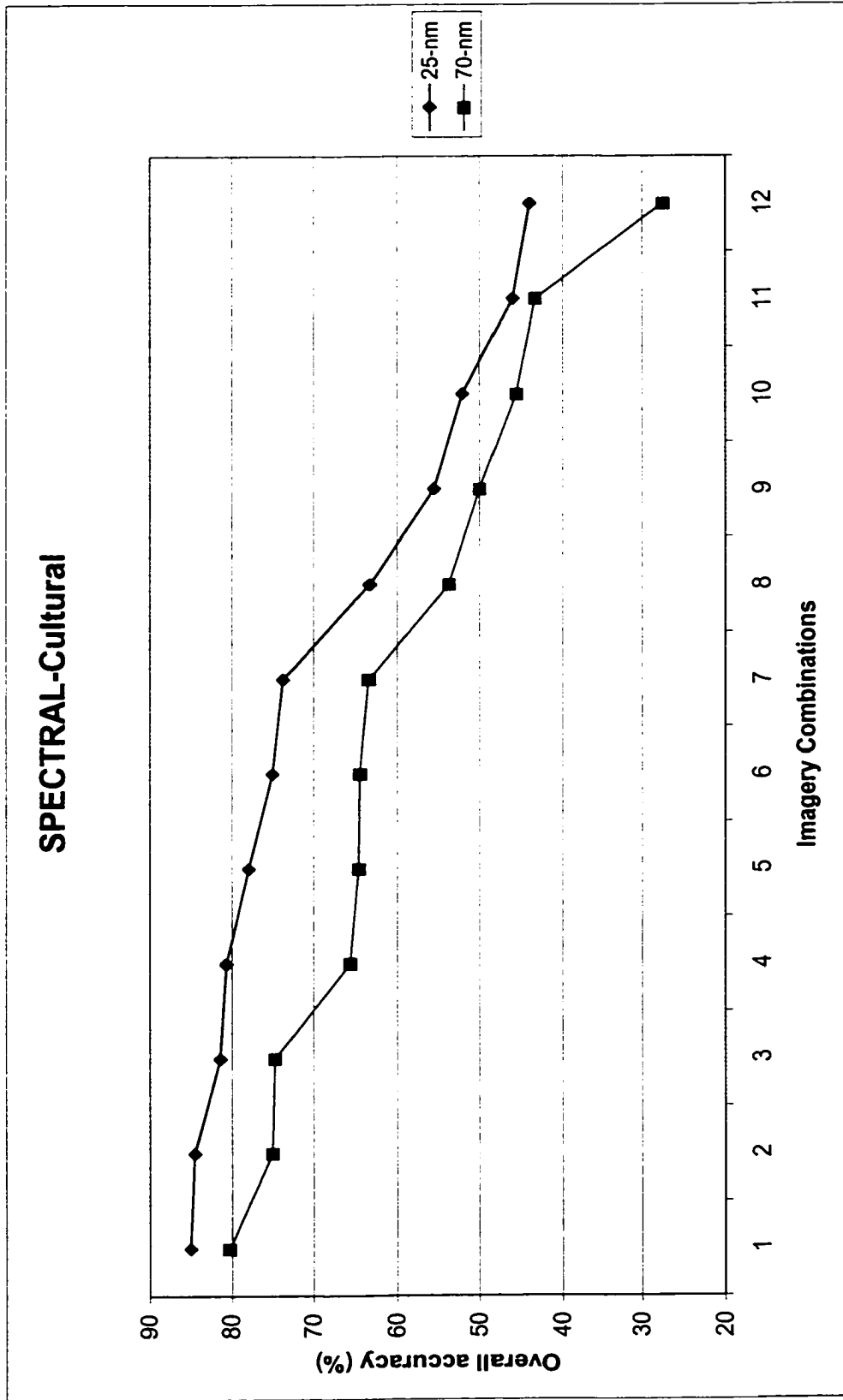
Figures 3a-c. Line plots depicting overall accuracy of each image combination by spatial pixel size 1-meter or 4-meter, reported for (a) all terrain features (natural and cultural), (b) natural features, and (c) cultural features. Imagery combinations plotted along the x-axis represent 6 training sample methods tested for 25nm and 6 training sample methods tested for 4m images, totaling 12 images. Overall accuracy scores (%) for classification were sorted and plotted from highest to lowest to illustrate score differences attributable to spatial pixel size contribution.

SPATIAL- Natural and Cultural

(a)

(b)

SPATIAL- Natural

Overall accuracy (%)

Imagery combinations

- 4-meter
- 1-meter

SPATIAL- Cultural

(c)

Overall accuracy (%)

Imagery combinations

Legend: ◆ 4-meter ■ 1-meter
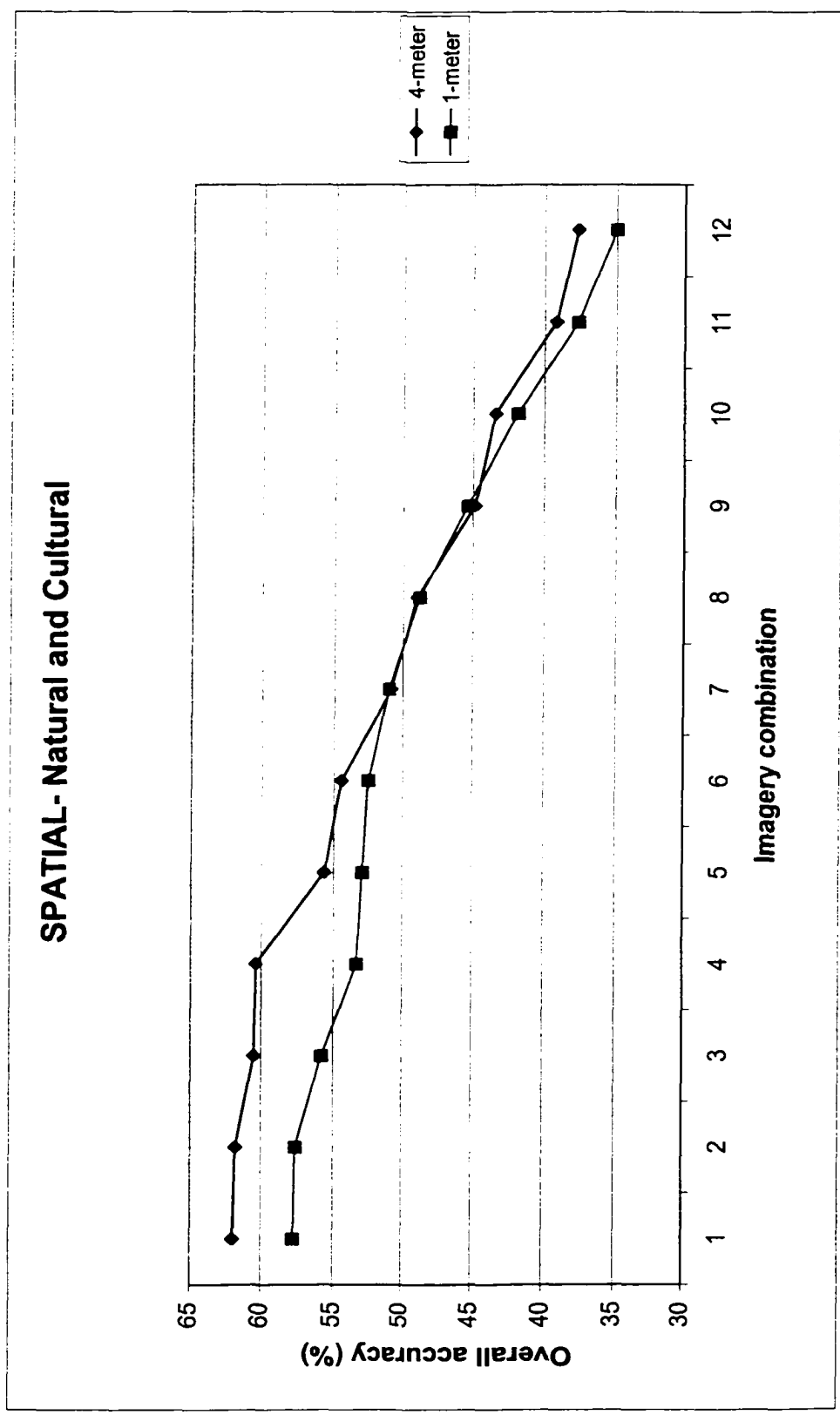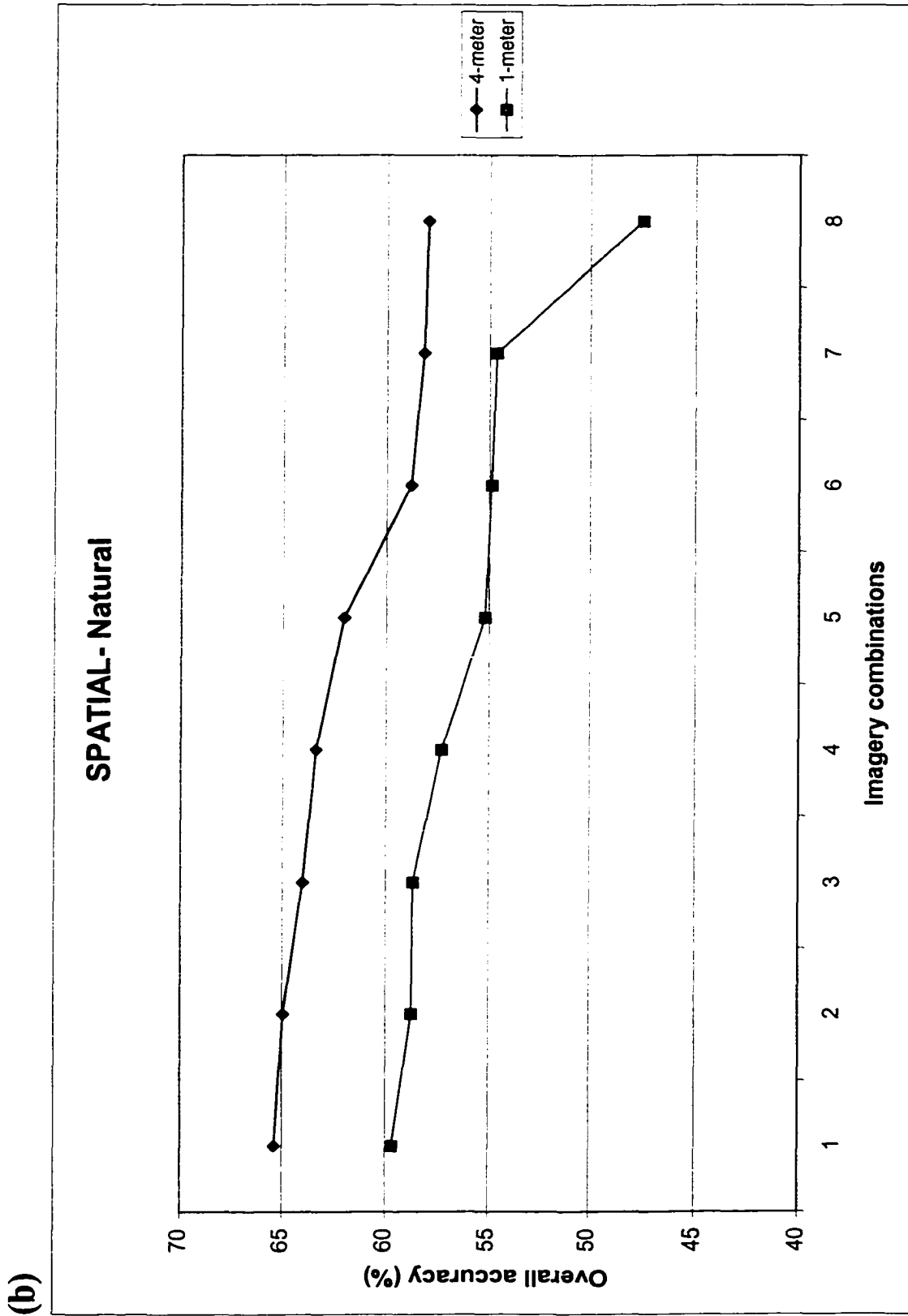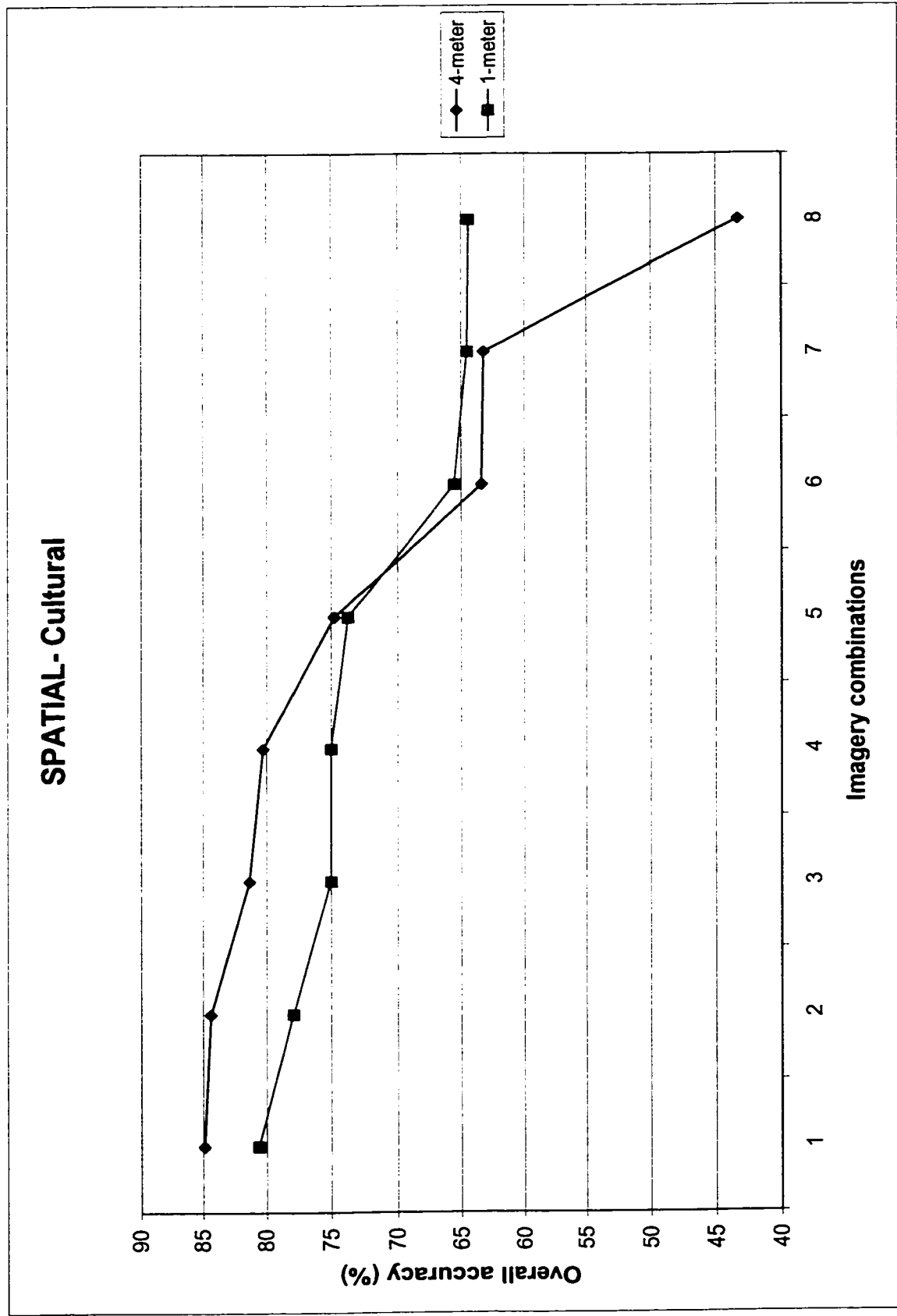
Figures 4a-c. Line plots depicting overall accuracy of each image combination of spectral

bandwidth and spatial pixel size, reported for (a) all terrain features (natural and cultural), (b)

natural features, and (c) cultural features. Six training sample methods are plotted along the

x-axis with the overall accuracy scores (%) for classification sorted and plotted from highest

to lowest to illustrate score differences attributable to the combination of spectral - spatial

resolution. Combination 70nm/1m is consistently lowest.

(a)

SPECTRAL-SPATIAL COMBINATION
(Natural and Cultural)

(b)

SPECTRAL- SPATIAL COMBINATION
(Natural)

Legend: 25-4 (♦), 70-1 (■), 70-4 (▲), 25-1 (×)

X-axis: Training Sample Methods (1, 2, 3, 4, 5, 6)

Y-axis: Overall accuracy (%) (30, 35, 40, 45, 50, 55, 60, 65, 70)

SPECTRAL - SPATIAL COMBINATION (Cultural)

Legend: 25-4, 70-1, 70-4, 25-1

X-axis: Training Sample Methods (1, 2, 3, 4, 5, 6)

Y-axis: Overall accuracy (%) (20, 30, 40, 50, 60, 70, 80, 90)
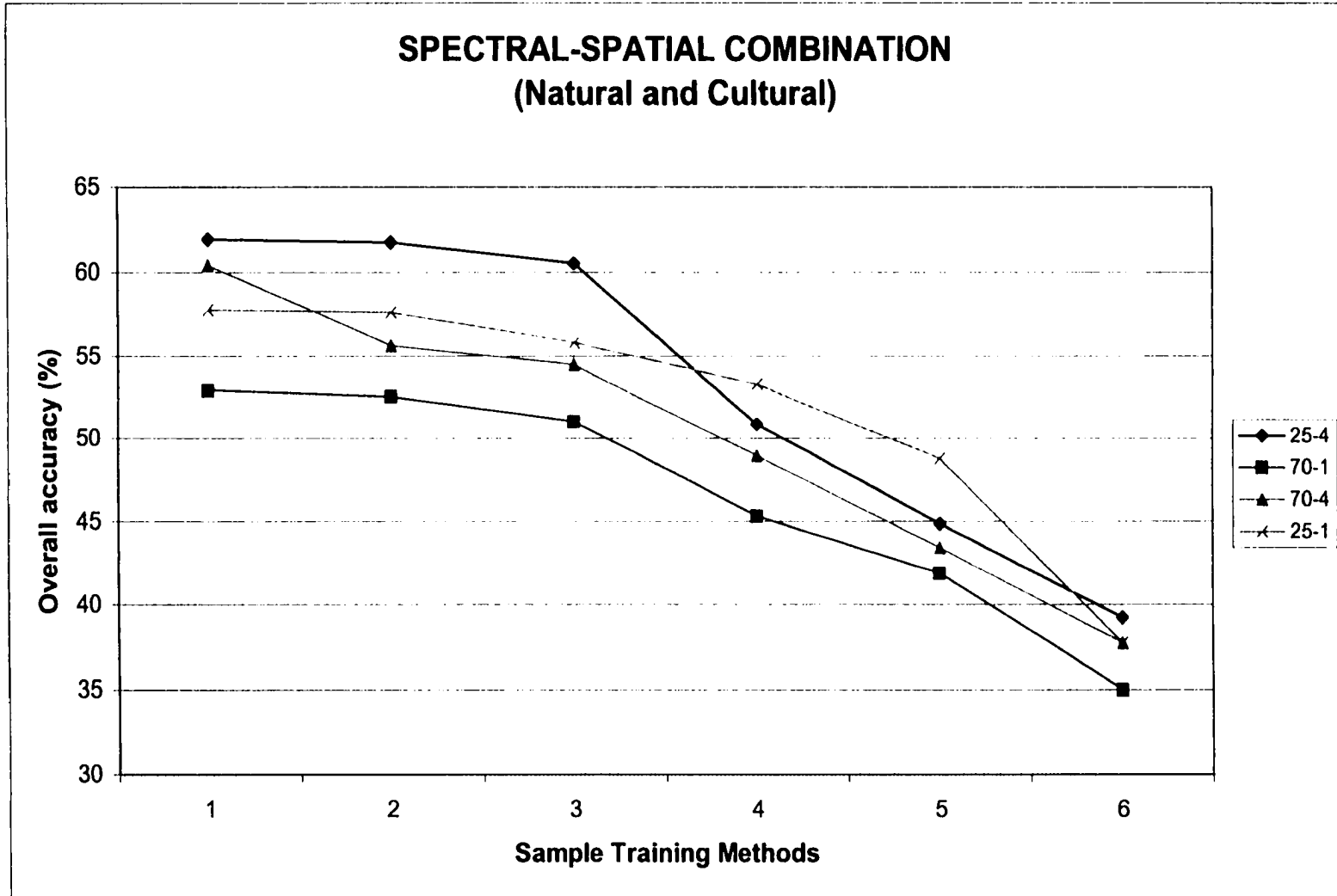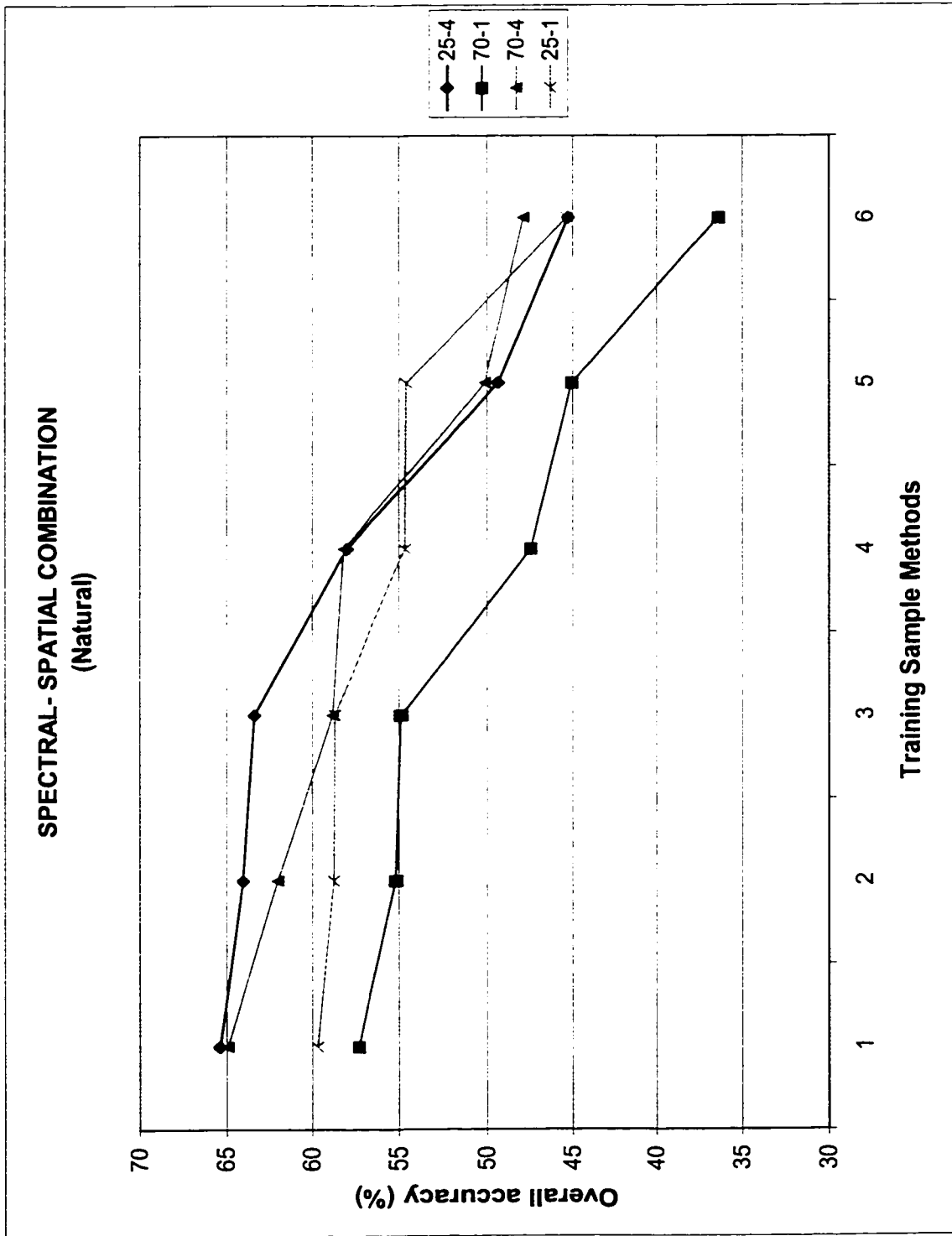
(c)
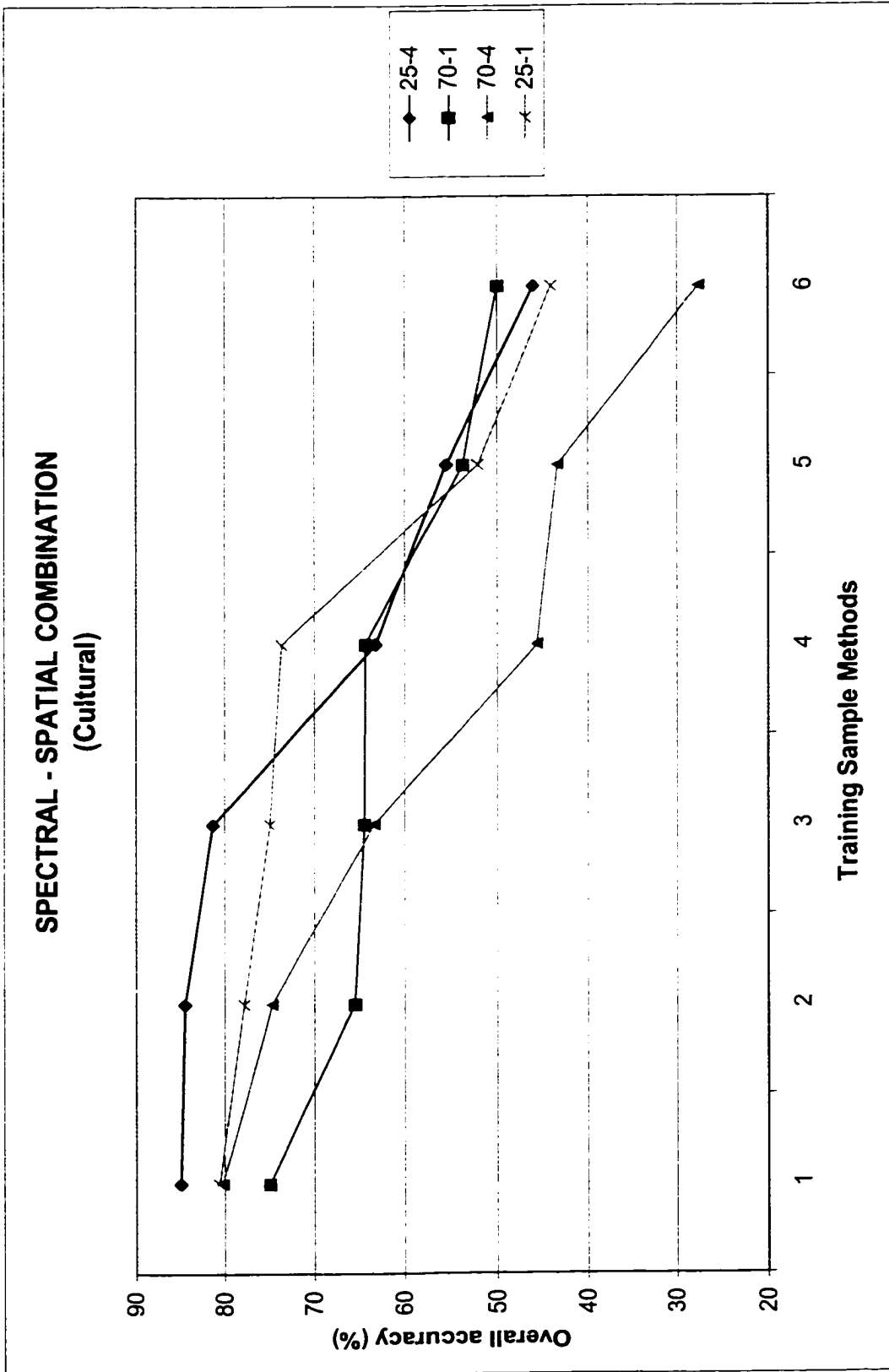
Figures 5a-c. Line plots depicting overall accuracy of training sample method, reported for (a) all terrain features (natural and cultural), (b) natural features, and (c) cultural features. Four imagery combinations (25nm/1m, 25nm/4m, 70nm/1m, 70nm/4m) are plotted along the x-axis with the overall accuracy scores (%) for classification sorted and plotted from highest to lowest to illustrate score differences attributable to the training sample method selected. Three methods: point, seed grow2, and seed grow5, had consistently poorest accuracy results regardless of features to be classified. Seed grow is a user-defined euclidean distance method that attempts to mimic a starting pixel statistics, polygon is a heads-up screen digitizing method subjectively determined by an analyst, and point method is selection of a single pixel, perhaps from a field global positioning system location.

(a)

Training Sample Methods
(Natural & Cultural)

(b)

Training Sample Methods
(Natural)

(c)

Training Sample Methods
(Cultural)
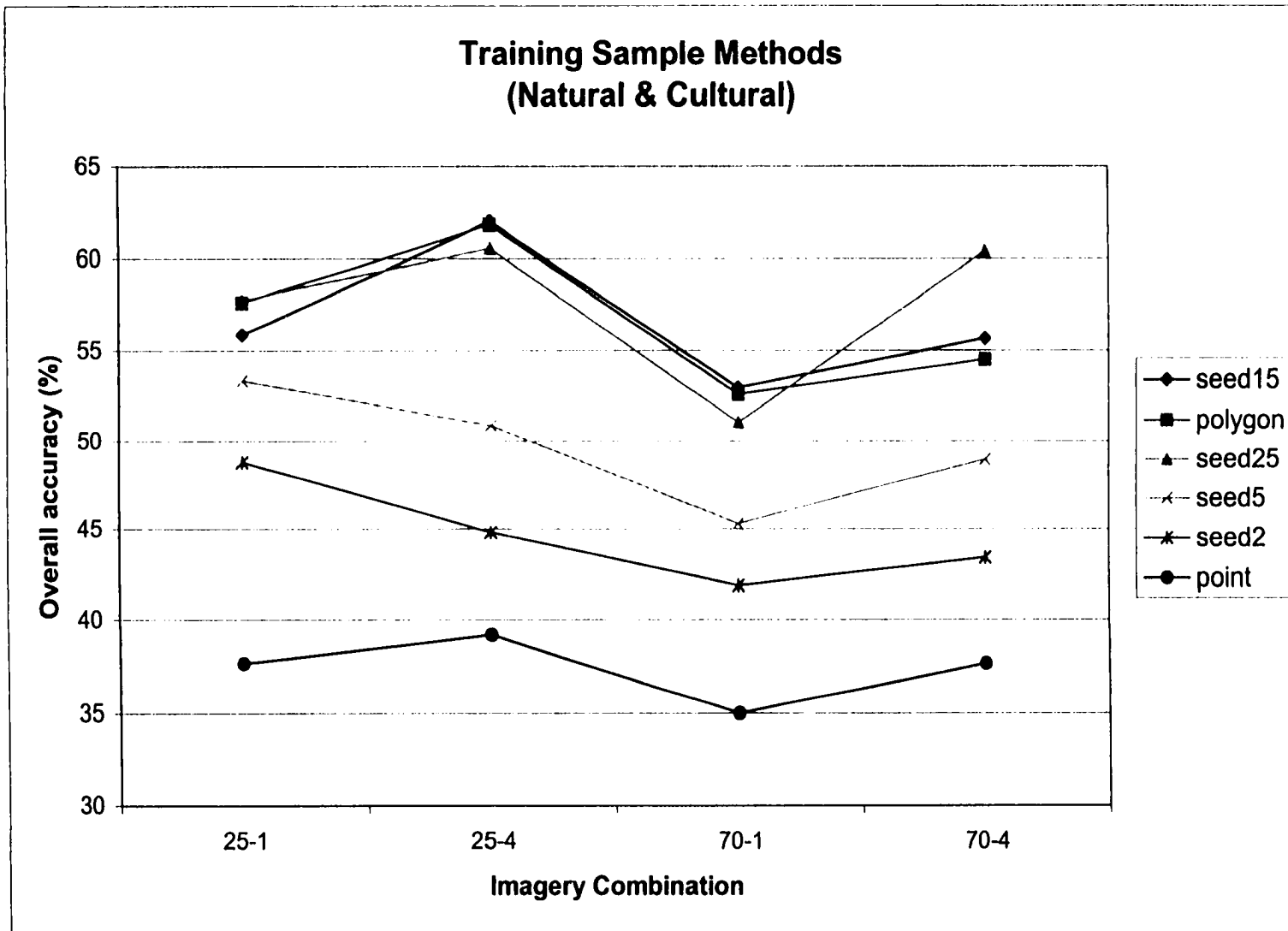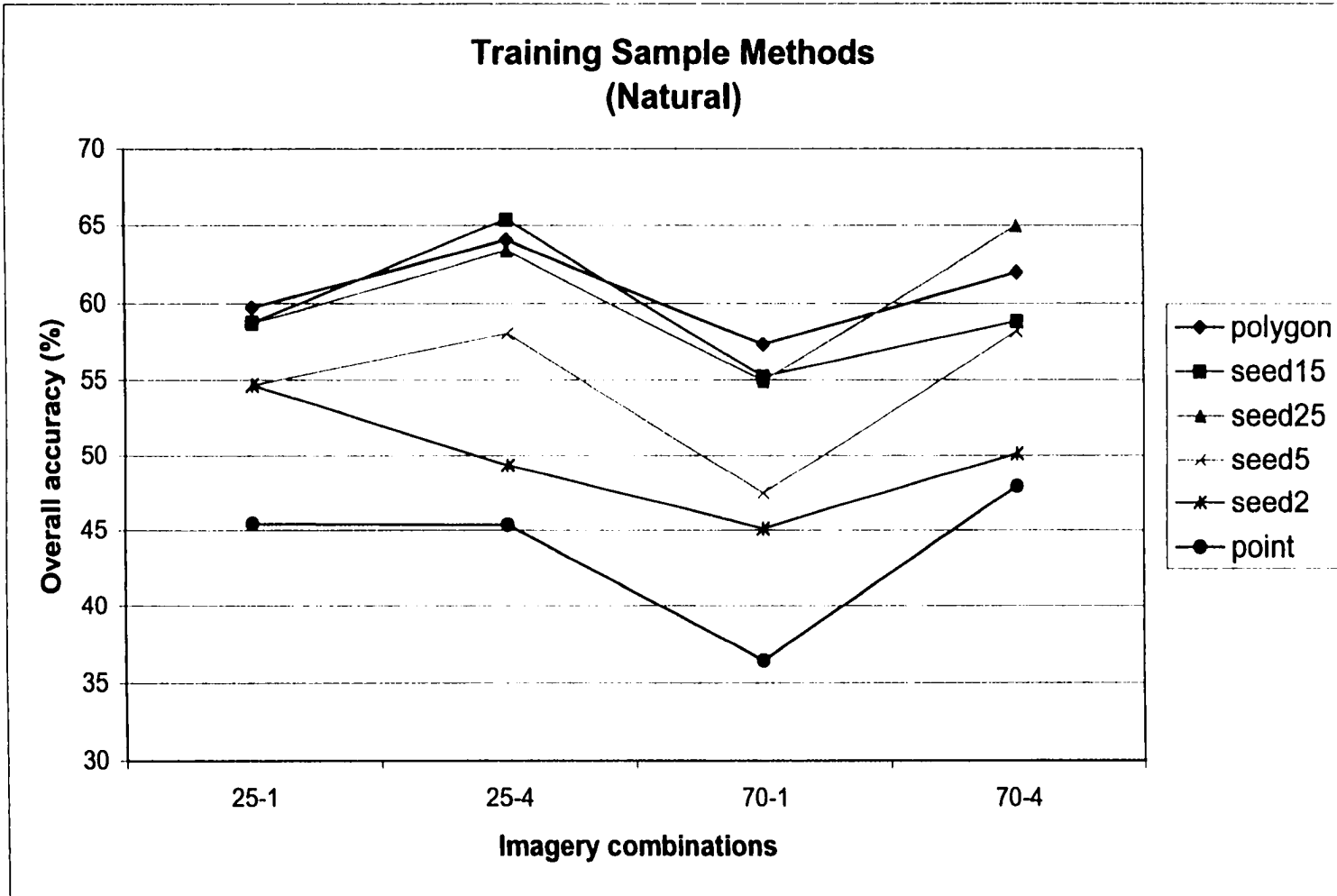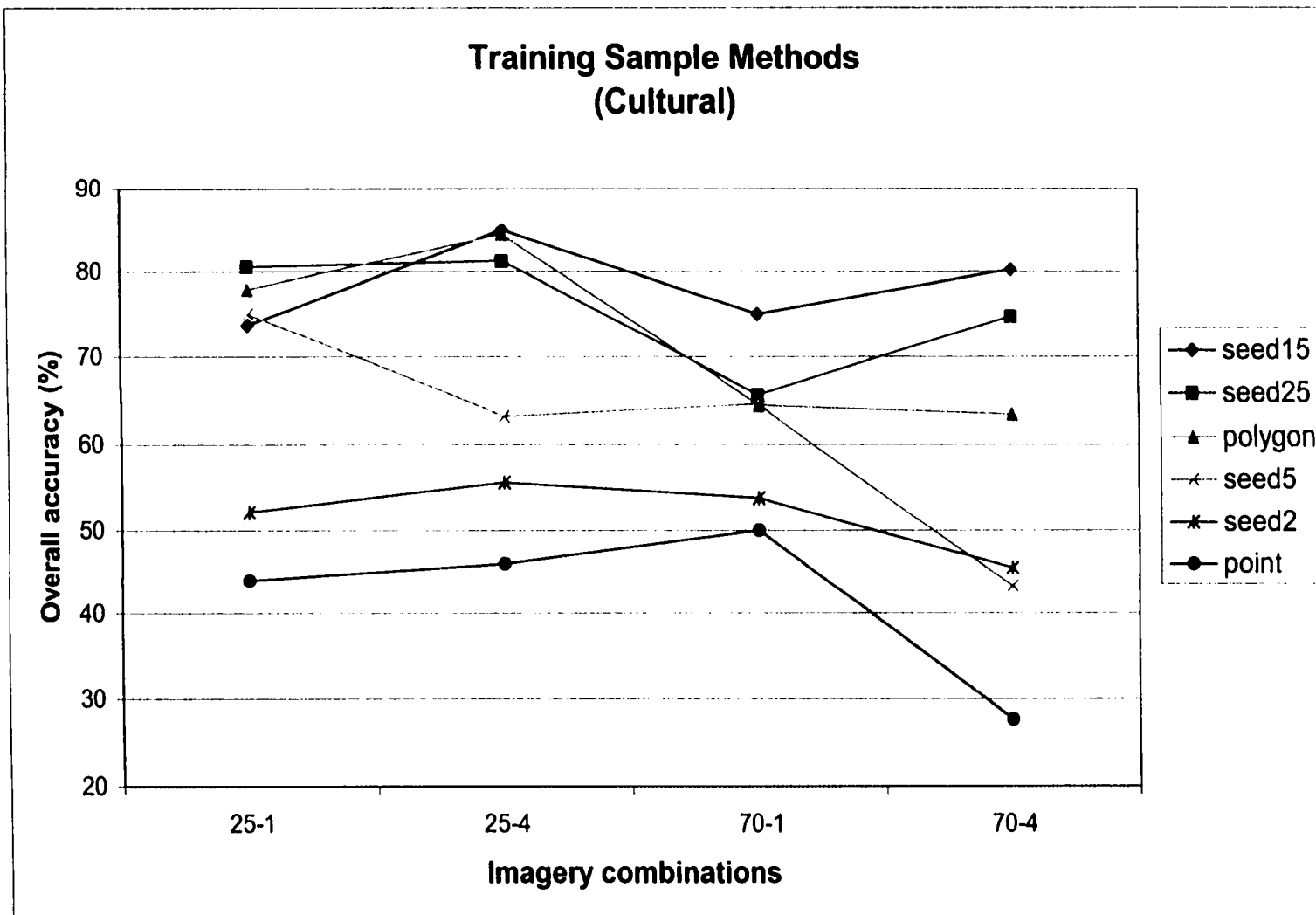
Figures 6a-c. Accuracy assessment Kappa score results for spectral, spatial, training method combinations, reported as a bar chart for (a) natural and cultural, (b) natural features, and (c) cultural features. The y-axis depict Kappa scores, reported as a value between 0.00 and 1.00, representing the amount of agreement between a classified cover type map and the truth set collected in the field. The x-axis shows the 24 possible images defined by spectral, spatial, and training sample method combinations. The top three Kappa scores are achieved from 25nm/4m imagery using training sample methods that acquire the most training pixels.

(a)

Kappa Scores for All Natural and Cultural Features Classification

(b)

Kappa Scores for Natural Features Classification

Kappa Scores for Cultural Feature Classification
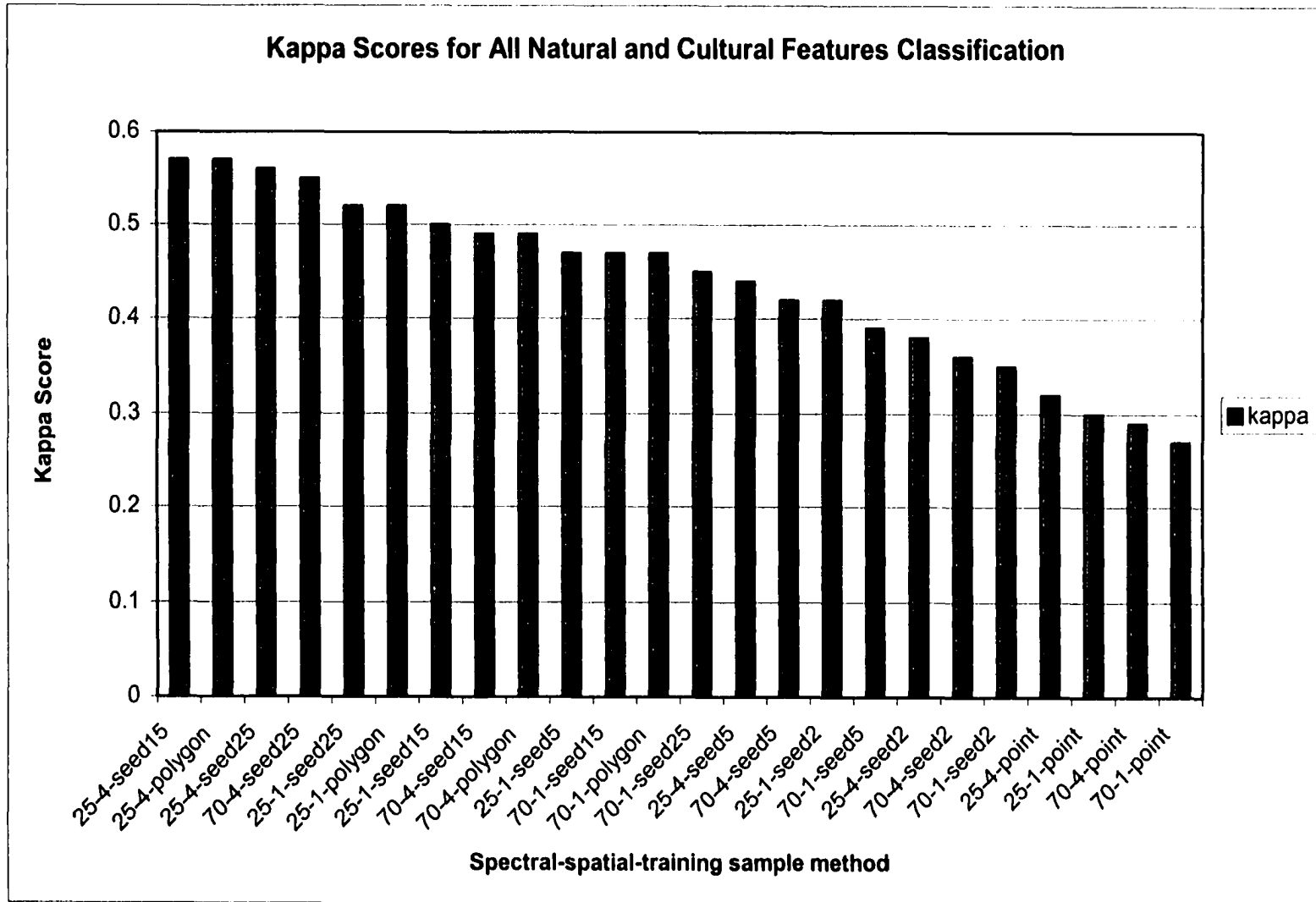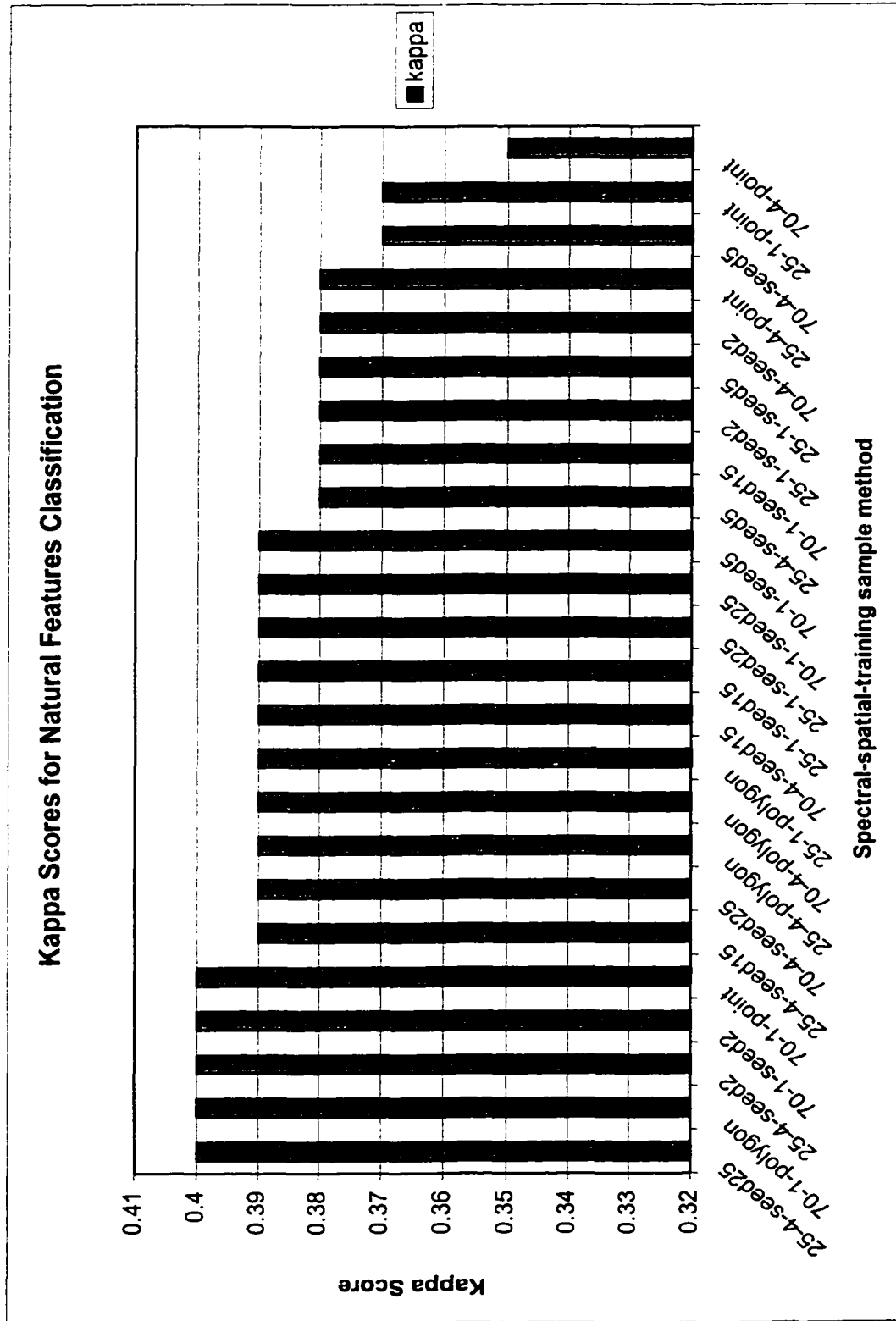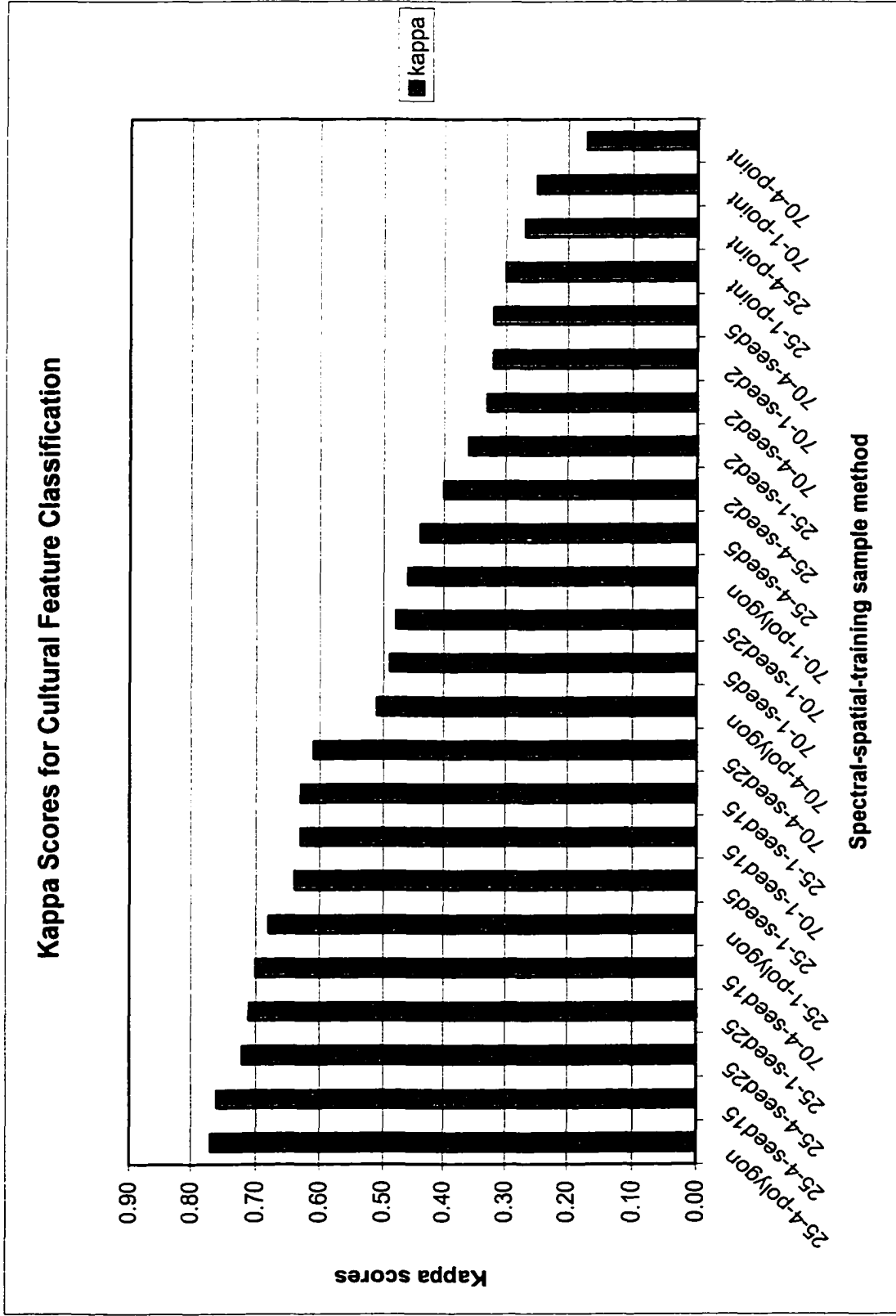
Chapter 2 to Chapter 3 Transition

The work presented in this past chapter provided insight into the capabilities of emerging high-resolution remote sensing platforms for classifying landscape cover types accurately. Chapter 3 investigates 1-meter spatial, 70-nm spectral imagery (imagery with resolution roughly equivalent to IKONOS panchromatic imagery that has been transformed with coincident 3-channel spectral data). IKONOS represents a new participant in the commercial spectral imagery community and another available data source from which resource managers must choose the best applicable imagery. The airborne image set proved suitable for classification of categorical biomass index differences in homogeneous stands of *Phragmites australis* (common reed). This capability for structural mapping is an extension to simpler cover class thematic mapping. Field data and image reflectance values within *P. australis* stands are statistically compared. The approach offers a potential method for remote monitoring of an historically unwanted plant that often out competes native plants for habitat.

Chapter 3

Remote Identification of Biomass Index Differences in

Phragmites australis Cav. Stands from

High-Resolution Spectral Imagery

Abstract

Phragmites australis was characterized remotely using high spatial resolution airborne multi-spectral imagery. Different spectral reflectance values were observed across monotypic reed-stand sample plots, believed to represent structural differences such as stand height, stem counts, average culm diameter and herbaceous understory cover percent. Reflectance values were acquired from the imagery at ten sample locations, followed by field measurements of the four structural variables cited above at coincident geographic locations on the ground. Statistical cluster trees of sample plot reflectance values were compared to clusters and their members that defined corresponding field data. Classes from the red-channel reflectance values came close to a direct match with the classes and members from the field data, misclassifying only one sample plot from the moderate to the low biomass index class. A high biomass index class was clearly separable with identical *P. australis* sample plots selected as members of the cluster. Analysis of variance and multiple regression confirmed that red-channel reflectance values best predicted biomass index field data categorized into classes: low, moderate and high. The addition of a green-, blue-, and NIR-image channel increased the predictive power of image reflectance values to classify *P. australis* into low, moderate and high biomass index classes. Remote identification of high biomass index stands may help to target remediation efforts.

Introduction

Phragmites australis Cav. (common reed grass) is generally considered an invasive plant species along the eastern coast of the United States, providing both minimal food and cover for resident wildlife (Marks *et al*, 1994; Pykes *et al*, 1999; Weinstein and Balletto, 1999). It is a facultative wetland species that has adapted uniquely well to low, marshy areas of the Atlantic Coast (Silberhorn, 1999). High brackish and freshwater inland marsh systems may be dominated quickly by this species due to its rapid lateral expansion at the expense of native species. While there is little historical quantitative data on percentage cover of *P. australis* in the eastern United States (Rice *et al*, 2000), one study originating from Connecticut salt marshes suggests extensive colonization (Roman *et al*, 1984); Delaware salt marshes are now dominated by *P. australis* (Hellings and Gallagher, 1992); and Virginia's fifteen constructed wetlands are showing signs of extensive invasion (Havens *et al*, 1997). *Phragmites australis* can grow exceptionally tall, extending upwards of 4-meters (Weinstein and Balletto, 1999) and aggressively out-competes native plants such as big cordgrass (*Spartina cynosuriodes* L.) and wild rice (*Zizaniopsis miliacea* Michx.) through reproduction from both its rhizome and seed head (Silberhorn, 1999). They are a particularly opportunistic species for invasion of soil disturbed naturally (e.g., at a high water rack line; created from decline in hydro period) and by anthropogenic means (e.g., excessive sedimentation) (Havens *et al*, 1997). These mono-culture environments are believed by some to reduce diversity and habitat quality (Pyke *et al*, 1999; Weinstein and Balletto, 1999; Rice *et al*, 2000). *Phragmites australis* has been shown to restrict tidal flow and drainage and thereby inhibit nutrient exchange (Pyke and Havens, 1999; Weinstein and Balletto, 1999), impounds and restrict interior *Spartina* communites from receiving needed water

flow, fragments *Spartina* vegetation communities, reduces plant to water interface for exchange of processes, and affects ingress and egress of fish (Weinstein and Balletto, 1999). Other researchers have shown neckton abundance to be statistically similar between *S. alterniflora* L. and *P. australis* dominated nurseries (Meyer *et al*, 2001; Able *et al*, 2001).

Levine *et al* (1998) suggested New England salt marsh plant species were limited at the lower elevation by waterlogged soil and at the higher elevation by competition among species. Pyke and Havens (1999) showed a negative linear relationship between sediment depth and proliferation of *P. australis*, with accumulation of sediments closer to creek channels. They described ideal conditions for *P. australis* as oxidized soil just below the high water line that did not accumulate sediments. Amsberry *et al* (2000) supported these claims in their studies where transplanted *P. australis* would die off when relocated to the lower marsh zone that is deficient in available oxygen and waterlogged by daily tides. Higher marsh development is promoted by the falling out of solution of suspended sediments as tidal sheet flow reduces in velocity when it reaches dense stands of *P. australis* (Weinstein and Balletto, 1999). Rooth and Stevenson's (2000) coastal study results indicated an increase in elevation for *P. australis* stands despite no increase in sediment delivery to the environment, suggesting that litter accumulation and below ground accumulation was increasing the substrate elevation. The ability of *P. australis* to alter the environment physically to prepare better for its advance into neighboring communities is complemented by its ability for lateral movement from the upper marsh into the lower marsh by clonal integration (Amsberry *et al*, 2000). This physiological process provides a mechanism for *P. australis* to creep into the edges of environments originally inhospitable to them (Amsberry *et al*, 2000).

Monitoring the expansion of *P. australis* has been suggested from both indirect and direct approaches. Roman *et al* (1984) stated that growth and distribution of marsh vegetation other than *P. australis* could provide indicators (or indirect surrogate variables) as to the stage of conversion of a marsh from an unrestricted tidal flow creek with minimal *P. australis* to a fully degraded marsh dominated by *Phragmites*. Shrub specie increases (e.g., *Iva frutescens* L.) and decreases in *S. alterniflora* tall form along creek banks were cited as specific indicators of vegetation change in a restricted marsh (Roman *et al*, 1984). Shoot density at 14 marsh study sites in Massachusetts were measured directly and analyzed for steepness of transition between community types with shoot density analyzed by ANOVA and Tukey post hoc pair-wise comparison (Keller, 2000). Results from this work were inconclusive and long-term research was identified as necessary to examine the rate of spread of *P. australis* into established communities (Keller, 2000). Rice *et al* (2000) found high biomass rates in two salt marsh study sites in the Chesapeake Bay area associated with high intrinsic rates of *P. australis* expansion with a third salt marsh site exhibiting low biomass but high expansion rate (Rice *et al*, 2000). Growth rate differences computed for older and newer stands of *P. australis* indicated highest rates of area expansion for the youngest stands (Rice *et al*, 2000). Remote monitoring of *P. australis* could provide a rapid, non-intrusive vegetation classification assessment method.

The purpose of this work was to determine if high-resolution multispectral imagery could be used for classifying structural differences in *P. australis* stands. If imagery proved useful for distinguishing stands of differing structure, follow-on field research recommended

by Keller (2000) would examine the rate of spread of *P. australis* into neighboring

communities. Specifically, stands of highest biomass index would be likely to expand

laterally first, thereby testing earlier findings of Rice *et al*, (2000), where growth rate was not

related to biomass or abundance. Numerous plots of *P. australis* were tested for remote

characterization from high-resolution airborne multispectral imagery. Ten *P. australis* stands

were subsequently visited to validate the hypothesis:

(H_o): imagery reflectance values are not related to *P. australis* biomass index.

(H_a): imagery reflectance values are a function of *P. australis* biomass index.

Methods

Site Description

Eighteen barrier islands make up a chain trending northeast-to-southwest off of

Virginia's Eastern Shore (Figure 1. Location map of Parramore Island, Virginia). Parramore

Island was selected as the primary study site; it is the central-most island in this barrier chain.

Since the late 1980's Parramore Island has been privately owned and access to the island has

been restricted. No permanent human population inhabits the island and activities such as

agriculture, hunting, logging or similar activities are prohibited. Island orientation is

approximately 15 degrees east of north and it has the classic drumstick shape indicating

rotational instability (Haynes, 1979). The island is approximately 10-kilometers long by 1.5-

kilometers wide and is separated from the mainland by a series of bays, salt marsh and small

tidal creeks. Parramore exhibits classic dune and valley geomorphology with (from seaward)

a sandy beachfront, dune / ridge sequence, maritime forest, inland marsh, and a bay-side

marsh complex.

Barrier island dune and valley complexes represent unique geomorphological

conditions that support very distinct vegetation zonation, a direct response to environmental

conditions such as salinity, period of inundation (Mitsch and Gosselink, 1993), and tidal

range (Frey and Basan, 1974). Homogenous stands of cattails (*Typha angustifolia*) and *P.*

australis are found growing within Parramore Island's upper valley marshes. The high marsh

also supports low-density, short-height marsh elder (*I. frutescens*) and groundsel-tree

(*Baccharis halimifolia*), found in co-existence with an herbaceous component that includes *S.*

patens and *T. angustifolia*. A comprehensive description of a Virginia barrier island

ecosystem can be found in McCaffrey and Duesser (1990) and Scott (1991). Figure 2 shows

the northern end of Parramore Island where P. australis co-dominates in the higher marsh

along with *S. patens* and *T. angustifolia*. *Phragmites australis* is considered to be a

management problem along the coastal plain of Virginia (Pyke and Havens, 1999).

Imagery data acquisition

Digital multispectral imagery was obtained over the Parramore Island study site on

May 30, 1999 (unpublished data) from a small, lightweight 4-camera imaging system fitted

with 25 nanometer wide bandpass interference filters centered at 450 (blue), 550 (green), 650

(red) and 800 (near infra-red) nanometer band centers. Spatial ground sample detection was

approximately 1.5-meters. The camera system named the Computerized Airborne Multi-

camera Imaging System (CAMIS) was purchased in 1999 by the U.S. Army Topographic

Engineering Center as a beta test system from FlightLand Data, Inc, located in Boston, MA.

Ten field plots of *P. australis* were selected randomly from a multispectral imagery

vegetation classification. A mean spectral reflectance was computed for each plot by

acquiring approximately 30 to 36, 1.5m pixels from each stand, with the position of the

central-pixel identified by geographic coordinates. Pixels were selected visually by

digitizing a polygon around the central pixel within the *P. australis* class type. The central

geographic coordinates were used for location in the field. Reflectance values were acquired

for the blue (450 nm), green (550 nm), red (650 nm), and near infra-red (780 nm) image

channels. A normalized difference vegetation index (NDVI) value was computed and

reported for each of the ten plots.

Field plots

Field data were acquired in early November 1999, late enough in the growing season that

P. australis had entered senescence. A one-meter quadrat plot was used in the field to

delineate sample plots. Average height range (reported by ½ meter), stems per meter

(density), average culm (stem) diameter, and percentage cover of all individual species were

recorded for each data point. Stand height range was calculated by tape measure. All stems

within the quadrat equal to or greater than 1-meter in height were counted. Diameters of all

stems greater than 1-meter in height within a 1/4-meter-quadrat were measured 15cm above

ground level, and an overall mean diameter for the full quadrat was estimated. *Spartina*

patens cover was visually estimated on a decile percentage scale.

Phragmites australis begins growth in the spring usually after the last frost

(http://www.fs.fed.us/database). Shoots emerge in the April to May timeframe in

Connecticut (Haslam, 1969) and in February in the Southeast (Leithead *et al*, 1971).

According to the National Oceanic and Amospheric Agency, March 23rd represents the 50%

probability date for the end of the frost season in Norfolk, Virginia, a location that is

approximately 50 miles south of Parramore Island and also along the coast (NOAA. 1988).

March 23 seems to be a reasonable approximation for Parramore given the Norfolk data and

suggested times of shoot emergence for Connecticut to the north and the southeastern states.

Period of shoot emergence can be between one and three months long (Cross *et al*, 1989).

Accordingly, new shoots would likely have emerged at Parramore beginning late-March and

continued no later than the end of June, or one-month after the May 30 image acquisition

date. Older *P. australis* stems were no longer in senescence by May 30 so the collection date

was agreeable for measuring green biomass. Reflectance values for this study, therefore,

depicted *P. australis* stand conditions during the conclusion of the growing season.

Following emergence, new stems can grow up to 4cm per day

(http://www.fs.fed.us/database). This information suggests a possibility that a few of the

shorter stems counted and measured in the November timeframe actually emerged in June

after the May collect. Furthermore, it suggests that the diameter of some stems may have

increased slightly during the month of June. In classifying the May 30 imagery, there was no

attempt to separate out older stems, some dead, from new growth. Likewise, there was no

attempt to do so in the field. Common factors affecting spectral reflectance are soil and dead

biomass, and soil is only pertinent when there is a sparse canopy of less than 30% cover

(Gross *et al*, 1989). Dead biomass will cause the red channel spectral reflectance to increase,

and increases in red reflectance are correlated with decreased green biomass within a salt marsh community (Hardisky *et al*, 1986). The investigation proceeded without addressing approximate stem age and their potential phenological contribution to image reflectance. Each stem was considered equivalent regardless of age.

Statistical computation

Stands of *P. australis* were grouped into classes termed "low", "moderate", or "high" biomass index, with biomass index determined from equation 1. This new variable ("biomass index") was computed by first normalizing all the data using a linear scale transform with maximum score procedure (Malczewski, 1999) and converting all maximum measured values in categories "height", "stem count", and "culm diameter" to 1.0. Percent cover of other species, primarily *S. patens* but also *T. angustifolia*, detracted, rather than contributed, to the computation of a biomass index estimate and was only considered if biomass index class designation was not definitive. All normalized values were entered into the following equation to calculate the new variable:

$$H \times S \times C = B, \text{ where} \tag{1}$$

H = average plot stand height

S = stems per meter

C = average plot culm diameter

B = average plot biomass index

Field data were grouped statistically by an icicle-tree (dendrogram) clustering algorithm using Ward's method. This method is different from other clustering techniques because it

uses an analysis of variance approach for assessing distance between clusters, minimizing the sum of squares of clusters formed at each step (Stat Soft Inc., 1995). Cluster analysis attempts to group variables that are highly correlated with each other and excludes variables that are not. Cluster analysis can be carried out for either presence and absence (qualitative data) or quantitative data with nearly identical results (Magurran, 1988). To compute these clusters, percent cover of understory was not considered as a variable. Three clusters were selected because a long-term goal was to sub-divide remotely characterized *P. australis* stands into three groups of biomass index— low (1), moderate (2), and high (3) biomass index — with high biomass index area presumed, but as yet untested, to be the most likely to advance laterally first. Additional clustering methods using single linkage and complete linkage with euclidean and squared euclidean distance variation were evaluated and used to derive the original three cluster groupings with equivalent plot members. Field data clusters and their respective plot members provided patterns of cluster structure. Subsequent cluster analysis of the image reflectance channels identified clusters and plot members that most closely matched the field data. Essentially, an exploratory search for the "right" combination of image channel reflectance values was undertaken and included: all image channels, near infra red (NIR), NIR and NDVI channels, red channel, and all image channels except NDVI, again using the Ward's clustering method with euclidean distance.

A one-way analysis of variance (ANOVA) using the General Linear Model (GLM) within Statistica (StatSoft, Inc., 1995), designed to test single categorical variables against continuous data (reflectance values), was used to confirm the results of the reflectance value clusters (if the reflectance cluster plot members matched the field cluster plot members) or,

conversely, to demonstrate that reflectance cluster plot members did not match field cluster members (i.e., imagery reflectance values were too similar). To test the ANOVA, reflectance value plot data were coded with a categorical value of 1, 2 or 3, matching the equivalent field plot cluster membership. All reflectance plot data were grouped by the categorical value 1, 2, or 3, tested by ANOVA for spectral differences, and analyzed by a Tukey test to determine if the interaction found in the image channel data set is explainable by a combination of independent variables (Sokal and Rohlf, 1995). Post-hoc comparisons, such as the Tukey test, may be completed when categorical predictor variables yield unexpected results that need to be proven reliable by hypothesis testing (StatSoft, 1995). Tukey is a multiple comparison procedure wherein all variables are compared in a pairwise manner (Zar, 1999) taking into account the fact that more than two samples are computed (StatSoft, 1995). Whenever statistically significant F test scores are reported from an analysis of variance testing, there is an interest in assessing which groups are different from each other. Accordingly, Tukey was computed to understand better the contribution of reflectance channel variables in remotely distinguishing between biomass clusters low, moderate, and high. Finally, forward stepwise regression was applied to all image channel reflectance values to test the predictive power of each image channel in estimating biomass index class. Image channels are rank-ordered based upon their respective contribution in explaining the variance in biomass index class, and included into the linear regression model.

Results

Table 1 gives the reflectance values of the *P. australis* sample plots, and Table 2 reports the coincident vegetation structural data measured in the field. Normalized field data are

given in Table 3, with a *P. australis* biomass index class assigned for each field plot. Biomass index values were rank-ordered from smallest to largest. A percentage change of greater than 25% in biomass index scores, comparing the smaller preceding index score to the next higher index score, was used to quantitatively delineate class thresholds Low, Moderate, and High. A low class was easily separated out, as plot members phrag24 and phrag27 each had less than a 1 per cent biomass index score. A review of the raw field data in Table 2 illustrated that these sample sites contained an herbaceous *S. patens* understory and had the smallest average culm diameters. Biomass index class 1 was termed "Low", for low biomass index. Biomass index class 2 was termed "Moderate", and contained plot members phrag20, phrag21, phrag22, phrag23, phrag 28, and phrag25. The term moderate was assigned because raw stem counts were all between 165 and 216 stems per meter and the biomass index computed values were reported between 0.20 and 0.40. Biomass index class 3 was called "High", and contained phrag21 and phrag22, with respective biomass index values of 0.55 and 0.79. Raw stand height and average culm diameter values were highest for these two plots. These two high biomass index sample plots are stands that warrant close monitoring for advancement. Figure 3 is a bar chart that depicts normalized field data measured at each sample plot with low biomass index plots identified on the left, moderate in the center, and high on the right of the chart.

Figure 4 is the dendrogram from the classification of *P. australis* biomass index values computed from normalized field plot data. Cluster analysis suggested four clusters identified at linkage distance 0.4 to 0.8, or perhaps three clusters as identified at linkage distance 0.8. Regardless if four or three clusters are designated, there is a distinctive high biomass index

class of *P. australis* with plot members phrag21 and phrag22, and a low biomass index class

with plot members phrag24 and phrag27. The remaining sample plots can be separated into

two classes (using linkage distance 0.4 to 0.8) or combined into one class (linkage distance

0.8) and are members of the moderate biomass index cluster. To simplify further

investigations, all moderate biomass plots were classed together as designated at linkage

distance 0.8, suggesting a total of three field clusters. There was a perfect match between

low, moderate, and high cluster groupings and plot memberships determined from the cluster

analysis method and from rank ordering and identification of 25% changes in biomass index

method discussed earlier. Clusters were computed for imagery reflectance values selected

from: all image channels, NIR channel, NIR and NDVI channels, red channel, and all image

channels except NDVI. Figure 5 is a dendrogram of the red channel, the channel that

resulted in cluster membership most nearly identical to the field data cluster members. Red-

channel clusters correctly separated out *P. australis* plots phrag21 and phrag22 as members

of the high biomass index class. Low biomass index class correctly identified plot members

phrag24 and phrag27, while plot member phrag26 plot was incorrectly included within the

low biomass index class. An "all-image-channels" combination attempt was also largely

successful, but it failed to group correctly low biomass index class members (phrag24 and

phrag27) together within the very first clustering step. The other three image channel

combination attempts (NIR, NIR and NDVI, and all-image-channels-except-NDVI) resulted

in class memberships that did not match the field data.

Image channel data was evaluated using ANOVA and Tukey tests. One-way analysis of

variance results were computed using the average digital numbers (reflectance values) for

each channel as the dependent variable and the classes codes 1, 2, 3, representing low, moderate and high biomass index, as the independent variable. Results are given in Table 4. The red-, green-, and NDVI-channels were significant at the 95% confidence with 9 d.f. (Red: F-stat = 14.98, p-value = 0.003; Green: F-stat = 6.57, p-value = 0.02; NDVI: F-stat= 5.92, p-value = 0.03). A post-hoc comparison Tukey test was performed to determine which *P. australis* biomass index classes were most different from another, based on all image channel reflectance values. Post-hoc comparison techniques specifically took into account the fact that more than two samples were taken in this test (in this case 3 biomass index classes). Tukey difference between the low- and high-biomass index classes was 0.08, and between the moderate and high biomass index class was 0.36. An additional Tukey test was computed for the red-channel reflectance values only and the differences between the low and high index classes was 0.002, and between the moderate and high biomass index class was 0.09. Tukey results are given in Table 5. Multiple regression test results report a significant (p-value= 0.004, d.f. = 9) and high score (r^2 = 0.97) for all five image channel reflectance values. A forward stepwise regression identifies four image channels (green, blue, red, NIR) as contributing to the overall prediction, with the red-channel explaining 79% of the variance; red and NIR explaining 85% of the variance; red, NIR, and green explaining 90% of the variance; and red, NIR, green, and blue explaining 96% of the variance. The NDVI index contributes 1% additional explanation (Table 6. Stepwise multiple regression results for imagery channel reflectance values prediction of biomass index class).

These results indicate that identification of structural changes in *P. australis* can be remotely differentiated by high spatial resolution multispectral imagery. The green-channel,

red-channel, and NDVI were each statistically significant in defining biomass index class. The red-channel reflectance values achieved better F, r^2, and p-value analysis of variance scores, and were responsible for the generation of clusters and cluster members most equivalent to the field data clusters. Tukey test results for all- image channels suggested that there was very good separability between the lowest biomass index class and the high class. The 0.36 score indicated it would be difficult to classify a *P. australis* site confidently as high versus classifying it as moderate. A measure of confidence (e.g., 64% confident the site is high biomass index) could be a preliminary consideration but additional sample field plots would be needed to address confidence levels adequately. A solution could be to use only the red-channel as Tukey separability results were excellent for this channel alone. A score of 0.002 indicated that red-channel reflectance differences could be used to distinguish a *P. australis* site correctly between low and high biomass index classification 499 out of 500 times. Separability between moderate and high biomass index classes reported a score of 0.08, meaning that more than 90% of the time the two classes could be correctly distinguished one from the other. An r^2 value of 0.79, for the red-image channel in predicting biomass index class, suggests that 21% of the variance in the prediction has not been explained. Inclusion of the green-, blue-, and NIR-channels eliminated 18% of the unexplained variance in this data set, as reported by stepwise multiple regression result r^2 = 0.97.

Remote identification of individual structural variables (stand height, stem count, culm diameter, under story per cent) is not suggested as a result of this work. Rather, each of the structural variables measured in the field contributed to an understanding of total plot

biomass computed from equation 1 algorithm. Conversion of the raw field measurements into normalized scores was necessary to reduce the importance of stem count data and increase the importance of culm diameter and stand heights. With all three variables equally weighted, the algorithm to compute biomass indices enabled an overall comparison across field plots. Additionally, clusters and their members first computed from the non-normalized *P. australis* field variables did not match with clusters and members computed from the imagery reflectance values.

Discussion

The original null hypothesis, H_{o1}-imagery reflectance values are not related to *P. australis* biomass index, was rejected. Following a normalization of *P. australis* stem count, stand height, and culm diameter data, Ward's method of cluster analysis demonstrated similar agreement in field plot groupings derived independently from the field data and the imagery red channel reflectance values. This finding suggests that the imagery red channel alone was able to distinguish biomass index differences of the *P. australis*. The clustering did not suggest an ability to rank order the field plots from high to low. Once a plot has been rank ordered by field investigation into a high, moderate or low biomass index class, all additional plots within the remotely sensed grouping could be considered to be of the same biomass index class. Additionally, statistical tests for ANOVA and stepwise regression affirmed a relation between the red channel reflectance values and the grouped field plot data.

Red channel mean reflectance values per sample plots followed an inverse pattern with biomass index values. Table 7 relates highest red reflectance values to lowest biomass values. The data are evidence of the chlorophyll absorption capacity of the 650nm-centered red channel, where higher *P. australis* biomass resulted in less reflected energy for the airborne camera to record. Conversely, lowest biomass index plots reflected the highest amounts of energy in the red channel, despite the existence of a *S. patens* herbaceous understory. Figure 6 illustrates the relationship between red channel reflectance, recorded in digital numbers (0-255), and the biomass indices classed into low, moderate, and high groupings.

Remote sensing enabled an assessment of the quantitative differences in *P. australis* biomass. A logical following question to be addressed is: Is there a propensity for high biomass *Phragmites* (as classified remotely) to advance laterally first, before the remotely classed moderate and low biomass groups? An eventual goal would be to assess *P. australis* stands remotely and determine stands most likely to advance laterally. Fifteen constructed wetland plots under invasion by *P. australis* have been measured by Havens *et al* (1997) and could provide a baseline of information for evaluating lateral advancement. Spectral imagery would be needed over the sites. Rice *et al*'s (2000) work is particularly important as it showed highly established *P. australis* stands measured growth rates much lower than newly established stands. These findings suggest that moderate or low biomass stands, as identified from remote sensing, could be the most likely to advance.

Clearly, other factors have been shown to control the advancement of *P. australis* and were cited earlier in this paper, including salinity, oxygen, and period of inundation. Huggett (1995) suggests that multivariate statistical methods are the best strategy for investigating ecosystems. Given sufficient biomass, salinity, oxygen, age of stand (if known) and hydroperiod independent variable data, and annual lateral advancement of *P. australis* dependent variable data, a researcher could apply several multivariate techniques to investigate the contribution of each independent variable. This would better prepare managers for stands in need of immediate attention. Advancement of *P. australis* area across a landscape can be measured from a temporal series of remote images.

Much research on *P. australis* has focused on the biogeochemical conditions under which expansion occurs. Changes in vegetation patterns can be a direct expression of the response of a wetland ecosystem to manmade pressures such as population growth, surrounding development, freshwater withdrawal for industrial purposes (Havens *et al*, 1997), and tidal flow restriction behind manmade constriction structures (Roman *et al*, 1984). Inundation is minimized with increasing elevation above high tide, and so Rooth and Stevenson (2000) investigated the probable causes for elevation increase under *P. australis* stands. They found elevation increases over a short duration of time attributable to below substrate *P. australis* rhizome development and above ground litter accumulation. Rooth and Stevenson (2000) suggested that *P. australis* be considered as a potential control technique for combating sea level rise, but given the plethora of evidence provided by others that *P. australis* restriction of tidal flow impacts negatively on nutrient exchange from marsh to estuary, this option for sea level rise control seems unlikely to be implemented.

Subsequent research should test the ten original plots examined for this work. Area measurements can be completed using imagery analysis tools. If such research confirms that high biomass stands do expand their aerial extent before lower biomass stands, a shift in *P. australis* monitoring and management methodologies would be warranted. Remote prediction of lateral expansion would help to target remediation efforts to those sites at greatest risk only.

Conclusion

Phragmites australis was characterized remotely using high spatial resolution airborne multi-spectral imagery. Different spectral reflectance values were observed across monotypic reed-stand sample plots, believed to be representative of structural differences such as stand height, stem counts, average culm diameter and herbaceous understory cover per cent. Reflectance values were acquired from the imagery at ten sample locations, followed by field measurements of the four structural variables cited above at coincident geographic locations on the ground. Field data were normalized and biomass index values computed for each plot.

Field plots were classified manually into one of three groups based on the computed biomass index values: low, moderate and high. A statistically objective approach confirmed these classes and the membership of sample plots within each class. A dendrogram of the raw field data (Variables: "average stand height", "average culm diameter", and "stem count") from Ward's method with euclidean distance measures revealed three identical

groups of equivalent sample plot members. Dendrograms of the sample plot reflectance values were compared with the pattern and structure of previously defined field data clusters and their members. Red-channel reflectance values came close to a direct match, misclassifying only one sample plot from the moderate to the low biomass class. Perhaps most importantly, a high biomass class was clearly separated with correct *P. australis* sample plots selected as members of the cluster.

Analysis of variance and multiple regression testing confirm that red-channel reflectance values were best for predicting low, moderate, and high *P. australis* biomass index field classes. The addition of a green-, blue-, and NIR-image channel increased the predictive power of image reflectance values to classify *P. australis* into low, moderate and high biomass classes from 0.79 for the red-channel alone to 0.97 for all image channels.

Phragmites australis has been described as an aggressive eastern United States species that merits the continued attention of natural resource managers. Understanding the physical, chemical and biological processes under which this invader might likely expand is critical. Management activities that increase tidal flow across a marsh should increase salinity and inundation, decrease oxygen and potential for sediment build-up, and thereby hinder the ability for *P. australis* to propogate laterally (Roman *et al*, 1984; Havens *et al*, 1997; Weinstein and Balletto, 1999). Long-term research is needed to examine the rate of spread of *P. australis* into established communities (Keller, 2000). Related future research is specifically needed to examine the expansion rates of high-density *P. australis* (as measured from remote sensing) to determine if these stands are indeed the first to laterally expand at

the expense of adjacent communities. Remote sensing could have potential value as an early warning detection system for the identification of stands most prone to expansion. As *P. australis* expands in territory, elimination of higher value communities and overall decline in ecosystem health characterized by loss of plant diversity/complexity, loss of shelter/habitat, and decline in food source is potentially at stake.

References

Able, K.W. and Hagan, S.M., 2000. Effects of common reed invasion on marsh and macrofauna: response of fishes and decapod crustaceans. *Estuaries*, 23 (5): 633-646.

Amsberry, L., Baker, M.A., Ewanchuk, P.J., and Bertness, M.D., 2000. Clonal integration and the expansion of *Phragmites australis*. *Ecological Applications*, 10 (4): 1110-1118.

Cross, D.H., and Fleming, K.L. 1989. Control of *Phragmites* or common reed. Fish and Wildlife Leaflet 13.4.12. Washington, DC: U.S. Department of the Interior, Fish and Wildlife Service. 5 p.

Gross, M.F., Hardisky, M.A., and Klemas, V., 1989. Chapter 11- Applications to coastal wetlands vegetation. In Theory and Applications of Optical Remote Sensing, ed. Ghassem Asrar, John Wiley and Sons, New York.

Hardisky, M.A., Gross, M.F., and Klemas, V., 1986. Remote sensing of coastal wetlands. *BioScience*, 36: 453-460.

Haslam, S.M., 1969. The development and emergence of buds in *Phragmites communis* Trin. *Annals of Botany*. 33: 289-301.

Havens, K.J., Priest, W.I., and Berquist, H., 1997. Investigation and long-term monitoring of

    Phragmites australis within Virginia's constructed wetland sites. *Environmental*

    Management, 21 (4): 599-605.

Hellings, S.E., and Gallagher, J.L., 1992. The effects of salinity and flooding on *Phragmites*

    australis. *Journal of Applied Ecology*, 29 (1): 41-49.

Keller, B.E.M., 2000. Plant diversity in *Lythrum, Phragmites*, and *Typha* marshes,

    Massachusetts, USA. *Wetlands Ecology and Management*, 8 (6):391-401.

Leithead, Horace L., Yarlett, Lewis L., Shiflet, Thomas N. 1971. 100 native forage grasses in

    11 southern states. Agricultural Handbook 389. Washington, DC: U.S. Department of

    Agriculture, Forest Service, 216 p.

Levine, J.M., J.S. Brewer, and Bertness, M.D., 1998. Nutrients, competition, and plant

    zonation in a New England salt marsh. *Journal of Ecology*, 86: 285-292.

Marurran, A.E., 1988. Ecological Diversity and Its Measurement, Princeton University

    Press, New Jersey.

Malcaewski, J., 1999. Chapter 4- Evaluation criteria. In GIS and Multicriteria Decision

    Analysis, John Wiley & Sons, Inc., New York.

Marks, M., Lapin, B., and Randall, J., 1994. *Phragmites australis* (P.communis): Threats, management, and monitoring. *Natural Areas Journal*, 14:285-294.

Meyer, D.L., Johnson, J.M., and Gill, J.W., 2001. Comparison of nekton use of *Phragmites australis* and *Spartina alterniflora* salt marshes in the Chesapeake Bay, USA, Marine Ecology Progress Series, Volume 209, 71-84.

National Oceanic and Atmospheric Agency, 1988. Freeze/Frost Data (Climatography of the U.S., No. 20, supplement No. 1).

Pyke, C.R., and Havens, K.J., 1999. Distribution of the invasive reed *Phragmites australis* relative to sediment depth in a created wetland. *Wetlands*, 19 (1): 283-287.

Rice, D., Rooth, J., and Stevenson, J.C., 2000. Colonization and expansion of *Phramites australis* in upper Chesapeake Bay tidal marshes. *Wetlands*, 20 (2): 280-299.

Roman, C.T., Niering, W.A., and Warren, R.S., 1984. Salt marsh vegetation change in response to tidal restriction. *Environmental Management*, 8 (2): 141-150.

Rooth, J.E., and Stevenson, J.C, 2000. Sediment deposition patterns in *Phragmites australis* communities: Implications for coastal areas threatened by rising sea-level. *Wetlands Ecology and Management*, 8 (2-3): 173-183.

Silberhorn, G. M., 1999. Common Plants of the Mid-Atlantic Coast: A Field Guide. 3rd ed.,

The Johns Hopkins University Press, Baltimore.

Slocum, K.R., in work. Association of Vegetation Type to Elevation, Soil Type, and Soil

Compaction at Parramore Island, Virginia.

Sokal, R.R., and Rohlf, F.F., 1995. Chapter 13- Assumptions of analysis of variance. In

Biometry: The Principles and Practice of Statistics in Biological Research, W.H.

Freeman and Company, New York.

StatSoft, Inc, 1995. Statistica, General Linear Model: clustering, one-way analysis of

variance, and stepwise multiple regression (computer program), Vol. III, Tulsa,

Oklahoma.

Zar, J.H., 1999. Chapter 11- Multiple comparisons. In Biostatistical Analysis, 4th ed.,

Prentice-Hall, Inc., New Jersey.

http://www.fs.fed.us/database/feis/plants/graminoid/phraus/botanical_and_ecological_charac

teristics.html, Botanical and ecological characteristics, Species: *Phragmites australis*.

Table 1. Reflectance values of *P. australis* sample plots are provided. "Plots" represent the sample locations and "blue", "green", "red", "NIR" (near infra-red), and "NDVI" (normalized difference vegetation index) represent image channels, or indices, from the multi-spectral image source. Values are digital numbers from the imagery between 0 and 256.

Plots	Blue	Green	Red	NIR	NDVI
phrag20	84.1	92.3	29.8	50.3	160.0
phrag21	83.8	86.0	27.1	52.4	167.4
phrag22	82.6	89.7	27.5	60.8	175.0
phrag23	85.2	84.9	29.5	39.2	145.4
phrag24	90.6	101.3	35.1	49.6	149.7
phrag25	88.3	95.3	29.7	51.1	161.1
phrag26	91.8	99.1	33.8	53.9	156.7
phrag27	89.3	103.5	35.6	57.4	156.5
phrag28	84.6	91.7	30.6	47.1	154.6
phrag29	84.4	91.5	28.9	49.8	161.5

Table 2. *Phragmites australis* field data, prior to normalization. "Plots" represent the sample locations; "height-range" represents the minimum and maximum stand height in meters found at the sample site; "low height" is the minimum stand height in meters found at the sample site; "stems" are the number counted within a 1m quadrat equal to or greater than 1m in height; "under" is the percentage of herbaceous understory (typically *S. patens*) found within the plot; and "culm" is the average diameter in millimeters of all stems greater than 1m in height, measured within a quarter-quadrat, measured 15cm above ground level.

Plots	Height-Range (m)	Low Height (m)	Stems (#)	Under (%)	Culm (mm)
phrag20	2-2.5	2.0	152	0	6.0
phrag21	2.5-3.0	2.5	162	0	7.0
phrag22	2.5-3.5	2.5	216	0	7.6
phrag23	2-2.5	2.0	102	0	4.8
phrag24	1.5-2	1.5	39	55	3.1
phrag25	1.5-2	1.5	165	0	5.7
phrag26	1.5-2	1.5	273	0	4.7
phrag27	1.0-1.5	1.0	14	70	4.0
phrag28	1.5-2	1.5	172	50	4.2
phrag29	2-2.5	2.0	254	0	4.1

Table 3. Normalized field data are given, computed against data in Table 2 from a linear scale transform with maximum score procedure (Malczewski, 1999). In the following table, "plots" represents the sample plot location, "height" represents the normalized average plot stand height, "stems" represents the normalized number of stems in a sample plot, "culm" represents the normalized average diameter of stems measured 15cm above ground, "under" represents the normalized understory percentage of herbaceous plants, "biomass class" represents the categorical classification of biomass index value. "Biomass index" values are computed from the equation:

H * S * C = B, where
        H = average plot stand height
        S = stems per meter
        C = average plot culm diameter
        B = average plot biomass index

A *P. australis* categorical biomass class was assigned to each field plot. Three class groupings of biomass index values were computed, therefore, three categorical biomass classes were assigned. Biomass class 1 was named "Low", for low biomass, and contained plot members phrag24 and phrag27; biomass class 2 was termed "Moderate", and contained plot members phrag20, phrag21, phrag22, phrag23, phrag 28, and phrag25; biomass class 3 was called "High", and contained phrag21 and phrag22.

Plots	Height	Stems	Culm	Under	Biomass Index	Biomass Class
phrag20	0.8	0.56	0.79	0	0.35	Moderate
phrag21	1.0	0.59	0.92	0	0.55	High
phrag22	1.0	0.79	1.00	0	0.79	High
phrag23	0.8	0.40	0.63	0	0.20	Moderate
phrag24	0.6	0.14	0.41	0.55	0.03	Low
phrag25	0.6	0.60	0.75	0	0.27	Moderate
phrag26	0.6	1	0.62	0	0.37	Moderate
phrag27	0.4	0.051	0.53	0.7	0.01	Low
phrag28	0.6	0.63	0.55	0.5	0.21	Moderate
phrag29	0.8	0.93	0.54	0	0.40	Moderate

Table 4. One-way ANOVA results between reflectance values of image channels (and indices) are listed in the following table. For purposes of this test, phrag28 plot was identified as a member of biomass cluster "Moderate". The red-, green-, and NDVI-channels were significantly different at the 95% confidence with 9 degrees of freedom (Red: p-value = 0.003; Green: p-value = 0.02; NDVI: p-value = 0.03).

Image channel	r^2	F-stat	F-critical	p-value	df
Blue	0.49	3.30	4.74	0.10	9
Green	0.65	6.57	4.74	0.02	9
Red	0.81	14.98	4.74	0.00	9
NIR	0.36	1.97	4.74	0.21	9
NDVI	0.63	5.92	4.74	0.03	9

Table 5. Tukey test results for (a) all image channels and (b) red-channel reflectance values only. (a) A post-hoc comparison Tukey test was computed to determine which *P. australis* biomass index classes were most different from another, based on all image channel reflectance values. "Low", "mod", and "high" represent biomass index class designations. Post-hoc comparison techniques specifically took into account the fact that more than two samples were taken in this test (in this case 3 biomass classes). Tukey test results show that the difference between low- and high-biomass classes was 0.08, and between the moderate and high biomass class was 0.36. Tukey test results for all- image channels suggested that there was very good separability between the lowest biomass class and the high class. The 0.36 score indicated it would be difficult to classify a *P. australis* site confidently as high versus classifying it as moderate. (b) An additional Tukey test was computed for the red-channel reflectance values only and the differences between the low and high biomass classes was 0.002, and between the moderate and high biomass class was 0.08. A score of 0.002 indicated that red-channel reflectance differences could be used to distinguish a *P. australis* site correctly between low and high biomass classification 499 out of 500 times. Separability between moderate and high biomass classes reported a score of 0.08, meaning that more than 90% of the time the two classes could be correctly distinguished one from the other.

(a)

	Low (1)	Mod(2)	High (3)
Low (1)	-----	0.28	0.08
Mod (2)	0.28	-----	0.36
High (3)	0.08	0.36	-----

(b)

	Low (1)	Mod (2)	High (3)
Low (1)	-----	0.01	0.002
Mod (2)	0.01	-----	0.08
High (3)	0.002	0.08	-----

Table 6. Summary of stepwise multiple regression for all imagery channel reflectance values to test for estimation of biomass class. A forward stepwise regression identifies the order of the five image channels (green, blue, red, NIR) as contributing to the overall prediction, with the red-channel explaining 79% of the variance; red and NIR explaining a cumulative 85% of the variance; red, NIR, and green explaining a cumulative 90% of the variance; red, NIR, green, and blue explaining 96% of the variance, and lastly the NDVI contribution helping to explain 97% of the variance. Red channel results are highly significant (p-value = 0.00). "In/out" represents the stepwise order in which variables explained biomass class. These results indicate that identification of biomass index changes in *P. australis* can be remotely differentiated remotely by high spatial resolution multispectral imagery, with the red-channel alone explaining all but 21% of the variance in estimation of biomass class. Red-channel reflectance values achieved better p-values, and were responsible for the generation of clusters and cluster members most equivalent to the field data clusters.

Image Channel	+in/-out	Pearson's r	r^2	r^2 change	p-level
Red	1	0.89	0.79	0.79	0.00
NIR	2	0.92	0.85	0.07	0.12
Green	3	0.95	0.90	0.05	0.12
Blue	4	0.98	0.96	0.06	0.05
NDVI	5	0.99	0.97	0.01	0.30

Table 7. Biomass indices rank ordered, lowest to highest, with corresponding red image channel mean values for each plot location. Note that the low biomass classes have the highest red-means and the high biomass classes have the lowest red-means. This follows convention, as the red channel (650nm band center) is noted for vegetation absorption and areas with highest vegetation are absorbing energy and returning less reflected energy.

Plot ID	Red-means	Ranked Biomass Index	Biomass Class
phrag27	35.6	0.01	LOW
phrag24	35.1	0.03	LOW
phrag23	29.5	0.20	MOD
phrag28	30.6	0.21	MOD
phrag25	29.7	0.27	MOD
phrag20	29.8	0.35	MOD
phrag26	33.8	0.37	MOD
phrag29	28.9	0.40	MOD
phrag21	27.1	0.55	HIGH
phrag22	27.5	0.79	HIGH

Figure 1. Location Map of study site at Parramore Island, Virginia. Eighteen barrier islands make up a chain trending northeast-to-southwest off of Virginia's Eastern Shore. Parramore Island is the central-most island in this barrier chain. No permanent human population inhabits the island and activities such as agriculture, hunting, logging or similar activities are prohibited. The island is approximately ten kilometers long by one and a half kilometers wide and is separated from the mainland by a series of bays, salt marsh and small tidal creeks. Barrier island dune and valley complexes represent unique geomorphological conditions that support very distinct vegetation zonation. Homogenous stands of cattails (*T. angustifolia*) and common reed (*P. australis*) are found growing within Parramore Island's upper valley marshes. The high marsh also supports low-density, short-height marsh elder (*I. frutescens*) and groundsel-tree (*B. halimifolia*), found in co-existence with an herbaceous component that includes *S. patens* and *T. angustifolia*.

Parramore Island

3-33

Figure 2. Photograph of invading *P. australis* stand (left side) with *S. patens* shown in the foreground. The individual in the photograph provides an indication that the height of the stand is greater than 2m.

Figure 3. Bar chart of normalized *P. australis* field data, measured at each sample plot location, with "low" biomass plots grouped together on the left, "moderate" grouped in the center, and "high" grouped at the right side of the x-axis. Y-axis represents the normalized value of each structural legend attribute scaled from 0.00 to 1.00. X-axis gives the sample plot study site names. Bars shown in the plot represent average height, number of stems, average culm diameter, and percentage of understory. If an understory bar is not shown for a sample plot, the percentage is 0.

Phragmites australis field data
(Parramore Island, November 2000)
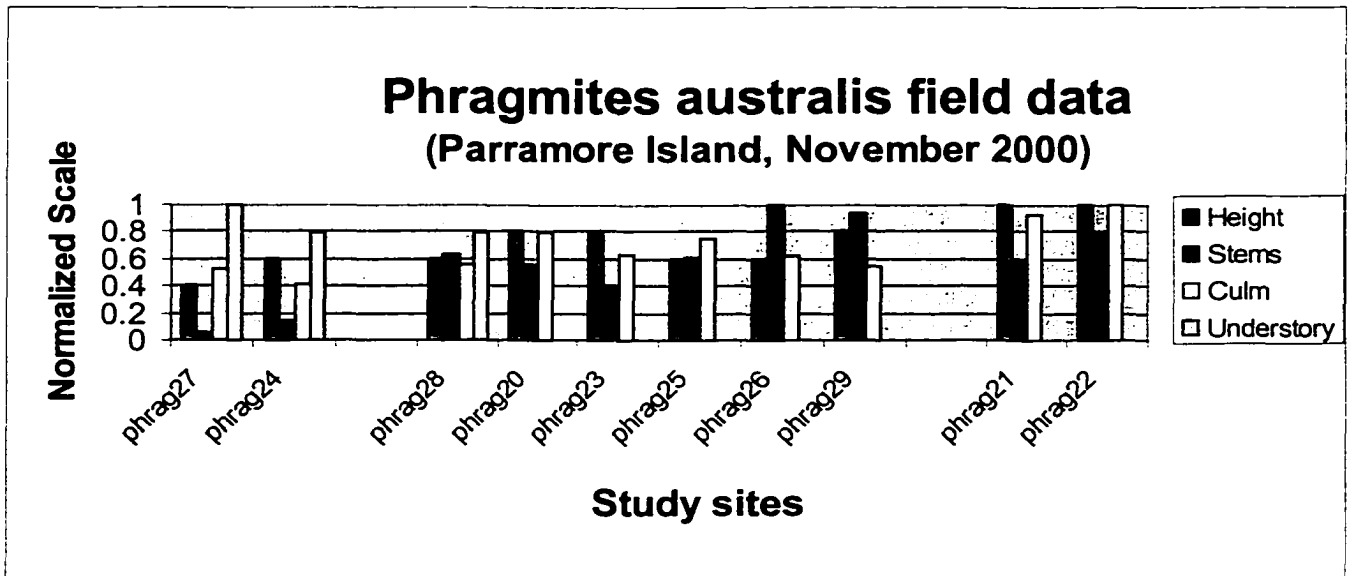
Figure 4. Dendrogram computed from Ward's method of clustering *P. australis* biomass index values, computed from normalized field plot data for stem count, stand height and culm diameter. Cluster analysis results suggest four clusters identified at linkage distance 0.4 to 0.8, or perhaps three clusters as identified at linkage distance 0.8. Regardless if four or three clusters are designated, there is a distinctive high biomass index class of *Phragmites australis* with plot members phrag21 and phrag22, and a low biomass index class with plot members phrag24 and phrag27. The remaining sample plots can either be separated into two classes (linkage distance 0.4 to 0.8) or combined into one class (linkage distance 0.8), representing the members to the moderate biomass index cluster.

Tree Diagram for 10 Cases
Ward's method
Euclidean distances
Computed from Normalized Stem Count, Stand Height, Culm Diameter
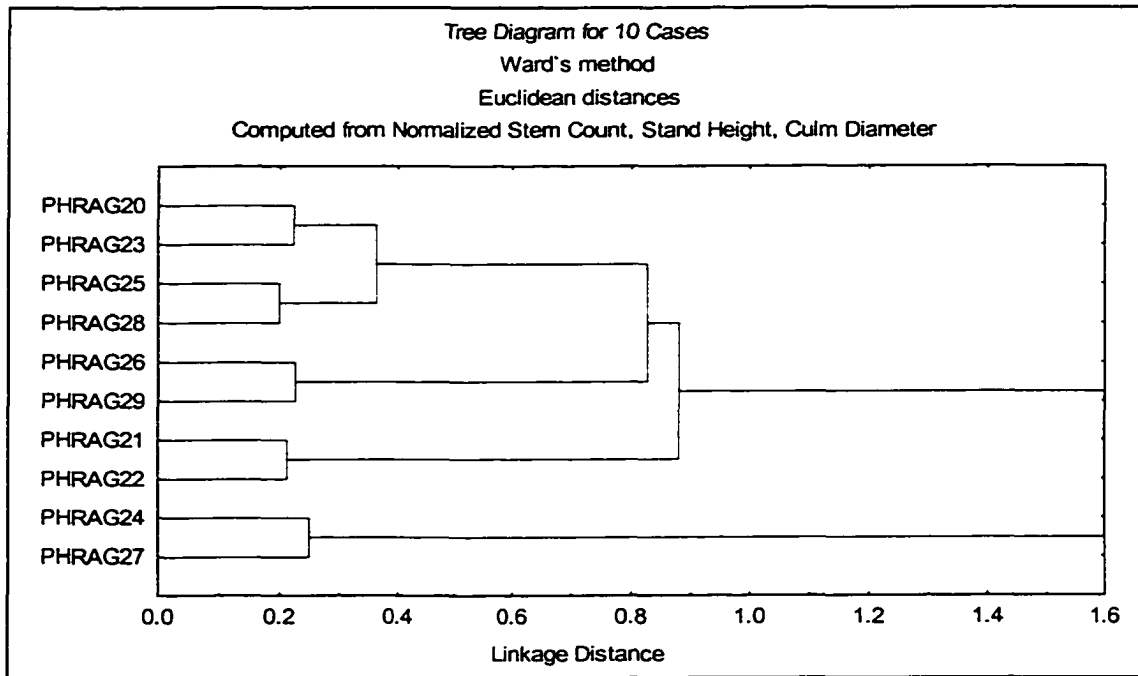
Figure 5. Dendrogram computed from Ward's method of clustering red-channel reflectance values, the channel that resulted in cluster membership most nearly identical to the field data cluster members. Red-channel clusters correctly separated out *P. australis* plots phrag21 and phrag22 as members of the high biomass class. Low biomass class correctly identified plot members phrag24 and phrag27, while plot member Phrag26 plot was incorrectly included within the low biomass class. Attempts at clustering other image channels, or combinations thereof, were unsuccessful at matching the field data clusters and class memberships.

Tree Diagram for 10 Cases
Ward's method
Euclidean distances
Imagery DNs Multispectral Red Channel (650 nm)
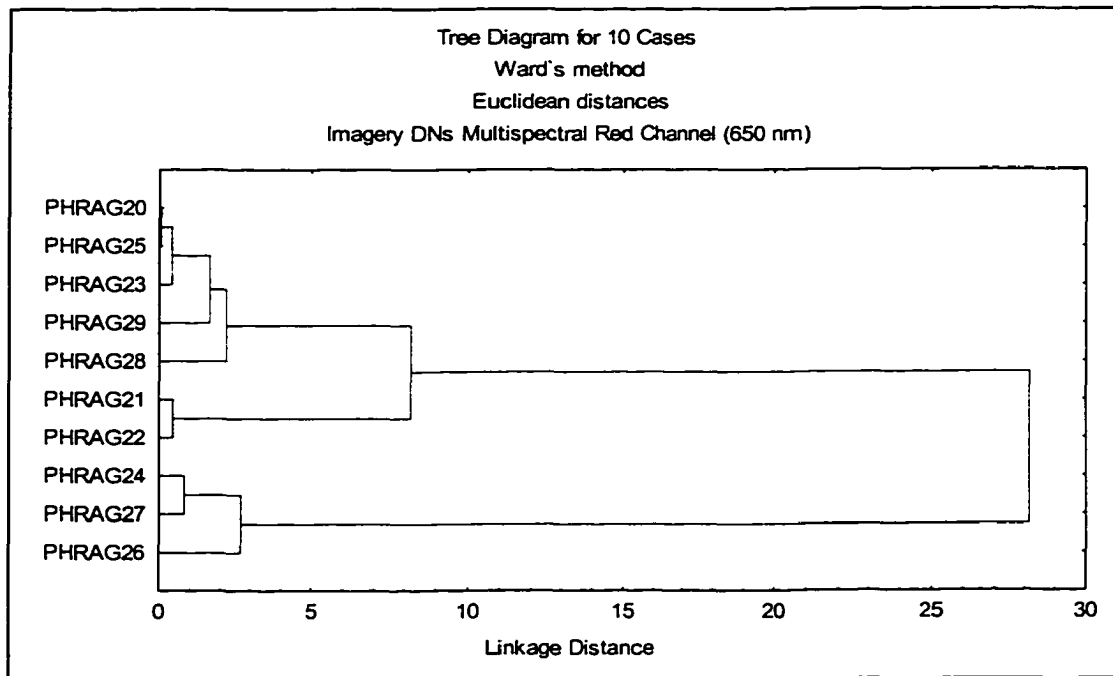
Figure 6. Biomass indices were rank ordered, lowest to highest, and graphed per field sample plot by their corresponding imagery red-channel digital number means. Note that biomass indices categorized low had the highest reflectance values while high biomass indices had the lowest reflectance values. This is due to the vegetation absorption characteristic of the 650nm red-channel wavelength in the electromagnetic spectrum. Areas on the ground with less vegetation return greater amounts of reflected energy. Only field plot "phrag26" showed an inclination towards higher red-channel DNs, which explained it's erroneous inclusion into the red-channel cluster low category.

Red-channel reflectance means

Means to Red channel DNs

Red-means

Phragmites australis field plot IDs

phrag27 phrag24 phrag23 phrag28 phrag25 phrag20 phrag26 phrag29 phrag21 phrag22
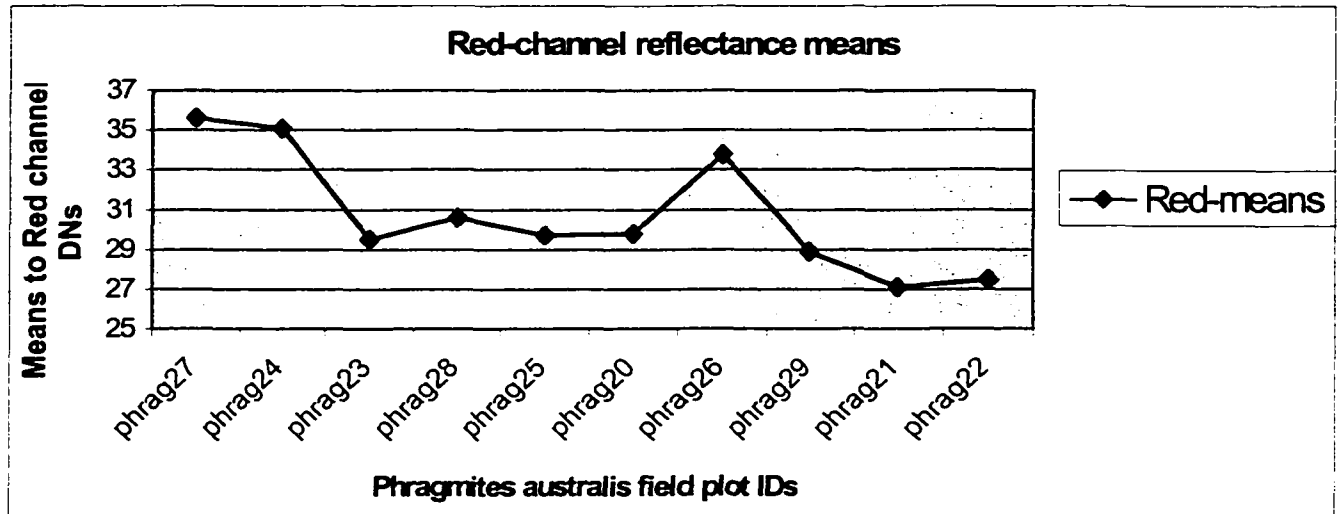
Chapter 3 to Chapter 4 Transition

This past chapter described that *P. australis* could be rank ordered into high, moderate, and low biomass index classifications. Even after a careful spectral and statistical classification process, there are often problems with an imagery-derived map product that are visibly evident to a user based on his or her knowledge of the environment and ecological processes. Chapter 4 addresses a post-classification method for corrective changes to imagery-derived landscape cover maps implemented using spatially explicit knowledge rules. Prototype corrective rules developed from textbooks, field experience, and gleaned from expert-knowledge, were subsequently developed into a spatial model within commercial image processing software. Geographic areas such as a coastal environment, and varying elevation strata within mountainous areas, are examples of zonal physiographic areas that lend themselves to general ecological rule correction. Revised landscape cover maps were compiled and the pre-and post-rule correction map products were compared.

Chapter 4

Prototype Ecology-based Models for Correcting Imagery–Derived

Vegetation Classification Errors

Abstract

Maps of imagery-derived classes might contain errors that are readily visible to the analyst and need automated correction. Simple "off-the-shelf" algorithms might not do the required correction. Eleven landscape classes generated previously from imagery were post-classified using a new set of rules. A review of the final map showed classes that should never have existed. Accordingly, a set of rules was developed combining the author's field experience on site and literature sources about barrier island complexes. This paper goes sequentially through a methodology in which ecology-based knowledge rules were translated into targeted corrections of incorrect vegetation classes. Rules were translated into conditional statements related to pixel adjacency and used neighborhood proximity and selected filtering options to eliminate or increase pixel classes. Targeted vegetation class corrections resulted in an improved end classification with more than 20% of the initially classified pixels converted to other classes. Over- or under-estimation of vegetation extent could adversely affect management decisions. In spite of the absence of an adjacency correction tool within ERDAS Imagine, modification to the existing modeling tools resulted in the implementation of a successful prototype for consideration and evaluation.

Introduction

It is probable that uncertainty in the assignment of various landscape classification cover types is a source of error that needs correcting (Wilkinson, 1996; Zhang et al, 2001). Visual identification of errors is often possible, especially to someone familiar to the area or with knowledge about the environment. Therefore, expertise about an area should improve the accuracy of the resulting map and should be incorporated into it when possible. Software image processing classification tools are available in many packages that address an entire image scene. Examples of such classifiers include discriminant analysis, maximum likelihood, minimum distance and contextual classifiers (Hubert-Moy *et al*, 2001). Contextual techniques were introduced to place prior constraints on pixel classifications usually based on neighboring pixels with the assignment of pixels based on neighboring spectral information and the thematic class of neighboring pixels (Landgrebe; 1980; DiZenso, 1987, Hubert-Moy *et al*, 2001). Following classification, other tools exist for correction of the imagery. For example, filters are often used to remove "speckle", or spurious pixels from a map. However, a ready to use tool that provides a user with the ability to target classification corrections to a particular cover classes as directly related to adjacency with another cover classes is does not exist as the author knows. Conventional contextual algorithms do not actually target corrections, and may perform well in one part of an image while performing poorly in another (Chalmond *et al*, 2001).

However, the commercially available tool that most closely approximates a targeted post-classification correction is the contextual algorithm. Pixel classification from contextual algorithms is based on the strength of the spatial relation to neighboring pixels in either a pre-

or post-classification phase and is called contextual classification (Kartikeyan *et al*, 1993; Fuller and Jones, 1995; and Stuckens *et al*, 2000). ERDAS Imagine (ERDAS, 1999) image processing software has a module that incorporates user knowledge into a post-classification process. However, when tested, the module was deemed to be inflexible because it could not achieve the type of correction results sought for this work. Rules designed to post-classify a map must maintain the original integrity of the correctly classified landscape. The framework, or methodology, in which rules are generated should be capable of modification to account for short- and long-term site condition changes. Sufficient flexibility in the way that the rule is constructed would encourage its wider use for many environmental study sites.

Remote sensing has been tested as a tool for ecosystem management. Nagendra (2001) reviewed the potential from remotely sensed data for mapping vegetation directly and for determining habitat suitability indirectly. Nagendra identified conditions under which remote characterization of biodiversity is possible and insists that there is continued need for relating field and spectral image data. Wessman *et al* (1998) said that remotely acquired imagery can be used to detect ecosystem processes and landscape relationships, such as edge configuration, habitat area, fragmentation, and human use. Cihlar *et al* (2000) found that land cover is a key for land use and land management decisions as it is a critical biophysical factor that determines the functioning of terrestrial ecosystems in biogeochemical cycling, hydrological processes, and interation between surface and atmosphere. Delbaere and Gulinck (1995) said that between 1987 and 1994, the journal *Landscape Ecology* published no papers that referred directly to remote sensing. Jennings (2000) acknowledges that

remotely sensed imagery has not been readily available in the past, and that accepted methods of classification based on ecology are now developed. The gap between landscape policy and remote sensing needs to be bridged, especially given the advantage of, among many cited benefits, remote sensing for vegetation cover mapping.

Incorporating prior knowledge into remote sensing classifications has predominantly been based upon image- or GIS-data. Mason et al, (1988) were among the first to investigate the use of digital map data as an ancillary source to assist in the segmenting and classifying of remotely sensed images. Tonjes *et al* (1999) attempted to automate the interpretation of imagery by using common *a priori* knowledge about a landscape. General rules provided data and model strategies for image classification including the use of topological relationships that provide information about neighboring properties of objects. Knowledge was transferred horizontally within the same layer and allowed constraints to be placed on the classification. Laferte *et al* (2000) proposed tree-based contextual techniques where a single classification was replaced by a set of classifications at multiple scales. Sanders and Tabuchi (2000) evaluated airborne radar for large-scale flood risk assessment to improve flood models. Quattrochi *et al* (2001) combined spectral land cover with thermal imagery to better understand heat island conditions in urban environments. Previous post-classification work includes attempts to improve accuracy within GIS to refine original map class boundaries based on zoning and demographic data (Harris and Ventura, 1995) and Hutchinson's (1982) work with post-classification sorting. Harris describes the use of post-classification rules as deterministic and best suited to areas with well-defined boundaries between cover types. Hutchinson describes the benefits of post-classifications as simple,

quick and easily implemented; efficient in dealing with problem landscape classes only; the ability to include multiple types of ancillary data in developing decision rules; and, the ability to easily create the decision rules.

The purpose of this project was to define a replicable method for post-classification correction of an imagery-derived landscape class map. The aim of this method was to target incorrect pixels for correction based on their topological inter-relationship and sound ecological principles.

Methods

Study site

Parramore Island, Virginia, a vegetated transverse dune and valley barrier island, was selected as the study site to demonstrate the correction of incorrectly mapped landscape pixels using ecological knowledge. There is sufficient understanding of mid-Atlantic barrier islands and coastal wetland ecosystems in general (Scott, 1991; Mitsch and Gosselink, 1993; Silberhorn, 1999) and specific knowledge of Parramore Island's ecological relationships (Slocum *et al*, in work). Spatial relationships between vegetation species are clearly evident on Parramore Island, as well as at other mid-Atlantic coastal sites. Lowest elevation grass communities (eg., *Spartina alterniflora,* Loisel) are adjacent to and are inundated daily by saltwater. These typically expansive monotypic stands change to higher marsh reed, grass and sedge communities exhibiting greater diversity across an exceptionally narrow elevation range (e.g., *Spartina patens, Distichlis spicata, Typha angustifolia and Juncas roemerianus*). It is common to find invasive *Phragmites australis* in this higher salt marsh environment,

also. At the edges of the high marsh, at the base of the Parramore Island's dune formations, are small shrubby communities of *Iva frutescens* and *Bacharris halimifolia*. Moving up the dune side slope one next encounters high-density shrub communities such as *Myrica cerifera*. At Parramore, this zone of vegetation was generally from 10 and 20 meters wide. Finally, *Pinus taeda* was the dominant species of the maritime forest that occupied the mid- and top-slopes of the dunes. This ecological ordering of vegetation was a recurring sequence that seems to be controlled by hydrogeochemical processes, such as hydrologic cycling of fresh- and salt-water, subtle changes in elevation, and soil strength (Oertel and Kraft, 1994; Hayden *et al*, 1995).

A dune and valley barrier island complex functions geographically in such a way that the spatial pattern is generally parallel to the main coastline and beach-front (Ahnert, 1996). The back-bay side of a barrier island is protected from storm events and most aeolian sand accretion (Hayden *et al*, 1995). On the other hand, the beach side of the complex has primary and secondary dunes in parallel to the main shoreline, with beach grasses commonly thriving in these environments (Christensen, 1988). The accretion zone of a barrier island provides habitat that is suitable for beach grasses (Christensen, 1988; Shao *et al*, 2000). This zone is easily identified at Parramore and other mid-Atlantic islands by the drumstick-like shape caused by island rotation and long-shore transport of sands (Scott, 1991). These sandy beach- and channel-side areas are higher in elevation and naturally much drier than the valley complexes (Hayden *et al*, 1995). Winding creek channels provide a daily conduit for the introduction of tidal salt water to penetrate the lower, and sometimes upper, marsh communities with creek meanders indicating level landscape areas with uniform soil

conditions that provide little structural resistance to lateral relocation of the channel (Ahnert, 1996). Soil in the marsh, especially low marsh, is typically clay and silt-laden sediment delivered by the tides (Ahnert, 1996).

Multispectral imagery was obtained for the island at a ground resolution of approximately 1.5-meters in May 1999. The pixels from the image were classified into 11 total classes, including 9 vegetation classes. An 11-classification map product (with 9-vegetation classes). There was no extensive image processing to improve the aesthetic appearance of the map. An examination of the classes on the map revealed problem areas in need of correction; these will be described below.

Landscape Classification

Spatial ecology-based knowledge was incorporated as part of the following sequence: (1) ascertain or identify ecological rules, or knowledge, pertinent to the geographic study area; (2) identify classification problem areas from the ecological knowledge acquired about the study area; (3) convert study area knowledge into IF-THEN-ELSE rule structure and; (4) convert IF-THEN-ELSE statements into an ERDAS Imagine spatial modeling environment using modified tools included in Imagine. Steps within this sequence were briefly examined and are provided later. Map corrections were applied using a prototype methodology and the accuracy of a new landscape classification map was reassessed in terms of changes in the area of cover type. Pixel classes changed as a result of the new model were verified from field information. Multiple rules can easily be developed for any study site, but in

preference, a single spatial model was created to show that individual rules can be incorporated into one large combined model.

The integration of user-defined knowledge that specifically targeted particular classes based on the spatial strength of neighboring pixels was not considered. Rather, rule development was developed from field expertise and related literature sources (Scott, 1991; Mitsch and Gosselink, 1993; TNS, 1995). Pixels that were incorrectly classified into vegetation landscape classes, inconsistent with an expected ecological spatial distribution, were corrected based on user-defined rules acting upon the spatial relationships of the vegetation data alone. A low-pass 3-pixel by 3-pixel filter was applied as a preliminary processing step, prior to the ecology-based rule model, to remove any spurious, unwanted "speckle" from the landscape classification.

The landscape classes derived from image exploitation included 9 vegetation types, sand, and water. Vegetation was classed at both the species and community level. A supervised classification using a maximum likelihood classifier algorithm was used to obtain the class maps. A map of classes was considered to be the final product. Application of a rule-based correction model aimed to improve each of the classifications provided. The class themes were:

1. *Spartina patens* (salt meadow hay);

2. *Spartina alterniflora* (cordgrass);

3. *Myrica cerifera* (wax myrtle) constituting high density shrub;

4. *Iva frutescens* (marsh elder) and *Baccharis halimifolia* (groundsel tree) together

   constituting low density shrub;

5. *Typha angustifolia* (cattails);

6. *Phragmites australis* (common reed);

7. *Pinus taeda* (loblolly pine) dominant within the maritime forest;

8. *Ammophila breviligulata* (dune grass);

9. *Juncus roemerianus* (black needlerush);

10. Sand;

11. Water.

Four principal steps defined the prototype methodology for including knowledge

rules into a post classification correction. The study site description presented earlier

provided all the background information necessary to formulate general knowledge rules.

This background knowledge defined the first step. Second, six independent mis-

classification problem areas were identified from the class map using the ecological

knowledge acquired about the study site in step one. Third, all classification problems were

translated into computer programming language, with IF-THEN-ELSE statements compiled

for the correction of the mis-classified pixels. Fourth, ERDAS Imagine's Spatial Modeler

module was adopted for incorporating conditional corrective statements compiled in step 3,

together with existing image processing algorithms for neighborhood size and focus majority

filters. Spatial Modeler provided a suitable framework for rule development that would

make the modeling technique available to other users and would facilitate modification of the

rules in the future. Ultimately, a single large spatial model was written that incorporated all

six corrections identified. The changes could also have been done as 6 independent spatial models. Corrections were tested individually on small segments of the map, followed by the integration of individual models into the large comprehensive model that acted sequentially upon and updated corrections to the entire landscape map.

Results

Problems in the vegetation classification map were identified by examining each landscape class, one at a time. Several factors were considered during this visual assessment of landscape class accuracy, including daily tidal inundation, expected location of vegetation along beach side dunes, anticipated neighboring vegetation classes, and implications of shadows from the forest. For efficiency in the project, six representative problem areas were selected and examined for post-classification error correction. Additional difficulties with the original classification were discovered that could have been addressed (e.g., forest adjacent to low density shrub, *P. australis* within the forest, and *S. alterniflora* adjacent to forest) but were not selected for correction to simplify the investigation.

The first issue for correction was erroneously classified pixels of high-density shrub spuriously located within the *S. alterniflora*. High-density shrub vegetation would not be found immediately adjacent to the lower marsh community without an intermediate high marsh community. *Spartina alterniflora* is typically a monotypic community without interspersed competing species. Therefore, conversion of high-density shrub pixels to *S. alterniflora* was warranted. A second problem was tracts of low-density shrub pixels directly adjacent to maritime forest pixels. High-density shrub community would be expected

between these two communities. Accordingly, the question was not whether these pixels should be changed to high-density shrub, but rather, which vegetation class was incorrect and in need of conversion. It was the maritime forest classified pixels that needed to be changed based on information from two sources available at earlier image processing steps: first, a low transformed divergence score for class separability was recorded between high density shrub and maritime forest and a high score for separability between low-density and high-density shrub classes; second, a low producers accuracy assessment score (columnar scores based on reference field data) was computed for high density shrub class attributable to an over-classification of the maritime forest class. Accordingly, maritime forest adjacent to low density shrub needed to be converted to high-density shrub. The width of pixel conversion was determined to be 10 meters based on observations in the field. A third correction needed was the elimination of *A. bevigulata* in areas of the back-bay, which was located within the *S. alterniflora* class. Dune grass was not expected in the lower back marsh between the barrier island and the main-coastline, but rather along the island's beach front dunes or the drumstick-shaped, accreting end of the island where dune formation was prevalent. A fourth correction was to eliminate small pockets of *S. alterniflora* identified in upland areas. A lack of meandering creeks that occur only in the silt and clay of the lower marsh communities and the adjacency of *S. alterniflora* pixels to upland vegetation were the determining factors in the need for correction. Sand was eliminated from the sound-side *S. alterniflora* marsh as a fifth correction. This is an area of silt and mud. Lastly, pixels were incorrectly classed as *S. alterniflora* within beach-front coastal dunes probably due to the effects of shadows from the maritime forest.

Corrections required to improve the landscape classification were coded into logical IF-THEN-ELSE statements. The following conditional statements satisfy the correction needs cited above.

1) IF vegetation class = high-density OR low-density shrub pixel AND the pixel is adjacent to *S. alterniflora* pixel, THEN reclassify the pixel as *S. alterniflora*, ELSE do not change the pixel class.

2) IF vegetation class = low-density shrub pixel AND the pixel is adjacent to maritime forest pixel, THEN reclassify the maritime forest pixel as high-density shrub within a buffering distance of 10 meters (or approximately 7 pixels), ELSE do not change the pixel class.

3) IF vegetation class = *A. bevigulata* pixel AND the pixel is adjacent to *S. alterniflora* pixel, THEN reclassify the pixel as *S. alterniflora*, ELSE do not change the pixel class.

4) IF vegetation class = *S. alterniflora* pixel, AND the pixel is adjacent to *S. patens*, OR *T. angustifolia*, OR *P. australis*, OR low-density shrub, OR high-density shrub, OR maritime forest, AND the *S. alterniflora* pixel originates from within a small isolated pocket of *S. alterniflora* pixels whose maximum width is less than or equal to 20 pixels**, THEN reclassify the pixel as *S. patens*, ELSE do not change the pixel class.

5) IF vegetation class = Sand pixel, AND the pixel is adjacent to *S. alterniflora* pixel, THEN reclassify as *S. alterniflora*, ELSE do not change the pixel class

6) IF vegetation class = *S. alterniflora* pixel, AND the pixel is adjacent to sand pixel, THEN reclassify the pixel as sand, ELSE do not change the pixel class.

**Small isolated pockets of *S. alterniflora* were defined as 20m in width or less. The expectation was that 20m was sufficiently large to eliminate all unwanted *S. alterniflora* pixels, while still maintaining a reduced existence of legitimate *S. alterniflora*. All remaining legitimate *S. alterniflora* was then restored, or grown back, to its original size by reversing this correction step by 20m.

The ERDAS Imagine Spatial Modeler module allowed for existing algorithms to be easily combined together. Functionality to accomplish the IF-THEN-ELSE conditional statements were effected within existing capabilities of Imagine. The sequence in which models were started and completed was important. Corrections that affected the smallest number of pixels were completed first, and corrections that affected the greatest number of pixels were best completed last to make the process efficient. When small areas of misclassified pixels were not eliminated early in the sequence of model correction steps, they were invariably acted upon by following steps in the model that magnified their existence. An approach that minimized this difficulty was the identification of all corrections needed for post-classification at the outset, ordering the identified corrections into a smallest-to-largest sequence, and implementation of the rule-based modeling steps in the equivalent order.

It was tempting to address the elimination of unwanted pixels adjacent to multiple landscape classes in the hope of reducing the number of modeling steps necessary for correction. However, to do this in one step made the converse process of returning legitimate pixels to their original class size impossible. It was not possible to know initially which class(es) needed to be restored to their correct size. When changes were completed incrementally, one at a time, this problem was solved. Removal of pixels was sensitive to the size of the neighborhood window and type of filter employed. A custom-defined "majority filter" was applied that assigned each pixel into a vegetation class based on the majority of pixels belong to a vegetation class within the window. The filter window acted upon only those desired classification corrections identified by the IF-THEN-ELSE conditional rule statements. These rules were easily recoded and incorporated into the Focal Use- Majority Filter model through "USE-at" and "APPLY-at" options, enabled the targeting of corrections while maintaining the integrity of the remainder of the classification.

The final ERDAS spatial model integrated fifteen custom developed filters to address specific land cover classification errors identified from an imagery-derived map. A segment of the rule-based model designed under the Spatial Modeler is given as Figure 1 and an example of the functional syntax of the model is provided in Figure 2. The model may be copied, modified, and re-used.

Change attributable to model correction was assessed by identifying all pixels that were different from the original classification and model-corrected classification. A difference map was created from these changes. The percentage of pixels changed was

computed. Changes to the original vegetation classification map were substantial. Over 20 per cent (173 hectares out of a total of 850 hectares) of the land cover classes were re-classified by the ecology-based rules. Table 1 provides an example of 101 randomly located sampling points that coincide with changed landscape pixels. Fifty-one sample points were changed from class 7 (maritime forest) to class 4 (low-density shrub); thirteen sample points were changed from class 4 to class 3 (high-density shrub); and ten points from class 7 to class 3. The remaining 26 sampling points were evenly divided across 10 additional land cover class changes.

Vegetation classes were determined at each of the 101 sample locations for the original and post-classification map. Each change was evaluated against the modeling rules that were established to correct for errors. All changes between the original and post-classification samples were arrived at justifiably as a result of the rules. Total area for each landscape class was recorded for the pre- and post-classification correction modeling. An increase in area occurred for sand (3ha), *T. angustifolia* (3ha), low-density shrub (45ha), high-density shrub (24ha), and *S. patens* (12ha). Decreases in area were observed for *A. breviligulata* (6ha), maritime forest (64ha), and *S. alterniflora* (16ha). Changes in areas did not occur for *P. australis*, water, or *J. roemerianus*, as there were no rules to adjust these classes.

Several derivations of the imagery–derived vegetation map are provided for comparison. Figure 3a is the original multispectral imagery over Parramore Island shown in a false-color 4-3-2 band representation. Imagery was collected on May 30, 1999, from 1155

to 1257 local solar time. Eleven flightlines were flown south to north at an altitude of approximately 3,000 meters above mean sea level, which resulted in a nominal pixel size of approximately 1.5 meters. Figure 3b is the initial classification of the land cover classes from the raw imagery, prior to the application of any rule-based classification to improve the results. Figure 3c shows the resulting map compiled after running the spatial model and making corrections to the original class map. Legends for Figures 3b and 3c identify area in hectares of each class change. Increases and decreases in hectares correspond with the requested model corrections to the original classification. The spatial pattern is more reasonable, with speckle and misclassified pixel areas removed. The homogeneity typically found in vegetation complexes of the barrier island are evident in Figure 3c; this was not the case prior to the corrective actions applied to Figure 3b. Finally, Figure 3d is the difference map between Figures 3b and 3c, depicting those pixels affected by the incorporation of the rules. The difference pixels in Figure 3d present definite spatial pattern, oriented in a southwest to northwesterly trend, probably attributable to the distinctive geomorphology and corresponding vegetation zones found on the barrier island. Location of likely ecotones between maritime forest and high-density shrub communities are observable in this map also.

Changes to each class map were examined by enlarging the pre-and post-correction rule results. Figure 4 shows high- and low-density shrubs existing within a *S. alterniflora* community (original classification) and the subsequent removal of these shrub pixels from this lower marsh (corrected classification). Much of this erroneous classification can be attributed to a collection of wrack (dead grass and reeds) that had accumulated in small pockets of the lower marsh during earlier tidal events. Figure 5 shows *A. breviligulata* and

sand patches interspersed within a *S. alterniflora* community (original) and the removal of these pixel classes from the lower marsh (corrected). Sediment is typically silt or mud, and not sand, and beach grass would not survive in this halophytic environment. Figure 6 shows small isolated *S. alterniflora* patches within *S. patens* and maritime forest immediately adjacent to low density shrub (original) followed by the removal of *S. alterniflora* patches and with the forest edges replaced by additional high density shrub (corrected). Figure 7 demonstrates an incorrect classification of *S. alterniflora* in the near-shore beach-front (original) followed by its substantial reduction (corrected).

Depending on the purpose of the user of the landscape land cover information, one might envisage adjusting the classes to which pixels belong to give certain classes more emphasis. In either case, the aim should be to change only those pixels deemed to be in error and not to affect those that are correctly classified. Selection of an appropriately sized neighborhood window ensured that correct pixels were not inadvertently eliminated and incorrectly assigned pixels were the only ones permanently converted to an alternative, user defined class. By correcting misclassified pixels to the correct class and obtaining the correct aerial extent of this class, restoring legitimate pixels to their original aerial extent was achieved by always either adding the pixels back using an equivalent window size to that used for elimination of pixels or, vice versa, eliminating pixels by using an equivalent window size used for growth of pixels in a preceding model step. For example, IF-THEN-ELSE conditional statement number four removed clumps of mis-classified pixels that were 20m or less in size from the *S. alterniflora* class. Once mis-classed pixels were eliminated,

4-19

legitimate pixels were returned to their original aerial extent by reversing the proceeding step and growing pixels back.

Discussion

As Harris (1995) suggested, areas with well-defined land cover types, such as a coastal zone, are ideal for post classification deterministic rule development. The Parramore Island study site presented many general ecological deterministic rules that could be modeled. Rules were easily defined and implemented and the impact on the classification was obvious. Ten years ago Ton *et al* (1991) suggested that adoption of post-classification spatial guidance rules for improving the accuracy of land cover classifications would lead to new, unrecoverable problems. Thus, the ability to develop legitimate rules was questioned. Nevertheless, the possibilities for post-classification rules have been demonstrated in this work.

Hutchinson (1982) attempted to improve image classification using additional spatial data, such as thematic maps and other landscape characteristics. He grouped classification processes into three methods: pre-classification stratification, classifier modification, and post-classification sorting. Improvements in classification accuracy were observed for each of these methods. Despite this favorable finding for post-classification, deterministic rules were thought of as lacking in sophistication and crude in approach (Hutchinson, 1982). Perhaps that is what makes them so attractive and available for ready implementation by non-modelers. Hutchinson's disclaimer was that if post-classification was used, reliable ancillary data and the rules that were developed should match the natural situation closely. For

4-20

Parramore Island, the ecological rules model developed herein fulfills Hutchinson's requirement.

In concurrence with Kim's (1996) statement on contextual classification techniques, land cover types of spatially neighboring pixels are strongly related. Hubert-Moy *et al* (2001) considered that contextual classifiers worked especially well in summer environments compared to other available standard classification techniques, such as discriminant analysis, maximum likelihood classifiers, and minimum distance. If *a priori* contextual tools can be applied to improve landscape classification, they should be used. Abkar *et al* (2000) used a type of contextual classification method by applying available knowledge to segment data into classes. This environmentally specific work constrained the classification of the dependent variable to the existence of soil, elevation, and slope characteristics. Abkar's work was similar to that completed at Parramore in that the user and decision maker have taken control of the output by adjusting the model parameters. For both this and Abkar's work, aerial extent of thematic classes has been expanded and shrunk to increase or decrease at the expense of neighboring pixels. Abkar's work was not coded using a commercial image processing software package for later exploitation by other users as has been done here.

The prototype spatial model developed for this project may be modified for alternative study sites and environments. Additional landscape data sets were not needed to run the model; only the vegetation classification map was included and acted upon within the model. Other approaches for improving accuracy with post-classification that include Boolean-like integration of multiple geographic information system data sets for improving

Reproduced with permission of the copyright owner. Further reproduction prohibited without permission.

the output (Welch *et al*, 1992; Harris and Ventura, 1995) or decision-tree approaches that require complementary landscape data (Lees and Ritman, 1991) have not been discounted by the model suggested herein. A key feature of this model is the ease with which rules may be developed and implemented for use by untrained image analysts. Tools that foster the integration of knowledge from the landscape ecologist are needed within the remote sensing community (Ehlers, 1995).

The process of developing rules for a barrier island complex could be adapted to a different physiographic environment, but the identification of rule sets would likely not be as easily constructed. The barrier island environment has a well-defined sequence of vegetation that is elevation and water related. Rule development for Parramore Island specifically considered the level of landscape classification that was desired and feasible for interpretation from the available image source. Imagery-derived vegetation classes for this project was a hybrid of Anderson Level II (e.g., maritime forest, shrub communities, water) and Level III (e.g., species level vegetation and sand) (Skidmore and Turner, 1988). The narrow bandwidths (25nm) and high spatial pixel resolution (1.5m) supported this level of mapping. Post-classification rules should be appropriate to support the level of land cover classification achievable from an image source. For example, rules that ascribe structural differences expected between selected plant communities would probably not be helpful for correcting a basic land cover classification map.

A modified future version of spatial model proposed herein might include the use of spatial constraints place upon the landscape classification as determined from geostatistical

variogram model parameters. The variogram provides information about directional trends and spatial variability in the landscape cover classes would be of assistance in improving the final classification.

Conclusion

The purpose of this work was to develop a methodology in which ecology-based knowledge could be easily incorporated into post–classification landscape cover type corrections. A prototype method was applied in a spatial environment that showed that it was possible to incorporate ecological understanding of a study area into a model with conditional rules. Flexibility of rule construction allowed for the targeting of specific landscape features and close interaction by the analyst. The ability to select neighborhood window sizes and filter class options to facilitate the elimination, or incorporation, of pixels into classes was critical.

There were several advantages to the post-classification prototype: the model was developed using commercial "off the shelf" image processing software; the software can be adapted to easily correct a variety of land covers by modifying class codes within spatial model filters; the corrections were integrated to create a single map at the end; the model is portable and can be used for another study site by generating appropriate ecological rules; and a map reviewer can apply known or learned knowledge about a study site into the classification process. Knowledge for this project originated from field experience and literature searches, but could have originated from a source such as high-resolution air photo

interpretation where visual cues provide an immeasurable opportunity for improved classification.

The conversion of pixels based on an ecological expectation of land cover type adjacency was successfully demonstrated. An image analyst was able to define corrections to the image classification and recoded those corrective actions into conditional statements that became components of a larger spatial model. Over 20% (173 of the total 850 hectares) of initial land cover classification pixels were converted to alternative classes based on ecology-based rules.

An overall plan for improved vegetation classification derived from imagery might best include a combination of a) digital multi-spectral imagery for automated processing, b) air photo imagery (1:20000 scale and larger) to assist in gathering knowledge from the photographic interpretation process, c) strategically located field-truth and testing plots, and d) implementation of an ecology-based spatial model for post-classification correction. A recommendation for future work includes verification in the field of the accuracy of ecology based corrections as well as a spatial evaluation of the changed pixels (refer to Figure 4) through a geostatistical analysis.

References

Ahnert, F., 1996. Chapter 23-The littoral system. In <u>Introduction to Geomorphology</u>, John Wiley and Sons, Inc., New York, 286-316.

Chalmond, B., Graffigne, C., Prenat, M., and Roux, M., 2001. Contextual performance prediction for low-level image analysis algorithms. *IEEE Transactions on Image Processing*, 10 (7): 1039-1046.

Christensen, 1988. Chapter 11- Vegetation of the southeastern coastal plain. In <u>North American Terrestrial Vegetation</u>, edited by M.B. Barbour and W.D. Billings, Cambridge University Press, New York.

Cihlar, J., Latifovic,R., Chen, J., Beaubien, J., Li, Z., and Magnussen, S., 2000. Selecting representative high resolution sample images for land cover studies. Part 2: Application to estimating land cover composition. *Remote Sensing of Environment*, 72(2):127-138.

Delbaere, B., and Gulinck, H., 1995. A review of landscape ecological research with specific interest to landscape ecological modeling. Proceedings of a JRC Workshop, Leuven, 17-19 March 1994 (Institute for Remote Sensing Applications, JRC Ispra and Institute for Land and Water Management, Leuven), 5-27.

Dizenzo, S., DeGloria, S.D., Bernstein, R., and Kolsky, H.G., 1987. Gaussian maximum likelihood and contextual classification algorithms for multi crop classification. *IEEE Transactions on Geoscience and Remote Sensing*, 25:805-814.

Ehlers, M., 1995. Integrating remote sensing and GIS for environmental monitoring and modeling: where are we?. *Geo Info Systems*, 5(7): 36-43.

ERDAS Inc., 1995. ERDAS Imagine, image-processing software.

Fischer, R., Campbell, M., Anderson, J., Slocum, K., submitted for journal review. Vegetation classification from high-resolution airborne multispectral imagery.

Groom, G.B., Fuller, R.M., and Jones, A.R., 1996. Contextual correction: techniques for improving land cover mapping from remotely sensed images. *International Journal of Remote Sensing*, 17 (1): 69-89.

Gulinck, H., Dufourmont, H., Coppin, P., Hermy, M. 2000. Landscape research, landscape policy and earth observation. *International Journal of Remote Sensing*, 21 (13&14): 2541-2554.

Harris, P.M., and Ventura, S.J., 1995. The integration of geographic data with remotely sensed imagery to improve classification in an urban area. *Photogrammetric Engineering and Remote Sensing*, 61 (8): 993-998.

Hayden, B.P., Santos, M.C.F.V., Shao, G., and Kochel, R.C., 1995. Geomorphological controls on coastal vegetation at the Virginia Coast Reserve. *Geomorphology*, 13: 283-300.

Hubert-Moy, L., Cotonnec, A., Le Du, L., Chardin, A., and Perez, P., 2001. A comparison of parametric classification procedures of remotely sensed data applied on different landscape units. *Remote Sensing of Environment*, 75 (2): 174-187.

Jennings, M.D., 2000. Gap analysis: concepts, methods, and recent results. *Landscape Ecology*, 15 (1): 5-20.

Kartikeyan, B., Gopalakrishna, B., Kalubarme, M.H., and Majumder, K.L., 1994. Contextual techniques for classification of high- and low-resolution remote sensing data. *International Journal of Remote Sensing*, 15 (5): 1037-1051.

Kim, K.E., 1996. Adaptive majority filtering for contextual classification or remote sensing data. *International Journal of Remote Sensing*, 17 (5): 1083-1087.

Laferte, J.M., Perez, P., and Heitz, F., 2000. Discrete Markov modeling and inference on the quad-tree. *IEEE Transactions on Image Processing*, 9 (3): 390-404.

Landgrebe, D.A., 180. The development of spectral-spatial classifiers for earth observational data. *Pattern Recognition*, 12: 165-175.

Lees, B.G., and Ritman, K., 1991. Decision-tree and rule-induction approach to integration of remotely sensed and GIS data in mapping vegetation in disturbed or hilly environments. *Environmental Management*, 15 (6): 823-831.

Mitsch, W.J., and Gosselink, J.G., 1993. Part 3- Coastal wetland ecosystems. in <u>Wetlands</u>, 2nd ed., Van Nostrand Reinhold, New York.

Nagendra, H., 2001. Using remote sensing to assess biodiversity. *International Journal of Remote Sensing*, 22 (12):2377-2400.

Oertel, G.F., and Kraft, J.C., 1994. Chapter 6- New Jersey and Delmarva barrier island: description of Delmarva barrier islands. In <u>Geology of Holocene Barrier Island Systems</u>, edited by R. Davis, Jr., Springer-Verlag, New York, 207-232.

Scott, J, 1991. Section IV-The Atlantic Coast. In <u>Between Ocean and Bay: A Natural History of Delmarva</u>, Tidewater Publishers, Chesapeake, MD.

Silberhorn, G.M., 1999. <u>Common Plants of the Mid-Atlantic Coast: A Field Guide.</u>, 3rd ed., Johns Hopkins University Press, Baltimore, MD.

Shao, G., Young, D.R., Porter, J.H., and Hayden, B.P., 1998. An integration of remote sensing and GIS to examine the responses of shrub thicket distributions to shoreline changes on Virginia barrier islands. *Journal of Coastal Research*, 14 (1): 299-307.

Skidmore, A.K., and Turner, B.J., 1988. Forest mapping accuracies are improved using supervised nonparametric classifier with SPOT data. *Photogrammetric Engineering and Remote Sensing*, 54: 1415-1421.

Slocum, K.R., Jarrett, J., 2001, Anderson, J.E., Oliver, M.A., and Perry, J.E., in work. Accuracy of coastal landscape feature classification based upon varied imagery spectral bandwidth, pixel resolution, and training sample selection method.

Slocum, K.R., Perry, J.E., 2001, Oliver, M.A., and Krause, P., in work. Remote identification of biomass differences to *Phramites australis* stands from high-resolution spectral imagery.

Slocum, K.R., Perry, J.E., Anderson, J.E., Campbell, M., and Fischer, R., in work. Vegetation association with elevation, soil type, and soil compaction at Parramore Island, Virginia.

Stuckens, J., Copping, P.R., and Bauer, M.E., 2000. Integrating contextual information with per-pixel classification for improved land cover classification. *Remote Sensing of the Environment*, 71, 282-296.

The Nature Conservancy (TNS), 1995. NBS/NPS Vegetation Mapping Program, Vegetation Classification of Assateague Island National Seashore, 14 November.

Tonjes, R., Growe, S., Buckner, J., and Liedtke, C-E.,1999. Knowledge-based interpretation of remote sensing images using semantic nets. *Photogrammetric Engineering and Remote Sensing*, 65 (7): 811-821.

Welch, R., and Remillard, 1992. Integration of GPS, remote sensing, and GIS techniques for coastal resource management. *Photogrammetric Engineering and Remote Sensing*, 58 (11): 1571-1578.

Wessman, C.A., Cramer, W., Gurney, R.J., Martin, P.H., Mauser, W., Nemani, R., Paruelo, J.M., Penuelas, J., Prince, S.D., Running, S.W., and Waring, R.H., 1998. Chapter 5- Group report: remote sensing perspectives and insights for study of complex landscapes. In Integrating Hydrology, Ecosystem Dynamics, and Biogeochemistry in Complex Landscapes, edited by J.D. Tenhunen and P. Kabat, John Wiley and Sons, New York, 89-103.

Wilkinson, G.G., 1996. A review of current issues in the integration of GIS and remote sensing. *International Journal of Geographical Information Systems*, 10:85-101.

Zhang, J., and Stuart, N., 2001. Fuzzy methods for categorical mapping with image-based

land cover data. *International Journal of Geographical Information Science*, 15 (2):

175-195.

Table 1. Changes to map class themes as a result of the ecology-based model corrections, are listed in the partial table below. Sample points are identification numbers of pixels that have been changed from one class to another. X is the easting and Y is the northing coordinate of the pixel. Class values are identified in a Legend at the bottom of the table.

Sample Pt.	X	Y	Veg Class (Original)	Veg Class (Corrected)
Point 1	446694.895	4158992	2	4
Point 2	445198.699	4158331	7	
Point 3	445588.179	4158312	2	1
Point 4	445356.925	4155729	2	8
Point 5	445859.425	4157342	7	4
Point 6	447082.637	4158715	9	1
Point 7	446041.994	4158525	7	4
Point 8	446096.764	4158594	7	4
Point 9	444338.886	4156016	2	3
Point 10	445178.703	4155580	7	4
Point 11	445584.706	4156505	7	4
Point 12	445414.304	4155913	4	3
Point 13	444694.46	4156655	7	4
Point 14	446712.283	4158735	9	1
Point 15	445549.057	4156234	2	1
Point 16	444887.462	4158945	7	4
Point 17	444289.331	4156159	4	3
Point 18	444858.773	4156721	7	4
Point 19	446718.369	4158393	7	4
Point 20	445357.795	4155780	7	4
Point 21	445423.867	4157666	2	4
Point 22	445888.114	4158329	7	4
Point 23	446425.389	4158203	7	4
Point 24	445418.051	4157720	7	4
Point 25	447006.132	4158802	9	1
Point 26	445738.581	4158533	7	3
Point 27	445488.201	4156078	7	4
Point 28	445575.139	4158615	7	4
Point 29	445053.513	4155787	7	4
Point 30	445801.177	4156349	7	4
Point 31	444947.449	4157042	2	4
Point 32	444131.105	4155800	7	4
Point 33	443903.328	4155546	7	1
Point 34	445346.493	4157668	2	1
Point 35	444900.503	4157041	7	4
Point 36	446588.831	4158433	7	4
Point 37	445278.073	4157199	7	4
Point 38	445408.218	4157041	7	4
Point 39	446297.59	4157524	2	5
Point 40	445278.681	4158084	7	4
Point 41	446530.8	4158519	7	4
Point 42	445752.491	4156399	2	8
Point 43	445496.895	4158669	7	4
Point 44	444760.533	4156217	7	4
Point 45	444311.935	4155166	7	4
Point 46	446798.351	4158946	9	1
Point 47	445140.451	4157298	2	1
Point 48	446556.621	4158032	2	8
Point 49	445081.333	4155443	4	3
Point 50	446367.14	4158819	7	

Sample Pt.	X	Y	Veg Class (Original)	Veg Class (Corrected)
Point 51	445745.5	4156739.4	7	4
Point 52	446275	4158807.6	7	4
Point 53	445849	4159064.1	8	1
Point 54	446131.5	4157245.3	2	4
Point 55	445733.4	4157364.4	7	4
Point 56	445611.7	4158294.7	2	1
Point 57	446038.5	4158222.5	7	3
Point 58	446002	4158253.8	7	4
Point 59	446205.4	4157494	7	3
Point 60	446275	4158735.5	4	3
Point 61	445816	4156222.1	7	4
Point 62	445999.4	4158413.8	7	4
Point 63	444195.4	4155637	7	3
Point 64	446291.5	4158206.9	4	3
Point 65	445176.1	4158589.8	7	3
Point 66	446455.8	4158282.5	7	3
Point 67	445502.1	4157347.9	7	4
Point 68	444478	4155344.9	7	4
Point 69	444598	4158400.3	2	1
Point 70	444215.4	4155643.9	4	3
Point 71	446657.5	4158621.6	7	4
Point 72	445756.8	4156449	7	4
Point 73	446699.2	4158543.3	7	3
Point 74	470052.2	4158354.7	4	4
Point 75	445583	4157048	7	3
Point 76	445208.3	4157543.5	7	4
Point 77	446168.1	4158572.9	7	3
Point 78	444705.8	4155299.7	7	4
Point 79	447043.5	4158539	7	3
Point 80	444877.9	4157065.4	7	4
Point 81	445502.1	4157422.7	7	3
Point 82	445713.4	4158778.9	7	3
Point 83	445777.7	4157507.9	7	4
Point 84	445036.1	4155479.6	4	3
Point 85	445313.5	4156936.7	7	3
Point 86	444807.5	4156764.6	7	4
Point 87	446407.1	4158044.3	4	3
Point 88	445875.1	4157680	4	4
Point 89	446511.5	4157687	2	3
Point 90	446175	4158973.7	7	4
Point 91	444677.1	4155792.6	9	3
Point 92	445589.9	4156101.2	4	8
Point 93	445310	4155955.2	7	3
Point 94	445730.8	4157586.1	4	3
Point 95	445159.4	4157485.3	4	3
Point 96	446159.4	4157502.7	2	3
Point 97	445437.8	4158100.8	7	5
Point 98	446235.9	4157437.5	4	4
Point 99	445436.9	4156041.3	4	2
Point 100	444442.3	4155307.5	3	2
Point 101	445565.1	4158329.5	3	2

VEGETATION LEGEND

Class 1	S. patens
Class 2	S. altern.
Class 3	High Dens
Class 4	Low Dens
Class 5	Typha
Class 7	Forest
Class 8	Sand
Class 9	Grass

Figure 1. Sample segment of a larger integrated ecology-based spatial correction model developed with ERDAS Imagine, where each model output builds upon the results of the previous correction until a final corrected map product is derived.

Post Classification Error Correction- Ecology-Based Rule Implementation

Classified Image Needing Correction

n12_veg

FOCAL MAJORITY

Speckle Removal

n17_Custom_Integer

n14_memory

$FOCAL MAJORITY

Beach Grass-Remove at S. patens

n7_Custom_Integer

n3_memory

$FOCAL MAJORITY

Beach Grass-Remove at S. alterniflora

n26_Custom_Integer
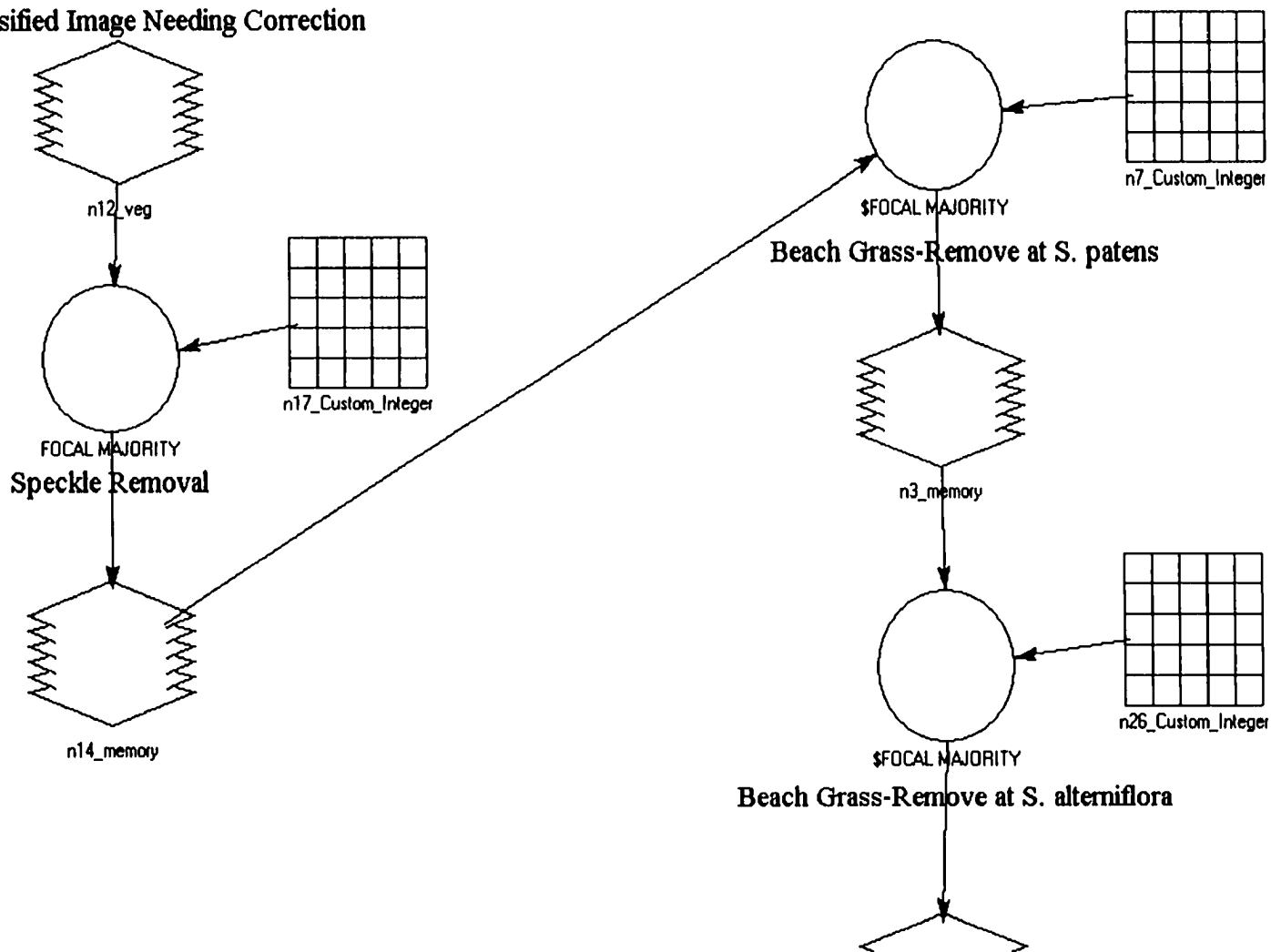
Figure 2. Sample syntax as applied to a focal majority function to target error correction of user-specified class themes, developed with ERDAS Imagine software.

.

Function Definition: $FOCAL MAJORITY

Available Inputs:

$n85_memory
$n98_Custom_Integer

Functions: [Focal (Scan)]

```
BOUNDARY ( <raster> , <matrix> )
BOUNDARY ( <raster> , <matrix> , <use_option> , <apply_option> )
FOCAL DENSITY ( <raster> , <matrix> )
FOCAL DENSITY ( <raster> , <matrix> , <use_option> , <apply_option> )
FOCAL DIVERSITY ( <raster> , <matrix> )
FOCAL DIVERSITY ( <raster> , <matrix> , <use_option> , apply_option )
FOCAL MAJORITY ( <raster> , <matrix> )
FOCAL MAJORITY ( <raster> , <matrix> , <use_option> , <apply_option> )
FOCAL MAJORITY ( <raster> , <matrix> , <threshold> )
FOCAL MAJORITY ( <raster> , <matrix> , <threshold> , <use_option> , <a
FOCAL MAX ( <raster> , <matrix> )
```

$FOCAL MAJORITY ($n85_memory, $n98_Custom_Integer, USE_VALUE 4, APPLY_AT_VALUE 7)|

Calculator keys:

```
%   "   /   *
7   8   9   .
4   5   6   +
1   2   3   _
.   0   )   ]
```

OK   Clear   Cancel   Help

Figures 3a - d. Multispectral imagery has been acquired and processed into classified imagery to demonstrate the impact of integrating post-classification rules. The images in figure 3 are shown in progressive order in the steps expected for correction and analysis.

Figure 3a is the original 4-channel multispectral imagery of Parramore Island shown in a false-color 4-3-2 band representation. Imagery was collected on May 30, 1999, from 1155 to 1257 local solar time. Eleven flight lines were flown south to north at an altitude of approximately 3,000 meters above mean sea level, which resulted in a nominal pixel size of approximately 1.5 meters.

Figure 3b is an initial classification of land cover classes from the raw imagery, prior to the application of any rule-based classification to improve the results. Speckle and misclassifications are visually evident.

Figure 3c shows the resulting map compilation after running the spatial model and making corrections to the original class map. Respective legends for Figures 3b and 3c identify the changes to class area in hectares. Spatial pattern is more reasonable with speckle and misclassified pixel areas removed in Figure 3c. Homogeneity typically found in vegetation complexes of the barrier island are evident in Figure 3c.

Lastly, Figure 3d is the difference map between Figures 3b and 3c, depicting those pixels changed by the incorporation of the rules. The difference pixels in Figure 3d present definite spatial pattern, oriented in a southwest to northwesterly trend.

(a)

(b)
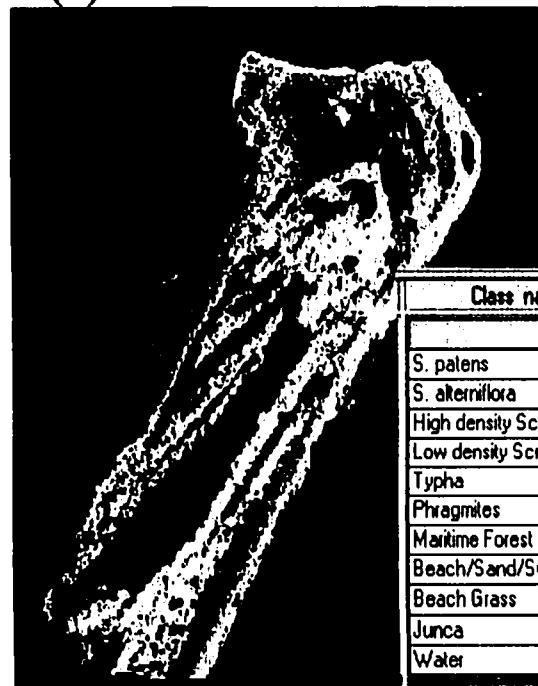
Class names	Color	Area NEW
		894.359
S. patens		151.369
S. alterniflora		115.06
High density Scrub/Shrub		30.2684
Low density Scrub/Shrub		86.723
Typha		28.5532
Phragmites		9.55849
Maritime Forest		186.676
Beach/Sand/Swash		61.8671
Beach Grass		20.873
Junca		1.10493
Water		175.744

(c)

(d)
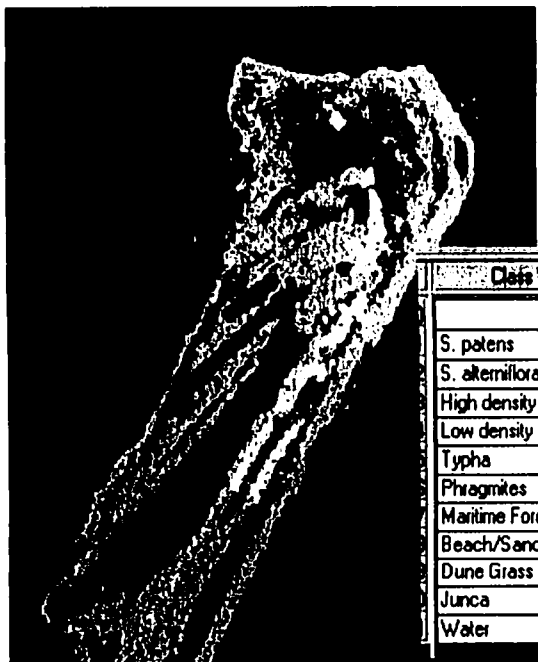
Class Names	Color	Area
		894.363
S. patens		163.347
S. alterniflora		99.5323
High density Scrub/Shrub		54.0161
Low density Scrub/Shrub		131.472
Typha		31.5411
Phragmites		9.43257
Maritime Forest		122.942
Beach/Sand/Swash		64.5774
Dune Grass		14.2981
Junca		1.08391
Water		175.55

Figure 4. Classification maps of cover classes at Parramore Island depicting results from: (a) Pre-corrections, with high and low-density shrubs (teal and aquamarine color) located within the *S. alterniflora* community (maroon color), and (b) Post-corrections, with high and low-density shrubs removed from *S. alterniflora*.
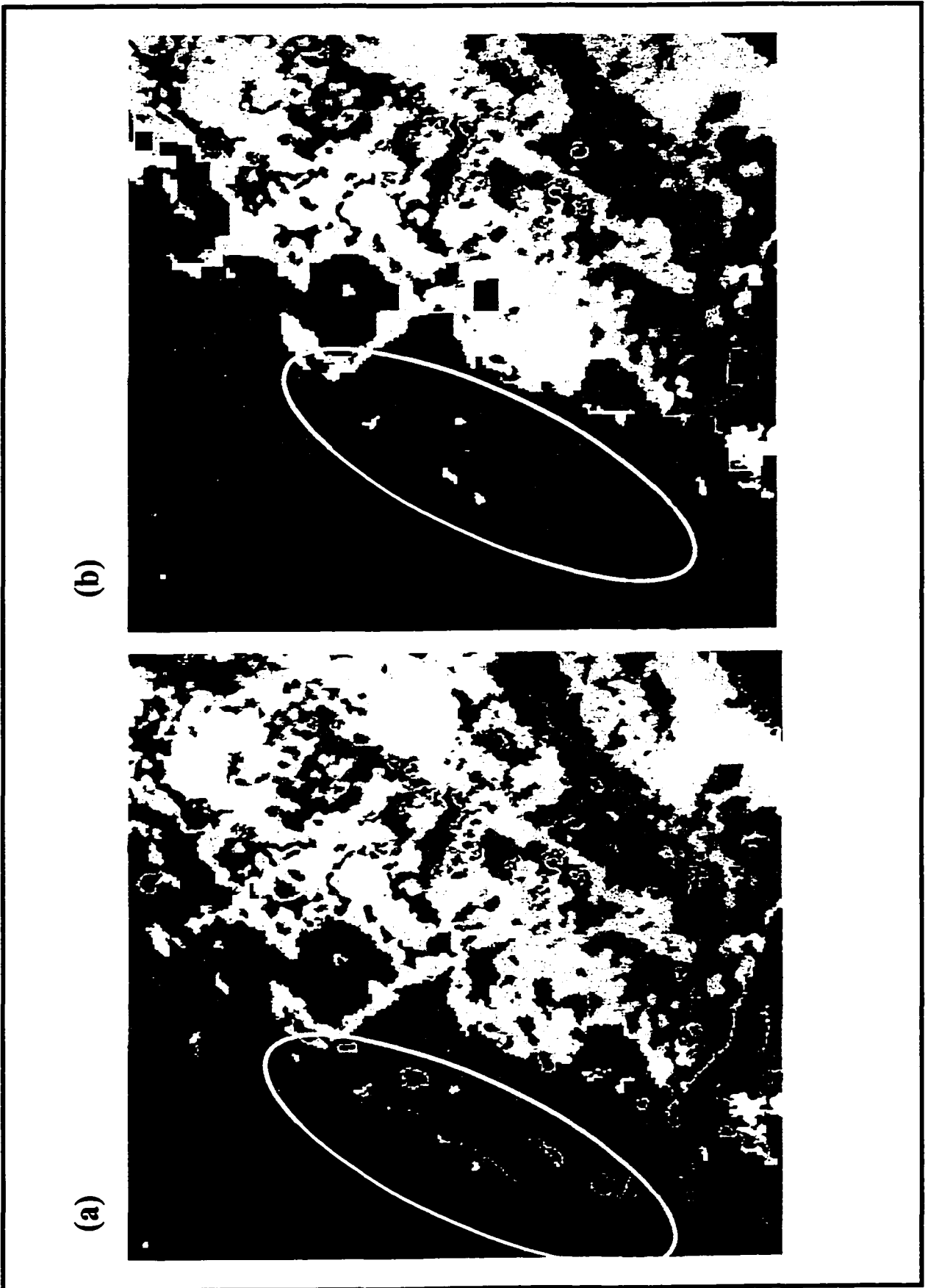
(b)

(a)

Figure 5. Classification maps of cover classes at Parramore Island depicting results from: (a) Pre-corrections, with both beach grass (yellow color) and sand (grey color) located within the *S. alterniflora* community (maroon color), and (b) Post-corrections, with beach grass and sand removed from *S. alterniflora*.

(a)

(b)
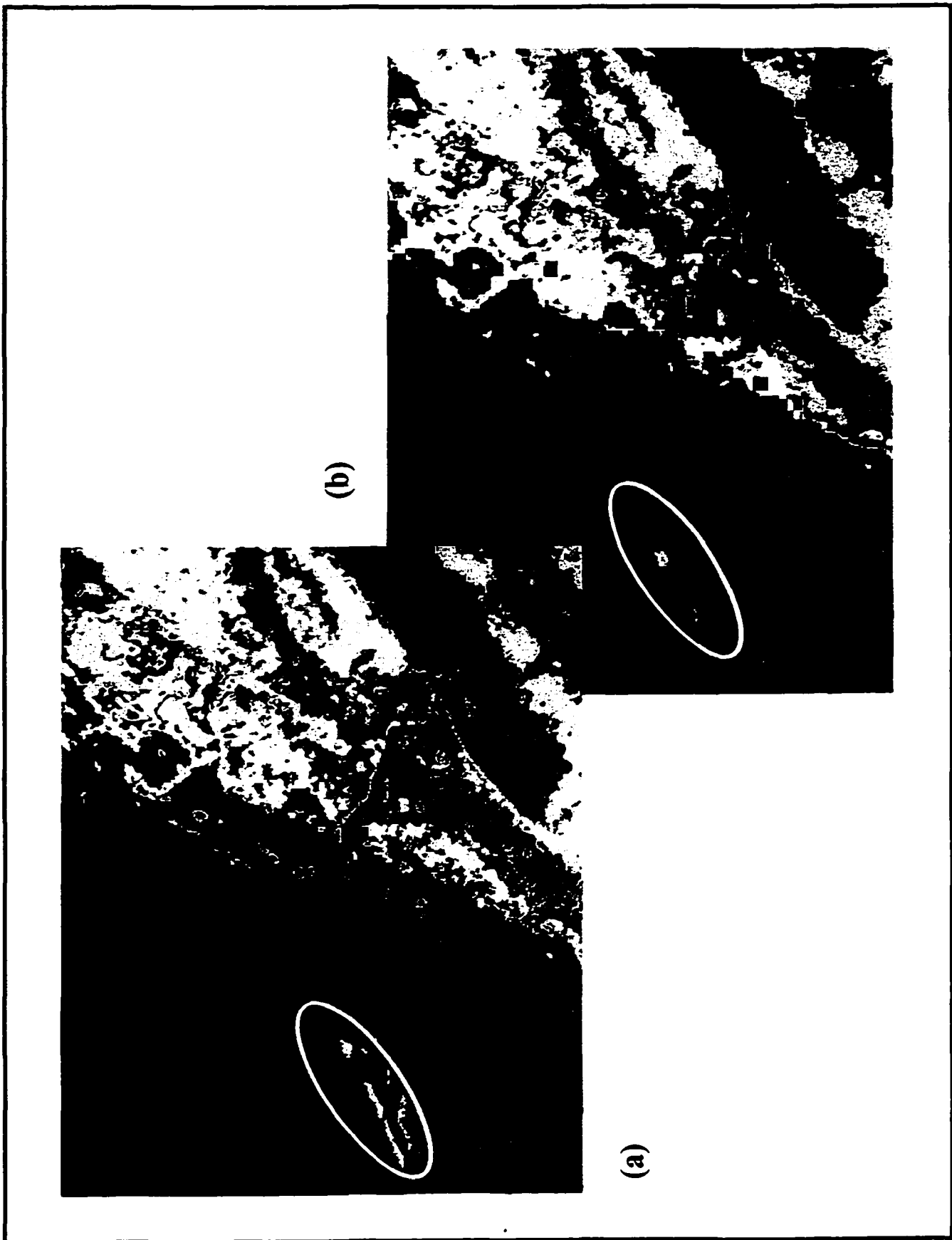
Figure 6. Classification maps of cover classes at Parramore Island depicting results from: (a) Pre-corrections, with both patches of *S. alterniflora* (maroon color) co-located within *S. patens* (brown color) and maritime forest (green) adjacent to low- density shrub without a high-density shrub buffer, and (b) Post-corrections, with *S. alterniflora* removed and forest converted to high density shrub.

(b)

(a)

Figure 7. Classification maps of cover classes at Parramore Island depicting results from: (a) Pre-corrections, with *S. alterniflora* (maroon color) located within the near-shore beach front, and (b) Post-corrections, with *S. alterniflora* substantially reduced but not yet eliminated. Follow-up corrections with forest adjacency are warranted.
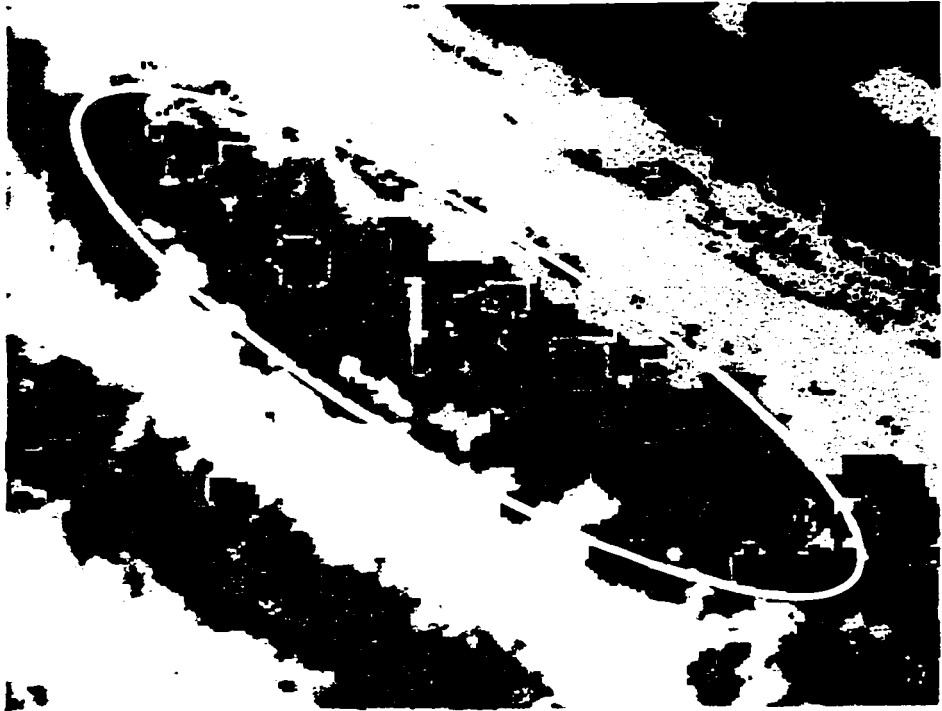
(b)
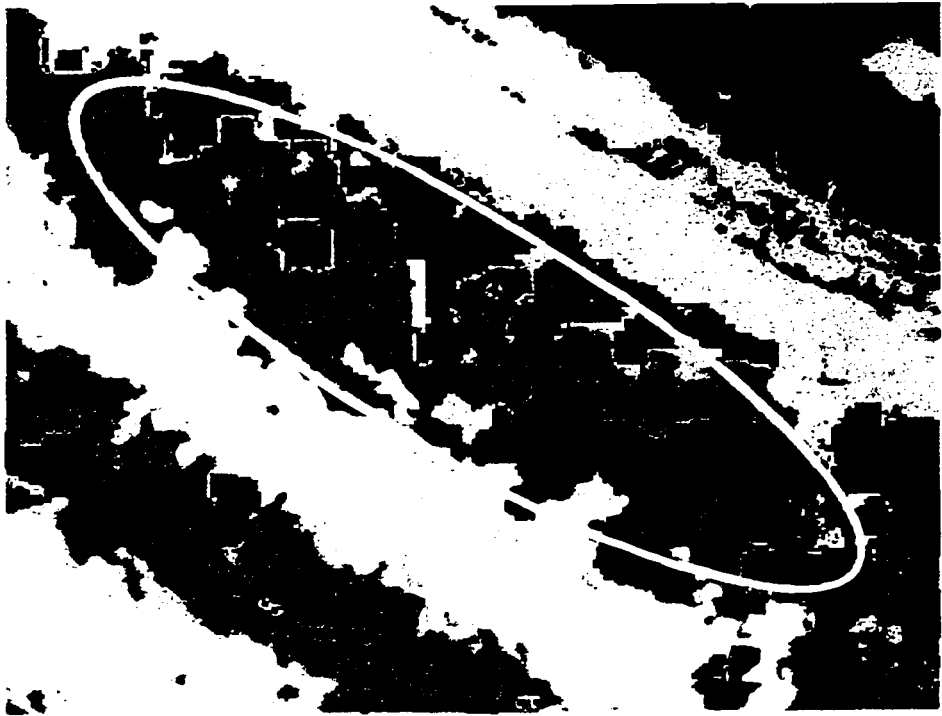
(a)

Chapter 4 to Chapter 5 Transition

Post-classification results documented in this past chapter describe a potential for producing rapid landscape classification based on sound ecological knowledge. Chapter 5 discusses the development of empirical models that use community based vegetation classifications as derived from high-resolution image sources as a surrogate variable for estimating a) soil type, b) soil compaction rate, and c) decimeter level elevation ranges. The predictive model relies on the accuracy of the vegetation characterization for the model to be dependable. Field data and coincident imagery was acquired across a Virginia coast barrier island. These data were used to assess statistical associations between categorical vegetation communities and estimated soil and elevation spatial data. While the findings of this chapter will not suggest replacement of time-tested field collection techniques for accurate mapping of soil properties, results of this work in the barrier island are promising for a rapid large-area approach tool for mapping soil type and strengths. This is true for the mapping of lower, upper and non-tidal areas based on vegetation and their observed preference for unique elevation strata.

Chapter 5

Vegetation Association with Elevation, Soil Type, and

Soil Compaction at Parramore Island, Virginia

Abstract

Barrier islands are among the earth's most dynamic environments. This manuscript presents the relationships between vegetation and a) elevation, b) soil type, and c) soil compaction strengths on a Virginia eastern shore barrier island. Measures of association tests suggest that barrier island vegetation is a valid variable for estimating elevation range in centimeters and soil properties: Vegetation type and categorized elevation range ($\chi^2 = 120$, p-value = 0.0059, d.f. = 84, and $V = 0.99$); vegetation type and soil type ($\chi^2 = 0.93$, p-value = 0.0000, d.f.= 21, $V = 0.86$); vegetation type and soil strength at depths of 30cm ($\chi^2 = 124$, p-value = 0.0000, d.f. = 82, $V = 0.96$) and 46cm ($\chi^2 = 124$, p-value = 0.0000, d.f. = 88, $V = 0.96$). Vegetation classification was used to estimate these ecological variables across the entire barrier island. Vegetation, therefore, became a surrogate variable for prediction.

Introduction

The terrestrial part of the coastal zone is subjected to continuing dynamic change. The barrier islands of the mid-Atlantic United States are particularly vulnerable to natural environmental changes. Over short distances there are striking gradients of plant salinity, soil properties, climate, and consequently in community composition, structure, and physiognomy (Christensen, 1988). These differences are interrelated. For example, soil processes and geomorphological processes are linked together within an environmental

landscape based on factors such as parent material, elevation gradient, and hydrologic weathering (Ruhe and Walker, 1978; Gerrard, 1991). The dynamic geologic history of the Atlantic barrier islands is well established, showing a landward shift from their original positions approximately 100 kilometers east over the last 18,000 years (Kraft *et al*, 1973; Bonan & Hayden, 1990; Hayden *et al*, 1991). Increased frequency and intensity of storms might have accelerated the erosion of some of the northern barrier islands of up to 13 meters per year in some areas (Dueser, 1990). Rapidly changing ecological conditions have inhibited the compilation of accurate records of these islands (Oertel *et al*, 1994). Expedient and cost effective methods for large area mapping are needed in coastal environments to assist resource managers to address issues such as sea level rise (Christensen, 1988; Nicholls *et al*, 1998; Jorgenson and Ely, 2001), loss of plant diversity (Garcia-Mora *et al*, 2000; Wood, 2001), and accumulation of pollutants (Knight and Pasternack, 2000). Land cover is a key input for decision support models and land management decisions (Cihlar *et al*, 2000). Remote sensing using moderate resolution (30m pixels) Landsat Thematic Mapper imagery has been used to classify land cover classification in the coastal areas, under the auspices of the National Oceanic and Atmospheric Administration's (NOAA) CoastWatch Change Analysis Project (C-CAP) (Jensen *et al*, 1993; Klemas *et al*, 1993).

Elevation and soil data have been acquired for many barrier islands from the US Geological Survey and Natural Resource Conservation Service respectively, however, data are still required. Several examples of data need can be cited. First, resolution of elevation data that is needed to support modeling and decision making in barrier islands is inappropriate with only meter-level vertical accuracy and a 30-meter interval between

observations (Kenward *et al*, 2000). A goal to map at an accuracy of +/-10 centimeter

vertical accuracy for nearby Assateague Island (Krabill, 2000) could not be achieved with

conventional elevation data. Remote sensing offers the only possibility to produce a time

series of elevation surveys of sufficient density for monitoring (Krabill *et al*, 2000). The

present elevation data do not enable the analysis of centimeter-level hydrologic relations that

exist between vegetation communities and tidal sequences in the barrier islands. Second,

interpolation from soil samples at point locations to provide predictions at unsampled

locations is a conventional mapping practice that introduces inevitable error. The reliability

of the predictions decrease as distance from sample locations increase (Cromley, 1992).

Third, since barrier islands are dynamic environments noted for rapid ecological change,

efficient monitoring methods are needed to document the present changes (Hayden *et al*,

1995). Frequently, updated high-resolution data are needed to satisfy the needs of the users

(Vogelmann, *et al*, 2001). Present methods of data collection (i.e., Interferometric Synthetic

Aperature Radar (IFSAR), Differential Global Positioning System (DGPS) survey, and

detailed sampling of soil data designed to minimize interpolation distances) can be

prohibitive in cost (Lyle, 1999; Atkinson, *et al*, 2000). A comprehensive description of the

environment will be beneficial and should help to alleviate the unavoidable difficulties of the

past in data acquisition (Huggett, 1995). Monitoring of temporal change is critical for coastal

zone management, and information about the amounts and types of change can be obtained

from image data (Michalek *et al*, 1993). Management/monitoring of vegetation communities

for stress, induced by drought, long-term inundation, naturally occurring senescence, or

infestations, using remote sensing infra-red reflectance (Rinker, 1994) should become part of

every resource manager's toolbox.

Barrier island dune, forest, and wetland complexes are unique geomorphological features that contribute to distinctive vegetation zones (Kraft *et al,* 1973; Bonan & Hayden, 1990; Hayden *et al,* 1991). They are a direct response to the environmental conditions such as salinity, inundation (Mitsch and Gosselink, 1993), and tidal range (Frey and Basan, 1974). Chesapeake Bay-side salt marsh communities are characterized by regularly inundated tall and short forms of monotypic smooth cord grass (*Spartina alterniflora,* Loisel) grading at higher elevations to complexes of mixed salt grass (*Distichilis spicata,* Greene) and salt meadow hay (*Spartina patens,* Muhl) in the high marsh that are less influenced by daily tides (Christensen, 1988). Marsh plant diversity increases with increased distance from salt-water inundation. Homogeneous stands of cattails (*Typha angustifolia* L.) and common reed (*Phragmites australis,* Cav.) can be found growing within upper valley marshes. The high marsh also supports low-density, short marsh elder (*Iva frutescens* L.) and groundsel-tree (*Baccharis halimifolia* L.), which co-exist with an herbaceous component that includes *S. patens* and *T. angustifolia* (Bourdeau and Oosting, 1959). A higher density shrub community is characterized by a transition from elder and groundsel-tree to taller (> two meters) and more closely spaced wax myrtle (*Myrica cerifera* L.). Dune systems support maritime forests dominated by loblolly pine (*Pinus taeda* L.), and less frequently black cherry (*Prunus serotina* Ehrh.), southern red cedar (*Juniperus virginiana* L.), and holly (*Ilex opaca* Ait.). Dune grass (*Ammophila breviligulata* Fern.) exists within the coastal dunes of the sandy beach zone. Nomenclature for the flora found at Parramore comes from Kartesz (1994). A comprehensive description of a Virginia barrier island ecosystem is given in McCaffrey and Duesser (1990) and Scott (1991).

Stable vegetated transverse dunes develop perpendicular to prevailing offshore winds in environments with sufficient available sand. Dune crests are asymmetrical in shape with a consistently less steep slope on the windward side (Strahler, 1962; Greenland and de Blij, 1977). In the formation of a transverse dune, a wavelike pattern of wind erosion and deposition results in the development of a steep slip face on the leeward side of the dune (Chorley *et al*, 1984). Addition of sand to the steep slip face, which typically has an angle of about 30-degress, will cause the dune to migrate (Davis, 1996). An understanding of dune formation aided in the designing of a technique to estimate crest height and location when concealed by maritime forest.

Barrier island soil type is affected by tidal and aeolian transport of sediment (Davies, 1973). Grain sorting occurs in sediments as daily and storm-driven tides relocate silt, clay and detritus throughout the marsh interior. Mud trapped in the marsh may originate from additional sources such as settling, flocculation of clays, formation of organoclays, and biogenic sediment trappings (Frey and Basin, 1974). Aeolian transport of beach sand has contributed to dune formation and migration. Sediment stability within a marsh area is related to the rooted plants and the shear strength of the resident sediments. Soil strength varies across a marsh environment (Frey and Basan, 1974).

Relationships between ecological variables have been intensively investigated (Milne, 1935; Grace, 1974; Walker, 1989; Moore, *et al*, 1993; Gessler *et al*, 1995; Huggett, 1995). Catenas were introduced by Milne (1935) to describe the lateral variation of soil on hill

slopes. Milne was also the first to recognize a vegetation catena associated with a soil catena

(Huggett, 1995). Others have related soil with landform and plant communities (Eyre, 1968;

Brady, 1974). Grace (1987) noted that plant species were limited by climate, soil,

topography and competition, but suggested that identifying interrelated variables would incur

costly and time-consuming field experiments. Walker (1989) investigated eight vegetation

stand types grouped according to moisture regimes and micro scale variations in topography.

Moore *et al.* (1993) looked at the idea of the spatial prediction of soil derived from slope and

wetness indices. Quantitative soil landscape models were proposed for terrestrial

environments that relied heavily on the use of available ecological variables, especially

elevation data, as independent predictors (Gessler *et al*, 1995). Huggett (1995) also

investigated soil occurring within distinctive classes based on relative topographic location.

Land cover will tend to exhibit spatial patterns when determined by landform and climate

(Steele, 2000). Chang and Islam (2000) analyzed the relationship between soil texture,

temperature, and moisture, with moisture and temperature collected from passive microwave.

Ecological relationships in nature are not random; structure and pattern become self-evident

as the spatial scales of investigation are changed (McBratney and Webster, 1983).

Remote sensing is a promising technology for characterizing barrier island ecology.

Inventory is considered a necessary starting point for resource management decision-making

(Lyle, 1999). As the ground detection resolution of satellite and airborne imagery continues

to increase, researchers should investigate new possibilities that these resources provide for

plant species-level mapping, structural vegetation change, and habitat change mapping.

Remote sensing began to show promise almost twenty years ago as a resource management

tool when a study of transverse dune morphological structure showed a positive correlation between remotely sensed measures of dune length, width, and distance between parallel dune crests (Chorley *et al*, 1984).

The purpose of this study was to investigate the statistical association between vegetation community types that were deemed to be capable of classification from remotely sensed source and: centimeter-level elevation, soil type, and soil compaction strength. As designated in earlier work by Smith (1996), remotely sensed vegetation classes are considered to be discrete units, contrary to their conventional treatment as continuous data due to compositional change over an environmental gradient. Discrete vegetation classification classes comprise part of larger classification schemes adopted by several United States federal government agencies: US Geological Survey Land Use Land Cover Classification System; US Fish and Wildlife Service Wetland Classification System; and the National Oceanic and Atmospheric Administration CoastWatch Land Cover Classification System, and these data are considered to be interpretable from remote sensing source (Jensen, 1996). Ultimately, field-based empirical relationships established between vegetation type and: elevation, soil type and soil compaction strength were applied to against vegetation classes identified from imagery.

Why would this be an important step in resource management? The use of vegetation community classes derived from imagery with a high spatial resolution to estimate centimeter-level elevation, soil type by category, and soil compaction strengths at incremental depths, would introduce an alternative, perhaps more affordable method of data

collection. Land managers need to know the spatial distribution of vegetation, soil, and elevation data to manage effectively (Wheatley *et al,* 2000). Complete area coverage afforded by the acquisition of imagery, classification of vegetation, and subsequent estimation of other ecological variables, would provide a level of spatial coverage otherwise unattainable from conventional sample plot-based field surveys. Establishment of empirical ecological relationships between vegetation community and elevation, or vegetation and soil properties, would assist land managers achieve a better understanding and ability to monitor change in the barrier island environment.

The following hypotheses were tested with a selected combination of nonparametric and multivariate statistics:

- Vegetation / elevation association, tested at the 95% confidence level:

    H_o = that elevation was the same regardless of vegetation community.

    H_a = that elevation varied because of vegetation community.

- Vegetation / soil type association, tested at the 95% confidence level:

    H_o = that soil type were equivalent regardless of vegetation community.

    H_a = that soil type varied because of vegetation community.

- Vegetation / soil compaction association, tested at the 95% confidence level:

    H_o = that soil compaction strengths, tested at 0cm, 5cm, 15cm, 30cm, and 46cm depths, were the same regardless of vegetation community.

H_a = that soil compaction strengths were different because of vegetation community.

Methods

Study Site

Linear barrier islands form a chain trending northeast from Long Island, New York, to southwest at the North Carolina Outer Banks (Schwartz. 1982). Their shorelines are long. The study site for this project was Parramore Island off the eastern shore of Virginia (Figure 1). It is the central island of this chain. Since the late 1980's Parramore Island has been privately owned and access has been restricted. No permanent human population inhabits it and activities such as agriculture, hunting, or logging are prohibited. The island orientation is approximately 15 degrees east of north and it has a classic drumstick shape indicating rotational instability (Haynes, 1979). The island is approximately 10-kilometers long by 1.5-kilometers wide, and it is separated from the mainland by a series of bays, salt marshes and small tidal creeks. Parramore exhibits classic dune and valley geomorphology with (from seaward) a sandy beachfront, dune / ridge sequence, maritime forest, inland marsh, and a bay-side marsh complex (Davies, 1973).

Imagery data acquisition

Digital multispectral imagery was obtained over the Parramore Island study site on May 30, 1999 (unpublished data) from a small, lightweight 4-camera imaging system fitted with 25 nanometer wide bandpass interference filters centered at 450 (blue), 550 (green), 650 (red) and 800 (near infra-red) nanometer band centers. Spatial ground sample detection was

approximately 1.5m. The camera system, named the Computerized Airborne Multi-camera Imaging System (CAMIS), was purchased in 1999 by the U.S. Army Topographic Engineering Center as a beta test system from FlightLand Data, Inc, located in Boston, MA. A false color image composite of the multispectral imagery is found at Figure 2a.

Vegetation

Forty-one sample sites were selected randomly from the imagery for field classification using 10m diameter sample plots. Dominant herbaceous and shrub vegetation was classified at the species level. All large woody vegetation was classified in a general category as maritime forest. These sites were used for imagery classification of vegetation and the development of empirical relationships with coincident elevation, soil type, and soil compaction. A discrete vegetation community class was identified in the field. Also, percentage of dominant vegetation cover was assigned to each sampling site as determined by averaging two independent observations. Dominant vegetation cover percentage was not a variable that was readily interpretable from remotely sensed data. Field data were classified into eight vegetation categories:

1. *Spartina alterniflora* (cordgrass);

2. *Spartina patens* (salt meadow hay);

3. *Typha angustifolia* (cattails);

4. *Phragmites australis* (common reed);

5. *Ammophila breviligulata* (dune grass);

6. *Iva frutescens* (marsh elder) and *Baccharis halimifolia* (groundsel tree, together constituting low density shrub);

7. *Myrica cerifera* (wax myrtle, constituting high density shrub); and

8. *Pinus taeda* (loblolly pine dominated maritime forest).

Statistical tests of categorical association

Elevation, soil type, and soil compaction variables were each evaluated for association with vegetation community using Pearson's Chi-square (χ^2) coefficient of association and Cramer's V, determined using Statistica software (StatSoft, Inc., 1995). Chi-square tests for the significance of a statistical relationship between categorical variables (for further explanation refer to Zar, 1999), but provides no measure of the strength of association. Cramer's V standardizes χ^2 so that the coefficient is within a more interpretable range of -1 to +1, representing the spectrum between complete disagreement (-1) and complete agreement (+1). Cramer's V provides a measure of the strength of the relationship between variables. The equation for computation of V is as follows:

Cramer's V = square root of (χ^2 / n min (r-1, c-1)) .... Equation 1

Where χ^2 = Chi Square value

            n = samples

            r = number of rows

            c = number of columns

A more thorough description of Cramer's V is given by Barber (1988) and Sokal and Rohlf (1995). Other statistics were applied on a variable by variable basis, identified in their respective methods section, and all tests were at the 95% confidence interval.

Each variable was estimated from vegetation using correspondence analysis (CA), applied as an exploratory technique whereby row and column data were compared using SYSTAT version 8.0 (SPSS, Inc., 1998) and BMDP (BMDP Statistical Software, Inc. 1992). It enabled visual interpretation of multivariate categorical data, specifically vegetation community types compared with soil type, soil compaction rates, and elevation. CA mathematically decomposes a Chi-square into principal components, and also maximizes correlation between pairs of variable points (BMDP Statistical Software, Inc., 1992). Analysis is similar to a principal components analysis (PCA) for categorical variables, with cases as the rows and variable categories as the columns. The distinction is that in PCA the trace of the covariance matrix sums to the total variance; in CA, the trace sums to the total of "Chi-square / n". CA analysis is carried out on an indicator or disjunctive matrix with coefficients and scale of variables chosen to maximize the variation between individuals (BMDP Statistical Software, Inc., 1992).

Elevation Field Data Acquisition and Analysis

Acquisition of centimeter-level elevation data were needed to test for minor changes in elevation that are associated with changes in vegetation type. Forty-one locations coinciding with the sample sites were measured with differential global positioning system (DGPS). Elevation measurements had an error between 5 and 10cm from true elevation height due to changing satellite geometry, instrument precision, and duration of site visit.

Only elevations for short form *S. alterniflora* were recorded; elevations for tall form *S. alterniflora*, found along the berms of tidal creeks, were not included. Elevation heights for maritime forest were acquired along lower dune slope elevations, approximately 1-meter beyond an observable ecotone boundary with high-density shrubs.

In addition to the Chi, Cramer's *V*, and CA statistical testing, analysis of variance (ANOVA), Tukey tests, and linear regression were used to test for differences in elevation for each of seven vegetation community type categories (minus *A. breviligulata*). A Tukey test identified the vegetation classes with statistically similar elevations and explainable by the effects of multiple variable interaction (Sokal and Rohlf, 1995). Post-hoc comparisons, such as the Tukey test, may be completed when categorical predictor variables yield unexpected results that need to be proven reliable by hypothesis testing (StatSoft, 1995). Tukey is a multiple comparison procedure wherein all variables are compared in a pairwise manner (Zar, 1999) taking into account the fact that more than two samples are computed (StatSoft, 1995). Whenever statistically significant F test scores are reported from an analysis of variance testing, there is an interest in assessing which groups are different from each other. The Tukey results enabled the re-coding of elevation data into vegetation types with similar elevation, reducing vegetation classes from seven to three: class one was *S. alterniflora* elevations alone; class two aggregated the elevations from *S. patens, T. angustifolia, P. australis*, and low density shrubs; and class three combined elevations acquired for *M. cerifera* and *P. taeda* dominated maritime forest locations. Elevations from these three class groups were statistically different from one another based on the analysis of variance test. Once group differences were confirmed, Pearson's Chi-square and Cramer's *V*

measure of association tests were computed for elevations from the original seven vegetation classes and those from the three combined vegetation classes.

Three preliminary elevation transects were acquired under Parramore's largest maritime forest, Italian Ridge dune. Relative height differences were measured across the crest of the underlying dune using a laser range finder. Locations were selected in the field based on understory line-of-sight. Field-based ratios were established between forest width (distance across the forest perpendicular to shoreline), measured using a standard surveyors tape, and a) dune crest height and b) dune crest location. Dune slope elevations were computed from crest height, crest location, and dune base elevation (maximum elevation reported for high-density shrub). This model was developed since maximum dune elevations were highly variable and the adoption of a single maximum elevation value would have misrepresented the true height of many forest locations.

Soil type data acquisition and analysis

Soil type data were acquired at forty-one vegetation type sample locations. A 61cm soil auger was used to acquire cores that were evaluated and classified in the field as one of four soil classes:

1. Saturated, fibrist and saprist epipedon surface over a saturated grayish sand, with no A horizon;

2. Moist, to very moist, to saturated histic epipedons and highly decayed organic surface, over a variable A horizon (2 to 8cm), over a moist to very moist grayish sand;

3. Dry to moist surface duff over a well defined A horizon (5 to 15cm) over a dry brownish sand;

4. Heterogeneous beach sand composed of random layers of unconsolidated sand and various types of detrital litter.

Soil compaction data acquisition and analysis

Soil compaction rates were measured at twenty locations pre-selected by stratified random sampling from imagery over Parramore Island to represent each vegetation type, with the exception of *A. breviligulata*. A 50cm soil strength penetrometer with incremental digital readout was used. Three 0cm (surface), 5cm, 15cm, 30cm, and 46cm depth replicate samples were collected at each site with measurements recorded in pounds per square inch (psi). Dominant site vegetation and closest adjacent vegetation type to the sampling locations were recorded. Identification of adjacent vegetation was to be used to determine if a soil strength gradient existed when moving from lower marsh to higher marsh. Accordingly, vegetation classes *S. patens, T. angustifolia, and P. australis* were sub-divided into lower and upper elevation categories based on their geographic position within the transitionary high marsh. This sub-division increased the number of vegetation classes related to soil compaction data from seven to ten. Vegetation was also re-grouped into three classes for statistical testing against soil compaction rates. The basis for the consolidation of classes was results obtained from vegetation-elevation analyses.

In addition to Chi-square, Cramer's V, and CA statistical tests, multivariate analysis of variance (MANOVA) and ANOVA tests were completed to test the relation between the vegetation groups and soil compaction data at each 0cm, 5cm, 15cm, 30cm, and 46cm depth. Soil compaction data were ranked into 19 classes, 1 to 19, using a lookup table created to group the raw values incrementally every 50 pounds per square inch and tested for association with the 10-class vegetation grouping.

Tidal effects

Tidal heights at Parramore Island vary across a lunar cycle. For May 1999, mean low water was 0.30m, mean high water was 1.52m, and mean sea level was 0.94m, computed at mean lower-low water datum (www.coops.nos.noaa.gov/data_retrieve.html). Daily tidal sequences submerge *S. alterniflora*, and periodically inundate the higher marsh species. High-density shrubs and maritime forest are above the 1.60-meter maximum tidal level, removing these vegetation communities from the effects of regular tidal inundation.

Results

Statistical association between vegetation community type and elevation

All field variables and corresponding data are detailed in Table 1. In evaluating this field data, initial ANOVA results indicated that elevation values grouped within 7 vegetation classes were significantly different (F-stat = 25.53, F-critical value = 3.97, p-value = 0.0000, d.f. = 39). Furthermore, Tukey test results for the 7-vegetation classes identified similar and dissimilar vegetation pairs (Table 2a). Vegetation classes 2, 3, 4, and 6, were very similar,

with values marked by asterisks in Table 2a indicate highly significant scores for a pair.

Scores based on a 0.0 to 1.0 scale, with 1.0 representing a perfect correlation, illustrate that

classes (2) *Spartina patens*, (3) *Typha angustifolia*, (4) *Phragmites australis,* and *(6) Iva*

frutescens and *Baccharis halimifolia* (together constituting low-density shrub) are co-existing

in a zone of elevation that is essentially equivalent. A re-grouped 3-class vegetation

grouping was selected based on these Tukey results and also based on the difficulty in

separating high-density shrub class from maritime forest class spectral information. The

three new groups comprise:

Group 1- *S. alterniflora*

Group 2- *S. patens*, *T. angustifolia*, *P. australis,* and *I. frutescens* and *B. halimifolia*

Group 3- *M. cerifera* and Maritime forest (dominated by *P. taeda*)

Figure 3 shows the elevation ranges for the original seven vegetation classes. The

upper maritime forest elevation range was purposefully adjusted with an additional crest

height data point with a more representative elevation range. Elevation range for each

vegetation class was determined by the low and high elevation value sampled for that class,

found in Table 3. A one-way ANOVA showed that elevation data for each vegetation class

was statistically different (F-stat = 34.30, F-critical value = 3.97, p-value = 0.0000, d.f. = 39).

Tukey test results for vegetation classes 1, 2, and 3 shows that they are very different from

one another with all results highly significant at the 95% confidence (Table 2b). Chi-square

and Cramer's *V* results for 3-vegetation classes versus elevation had highly significant scores

showing a positive statistical association between the two terrain variables (X^2 = 120 p-value = 0.0059, d.f. = 84, and V = 0.9884).

Correspondence analysis and a plot for 7-vegetation classes and elevation was computed (Figure 4). A non-significant Chi-square was computed as an intermediary result for Figure 4 (p-value = 0.144, d.f.=168). Five factors were needed to account for over 90% of the cumulative contribution explaining the association between variables. Factor 1, represented as "Dim"ension (1) or the x-axis, contributed only 21.33% with eigenvalue 1.00, and factor 2, represented as "Dim"ension' (2) or the y-axis, contributed only 21.33% with eigenvalue 1.00. The origin of a graph matrix is found at the intersection of the red vectors. At the end of each vector are elevation values and corresponding vegetation sample plots. Plot locations, shown by open circles, provide measurable distances (horizontally and vertically) from the origin, and this distance is an indication how far away the variable is in Chi-square euclidean distance from the overall marginal row profile. Horizontal and vertical distances between points (no diagonal distances) are approximate Chi-square distances between individual row profiles. The axes provide the scaled distances.

In Figure 4, the row, or vegetation variable, that contributed the most to Factor 1 was maritime forest (0.875). Likewise, the row variable contributing the most to Factor 2 was *S. alterniflora* (0.886). Column variables were the elevation values, and the contributing variables to Factor 1 were all the elevation values measured within maritime forest, and contributing variables to Factor 2 were all elevation values measured within *S. alterniflora*. This result supports the decision to divide elevation into groups, with *S. alterniflora* in a

group by itself, and maritime forest in a group joined only by high-density shrub. The plot itself also indicates that there are three primary zones grouping together elevation values and vegetation codes; unfortunately, variable symbols are plotting on top of each other and difficult to read. *Spartina alterniflora* is plotted at the top; high-density shrub and maritime forest are together on the far right; and *S. patens, T. angustifolia, P. australis*, and low-density shrub are together just off the origin.

Correspondence analysis of elevation zones, as justified from earlier findings, was used to compute a 2-axis plot for vegetation and elevation values (Figure 5). A highly significant Chi-square was computed as an intermediary result (p-value = 0.000, d.f.= 12). Two factors were needed to account for 100% of the cumulative contribution explaining the association between variables. Factor 1, represented as "Dim"ension (1) or the x-axis, contributed 52.28% with eigenvalue 1.00, and factor 2, represented as "Dim"ension (2) or the y-axis, contributed the remaining 47.72 with eigenvalue 0.913. The origin of a graph matrix is found at the intersection of the red vectors and at the end of each vector are elevation zones and vegetation sample plots. Blue circles represent elevation zones and vegetation plot locations are shown by open red circle symbols.

In Figure 5, the row, or vegetation variable, contributing the most to the Factor 1 was *S. alterniflora* (0.90). The row variables contributing the most to the Factor 2 were high-density shrub (0.346) and maritime forest (0.346). These results support the idea of three elevation zones and the appropriate vegetation members within the groups. The

correspondence plot suggests that perhaps low-density shrub (code 6) could be justifiably

separate from elevation zone 2, but that is the closest group to which it would belong.

Lastly, linear regression was used to determine the multiple contribution of three

elevation zones and four soil types in explaining the variation in vegetation type, and the

contribution of elevation in centimeters and soil type in explaining the variation in vegetation

type. The regression coefficient computed from the 3-zone elevation variable (r^2 = 0.86, p =

0.0000, n = 41, d.f. = 2,38) was a better predictor of vegetation than the regression computed

using raw elevation values (r^2 = 0.78, p = 0.0000, n = 41, d.f. = 2,38). The regression results

were further evidence to support the reduction of vegetation classes into three groupings so

that elevation could be considered a range of values (3-zones) and not absolute integer data.

Estimation of centimeter-level elevation was most successful after vegetation types

were re-grouped into 3 classes. Prior to re-grouping, overlap in elevation was evident in

pair-wise Tukey comparison tests between high-marsh plant species. Pair-wise test results,

known tidal range information, and the difficulty of classification separability between high-

density shrub and maritime forest, together endorsed the decision to combine seven

individual vegetation types into three merged classes. Re-grouping mostly removed

overlapping elevations and estimation of elevation ranges became simplified. The validity of

estimating centimeter-level elevations based solely on resident vegetation type was not

compromised by changing the methodology. A clearly defined lower elevation class

included *S. alterniflora* on its own. This monotypic lower marsh community grew between

1.16 and 1.32 meters in elevation. A high elevation class combined high-density *M. cerifera*

shrub, growing between 1.66 and 2.24 meters, with *P. taeda* dominated maritime forest at elevations greater than 1.99 meters. An overlap in elevation between *M. cerifera* and *P. taeda* noted at 1.99 to 2.24 meters could possibly signify the elevation range of an observable ecotone that separated these two distinct plant communities. The combination of *M. cerifera* high-density shrub and *P. taeda* observed forest types into a single elevation class eliminated mistakes in elevation estimating that would have resulted from a possible remote sensing misclassification between these two vegetation communities. The middle, or transition, elevation class included all high marsh species and occupied elevation in a narrow band of 1.40 to 1.68 meters above mean low water. Again, the importance attributed to the classification of vegetation was minimized as all four upper marsh species were re-coded (for elevation estimation only) to estimate an identical elevation range. Inclusion of invasive *P. australis* within this narrow elevation transition was noteworthy as other species at the same elevation are at greatest risk of natural eradication by this reed's prolific lateral rhizome expansion.

An elevation map was produced by reclassifying the vegetation class map from 7-classes to 3-classes and re-coding the 3-class vegetation map into elevation ranges: less than 1.40m, 1.40 to 1.66m, and greater than 1.66m. The elevation map estimated from vegetation type is shown in Figure 2d.

A methodology to estimate dune height and relative crest location under maritime forests was tested based on forest widths. Plotting the results of three test transects (Figure 6) illustrated geomorphological similarities across the dune. The y-axis measures the dune

heights, the x-axis the forest width, and the transect break points represent the dune crest locations. Table 4 contains the original transect data. For the three preliminary transects, ratios were computed based on H = dune height, LS = lee slope, and W = forest width:

Dune Height Estimate	Transect 1	Transect 2	Transect 3	Average Ratio
H / W =	0.30	0.30	0.37	0.32

The average ratio (0.32) multiplied by forest width (W) equaled the estimated dune height.

Average Ratio * W = H.

Side slopes were computed as a constant rate of elevation change using an approximate base dune elevation of two-meters to denote the forest boundary.

Crest Location Estimate	Transect 1	Transect 2	Transect 3	Average Ratio
LS / W =	0.21	0.18	0.19	0.19

The average ratio (0.19) multiplied by forest width (W) equaled the estimated location of the dune crest, determined as a function of distance measured from the lee slope forest edge (D).

Average Ratio * W = D

W - D = Dune Crest Location

Preliminary results suggest forest width measurements may provide a single predictor variable for modeling a maximum elevation value. Ratios calculated for forest width measurements (derivable from imagery) and dune height, and forest width and crest location, suggest that empirical models could be validated after tests with additional transect samples. Dune slope elevations were easily computed given estimated dune height and crest location.

Presently, determining maritime forest elevations demands labor-intensive field-surveys because the forest canopy conceals the ground elevation from possible airborne photogrammetric measurement.

Vegetation type association with soil type

Many vegetation types grew within a single class of soil. For example, *S. alterniflora* (n = 2), *S. patens* (n = 12), and *T. angustifolia* (n = 6) were observed on soil type one. *Phragmites australis* (n = 3) was found on soil type one and two. The existence of *Phragmites* upon soil type one, soil dominated by halophytic species such as *Spartina*, indicates its ability to adapt, compete and thrive in domains that were not necessarily preferential habitat (Amsberry *et al*, 2000). Low density shrubs such as *I. frutescens* (n = 8) were observed on soil types one and two, but usually two. High-density shrubs such as *M. cerifera* (n = 10) grew on soil types two and three, but usually two. Growth of *M. cerifera* in soil type three is likely explained as the ecotone area where there was a quarter meter of elevation agreement with the lower end of maritime forest elevation values. Tukey pair-wise comparisons suggested separability between *M. cerifera* and forest elevations were statistically attainable. *P. taeda* maritime forest grew on soil type three. Lastly, *A. breviligulata* (n = 3) was found on soil type four. Scores from Pearson's χ^2 = 93 (p-value of 0.00, d.f. = 21, n= 41) and Cramer's V = 0.85, both suggest a strong positive association between vegetation type and soil type.

Correspondence analysis was used to compute a 2-axis plot for vegetation and soil types (Figure 7). A highly significant Chi-square was computed as an intermediary result (p-value = 0.000, d.f.= 18). Two factors were needed to account for over 99.70% of the

cumulative contribution explaining the association between variables. Factor 1, represented as "Dim"ension (1) or the x-axis, contributed 67.54% with eigenvalue 0.865, and factor 2, represented as "Dim"ension (2) or the y-axis, contributed 32.16% with eigenvalue 0.412. The origin of a graph matrix is found at the intersection of the red vectors and at the end of each vector are soil type and vegetation sample plots. Vegetation plot locations are shown by open red circle symbols and blue symbols represent soil types.

In Figure 7, the row, or vegetation variables, contributing the most to Factor 1 were maritime forest (0.797) and *S. patens* (0.102). Several row variables contributed to Factor 2: high-density shrub (0.457), *S. patens* (0.184), low-density shrub (0.132), *S. alterniflora* (0.105), maritime forest (0.064), and *P. australis* (0.055). The vegetation variables are plotted in sequence, 1 to 7, and then 8 off to itself, essentially replicating the natural sequence of vegetation zonation attributable in part to soil type. The correspondence plot suggests that low-density shrub (code 6) could be justifiably separate from elevation zone 2, but that it is the closest group to which it would belong.

Cramer's V, Chi-square, and correspondence analysis results supported the compilation of an estimated soil type map (Figure 2c) based on the re-coding of the original eight vegetation classes into soil classes using Table 3. A reliability score could be assigned to each soil class by using field-data results. For example, a vegetation class such as *S. alterniflora* that is only found on soil type one, would result in a 100 per cent correct assignment of a site to a particular soil type, provided the vegetation was classified correctly in the first place. Field data for low- density shrubs (*I. frutescens*) showed a preference for both soil types one and two, but for type two 80 percent of the time. An 80 percent chance of

assigning soil type two to the *I. frutescens* vegetation class correctly would be included as a reliability attribute for determining soil type.

Estimation of soil types from vegetation type provided an island-wide image of the soils that would otherwise be difficult to acquire from strategically located field samples. Also, a map of complete soil cover provides increased insight into the physical processes of sediment delivery/generation and removal that have shaped the geomorphology of Parramore Island.

Vegetation type association with soil compaction rates

A MANOVA was completed to assess the effects of multiple independent variables vegetation type and grouped soil compaction values computed at five depths for 10-vegetation classes:

Depth	r^2	p-value	n
0cm	0.47	0.0137	60
5cm	0.24	0.0137	60
15cm	0.59	0.0001	60
30cm	0.88	0.0137	60
46cm	0.72	0.0000	60

The p-values at all depths were highly significant and vegetation type explained the variance in soil compaction at depths of 30 and 46cm the most effectively. Analysis of variance results for 10-, 7- and 3-vegetation classes (respectively) and soil compaction rates affirmed the MANOVA findings by returning significant p-values at all depths and increased

F-statistics as the measured depth increased (Table 5). The Chi-square and Cramer's V association test for the 10-, 7- and 3-vegetation classes and soil compaction strength produced scores of at least 0.85 for 30 and 46cm depths; all shallower depths produced smaller scores (Table 5). Similar to the MANOVA and ANOVA results, the scores for Chi-square and Cramer's V increased with depth measured. Figure 8 gives Cramer's V scores of association between soil compaction and 10-vegetation type classes, computed by depth. Figure 9a shows the average soil compaction rates at each of the five depths for all vegetation types. A simple box-and-whisker plot (Figure 9b) showed that the greatest variation among soil compaction rates was measured at 30cm (12in) and 56cm (18in) depths. Chi-square and Cramer's V scores supported mapping the estimated soil compaction strength for 30 and 46cm depths (Figure 2b). A 7-class vegetation map (minus *A. breviligulata*) was classified and the legend attributed using estimated soil compaction minimum and maximum rates found in Table 6, for 30 and 46cm depths. Means and standard deviations could have been included as attributes also. An attempt to classify soil compaction values into 19 rank ordered categories did not improve the statistical relation between vegetation type and soil compaction as both Chi-square and Cramer's V test scores decreased after grouping the compaction data values. Accordingly, this approach for estimation of soil strength was dismissed.

Soil compaction showed the strongest statistical relation with vegetation type at depths of 30 and 46cm, while at shallower depths (surface, 5cm, and 15cm) the relation was considerably less (Figure 9a). This graph supported the Chi-square and Cramer's V test statistics indicating that vegetation type was better at estimating soil compaction at depths of

30 and 46cm than at shallower depths. Maritime forest and high-density shrubs grew on soil with the greatest compaction rates at depths of 15cm and greater, helping to explain the stability of these environments against sediment loss. Maritime forest and high-density shrub also had the most variable soil strengths and, correspondingly, had the larger Chi-square and Cramer's V scores. *Spartina alterniflora* and lower elevation *S. patens* marsh grew in soil where the compaction rates were consistently less, distinguishing the lower marsh as an area with a potential for soil erosion and regenerative sedimentation. Lower marsh species (*Spartina* genus) were associated with low overall soil strengths at all depths.

Lastly, correspondence analysis evaluated 10 vegetation community types and soil compaction rates at 5 depths. Row and column pairs were decomposed into four components, with the first two components explaining 73.8% of the association (component 1, or the principal component, contributed 43.0% and component 2 contributed 30.8%). Figure 10 shows the first (axis 1) and second component (axis 2) with vegetation and soil compaction variable names plotted. Plotted distance from the origin, or intersection of the two axes, provides an indication of how far away each variable is in chi-square distance from the overall marginal row and column profile. For depth variables, soil compaction rates at 30cm (12in) and 46cm (18in) were very closely associated along the first component axis and closely associated with the second component; 15cm (6in) and 5cm (2in) were closely related but far removed from the first and second components; and surface measurements were plotted in isolation and exceptionally far away from both axis. All vegetation communities hovered about the origin, or right on the primary component axis, except for marsh species lower *S. patens* and *S. alterniflora*. A review of the raw data shows these communities to

have the least range in compaction rates at all depths of all the vegetation communities studied. *Phragmites australis* samples acquired from upper and lower elevations were plotted as equivalent in coordinate space suggesting a laterally monotypic soil condition; accordingly, "hiaust", or upper *P. australis*, had to be plotted by hand to show it's coincident graph location with "loaust", lower *P. australis*. Conversely, *S. patens* and *T. angustifolia*, while also divided into upper and lower sampling sites, were plotted away from each other in coordinate space.

The interpretation of Figure 10 concurred with prior statistical findings that suggested that soil compaction rates at 30cm (in12) and 46cm (in18) were most closely associated with vegetation community. These variables plot directly on, or just off, the first axis. Additional information conveyed by this graphic was that *S. alterniflora* and *S. patens* had the poorest association with compaction rates of all the community types and surface (zeroin) soil compaction rates had poor association with any vegetation type. Correspondence analysis also provided a highly significant cumulative Chi-square measure of association for the compaction rates at all depths ($\chi^2 = 686$, p-value = 0.00).

Discussion

Current landscape cover maps are critical to resource managers charged with decision-making. Historically, much research involving ecological relationships focused on landform or elevation as the dependent variable. With the advent of emerging Light Detection and Ranging (LIDAR) technology (Hill *et al*, 2001), suggested as capable of achieving elevations within 10cm absolute accuracy (Krabill *et al*, 2000), coastal zone

elevation models could also be useful as a predictor variable for vegetation and soil properties. LIDAR elevation values would be a likely complement to remotely-derived vegetation community class maps for the prediction of soil type and compaction rates.

Grace's (1987) contention that sorting out interrelated variables for determining plant species would incur costly and time-consuming field experiments was mostly correct. Empirical field relationships examined for this research project did consume significant time and effort. However, time spent judiciously in the field was sufficient to enable the mapping of all of Parramore Island. Multivariate statistics are well suited for sorting out interrelated variables and determining principal contributors.

Walker's (1989) investigation of vegetation types grouped according to moisture regimes and micro-scale variations in topography was analogous to the methods applied here. In the case of Walker's work, availability of independent data was the key to establishing the vegetation model. Ecological models should be designed to work with available data, remotely derived or otherwise (Wessman *et al*, 1998). Quantitative soil landscape models have been proposed for terrestrial environments that relied heavily on the use of available variables, especially elevation data, as independent predictor variables (Gessler *et al*, 1995). However, models that have relied historically on USGS digital elevation model data would be ineffective in the coastal zone where small changes in elevation occur that are within the vertical error of the data (Skidmore and Turner, 1988).

Moore *et al* (1993) and Steele (2000) investigated the spatial component of soil as related to slope or landform. In a coastal zone, landform is a principal factor in determining amount of hydrological coupling with the vegetation. Ecological relationships in the coastal environment, especially a barrier island, are distinctly zonal and related to landform. Spatial pattern and structure were evident on Parramore Island, perhaps futher explained by geostatistical methods (Webster and Oliver, 2001).

Soil information is necessary for judicious natural resource management and only a few industrialized countries have complete detailed surveys (McKenzie *et al*, 2000). McKenzie *et al* (2000) questioned the efficiency of conventional methods for acquiring soil data. They recommended the use of terrain analysis to assist in the classification of soils. Vegetation as a predictor variable also satisfies this recommendation. The McKenzie *et al* (2000) solution was to develop process-based relationships between terrain and soil due to their dissatisfaction with empirical models not being portable from one site to another. The extendability of empirical models depends on the uniqueness of the study site. For example, Parramore Island has neighbors within its 18-island chain that are geomorphically similar. Models developed for Parramore Island should be tested on these islands to test model portability and validate, or invalidate, the McKenzie claim.

Remote estimation of centimeter-level elevation could provide a tool for the rapid prediction of flood prone barrier island areas. Temporal mapping of tidal marsh vegetation could provide an efficient, preliminary indication of an increase or decrease in centimeter-level elevation change, as well as the anticipated impact on fishery productivity in adjacent

estuaries. Tidal flow effects the exchange of nutrients between marsh and estuary, and reduced velocities in tidal creeks and sheet flow will cause increased sedimentation that may decrease fish recruitment and survival (Weinstein and Balletto, 1999). Positive relationships between areas of marsh and commercial fishery productivity have been documented previously (Gosselink, 1984; and Costanza *et al*, 1989). Small changes in elevation can affect vegetation community structure and diversity. Management decisions that may increase sediment delivery and raise overall marsh elevation, or decrease sediment accretion and lower marsh elevation, will ultimately have an impact on vegetation communities.

Given the horizontal inaccuracies allowed by the U.S. National Map Accuracy Standard (0.5mm) and a purity (accuracy) of 0.80 of a typical soil map (Lyle, 1999), horizontal inaccuracy can be expected if attempting to align, for example, soil, elevation, and vegetation map data geographically. Lyle computed the accuracy of a new map after cubing the 0.80 error in each separate map (0.8 x 0.8 x 0.8) to arrive at a horizontal accuracy for the combined map of approximately 0.51. If one was to use vegetation community types derived from imagery and then recode the vegetation to estimate soil type, as was done for this work, the source of horizontal error would be restricted to the initial vegetation classification.

Tidal inundation within a lower marsh provides a physical mechanism for dynamic equilibrium between erosion (from existing marsh soil) and deposition of new sediment as sheet-like tidal flow encounters marsh grass resistance, causing the velocity to decrease, and suspended loads to be deposited (Friedrichs and Perry, 2001). Lower compaction rates encourage air spaces in the soil that are critical for the transfer of oxygen to the root zone of

the vegetation. Measurements from Parramore Island confirm that the variation in soil compaction strength is directly associated with resident vegetation. In addition, uniform horizontal and vertical compaction rates exist in association with monotypic vegetation such as *S. alterniflora,* and the more biologically diverse vegetation complexes were associated with increasing variation in soil compaction horizontally and vertically. This finding suggests that vegetation diversity requires soil compaction strengths that are variable in both the horizontal (aerial) and vertical (depth) dimensions. Accordingly, constructed wetlands may need to mimic naturally occurring soil compaction rates if they are to achieve desired biological diversity levels.

Two additional ecological phenomena appear capable of being estimated from image-derived vegetation classes: a) nutrient cycling and b) invasive species advancement. Salt marsh vegetation is believed to be among the most productive on earth with annual estimates of 80 metric tons per hectare of plant material in the southern coastal plain of North America (Mitsch and Gosselink, 1993). High marsh consistently functions as a geochemical sink while lower marsh accounts for variable flux in dissolved organic nitrogen (DON) and dissolved organic phosphorous (DOP) (Wolaver, 1981). High marsh bacteria require DON and DOP for the decomposition of detritus and its release into the estuary in soluble form. Particulate nitrogen and phosphorous are removed by both low and high marshes due to settling of suspended loads (Wolaver, 1981). Given the substantial productivity of salt marsh communities, nutrient flux from these environments into adjoining estuaries are essential for overall sustainability of the ecosystem. Classification and temporal monitoring of vegetation

changes, such as those occurring in *Spartina* marsh communities, can be accomplished from a high-resolution image source.

Imagery classification was successful at separating reed classes, *T. angustifolia* and *P. australis,* from the salt meadow hay *S. patens* class. This result bodes well as a basis for using remotely sensed data for the future management of invasive species. The complexity and distribution of the reed species, especially *P. australis,* is of immediate importance to resource land managers responsible for maintaining biodiversity and wildlife habitat, because it is believed by many to provide little nutritional food source and minimal shelter for wildlife (Pyke, 1999; Silberhorn, 1999). Annual monitoring using a classification of high spatial resolution imagery would quantify changes in the aerial extent of each community and, based on these, control and eradication measures could be implemented.

Conclusion

The aim of this study was to describe an ecological association between vegetation communities and a) elevation, b) soil type, and c) soil compaction strength based on statistical significance. Vegetation communities were selected purposefully because of their ability to be remotely classified into a land cover map from remote sensing. Field data were collected to statistically test the significance and strength of association between ecological variables. Vegetation field data was used in the development of empirical models.

The statistical relationship between seven initial vegetation classes and absolute elevation value was small due to an overlap in elevation for the high marsh vegetation.

Correspondence analysis of elevation values and vegetation classes illustrated this overlap in elevation in a 2-factor plot. Accordingly, vegetation was re-grouped into low marsh, transitionary high marsh, and upper elevation communities. Statistical tests were re-computed and the results improved predictive power of vegetation type as an estimator of centimeter-level elevation ranges. High marsh vegetation was measured within a narrow elevation range of 1.40 to 1.66m suggesting intense competition between the species. Maritime forest was established on ground at or above 2.0m elevation. At the other end of the spectrum, *S. alterniflora* was dominant at elevations of less than 1.32m. Elevation changes, measurable at the centimeter-level, provide compelling evidence of plant tolerance/intolerance to tidal inundation. Elevation clearly defined and restricted the location of individual plant species and created a distinctive zonal pattern of vegetation diversity.

Soil type was shown to have a strong association when tested against eight vegetation types: *S. alterniflora, S. patens, T. angustifolia, P. australis, I. frutescens, M. cerifera,* maritime forest (*P. taeda*), and *A. breviligulata* ($\chi^2 = 0.93$; p-value = 0.0000; df.= 21; $V = 0.86$). Correspondence plot Figure 7 illustrated this strong relationship as vegetation communities were closely aligned with appropriate soil types. However, when compared to grouped vegetation types (Group 1- *S. alterniflora*; Group 2- *S. patens, T. angustifolia, P. australis, I. frutescens;* Group 3- *M. cerifera* and maritime forest; Group 4- *A. breviligulata*), groupings similar to those used for elevation zone designation, the test statistics dropped considerably ($\chi^2 = 0.58$; p-value = 0.0000; d.f.= 9; $V = 0.68$). Results were better when vegetation types were evaluated independently against soil type.

The estimation of soil type within the barrier island was limited to four possible soil choices:

1. Saturated, fibrist and saprist epipedon surface over a saturated grayish sand, with no A horizon;

2. Moist, to very moist, to saturated histic epipedons and highly decayed organic surface, over a variable A horizon (2 to 8cm), over a moist to very moist grayish sand;

3. Dry to moist surface duff over a well defined A horizon (5 to 15cm) over a dry brownish sand;

4. Heterogeneous beach sand composed of random layers of unconsolidated sand and various types of detrital litter.

Soil compaction was related closely to vegetation type at depths of 30 and 46cm. Cramer's V scores of association between 30 and 46cm soil compaction rates and vegetation community types for 10, 7 and 3-vegetation classes were always 0.85 or greater, on an absolute scale of 0.0 to 1.0. Re-grouping vegetation from 10- to 7- to 3-classes positively improved association test scores at 30 and 46cm depths. Soil compaction values for the surface and shallower depths (5 and 15cm) showed little association with vegetation type. Estimation of soil compaction at shallow depths was impractical based on the results at Parramore Island.

Vegetation diversity and the structural complexity of ecosystems appear to be measurable from high-resolution imagery. Complexity might be shown to be part of a larger,

more homogeneous spatial scale of diversity, perhaps best evaluated through a geostatistical analysis of imagery (Oliver *et al*, 2000). A standard ecological diversity score can be computed for vegetation communities on Parramore Island and compared with imagery–derived scales of spatial variation. Spatial variation might be determined using the variogram (a geostatistical tool) for a normalized difference vegetation index (NDVI) spectral image band acquired over the island. This spatial scale of variation could have a short- and long-range component and thus could be used to guide further sampling and also the degree of detail required for future mapping based on classification (Oliver et al, 2000; Oliver *et al*, in press). Elevation data acquired from LIDAR is sufficiently detailed (~1m horizontal postings and ~15cm vertical accuracy) for variogram analysis and again might reveal whether there are short- and long-range components in the variation. Elevation and NDVI variograms could be compared in identical cardinal directions and if they have similar spatial components this would suggest that the effects of elevation can be detected from the imagery. The variogram for one feature (NDVI or elevation) could be used to help estimate the other feature using co-kriging (geostatistical prediction). Soil data are more difficult to acquire than either vegetation or elevation. Variograms of soil properties can be computed from the sample data and used to estimate values at unsampled places across the island by kriging (Webster and Oliver, 2001), thereby complementing the empirical models for estimating soil type and compaction strength established in this study. Kriging uses the variogram and the data to provide optimal unbiased estimates. The reliability of the estimated values of soil properties could be determined using the kriging variance which is calculated at the same time as the predictions by kriging.

Together, remote sensing and association among ecological variables aid large-area analysis of barrier islands and inter-relations with neighboring ecosystems. Remote sensing offers a "top-down" technology critical for determining the scale of variation and characterization of large areas of land. Estimation of centimeter level elevation, soil type, and soil compaction strength complements image analysis by providing an alternative to exhaustive ground-level surveys needed for measurement and calibration. Estimation of soil variables would not have been obtained *directly* via image analysis and surely would have been costly and time consuming to acquire through intensive field analysis. Remote sensing together with methods that relate ecological variables will assist coastal zone managers in ecosystem management and decision-making.

Remote sensing may also be used to address specific resource management issues identified earlier. Shoreline erosion along the coasts of the barrier islands can be mapped and quantified from high-resolution image source. Any necessary erosion mitigation efforts can be targeted and monitored. Rapidly changing ecological conditions that historically inhibited compilation of accurate records of the islands (Oertel *et al*, 1994) can now be accounted for with timely remote sensing missions. Airborne missions may be flown at any time while satellite data is on a fixed schedule. Archival imagery could be viewed and compared with coincident imagery collects for studying the effects of sea level rise (Christensen, 1988; Nicholls *et al*, 1998; Jorgenson and Ely, 2001). As global warming continues, sea level rise can be expected to accelerate. Combining a LIDAR high resolution elevation model with a spectral image classification map into a 3-dimensional display would provide an excellent graphic tool for visualization of future sea level rise impacts, such as the

potential loss of plant diversity suggested by Garcia-Mora *et al* (2000) and Wood (2001). If

disturbances are having a profound effect on plant life, as suggested by Huggett (1995), the

effect must be documented and mitigated.

A logical first step is to map vegetation change, a step that remains ripe for remote

sensing contribution. Mapping of vegetation communities from imagery provides a synoptic

view of vegetation fragmentation. People's existence within the barrier islands should be

monitored and routinely compared for direct links to excess nutrient loadings, over-fishing,

introduction of overheated water from factories, habitat loss, accumulation of pollutants,

sedimentation, marine and beach debris, and oil spills within the coastal zone. Our existence

is spatially related to these anthropogenic disturbances and again may best be evaluated using

image source as a reference tool. Resource managers have developed decision support

models and land decision models but they demand land cover data to run (Cihlar *et al*, 2000).

This data can either come from field collections, image classifications or both. A

combination of field and imagery are recommended, perhaps with the opportunity to apply

geostatistical techniques for mapping into the mix in the near future.

References

Amsberry, L., Baker, M.A., Ewanchuk, P.J., and Bertness, M.D., 2000. Clonal integration and the expansion of *Phragmites australis*. *Ecological Applications*, 10 (4): 1110-1118.

Atkinson, P.M., Fody, G.M., Curran, P.J., and Boyd, D.S., 2000. Assessing the ground data requirements for regional scale remote sensing of tropical forest biophysical properties. *International Journal of Remote Sensing*, 21 (13&14): 2571-2587.

BMDP Statistical Software, Inc., 1992. In Part 1 and 2: Correspondence analysis, BMDP Statistical Software Manual, Volume 2, ed. W.J. Dixon, 683-756.

Barber, G.M., 1988. Chapter 11-Correlation analysis. In Elementary Statistics for Geographers, The Guilford Press, New York, 367-408.

Bonan, G. and Hayden, B., 1990. Using a forest stand simulation model to examine the ecological and climatic significance of the last Quaternary pine-spruce pollen zone in eastern Virginia. *Quaternary Research*, 33, 387-415.

Bourdeau, P.F., and Oosting, H.J., 1959. The maritime live oak forest in North Carolina. *Ecology*, 40: 148-152.

Brady, N.C., 1974. Chapter 12, In The Nature and Properties of Soils, 8th ed., MacMillan Publishing Company, Inc., New York.

Cihlar, J., Latifovic,R., Chen, J., Beaubien, J., Li, Z., and Magnussen, S., 2000. Selecting representative high- resolution sample images for land cover studies. Part 2: Application to estimating land cover composition. *Remote Sensing of Environment*, 72 (2): 127-138.

Chang, D-H., and Islam, S., 2000. Estimation of Soil Physical Properties using Remote Sensing and Artificial Neural Network, *Remote Sensing of Environment*, 74 (3): 534-544.

Christensen, N.L., 1988. Chapter 11- Vegetation of the southeastern coastal plain. In North American Terrestrial Vegetation, edited by M.G. Barbour and W.D. Billings, Cambridge University Press, New York.

Costanza, R., Farber, S.C., and Maxwell, J., 1989. Valuation and management of wetland ecosystems. *Ecological Economics* 1, 335-361.

Chorley, R.J., Schumm, S.A., and Sugden,D.E., 1984. Aeolian processes and landforms- Chapter 16. In Geomorphology, Methuen Press, New York.

Cromley, R. G., 1992. Chapter 6. In Digital Cartography, Prentice-Hall, Inc. New Jersey.

Davies, J.L., 1973. Geographic Variation in Coastal Development, edited by K.M. Clayton, Hafner Publishing Company, New York.

Davis, R.A., 1996. Coasts, Prentice-Hall, Inc., New Jersey.

Eyre, S.R., 1968. Vegetation and Soils, 2nd ed., Edward Arnold Publishers Ltd., London.

Frey, R., and Basan, P., 1978. Coastal salt marshes. In *Coastal Sedimentary Environments*, edited by R.A. Davis, Springer-Verlag, New York.

Friedrichs, C.T., and Perry, J.E., 2001. Tidal salt marsh morphodynamics. *Journal of Coastal Research*, Special Issue, 27: 7-38.

Garcia-Mora, M.R., Gallego-Fernandez, J.B., and Garcia-Novo, F., 2000. Plant diversity as a suitable tool for coastal dune vulnerability assessment. *Journal of Coastal Research*, 16 (4): 990-995.

Gerrard, 1991. The status of temperate hillslopes in the Holocene. *The Holocene*, 1:86-90.

Gessler, P.E., Moore, J.D., McKenzie, N.J., and Ryan, P.J., 1995. Soil-landscape modeling and spatial prediction of soil attributes. *International Journal of Geographical Information Systems*, 9 (4): 421-432.

Gosselink, J.G., 1984. The Ecology of Delta Marshes of Coastal Louisiana: A Community

Profile, U.S. Fish and Wildlife Service, Biological Services, FWS/OBS-84/09,

Washington, D.C., 134.

Grace, J., 1987. Climatic tolerance and the distribution of plants. *New Phytologist*, 106

(Supplement): 113-130.

Greenland, D., and de Blij, H.J., 1977. Chapter 21- Ice, waves, and wind. In The Earth in

Profile: A Physical Geography, Canfield Press, San Francisco.

Huggett, R.J., 1995. Geoecology-An Evolutionary Approach, Routledge, New York.

Hayden, B., Dueser, R., Callahan, J., and Shugart, H., 1991. Long-term research at the

Virginia Coast Reserve. *Bioscience*, 41 (5): 310-318.

Hayden, B.P., Santos, M.C.F.V., Shao, G., and Kochel, R.C., 1995. Geomorphological

controls on coastal vegetation at the Virginia Coast Reserve. *Geomorphology*, 13:

283-300.

Haynes, M.O., 1979. Barrier island morphology as a function of tidal and wave regime. In

Barrier Islands, edited by Letherman, Academic Press, New York, 1-27.

Huggett, R.J., 1995. Geoecology-An Evolutionary Approach, Routledge, New York

Hunt, R.J., 1997. Do created wetlands replace the wetlands that are destroyed? USGS Fact Sheet FS-246-96, http://wwwdwimdn.er.usgs.gov/widocs/wetlands/FS_246-96.html.

Jensen, J.R., Cowen, D.J., Althausen, J.D., Narumalani, S., and Weatherbee, O., 1993. Evaluation of the CoastWatch change detection protocol in South Carolina. *Photogrammetric Engineering and Remote Sensing*, 59 (6): 1039-1046.

Jensen, J.R., 1996. Thematic Information extraction: image classification. In Introductory Digital Image Processing, A Remote Sensing Perspective, Prentice Hall, New Jersey, 197-256.

Jorgenson, T., and Ely, C., 2001. Topography and flooding of coastal ecosystems on the Yukon-Kuskokwim Delta, Alaska: implications for sea-level rise. *Journal of Coastal Research*, 17 (1): 124-136.

Kartesz, J.T., 1994. A synonymized checklist of the vascular flora of the United States, Canada, and Greenland. Vol.1. Checklist. Timber Press, Portland, OR, 622.

Kenward, T., Lettenmaier, D.P., Wood, E.F., and Fielding, E., 2000. Effects of digital elevation model accuracy on hydrologic predictions. *Remote Sensing of Environment*, 74 (3): 432-444.

Klemas, V.V., Dodson, J.E., Ferfuson, R.L., and Haddad, K.D., 1993. A coastal land cover classification system for the NOAA CoastWatch Change Analysis Project. *Journal of Coastal Research*, 9 (3): 862-872.

Knight, M.A. and Pasternack, G.B., 2000. Sources, input pathways, and distributions of Fe, Cu, and Zn in a Chesapeake Bay tidal freshwater marsh. *Environmental Geology*, 39 (12): 1359-1371.

Krabill, W.B., Wright, C.W., Swift, R.N., Frederick, E.B., Manizade, S.S., Yunger, J.K., Martin, C.F., Sonnta, J.G., Duffy, M., Hulslander, W., and Brock, J.C., 2000. Airborne laser mapping of Assateague national seashore beach. *Photogrammetric Engineering & Remote Sensing*, 66 (1): 65-71.

Kraft, J., Biggs, R., and Halsey, S., 1973. Morphology and vertical sedimentary sequence models in Holocene transgressive barrier systems. In <u>Coastal Geomorphology</u>, edited by D. Coats, SUNY Binghampton, 321-354.

Lyle, J.T., 1999. <u>Design for Human Ecosystems</u>, Island Press, New York.

McBratney, A.B., and Webster, R., 1983. How many observations are needed for regional estimation of soil properties? *Soil Science*, 177-183.

McCaffrey, C.A., and Duesser, R.D., 1990. Plant associations on the Virginia barrier islands. *Virginia Journal of Science*, 41 (4a) 282-299.

McKenzie, N.J., Gessler, P.E., Ryan, P.J., and O'Connell, D.A., 2000. Chapter 10-The role of terrain analysis in soil mapping, In Terrain Analysis- Principles and Applications, edited by J.P. Wilson and J.C. Gallant, John Wiley and Sons, Inc., New York, 245-266.

Michalek, J.L., Wegner, T., Luczkovich, J., and Stoffle, R.,1993. Multispectral change vector analysis for monitoring coastal marine environments. *Photogrammetric Engineering and Remote Sensing*, 59 (3) 381-384.

Milne, G., 1935. Composite units for the mapping of complex soil associations. *Transactions of the 3rd International Congress on Soil Science*, 1:325-347.

Mitsch, W.J. and Gosselink, J.E., 1993. Chapter 8- Tidal salt marshes. In Wetlands, 2nd ed. Van Nostrand Reinhold, New York.

Moore, J.D., Gessler, P.E., Nielsen, G.A., and Petersen, G.A., 1993. Soil attribute prediction using terrain analysis. *Journal of Soil Science America*, 57, 443-452.

Nicholls, R.J., Leatherman, S.P., Dennis, K.C., and Volonte, C.R., 1994. Impacts and responses to sea-level rise: qualitative and quantitative assessments. *Journal of Coastal Research*, Special Issue 14, 26-43.

Oertel, G.F., and Kraft, J.C., 1994. Chapter 6- New Jersey and Delmarva barrier islands, description of Delmarva barrier islands. In <u>Geology of Holocene Barrier Island Systems</u>, edited by R. Davis, Jr., Springer-Verlag, New York, 207-232.

Oliver, M., Webster, R., and Slocum, K., 2000. Filtering SPOT imagery by kriging analysis. *International Journal of Remote Sensing*, 21(4): 735-752.

Oliver, M.A., Shine, J., Slocum, K.R., in press. Using the variogram to explore imagery of two different spatial resolutions. *International Journal of Remote Sensing*.

Pyke, C.R., and Havens, K.J., 1999. Distribution of the invasive reed *Phragmites australis* relative to sediment depth in a created wetland. *Wetlands*, 19 (1): 283-287.

Rinker, J.,1994. <u>Remote Sensing Tutorial: Multiband, Multispectral, Hyperspectral</u>. U.S. Army Topographic Engineering Center.

Ruhe, R.V. and Walker, P.H., 1968. Hillslopes and soil formation open systems. *Transactions of the 9th International Congress of Soil Science*, Adelaide 4: 551-560.

Schwartz, M.L., ed., 1982. The Encyclopedia of Beaches and Coastal Environment-, Encyclopedia of Earth Sciences, Volume XV, Hutchinson Ross Publishing Company, Stroudsburg, Pennsylvania.

Scott, J., 1991. Between Ocean and Bay: A Natural History of Delmarva, Tidewater Publishers, Chesapeake, Maryland, Sect. IV, 157-180.

Sokal, R.R. and Rohlf, F.J., 1995. Chapter 15- Correlation. In Biometry, 3rd ed., W.H. Freeman and Company, New York, 593-608.

Silberhorn, G.M., 1999. Common Plants of the Mid-Atlantic Coast: A Field Guide, 3rd ed., Johns Hopkins University Press, Baltimore, MD.

Skidmore, A.K., and Turner, B.J., 1988. Forest mapping accuracies are improved using supervised nonparametric classifier with SPOT data. *Photogrammetric Engineering and Remote Sensing*, 54: 1415-1421.

Smith, R.L., 1996. Appendix B, Ecology and Field Biology, 5th ed., Harper Collins, New York.

SPSS, Inc., 1998. SYSTAT software, version 8.0, Correspondence analysis module.

StatSoft, Inc., 1995. Statistica, Basic Statistics and Tables (Computer Program), In Basic Statistics and Tables, Gamma, Statistica for Windows, Vol. III, Tulsa, OK.

Steele, B.M., 2000. Combining multiple classifiers: an application using spatial and remotely sensed information for land cover type mapping. *Remote Sensing of Environment*, 74 (3): 545-556.

Strahler, A.N., 1962. Chapter 28-Landforms made by wind. In Physical Geography, 2nd ed., John Wiley & Sons, Inc., New York.

Vogelmann, J.E., Howard, S.M., Yang, L., Larson, C.R., Wylie, B.K., and van Driel, N., 2001. Completion of the 1990s national land cover data set for the conterminous United States from Landsat Thematic Mapper data and ancillary data sources. *Photogrammetric Engineering and Remote Sensing*, 67 (6): 650-662.

Walker, E.P., Binnian, E., Evans, B.M., Lederer, N.D., Nordstrand, E., and Webber, P.J., 1989. Terrain, vegetation, and landscape ecology of the R4D research site, Brooks Range Foothills, Alaska. *Holarctic Ecology*, 12:238-261.

Webster, R., and Oliver, M.A., 2001. Geostatistics for Environmental Scientists, John Wiley and Sons, Ltd., Chichester, UK.

Weinstein, M.P., and Balletto, J.H., 1999. Does the common reed, *Phragmites australis*, affect essential fish habitat? *Estuaries*, 22 (3B): 793-802.

Wessman, C.A.,, Cramer, W., Gurney, R.J., Martin, P.H., Mauser, W., Nemani, R., Paruelo, J.M., Penuelas, J., Prince, S.D., Running, S.W., and Waring, R.H., 1998. Chapter 5- Group report: remote sensing perspectives and insights for study of complex landscapes. In Integrating Hydrology, Ecoxsystem Dynamics, and Biogeochemistry in Complex Landscapes, edited by J.D. Tenhunen and P. Kabat, John Wiley and Sons, New York, 89-103.

Wheatley, J.M., Wilson, J.P., Redmond, R.L., Zhenkui, M., DiBenedetto, J., 2000. Chapter 15-Automated land cover mapping using Landsat Thematic Mapper images and topographic attributes. In Terrain Analysis- Principles and Applications, edited by J.P. Wilson and J.C. Gallant, John Wiley and Sons, Inc., New York, 245-266.

Wolaver, T.G., 1981. Nitrogen and phosphorous exchange between a mesohaline marsh and the surrounding estuary, University of Virginia, Dissertation.

Wood, B., 2001. Maintaining vegetation diversity on reserves: the relationship between persistence and species richness. *Biological Conservation*, 97 (2): 199-205.

Zar, J.H., 1999. Chapter 11- Multiple comparisons. In Biostatistical Analysis, 4th ed., Prentice-Hall, Inc., Jew Jersey.

http://www.co-ops.nos.noaa.gov/data_retrieve.html. NOAA/NOS Historic Monthly Mean

Water Level Data.

Table 1. Field variables and corresponding data. Vegetation, soil, and elevation zone are categorical data values, while percent cover of vegetation and elev (m) are integer values. Plot ID is the sample identification number corresponding to the field sample location. Veg values 1, 2, 3, 4, 6, 7, and 8 represent: *S. alterniflora, S. patens, T. angustifolia, P. australis,* low-density shrub, high-density shrub, and maritime forest. Soil values are represented as follows: 1 = Saturated, fibrist and saprist epipedon surface over a saturated grayish sand, with no A horizon; 2 = Moist, to very moist, to saturated histic epipedons and highly decayed organic surface, over a variable A horizon (2 to 8cm), over a moist to very moist grayish sand; 3 = Dry to moist surface duff over a well defined A horizon (5 to 15cm) over a dry brownish sand; 4 = Heterogeneous beach sand composed of random layers of unconsolidated sand and various types of detrital litter. Elevation zones are represented as follows: 1 = 1.16 to 1.32m; 2 = 1.40 to 1.66; 3 = 1.66 to 2.24 (or higher).

Plot ID	Veg	Percent Cover	Soil	Elev zone	Elev (m)
181	1	50	1	1	1.16
182	1	50	1	1	1.20
100	1	50	1	1	1.32
200	1	50	1	1	1.23
1	2	100	1	2	1.40
2	2	100	1	2	1.48
3	2	50	2	2	1.48
12	2	100	1	2	1.49
19	2	100	1	2	1.54
13	2	100	1	2	1.55
14	2	80	1	2	1.57
37	2	100	1	2	1.58
9	2	90	1	2	1.58
17	2	100	1	2	1.60
33	2	100	1	2	1.63
34	2	100	1	2	1.65
29	2	50	1	2	1.65
4	3	75	2	2	1.50
23	3	100	1	2	1.56
38	3	100	1	2	1.56
11	3	50	1	2	1.57
10	3	70	1	2	1.63
30	3	80	2	2	1.66
5	4	100	2	2	1.51
6	4	10	2	2	1.58
32	4	100	1	2	1.60
31	4	100	1	2	1.63
15	6	50	1	2	1.58
24	6	50	2	2	1.59
20	6	100	2	3	1.68
7	7	100	3	3	1.66
28	7	75	2	3	1.69
36	7	75	2	3	1.72
22	7	90	2	3	1.80
18	7	100	2	3	1.89
35	8	50	3	3	1.99
21	8	50	3	3	2.19
25	8	55	4	3	2.51
26	8	60	3	3	2.69
8	8	40	3	3	7.08

Table 2. (a) Tukey results of pair wise comparisons for 7-vegetation classes. Earlier ANOVA results indicated that elevations grouped within 7 vegetation classes were significantly different (F-stat = 25.53, F-critical value = 3.97, p-value = 0.0000, d.f. = 39). Tukey test results for the 7-vegetation classes identified similar and dissimilar vegetation pairs based on the test scores returned. Tukey scores are based on a 0.0 to 1.0 scale, with 1.0 representing a perfect correlation and values marked with an asterisk (*) indicating a highly significant score for a vegetation pair. Scores below indicate that classes (2) *S. patens*, (3) *T. angustifolia*, (4) *P. australis*, and (6) *I. frutescens* and *B. halimifolia* (together constituting low-density shrub) are co-existing in a zone of elevation that is essentially equivalent.

	1	2	3	4	6	7	8
1	1.0000						
2	.0052*	1.0000					
3	.0064*	.9993	1.0000				
4	.0369*	.9999	1.0000	1.0000			
6	.0186*	1.0000	.9999	.9999	1.0000		
7	.0002*	.0069*	.0664	.1764	.0469*	1.0000	
8	.0001*	.0001*	.0001*	.0001*	.0001*	.0002*	1.0000

(b) Tukey results of pair wise comparisons for 3-vegetation classes. All values are highly significant. A re-grouped 3-class vegetation grouping was selected based on earlier 7-vegetation class Tukey results (Table 2a) and, also, based on the difficulty in separating high-density shrub class from maritime forest class spectral information. The three new groups comprise:

Group 1- *S. alterniflora*
Group 2- *S. patens*, *T. angustifolia*, *P. australis*, and *I. frutescens* and *B. halimifolia*
Group 3- *M. cerifera* and Maritime forest (dominated by *P. taeda*)

	1	2	3
1		.0049	.0001
2	.0049		.0001
3	.0001	.0001	

Table 3. Variables in this table include: vegetation type, elevation ranges (low and high) in meters, elevation class, soil class, and probability (%) of correctly estimating soil class from the field data that was collected. Elevation range for the three new vegetation classes was determined by selecting the lowest and highest elevation in the grouping. The values in parentheses beneath column "soil class" represent a secondary soil class in which the vegetation type was found.

Vegetation Type	Low Elev. (m)	High Elev. (m)	Elev. Class	Soil Class	Prob (%)
S. alterniflora (short form)	1.16	1.32	1	1	100
S. patens	1.40	1.65	2	1 (2)	92
T. angustifolia	1.56	1.63	2	1 (2)	67
P. australis	1.51	1.66	2	2 (1)	50
I. frutescens, B. halimifolia	1.48	1.68	2	2 (1)	67
M. cerifera	1.66	2.24	3	2 (3)	50
P. taeda maritime forest	1.99	7.08	3	3 (4)	80
A. breviligulata	n/a	n/a	n/a	4	100

Table 4. Dune transect data acquired to support the development of a methodology to estimate maximum height and crest based on forest width measurements. Three preliminary transects were run (sample transects 1, 2 and 3). Measurements acquired along the transect included: dune crest height in meters (height); width of the leeward, steeper side of the dune in meters (short); width of the windward, shallower side of the dune (long); total width of the dune in meters (short and long). Ratios were computed from these field data to compute: crest location (short / (long + short) and dune height A methodology to estimate dune height and relative crest location under maritime forests was tested based on forest widths. Plotting the results of three test transects (Figure 4) illustrated geomorphological similarities across the dune. The y-axis measures the dune heights, the x-axis the forest width, and the transect break points represent the dune crest locations. Table 4 contains the original transect data. For the three preliminary transects, ratios were computed based on H = dune height, LS = lee slope, and W = forest width: (height / (short + long).

	Height (m)	Short (m)	Long (m)	Short & Long (m)	Short / Long + Short (ratio)	Height / Short + Long (ratio)
Sample transect 1	7.13	4.72	17.99	22.71	0.21	0.30
Sample transect 2	4.42	2.65	11.80	14.45	0.18	0.30
Sample transect 3	7.01	3.54	14.75	18.29	0.19	0.37

Table 5. Statistical results of 10-, 7-, and 3-vegetation classes tested for their analysis of variance (F-stat, F-critical, p-value, and degrees of freedom) and measures of association (Cramer's V, Chi square, p-value, and degrees of freedom) with soil compaction values measured at depths of 0-, 5-, 15-, 30-, and 46cm. The p-values at most depths were significant at the 95% confidence level. Vegetation type explained the variance in soil compaction at depths of 30- and 46-cm the most effectively, regardless of the number of vegetation classes. Analysis of variance (ANOVA) results for 10-, 7- and 3-vegetation classes (respectively) and soil compaction rates affirmed the MANOVA findings by returning significant p-values at most depths and increased F-statistics as measured depths increased. The Cramer's V and Chi-square association test for the 10-, 7- and 3- vegetation classes and soil compaction strength produced scores of at least 0.85 for 30- and 46-cm depths; all shallower depths produced smaller scores. Similar to the MANOVA and ANOVA results, scores for Chi-square and Cramer's V increased with measured depth.

10 Veg Classes Depth	F-Stat	F-Crit	p-value	d.f.	Cramer's V	Chi	p-value	d.f.
46-cm (18-in)	359	3.9	0.0000	135	0.85	457	0.04	405
30-cm (12-in)	226	3.9	0.0000	135	0.85	452	0.01	378
15-cm (6-in)	195	3.9	0.0000	135	0.74	342	0.08	306
5-cm (2-in)	187	3.9	0.0000	135	0.66	272	0.00	207
0-cm (0-in)	80	3.9	0.0000	135	0.45	128	0.01	90
7 Veg Classes Depth	**F-Stat**	**F-Crit**	**p-value**	**d.f.**	**Cramer's V**	**Chi**	**p-value**	**d.f.**
46-cm (18-in)	362	3.9	0.0000	135	0.87	308	0.04	264
30-cm (12-in)	230	3.9	0.0000	135	0.89	322	0.00	246
15-cm (6-in)	203	3.9	0.0000	135	0.75	232	0.05	198
5-cm (2-in)	201	3.9	0.0000	135	0.59	144	0.22	132
0-cm (0-in)	103	3.9	0.0000	135	0.40	65	0.29	60
3 Veg Classes Depth	**F-Stat**	**F-Crit**	**p-value**	**d.f.**	**Cramer's V**	**Chi**	**p-value**	**d.f.**
46-cm (18-in)	365	3.9	0.0000	135	0.96	127	0.00	88
30-cm (12-in)	232	3.9	0.0000	135	0.96	124	0.00	82
15-cm (6-in)	207	3.9	0.0000	135	0.73	72	0.3	66
5-cm (2-in)	210	3.9	0.0000	135	0.60	49	0.28	44
0-cm (0-in)	122	3.9	0.0000	135	0.44	26	0.17	20

Table 6. Summary of the minimum and maximum soil compaction values, measured in pounds per square inch (psi), grouped by vegetation type at 0, 5, 15, 30, and 46cm depths. A 7-class vegetation table (minus *A. breviligulata*) lists the minimum and maximum soil compaction rates sampled at each of the five depths. Compaction rates were measured in the field with a 50cm soil penetrometer.

Vegetation	0cm	5cm	15cm	30cm	46cm
S. alterniflora	0-20	40-142	106-147	101-137	117-152
S. patens	5-50	25-101	45-101	81-244	71-504
T. angustifolia	0-40	5-142	25-295	132-310	188-498
P. australis	5-30	25-117	56-137	106-213	218-437
I. frutescens	20-45	66-71	122-152	254-412	280-376
M. cerifera	20-25	45-61	91-168	519-758	310-946
P. taeda	15-50	30-96	167-290	458-483	524-616

Figure 1. Location map of study site at Parramore Island, Virginia. Eighteen barrier islands make up a chain trending northeast-to-southwest off of Virginia's Eastern Shore Parramore Island is the central-most island in this barrier chain. No permanent human population inhabits the island and activities such as agriculture, hunting, logging or similar activities are prohibited. The island is approximately ten kilometers long by one and a half kilometers wide and is separated from the mainland by a series of bays, salt marsh and small tidal creeks. Barrier island dune and valley complexes represent unique geomorphological conditions that support very distinct vegetation zonation. Homogenous stands of cattails (*T. angustifolia*) and common reed (*P. australis*) are found growing within Parramore Island's upper valley marshes. The high marsh also supports low-density, short-height marsh elder (*I. frutescens*) and groundsel-tree (*B. halimifolia*), found in co-existence with an herbaceous component that includes *S. patens* and *T. angustifolia*.

Parramore Island

Figure 2. (a) Multispectral 4-channel imagery, acquired in May 1999, displayed as a false color composite image of Parramore Island, Virginia. (b) Vegetation classes were derived from the imagery using a supervised classification method, and the vegetation classes attributed by soil compaction strength estimated for12- and 18-inch depths. These estimates were based on earlier ANOVA and Cramer's tests indicating strength of association. (c) A soil type class map was compiled by a simple recode of vegetation classes that had been grouped into three categories. Each vegetation class had a corresponding soil type that was mapped. (d) Lastly, an elevation class map was also re-coded from vegetation classes that had been grouped into three categories.

(a)

(b)

Vegetation Class, w/ Soil Compaction Range (psi) Attributed at 12- and 18-inch depths

- *S. alterniflora* (101-137, 117-152)
- *S. patens* (81-244, 71-504)
- *T. angustifolia* (132-310, 188-498)
- *P. australis* (106-213, 218-437)
- *I. frutescens* (254-412, 280-376)
- *M. cerifera* (519-758, 310-946)
- *P. taeda* (458-483, 524-616)
- *A. breviligulata*
- Beach/sand
- Water

(c)

Soil type

- Type 1- Saturated
- Type 2- Moist
- Type 3- Dry
- Type 4- Sand
- Water

(d)

Elevation Range

- < 1.40 meters
- 1.40 - 1.68 meters
- > 1.66 meters
- Not classed
- Water

Figure 3. Elevation range (in meters) by vegetation community type at Parramore Island. The upper maritime forest elevation range was purposefully adjusted with an additional crest height data point to illustrate a more representative elevation range. Elevation range for each vegetation classes was determined by the low and high elevation value sampled for that class, shown along the x-axis. The y-axis represents elevation in meters. The graph depicts an overlap in habitat elevation for high marsh species *S. patens*, *T. angustifolia*, *P. australis*, *I. frutescens*, and *B. halimifolia*.

Elevation Range by Vegetation Type at Parramore Island

Legend:
- S. alterniflora
- S. patens
- T. angustifolia
- P. australis
- Low Density
- High Density
- Maritime Forest

X-axis: Low-Elev, High-Elev
Y-axis: 0–8
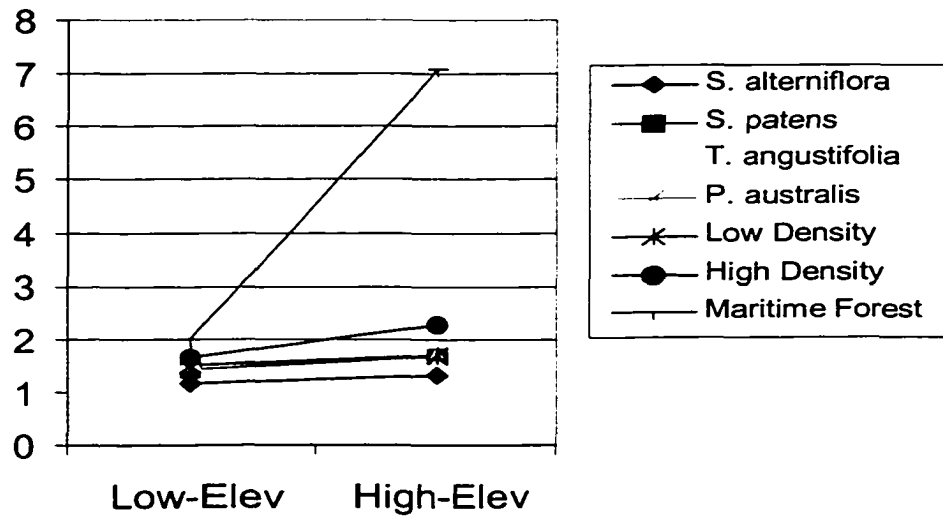
Figure 4. Correspondence analysis plot for vegetation and elevation with a non-significant Chi-square computed as an intermediary result (p-value = 0.144, d.f.=168). Five factors were needed to account for over 90% of the cumulative contribution explaining the association between variables. Factor 1, represented as Dim (1) or the x-axis, contributed only 21.33% with eigenvalue 1.00, and factor 2, represented as Dim (2) or the y-axis, contributed 21.33% with eigenvalue 1.00. The origin of the graph matrix is found at the intersection of the red vectors. At the end of each vector are vegetation sample plots. Plot locations, shown by open circles, provide measurable distances (horizontally and vertically) from the origin, and this distance is an indication of how far away the variable is in chi-square euclidean distance from the overall marginal row profile. Horizontal and vertical distances between points (no diagonal distances) are approximate chi-square distances between individual row profiles. The axes provide the scaled distances. The row, or vegetation variable, that contributed the most to the Factor 1 was maritime forest (0.875) and the row variable contributing the most to the Factor 2 was *S. alterniflora* (0.886). Column variables, or elevation values, contributing to Factor 1 were all the elevation values measured within maritime forest and contributing variables to Factor 2 were all elevation values measured within *S. alterniflora*. This result supported a decision to divide elevation into groups, with *S. alterniflora* in a group by itself, and maritime forest in a group joined only by high-density shrub. The plot itself also indicates that there are three primary zones grouping together elevation values and vegetation codes; unfortunately, variable symbols are plotting on top of each other and difficult to read. *Spartina alterniflora* is plotted at the top; high-density shrub and maritime forest are together on the far right; and *S. patens*, *T. angustifolia*, *P. australis*, and low-density shrub are together just off the origin.

Correspondence Plot
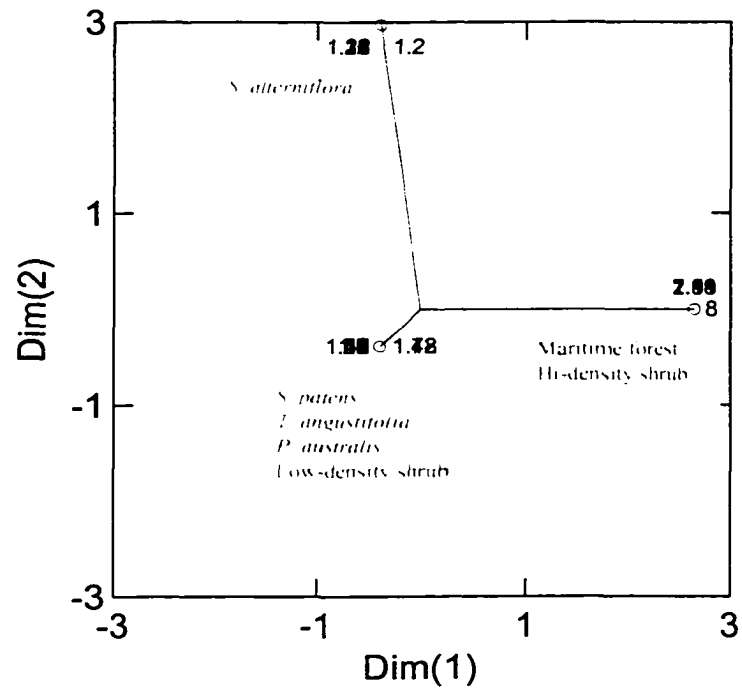
Figure 5. Correspondence analysis of elevation zones, as justified from earlier findings, was used to compute a 2-axis plot for vegetation and elevation values (Figure 5). A highly significant Chi-square was computed as an intermediary result (p-value = 0.000, d.f. = 12). Two factors were needed to account for over 100% of the cumulative contribution explaining the association between variables. Factor 1, represented as Dim (1) or the x-axis, contributed 52.28% with eigenvalue 1.00, and factor 2, represented as Dim (2) or the y-axis, contributed the remaining 47.72% with eigenvalue 0.913. The origin of a graph matrix is found at the intersection of the red vectors and at the end of each vector are vegetation sample plots. Vegetation plot locations are shown by open red circle symbols. Plot locations provide measurable distances (horizontally and vertically) from the origin, and this distance is an indication of how far away the variable is in chi-square euclidean distance from the overall marginal row profile. Horizontal and vertical distances between points (no diagonal distances) are approximate chi-square distances between individual row profiles. The axes provide the scaled distances. The row variable, or vegetation, that contributed the most to Factor 1 was *S. alterniflora* (0.897). The row variables contributing the most to Factor 2 were high-density shrub (0.394), maritime forest (0.315), *S. patens* (0.164), *T. angustifolia*, and *P. australis* (0.050). These results also support the idea of three elevation zones with selected vegetation membership within the groups. The correspondence plot suggests that perhaps low-density shrub (code 6) could be in its own elevation zone.

Correspondence Plot
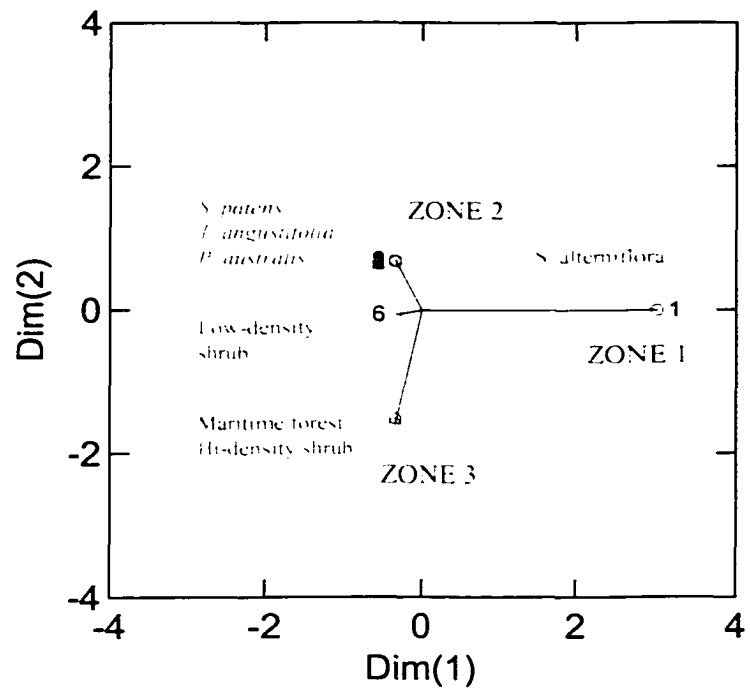
Figure 6. Plotting the results of three test transects illustrated geomorphological similarities across a vegetated transverse dune. A methodology to estimate dune height and relative crest location under maritime forests was tested based on forest widths. The y-axis measures the dune heights, the x-axis the forest width, and the transect break points represents the dune crest locations. For the three preliminary transects, ratios were computed based on H = dune height, LS = lee slope, and W = forest width. Strong similarities in crest shape and location suggests that modeling of crest height and location may be possible from a forest width measurement and the ratios computed from these test transects.

Transects Across Vegetated Transverse Dune

Elevation (meters)

Maritime Forest Width (meters- measured perpendicular to coast)

Transect 1
Transect 2
Transect 3
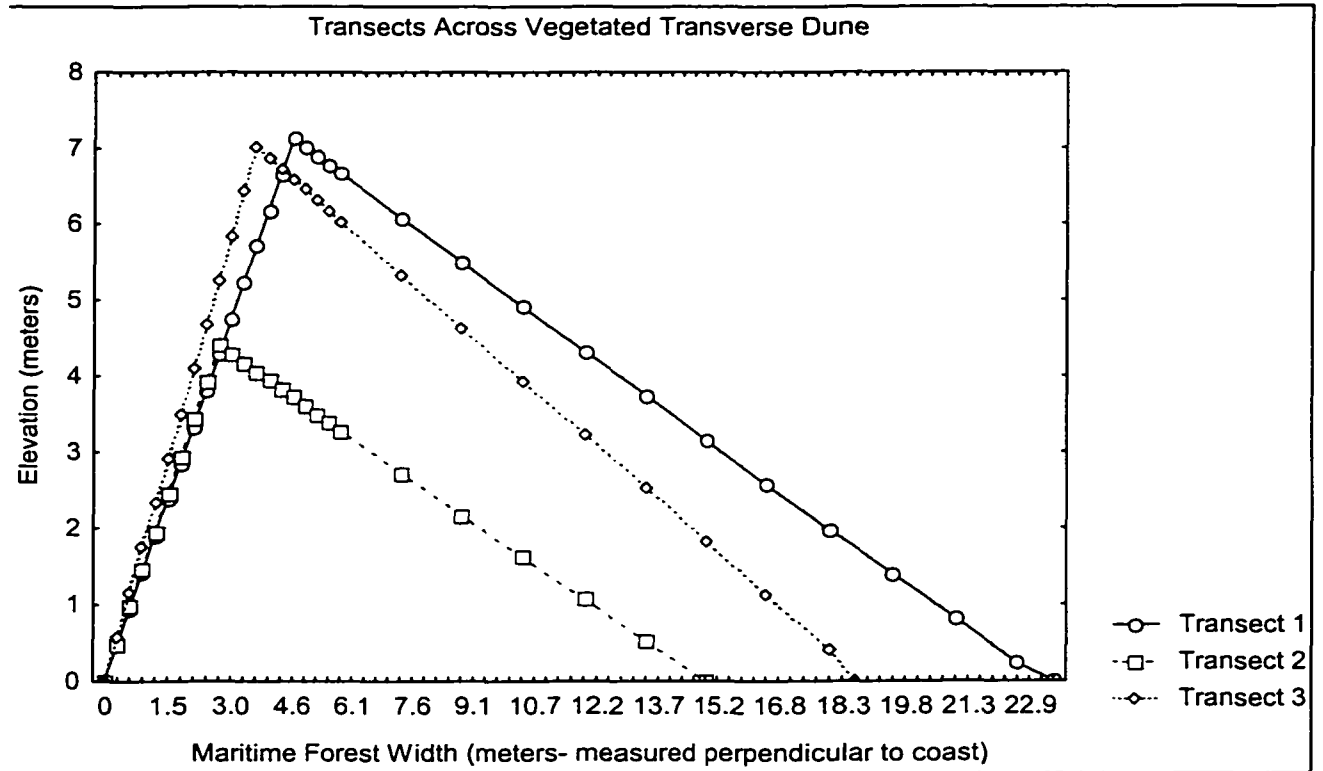
Figure 7. Correspondence analysis was used to compute a 2-axis plot for vegetation and soil types (Figure 7). A highly significant Chi-square was computed as an intermediary result (p-value = 0.000, d.f.= 18). Two factors were needed to account for over 99.70% of the cumulative contribution explaining the association between variables. Factor 1, represented as Dim'ension' (1) or the x-axis, contributed 67.54% with eigenvalue 0.865, and factor 2, represented as Dim'ension' (2) or the y-axis, contributed 32.16% with eigenvalue 0.412. The origin of a graph matrix is found at the intersection of the red vectors and at the end of each vector are vegetation sample plots. Vegetation plot locations are shown by open red circle symbols and blue symbols represent soil types. Plot locations provide measurable distances (horizontally and vertically) from the origin, and this distance is an indication of how far away the variable is in chi-square euclidean distance from the overall marginal row profile. Horizontal and vertical distances between points (no diagonal distances) are approximate chi-square distances between individual row profiles. The axes provide the scaled distances. The row variables, or vegetation, that contributed the most to Factor 1 were maritime forest (0.797) and *S. patens* (0.102). Several row variables contributed to Factor 2: high-density shrub (0.457), *S. patens* (0.184), low-density shrub (0.132), *S. alterniflora* (0.105), maritime forest (0.064), and *P. australis* (0.055). The vegetation variables are plotted in sequence, 1 to 7, and then 8 off to itself, in large part replicating a natural sequence of vegetation spatial pattern attributed in part to soil type. The correspondence plot suggests that low-density shrub (code 6) could be separate from elevation zone 2.

Correspondence Plot
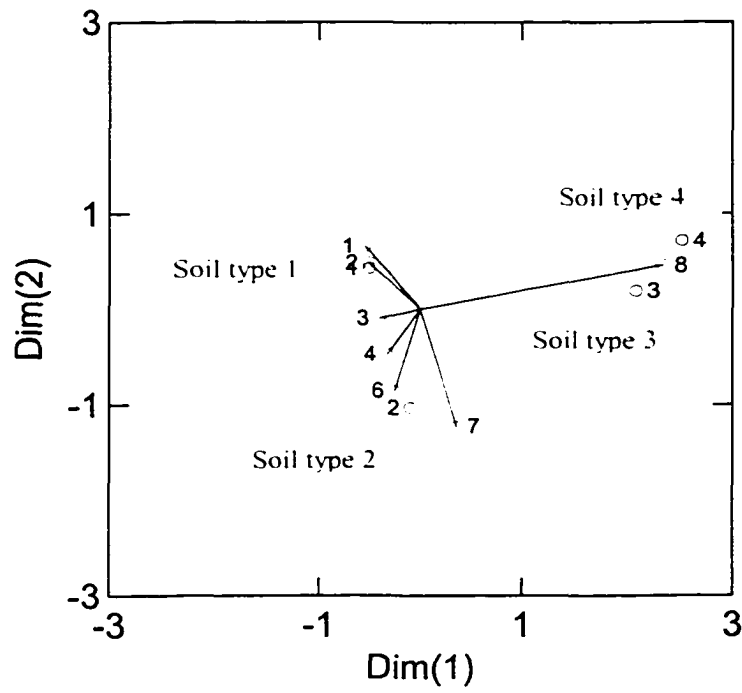
Figure 8. Cramer's V statistical test scores of association between 10-vegetation types and soil compaction rates at depths of: 0 (0cm), 2 (5cm), 6 (15cm), 12 (30cm) and 18in (46cm). The plot shows that strength of association increased (Cramer's V score increases) as the depth of compaction measurement increased.

Vegetation Type Association with Soil Compaction
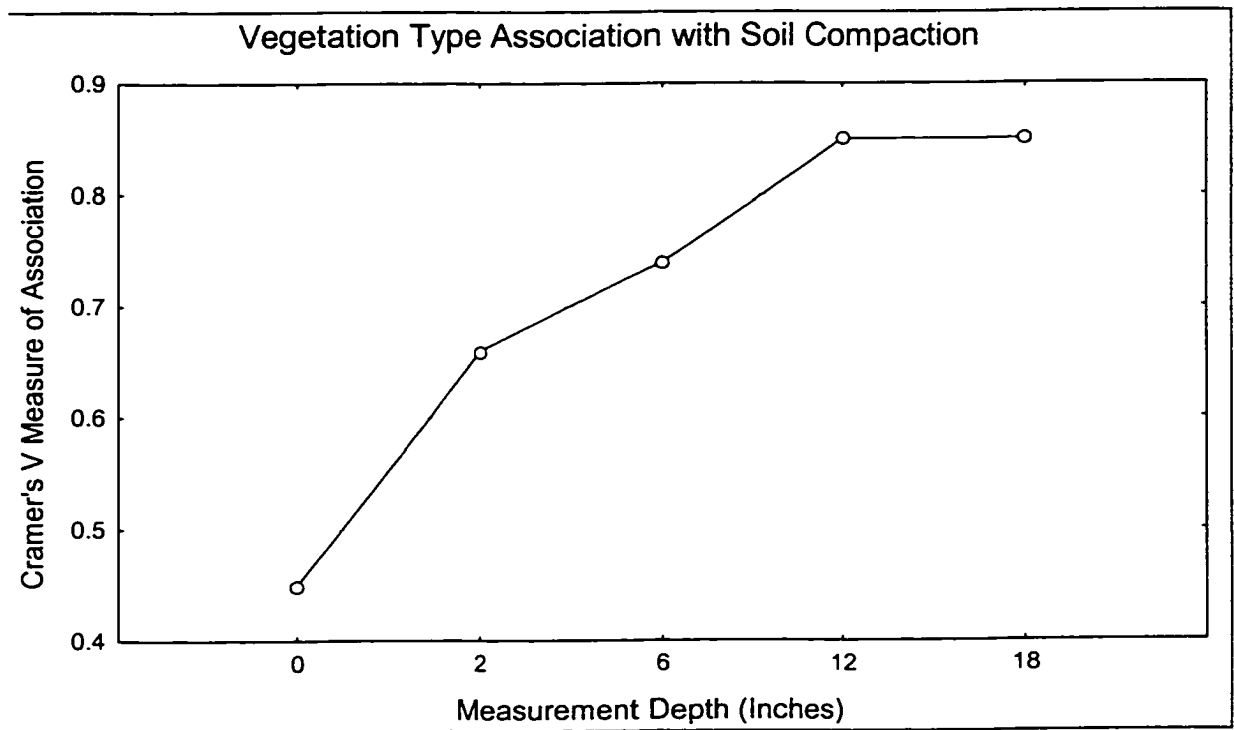
Figure 9(a)- Average compaction rate for soil at depths of 0, 2, 6, 12, and 18in for 10 vegetation classes. Y-axis gives compaction rates expressed in pounds per square inch. X-axis gives measurement depth in inches. Low marsh vegetation (*S. alterniflora*) has a lower compaction rate at all depths, while high-density shrub and maritime forest show continually increasing compaction rates with depth.

Average Soil Compaction Rates

Legend:
- S. alterniflora
- lower S. patens
- upper S. patens
- low T. angustifolia
- Up T. angustifolia
- Low P. australis
- Up P. australis
- Low density shrub
- High density shrub
- Maritime forest

X-axis: Measurement Depths (0-inches, 2-inches, 6-inches, 12-inches, 18-inches)

Y-axis: Compaction (pounds per square inch) (-100 to 800)
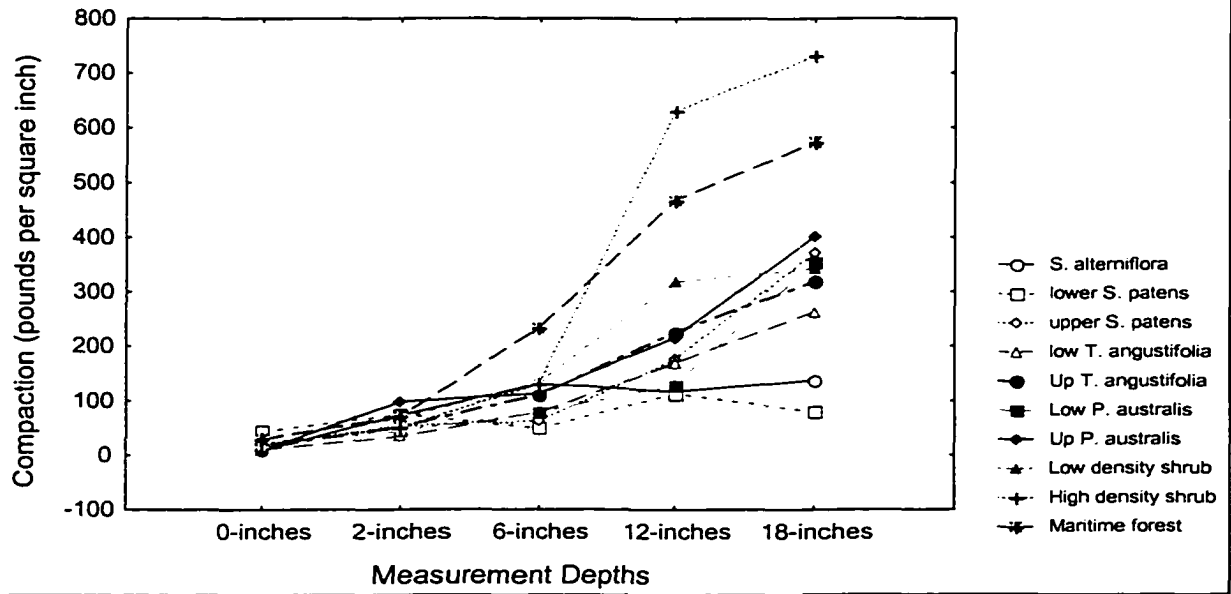
Figure 9(b)- Variability in soil compaction rates increased at deeper depths of 12 and 18 inches. A box-and-whisker plot shows that the greatest variation among soil compaction rates measured at these deeper depths. The ten vegetation types separate more effectively within the wider, more variable, range of soil compaction rates.

Soil Strength and Variability with Depth
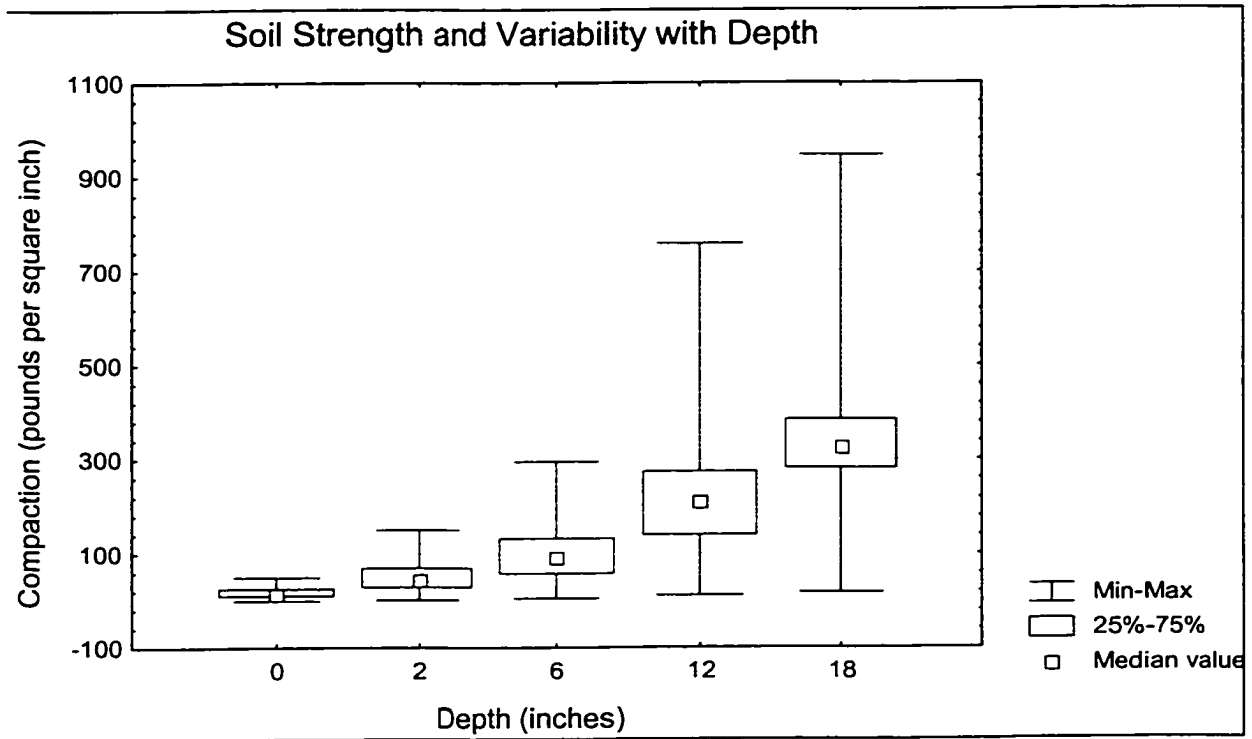
Figure 10. Correspondence analysis (CA) plot from an analysis of vegetation community types and soil compaction rates at 0, 5, 15, 30, and 46cm depths. CA decomposed row and column pairs into two components that explained 73.8% of the association, with the principal axis (axis 1) contributing 43.0% and the second axis (axis 2) contributing 30.8%. Vegetation type and soil compaction depth variables are plotted as point data with their respective distance from the origin, or intersection of the two axes, providing an indication of how far away each variable is in chi-square distance from the overall marginal row and column profile. For depth variables, soil compaction rates at 30 and 46cm were very closely associated along the first component axis and closely associated with the second component; 15 and 5cm were closely related but far removed from the first and second components; and surface measurements were plotted in isolation and exceptionally far away from both axis. All vegetation communities hovered about the origin, or right on the primary component axis, except the low marsh species, lower *S. patens* and *S. alterniflora*. This plot concurs with prior statistical findings that suggested that soil compaction rates at 30 and 46cm were most closely associated with vegetation community. Additional information conveyed by this graphic was that *S. alterniflora* and *S. patens* had the poorest association with compaction rates of all the community types.

<u>Vegetation Community Types</u>
salter = *S. alterniflora*
lowpats = lower elevation *S. patens*
hipats = higher elevation *S. patens*
lowing = lower elevation *T. angustifolia*
hiang = higher elevation *T. angustifolia*
lowaust = lower elevation *P. australis*
hiaust = higher elevation *P. australis*
low shrub = low density shrubs
hishrub = high density shrubs
marfor = maritime forest

<u>Soil Compaction Depths</u>
zeroin = 0in, or surface
in2 = 2in (5cm)
in6 = 6in (15cm)
in12 = 12in (30cm)
in18 = 18in (46cm)

PLOT OF ROWS AND COLUMNS

```
              ...+........+.......+.........+.......+.......+.......+.......+.....
              -                 |                                              -
     .6       +                 +                                              +
              -                 |                     zeroin                   -
              -                 |                                              -
              -                 |                                              -
              -                 |                                              -
              -                 |                                              -
     .4       +                 +                                              +
              -                 |                                              -
              -                 |                                              -
              -                 |                                              -
              -               hischrub                                         -
              -                 |                     lowpats                  -
              -                 |                                              -
     .2       +               in12                                            +
   A          -                 |                                              -
   X          -                 |                                              -
   I          -                 |                                              -
   S          -                 |                                              -
              -     lowang      |                                              -
   2          -               marfor                                           -
              -                 |                                              -
     0.       +--+--------+--------+-------+-------+-------+-------+-------+----+
              -       hiang      |                                              -
              -                 |        lowshrub                               -
              -                 |                                              -
              -     in18        |                                              -
              -       hipats    |                                              -
              -                 |                                              -
    -.2       +               lowaust        in6                              +
              -                 |                                              -
              -                 |                                              -
              -                 |            in2                               -
              -                 |                                              -
              -                 |           salter                             -
              -                 |                                              -
    -.4       +                 +                                              +
              -                 |
              ...+........+.......+.........+.......+.......+.......+.......+.....
                    -.20          0.0       .20        .60       1.0
                -.40        0.0         .40         .80         1.2
```

AXIS 1
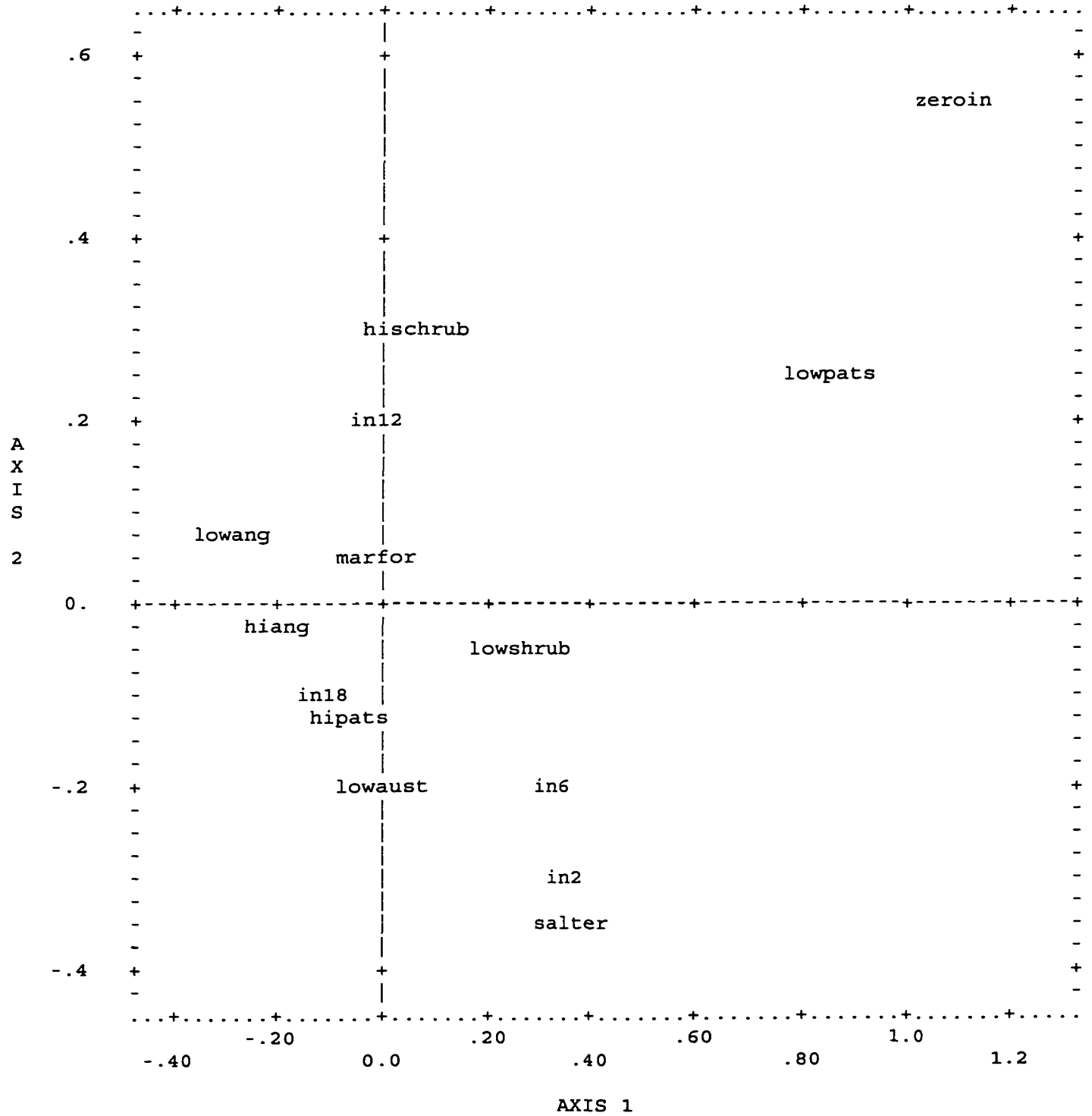
Chapter 5 to Chapter 6 Transition

In this past chapter, vegetation class was shown to relate statistically with several landscape variables: elevation, soil type, and soil compaction strength at 30- and 46cm. In the summary/concluding Chapter 6, discussion focuses on a need for the integration of remote sensing with ecology to advance our potential for informed resource management and decision-making. Remote sensing technology is advocated as a tool that should be used by resource managers. Additional resource management areas in which remote sensing has and could be used beyond those discussed in this manuscript are briefly addressed.

Chapter 6

Summary & Conclusion

Summary

Landscape data is baseline information needed for detailed studies of biodiversity, ecosystems, and sustainability (Cooke and Doornkamp, 1990; Lyle, 1999). Land managers need landscape information such as vegetation, soil, and terrain attributes to manage effectively (Wheatley *et al*, 2000). Landscape variables must be acquired in a cost- and time-efficient manner (Wheatley *et al*, 2000). The low cost of acquiring remotely sensed data over broad areas at regular intervals in time (Redfern and Williams, 1996), and the capability for coincident collection of multiple variables or themes of interest (de Blij and Muller, 1996), can provide these necessary landscape variables. Regularly updated data are needed because resource managers require current land cover for monitoring (Vogelmann *et al*, 2001). Acquisition of ground data is expensive and will need to be optimized in conjunction with remotely sensed imagery (Atkinson *et al*, 2000).

Remote sensing has been used for landscape characterization (identifying and describing by cover type), monitoring changes (presence or absence), and assessing the effect of change on the quality of the landscape in environmentally sensitive areas (Slater and Brown, 2000). For example, the Ecological Monitoring and Assessment Program (EMAP) of the Environmental Protection Agency uses biological indicators derived from satellite and airborne imagery to assess our national ecological resources. Historically, comprehensive descriptions of the environment have been difficult to acquire, but remote sensing and geographic information systems have greatly assisted in the process (Huggett, 1995).

Commercial satellite imagery has recently been offered for sale with spectral bandwidths of about 70nm and spatial pixel sizes of 4 and 1m for panchromatic imagery (IKONOS). For this study, 4m multispectral airborne imagery, with similarities to IKONOS satellite imagery, was acquired over two coastal Virginia study areas. One site, a coastal military installation, served as a test location for evaluating land cover classification accuracy for four combinations of spectral and spatial image resolution. The second site, a barrier island, was used to test for: the classification of categorical biomass index differences in an invasive species; the estimation soil properties and elevation data from the existence of vegetation communities; and the inclusion of a method to apply expert knowledge classification correction rules to improve an erroneous land cover classification.

Chapter 2 was an investigation at Fort Story, VA of spectral, spatial, and spectral and spatial resolution combined, as well as a review of six training sample methods used. Classification accuracy of maps compiled from imagery with wide bandwidths (75nm) was compared to the accuracy of map classifications derived from narrow bandwidths (25nm). Based on the independent contribution of bandwidth alone, the narrower bandwidth imagery returned higher Kappa and overall accuracy scores, in addition to improvements in the transformed divergence scores for training classes that were difficult to spectrally separate. Specifically, 25nm imagery resulted in higher accuracy cultural feature classifications, and a combination of natural and cultural features.

In a similar test, the independent contribution of spatial resolution was tested to determine if imagery with 4m pixels returned statistically equivalent image classifications to

imagery with 1m pixels. Transformed divergence scores of difficult to separate training sample pairs improved with the 4m imagery. Kappa scores suggest that natural features are better interpreted from 4m imagery than 1m imagery. Classification accuracy of natural features from 4m imagery was consistently 5% better than accuracy achieved from 1m imagery. Classification from cultural, and natural and cultural, features were statistically similar regardless of pixel size.

The joint contribution of spectral and spatial image resolution was evaluated. Accuracy results for the narrow bandwidth 25nm imagery with the larger 4m pixel size generally outperformed the other three image resolution combinations. The results were statistically different between 25nm/4m imagery and 70nm/1m imagery for a classification of natural, and natural and cultural features, but were not statistically different between 25nm/4m imagery and the remaining combinations.

Six training sample methods were compared. An effective number of training sample pixels were acquired from both the seed grow-15 and seed grow-25 methods, as determined from the successful accuracy assessment scores of image classifications processed using these methods. These methods offer an opportunity for a more replicable, objective training sample selection process. The polygon training sample method was also effective. Methods that collected the smallest training sample sizes were ineffective.

In summary of chapter 2, a resource manager should not select 70nm/1m imagery for classification when 25nm/1m, 25nm/4m, or 70nm/4m imagery is available. Consistently

higher Kappa accuracy scores were attained from the 25nm/4m imagery suggesting this image resolution combination is the better choice of the four evaluated by this study. If a resource manager were specifically interested in the classification of any individual landscape feature evaluated in this study, Appendix 2 provides detailed results of the accuracy attained for each feature, for each image resolution combination.

Chapter 3 describes a method for determining categorical measures of *P. australis* biomass indices from high-resolution multispectral imagery. *Phragmites australis* is an undesired opportunistic invader species that can quickly overtake native plant habitat. This species needs to be monitored to assure its lateral advance is controlled by remediation efforts. Field data (average plot stand height, stems per meter, and average culm diameter) and coincident multispectral imagery were acquired.

Biomass indices were computed for each stand from normalized field data by a linear scale transform with maximum score procedure (Malczewski, 1999). *Phragmites australis* biomass indices and various combinations of image channel reflectance values were evaluated by cluster analysis tools. Classes and class members defined by field data were closely matched to classes and class members defined by the red-channel of the imagery. The result of this study is that remotely sensed image data correctly separated *Phragmites* into stands of high, moderate and low-density biomass, as also classified from field verification. This result suggests that if the high-density stands were the first to expand laterally, and this is a question that warrants further investigation, remote sensing could be useful for targeting those high-density sites in need of immediate mitigation. Strategic attacks on laterally

advancing stands would help resource managers protect higher-value plant communities and avert a decline in ecosystem health attributable to loss of plant diversity/complexity, loss of shelter/habitat, and decline in food source.

Chapter 4 discusses a simple methodology for improving a land cover classification map of Parramore Island, VA. Cover classification maps defined from image processing often contain errors. It is not uncommon to find that some mistakes are plainly visible. Targeting these misclassifications can be difficult with the standard tools available within image processing software. In this study, ecological rules were introduced to target and correct classification mistakes strategically. A four-step process was implemented. First, ecological expert knowledge was acquired about the study site. This could be acquired from field expertise or literature sources. Second, misclassifications were visually identified based on the expert knowledge. Third, IF-THEN-ELSE conditional statements were loosely developed to address the mistakes. Lastly, these conditional statements were implemented within ERDAS Imagine Spatial Modeler image processing code as a post-classification correction model.

Conditional rules were converted into computer interpretable statements with ERDAS' Majority Focus optional statements. All rules were spatial in nature, in that change was effected only by adjacency of feature class pixels identified by the model analyst. The analyst defined the criteria for selected pixels to change to a new, ecologically sound feature class. Six rule corrections used to post-classify the Parramore Island cover class map resulted in the conversion of over 20 per cent (173 of the total 850 hectares) of the initial land

cover classification pixels to alternative classes. The method of post-classification correction described in Chapter 4 is portable in the sense that the rules can easily be changed and adopted to a new physiographic environment; the model template is extendable to new domains.

Chapter 5 describes Parramore Island and the use of field data to develop empirical models used to estimate elevation, soil type and soil compaction strength from vegetation community classes. Vegetation class was selected as the dependent variable because these types of data are considered to be readily interpretable from remote sensing source (Jensen, 1996). Accordingly, if vegetation classifications were established remotely, and empirical relationships were established between vegetation, soil, and elevation field data, then vegetation class maps could be used to estimate the other variables. Strong correlation between soil type and vegetation community enabled the estimation of soil type across the entire island. Strength of association non-parametric statistics were used to assess the inter-relationship between variables. Vegetation was related to elevation, soil type and soil compaction strength on Parramore Island.

Elevation heights were grouped into one of three categories. A Cramer's V score for a 3-vegetation class grouping versus the elevation values in those three classes resulted in a positive strength of association score of: 0.9884, with a value of 1.0000 representing perfect association between the variables. Elevation zones 1 and 2 had a minimum and maximum elevation height. Elevation zone 3 did not sample points to establish an upper elevation. Rather, maritime forest concealed the underlying dunes. Equations are provided in Chapter 5

that illustrate the development of ratios that were empirically developed from field transect data for estimation of dune height and crest location concealed by maritime forest. These ratios suggest consistency in dune shape, height, and crest location, with respect to overlying forest width.

Soil type was divided into four classes and compared to vegetation communities. Vegetation community class was shown to have a strong positive association with these four classes. The Cramer's V score: 0.85, suggests that vegetation could be used to estimate soil type locations on Parramore Island. A soil type map of the island was subsequently developed that provides insight into the physical processes of sediment delivery and removal that have shaped its geomorphology.

Soil compaction strength scores were recorded at depths of 0, 5, 15, 30 and 46cm. Vegetation type best explained the variance in soil compaction at the deeper 30 and 46cm depths as indicated by respective r^2 scores: 0.88 and 0.72. Cramer's V measures were computed for 10, 7 , and 3-vegetation classes and soil compaction strength with scores of at least 0.85 for both 30 and 46cm depths. The greater variation in the soil compaction rates for 30 and 46cm depths was responsible for the increased Cramer's V strength of relationship scores with vegetation type.

Conclusions

Remote sensing is an excellent tool to assist in the management of the coastal zone. It should not be over-promoted, however, as a single solution to landscape characterization

and ecological monitoring. To the contrary, the compilation of an accurately characterized landscape from remote imagery should rely upon: field truth for training sample development and testing data (albeit at a significantly reduced level were remote imagery not used); an image analyst trained in processing remotely acquired data; and individuals with biogeochemical expertise about the coastal study area that is to be inventoried. Up-to-date imagery and landscape classes derived from it are essential tools to help resource managers make informed decisions. Remote sensing should be driven by scientific hypothesis and any future modeling should account for a remote sensing and landscape process model merge (Wessman *et al*, 1998). To date, implementation of remote sensing in landscape ecology research and applications has been relatively scarce (Gulinck *et al*, 2000). Ecological models should be designed to use direct or derived variables from remote sensing (Wessman et al, 1998).

The future of remote sensing is bright. Detailed, accurate measurements of the ocean, land, and atmosphere are planned by satellite sensors. Many camera systems are already orbiting earth including the MODIS (Moderate-Resolution Imaging Spectroradiometer) measuring biological and physical processes such as plankton, land vegetation, and clouds; MISR (Multi-angle Imaging Spectro-Radiometer), measuring atmospheric aerosols; ASTER (Advanced Spaceborne Thermal Emission and Reflection Radiometer), providing 15m horizontal spatial resolution imagery for elevation and landform mapping, surface temperatures, and rock cover types, and MOPITT (Measurements of Pollution in the Troposphere) measuring methane and CO^2 (Glaze, 1999). LIDAR technology offers particular promise for the mapping of elevations at 15 to 100cm vertical accuracy in an

accurate, timely, and economical way (Hill *et al*, 2001). Hyperspectral sensors are currently acquiring data by airborne and satellite platform and hold promise for better spectral separation of biotic features due to narrower bandwidths. Ecological monitoring from remote imagery will continue, as testified to by the $30-million dollar annual remote sensing-based ecological monitoring and assessment program (EMAP), the National Science Foundation's continued investment in remote sensing for their Long Term Ecological Research (LTER) program, and the US Forest Service use of imagery for their forest health monitoring program (Stone, 1995).

Remote sensing offers a technological advantage to a resource manager. A simple way to determine if remote sensing is an appropriate tool for coastal zone landscape characterization is to overwhelmingly answer "yes" to the following questions.

- Are the desired landscape data useful for multiple projects?
- Is this, or should this site be routinely monitored?
- Is this project too large to map on the ground with available resources?
- Is the project site largely inaccessible?
- Is this a project site best understood from a complete picture (imagery) rather than a sampling of field points?

Additional areas of future research recommended for investigation that were not identified in the preceding chapters include:

◊ Chapter 2- Compare landscape classification accuracy from Landsat Thematic Mapper and SPOT XS imagery to the 25nm/1m, 25nm/4m, 70nm/1m, and 70nm/4m imagery used for this research.

◊ Chapter 3- Investigate other invasive plant stands for quantitative correlation between field and imagery. Also, visit additional geographic locations containing *P. australis* sites for validation of the present findings.

◊ Chapter 4- Comprehensive knowledge rules compiled for disparate environments should be compiled using other sources such as literature, expert advisors, and first hand field experience. The value added in applying this technique might be determined by comparing accuracy assessments of landscape classifications before and after applying the knowledge-based rules.

◊ Chapter 5- Apply the deterministic models for predicting soil type, soil compaction rates, and elevation from vegetation at other barrier islands along the mid-Atlantic Coast, test for accuracy, and validate or invalidate the portability of the model. Also, measure additional cross-sectional elevation transects of Parramore Island's transverse dunes to affirm preliminary findings that suggest dune height and crest location can be modeled from coincident maritime forest width.

References

Aplin, P., Atkinson, P.M., Curran, P.J., 1997. Fine spatial resolution satellite sensors for the next decade. *International Journal of Remote Sensing*, 18 (18): 3873-3881.

Atkinson, P.M., Fody, G.M., Curran, P.J., and Boyd, D.S., 2000. Assessing the ground data requirements for regional scale remote sensing of tropical forest biophysical properties. *International Journal of Remote Sensing*, 21 (13&14): 2571-2587.

Cooke, R.U., and Doornkamp, J.C., 1990. Geomorphology in Environmental Management-A New Introduction, 2nd ed., Clarendon Press, Oxford.

de Blij, J.J. and Muller, P.O., 1996. Physical Geography of the Global Environment, 2nd ed., John Wiley and Sons, New York.

Glaze, W.H., editor, 1999. Environmental News: NASA's flagship satellite will revolutionize study of climate change. *Environmental Science & Technology*, 33 (13): 271-272.

Gulinck, H., Dufourmont, H., Coppin, P., Hermy, M. 2000. Landscape research, landscape policy and earth observation. *International Journal of Remote Sensing*, 21 (13&14): 2541-2554.

Hill, J.M., Graham,L.A., and Henry, R.J., 2001. Wide-area topographic mapping and applications using airborne Light Detection and Ranging (LIDAR) technology. *Photogrammetric Engineering and Remote Sensing*, 6 (8): 908-914.

Huggett, R.J., 1995. Geoecology-An Evolutionary Approach, Routledge, New York

Jensen, J.R., 1996. Thematic Information extraction: image classification. In Introductory Digital Image Processing, A Remote Sensing Perspective, Prentice Hall, New Jersey, 197-256.

Lyle, J.T., 1999. Design for Human Ecosystems, Island Press, New York.

Malcaewski, J., 1999. Chapter 4- Evaluation criteria. In GIS and Multicriteria Decision Analysis, , John Wiley & Sons, Inc., New York.

Redfern, H., and Williams, R.G., 1996. Remote sensing – latest developments and user. *Chartered Institution of Water and Environmental Management*, 10 (6): 423-428.

Slater, J., and Brown, R., 2000. Changing landscapes: monitoring environmentally sensitive area using satellite imagery. *International Journal of Remote Sensing*, 21 (13&14): 2753-2767.

Stone, R. 1995. EPA streamlines troubled national ecological survey. *Science*, 268 (June 9): 1427-1428.

Vogelmann, J.E., Howard, S.M., Yang, L., Larson, C.R., Wylie, B.K., and van Driel, N., 2001. Completion of the 1990s national land cover data set for the conterminous United States from Landsat Thematic Mapper data and ancillary data sources. *Photogrammetric Engineering and Remote Sensing*, 67 (6): 650-662.

Wessman, C.A.,, Cramer, W., Gurney, R.J., Martin, P.H., Mauser, W., Nemani, R., Paruelo, J.M., Penuelas, J., Prince, S.D., Running, S.W., and Waring, R.H., 1998. Chapter 5- Group report: remote sensing perspectives and insights for study of complex landscapes. In Integrating Hydrology, Ecosystem Dynamics, and Biogeochemistry, Complex Landscapes, edited by J.D. Tenhunen and P. Kabat, John Wiley and Sons, New York, 89-103.

Wheatley, J.M., Wilson, J.P., Redmond, R.L., Zhenkui, M., DiBenedetto, J., 2000. Chapter 15- Automated land cover mapping using Landsat Thematic Mapper images and topographic attributes. In Terrain Analysis- Principles and Applications, edited by J.P. Wilson and J.C. Gallant, John Wiley and Sons, Inc., New York, 245-266.

Appendix 1. Sample plots of Fort Story field data.

id	X	Y	Oak/Holly	Mixed Forest	Loblolly	Amophilla	Maint grass	Asphalt	Concrete	Roof Grey	Roof Brown	Ocean	Sand	Clay	rip rap
1	409689	4087230			XXX										
2	409790	4087651										XXX			
3	409813	4087616											XXX		
4	409527	4087615						XXX							
6	409615	4087233			XXX										
7	409509	4087372						XXX							
8	409640	4087262			XXX										
9	409562	4087683										XXX			
10	409633	4087472	XXX												
11	409600	4087559					XXX								
13	409503	4087491					XXX								
14	409558	4087439	XXX												
15	409620	4087640					XXX								
17	409511	4087673													XXX
19	409479	4087700										XXX			
20	409637	4087380							XXX						
23	409820	4087651					.					XXX			
25	409815	4087633										XXX			
26	409521	4087590					XXX								
31	409530	4087578					XXX								
33	409846	4087487	XXX												
34	409508	4087508					XXX								
38	409644	4087318			XXX										
39	409778	4087215					XXX								
40	409762	4087365					XXX								
42	409776	4087460					XXX								
43	409562	4087657					XXX								
46	409844	4087299			XXX										
47	409810	4087693										XXX			
48	409777	4087421		XXX											
49	409544	4087665													XXX
50	409821	4087374							XXX						

Appendix 1- Sample of Fort Story Field Data Collection- February 2001

	ID1	ID2										
52	409559	4087515				XXX						
53	409788	4087537	XXX			XXX						
54	409682	4087546				XXX						
55	409644	4087648										XXX
56	409485	4087595										
57	409647	4087475	XXX			XXX						
58	409700	4087664		XXX							XXX	
61	409757	4087360										
64	409772	4087538	XXX			XXX						
65	409771	4087535	XXX									
66	409760	4087396		XXX								
67	409676	4087512				XXX						
68	409826	4087324		XXX								
70	409723	4087424		XXX		XXX						
71	409517	4087654										
72	409563	4087334			XXX							
73	409721	4087528	XXX									
74	409821	4087524	XXX									
75	409597	4087576				XXX		XXX				
77	409509	4087499										
78	409646	4087230			XXX							
79	409640	4087687								XXX	XXX	
80	409749	4087672										
82	409804	4087525	XXX			XXX						
83	409662	4087327							XXX			
85	409835	4087349										
87	409630	4087528					XXX					
90	409759	4087608										
91	409634	4087688				XXX						
95	409787	4087669								XXX	XXX	
96	409565	4087566				XXX						
97	409635	4087439	XXX			XXX						
98	409648	4087417										
99	409732	4087365		XXX								

#	ID1	ID2
100	409810	4087466
101	409648	4087297
103	409755	4087200
105	409705	4087234
107	409552	4087538
109	409789	4087370
110	409782	4087221
112	409660	4087461
113	409763	4087425
114	409618	4087489
115	409683	4087562
116	409561	4087654
118	409705	4087251
119	409758	4087692
121	409688	4087199
123	409773	4087632
124	409737	4087680
126	409531	4087670
127	409617	4087204
129	409821	4087510
130	409683	4087396
131	409539	4087470
132	409692	4087641
133	409634	4087321
134	409703	4087199
135	409768	4087630
137	409712	4087219
138	409828	4087256
140	409693	4087411
141	409720	4087209
144	409738	4087643
146	409542	4087507
147	409497	4087233
148	409825	4087570

Index	ID 1	ID 2
149	409585	4087595
151	409795	4087268
152	409799	4087404
153	409533	4087592
154	409597	4087473
155	409780	4087507
156	409599	4087593
158	409519	4087638
159	409777	4087607
160	409509	4087331
162	409778	4087429
164	409522	4087562
165	409775	4087431
166	409590	4087235
168	409698	4087361
169	409516	4087485
170	409850	4087218
173	409564	4087240
174	409488	4087622
177	409627	4087383
178	409508	4087515
180	409660	4087224
183	409809	4087672
186	409652	4087450
187	409566	4087435
188	409614	4087227
189	409665	4087268
191	409512	4087693
192	409642	4087276
193	409494	4087701
195	409592	4087379
196	409561	4087661
197	409702	4087670
199	409598	4087461

200	409506	4087473
203	409723	4087367
206	409579	4087264
209	409847	4087327
210	409710	4087240
212	409735	4087440
213	409840	4087632
214	409645	4087688
216	409839	4087411
217	409568	4087306
219	409856	4087270
220	409758	4087343
221	409517	4087567
222	409691	4087296
223	409519	4087544
225	409579	4087692
226	409800	4087248
230	409572	4087652
231	409719	4087646
233	409800	4087607
234	409828	4087239
236	409582	4087689
237	409563	4087477
239	409701	4087358
240	409761	4087337
242	409780	4087659
243	409654	4087340
247	409561	4087226
248	409624	4087437
249	409821	4087643
250	409650	4087253

Appendix 2. Accuracy assessment matrices for all image combinations, for natural and cultural, natural, and cultural features.

- 25nm/1m/point
- 25nm/1m/polygon
- 25nm/1m/seed15
- 25nm/1m/seed25
- 25nm/1m/seed2
- 25nm/1m/seed5

- 25nm/4m/point
- 25nm/4m/polygon
- 25nm/4m/seed15
- 25nm/4m/seed25
- 25nm/4m/seed2
- 25nm/4m/seed5

- 70nm/1m/point
- 70nm/1m/polygon
- 70nm/1m/seed15
- 70nm/1m/seed25
- 70nm/1m/seed2
- 70nm/1m/seed5

- 70nm/4m/point
- 70nm/4m/polygon
- 70nm/4m/seed15
- 70nm/4m/seed25
- 70nm/4m/seed2
- 70nm/4m/seed5

25-1-point-all

	Oak holly	Mixed	Loblolly	Dune grass	Maint grass	Ocean	Sand	Clay	Asphalt	Concrete	Roof-grey	Roof-brown	Rip rap	diagonal	row total	users acc
Oak holly	49	24	25	4	1	2	0	0	0	0	0	2	0		107	45.79
Mixed	12	9	8	0	3	0	0	0	0	0	0	0	0		32	28.13
Loblolly	17	11	11	0	0	0	0	0	0	0	1	0	0		40	27.50
Dune grass	12	12	13	18	3	0	0	0	0	0	0	0	0		58	31.03
Maint grass	16	10	7	4	56	0	0	0	0	0	0	0	0		93	27.50
Ocean	0	0	0	0	0	2	0	0	0	0	0	0	0		2	31.03
Sand	0	0	0	0	0	0	3	0	0	0	0	0	0		3	100.00
Clay	0	0	0	0	0	0	0	5	0	0	0	0	0		5	100.00
Asphalt	0	0	0	0	0	5	2	0	16	0	0	0	1		24	66.67
Concrete	0	0	0	0	0	0	0	0	0	10	0	0	0		10	100.00
Roof-grey	0	0	0	0	1	9	2	0	3	1	2	0	0		18	11.11
Roof-brown	0	0	1	1	0	0	0	0	0	0	0	4	0		6	66.67
Rip rap	3	1	4	7	11	15	16	5	31	10	7	3	12		125	9.60
														197		
col. total	109	67	69	34	75	33	23	10	50	21	10	9	13		523	37.67
producer acc	44.95	13.43	15.94	52.94	74.67	6.06	13.04	50.00	32.00	47.62	20.00	44.44	92.31			Overall Acc.

25-1-point-natural

	Oak holly	Mixed	Loblolly	Dune grass	Maint grass	Ocean	Sand	Clay	diagonal	row total	users acc
Oak holly	49	24	25	4	1	2	0	0		105	46.67
Mixed	12	9	8	0	3	0	0	0		32	28.13
Loblolly	17	11	11	0	0	0	0	0		39	28.21
Dune grass	12	12	13	18	3	0	0	0		58	31.03
Maint grass	16	10	7	4	56	0	0	0		93	28.21
Ocean	0	0	0	0	0	2	0	0		2	31.03
Sand	0	0	0	0	0	0	3	0		3	100.00
Clay	0	0	0	0	0	0	0	5		5	100.00
									153		
col. total	106	66	64	26	63	4	3	5		337	45.40
producer acc	46.23	13.64	17.19	69.23	88.89	50.00	100.00	100.00			Overall Acc.

25-1-point-cultural

	Asphalt	Concrete	Roof-grey	Roof-brown	Rip rap	diagonal	row total	users acc
Asphalt	16	0	0	0	1		17	94.12
Concrete	0	10	0	0	0		10	100.00
Roof-grey	3	1	2	0	0		6	33.33
Roof-brown	0	0	0	4	0		4	100.00
Rip rap	31	10	7	3	12		63	19.05
						44		
col. total	50	21	9	7	13		100	44.00
producer acc	32.00	47.62	22.22	57.14	92.31			Overall Acc.

25-1-polygon- all

	Oak holly	Mixed	Loblolly	Dune grass	Maint grass	Ocean	Sand	Clay	Asphalt	Concrete	Roof-grey	Roof-brown	Rip rap	diagonal	row total	users acc
Oak holly	45	26	6	0	0	0	0	0	0	0	1	0	0		78	57.69
Mixed	19	21	12	1	0	0	0	0	0	0	0	0	0		53	39.62
Loblolly	36	18	43	0	0	0	0	0	0	0	0	0	0		97	44.33
Dune grass	6	1	6	31	14	0	1	0	1	0	1	1	0		62	50.00
Maint grass	3	1	1	2	54	0	0	0	0	1	0	0	0		62	44.33
Ocean	0	0	0	0	0	8	0	0	0	0	0	0	0		8	50.00
Sand	0	0	0	0	0	0	15	0	0	3	0	0	0		18	83.33
Clay	0	0	0	0	0	0	0	10	0	0	0	0	0		10	100.00
Asphalt	0	0	0	0	1	5	1	0	40	1	0	0	3		51	78.43
Concrete	0	0	0	0	0	0	1	0	0	13	1	0	0		15	86.67
Roof-grey	0	0	0	0	6	5	4	0	3	2	6	1	2		29	20.69
Roof-brown	0	0	0	0	0	0	0	0	0	0	0	7	0		7	100.00
Rip rap	0	0	1	0	0	15	1	0	6	1	1	0	8		33	24.24
														301		
col. total	109	67	69	34	75	33	23	10	50	21	10	9	13		523	57.55
producer acc	41.28	31.34	62.32	91.18	72.00	24.24	65.22	100.00	80.00	61.90	60.00	77.78	61.54			Overall Acc

25-1-polygon-natural

	Oak holly	Mixed	Loblolly	Dune grass	Maint grass	Ocean	Sand	Clay	diagonal	row total	users acc
Oak holly	45	26	6	0	0	0	0	0		77	58.44
Mixed	19	21	12	1	0	0	0	0		53	39.62
Loblolly	36	18	43	0	0	0	0	0		97	44.33
Dune grass	6	1	6	31	14	0	1	0		59	52.54
Maint grass	3	1	1	2	54	0	0	0		61	44.33
Ocean	0	0	0	0	0	8	0	0		8	52.54
Sand	0	0	0	0	0	0	15	0		15	100.00
Clay	0	0	0	0	0	0	0	10		10	100.00
									227		
col. total	109	67	68	34	68	8	16	10		380	59.74
producer acc	41.28	31.34	63.24	91.18	79.41	100.00	93.75	100.00			Overall Acc.

25-1-polygon-cultural

	Asphalt	Concrete	Roof-grey	Roof-brown	Rip rap	diagonal	row total	users acc
Asphalt	40	1	0	0	3		44	90.91
Concrete	0	13	1	0	0		14	92.86
Roof-grey	3	2	6	1	2		14	42.86
Roof-brown	0	0	0	7	0		7	100.00
Rip rap	6	1	1	0	8		16	50.00
						74		
col. total	49	17	8	8	13		95	77.89
producer acc	81.63	76.47	75.00	87.50	61.54			Overall Acc.

25NM 1M SEED 15 NATURAL AND CULTURAL RAW DATA

	Oak holly	Mixed	Loblolly	Dune grass	Maint grass	Ocean	Sand	Clay	Asphalt	Concrete	Roof-grey	Roof-brown	Rip rap	diagonal	row total	users acc
Oak holly	42	21	13	2	1	0	0	0	0	0	1	0	0		80	52 50
Mixed	32	35	26	1	0	0	0	0	0	0	0	0	0		94	37 23
Loblolly	26	6	23	0	0	0	0	0	0	0	0	0	0		55	41 82
Dune grass	4	3	3	23	2	0	0	0	0	0	0	1	0		36	63 89
Maint grass	5	2	3	5	66	0	1	0	1	1	1	0	0		85	41 82
Ocean	0	0	0	0	0	9	0	0	0	0	0	0	0		9	63 89
Sand	0	0	0	0	0	0	14	0	0	3	0	0	0		17	82 35
Clay	0	0	0	0	0	0	0	10	0	0	0	0	0		10	100 00
Asphalt	0	0	1	0	1	15	0	0	36	0	0	0	2		56	64 29
Concrete	0	0	0	0	0	0	1	0	0	13	0	0	0		14	92 86
Roof-grey	0	0	0	0	0	0	0	0	0	1	3	0	0		4	75 00
Roof-brown	0	0	0	0	0	0	0	0	1	0	0	7	0		8	87 50
Rip rap	0	0	0	3	5	9	7	0	12	2	5	1	11	292	55	20 00
col total	109	67	69	34	75	33	23	10	50	21	10	9	13		523	55 83
producer acc	38 53	52 24	33 33	67 65	88 00	27 27	60 87	100 00	72 00	61 90	30 00	77 78	84 62			Overall Acc

25NM 1M SEED 15 NATURAL RAW DATA

	Oak holly	Mixed	Loblolly	Dune grass	Maint grass	Ocean	Sand	Clay	diagonal	row total	users acc
Oak holly	42	21	13	2	1	0	0	0		79	53 16
Mixed	32	35	26	1	0	0	0	0		94	37 23
Loblolly	26	6	23	0	0	0	0	0		55	41 82
Dune grass	4	3	3	23	2	0	0	0		35	65 71
Maint grass	5	2	3	5	66	0	1	0		82	41 82
Ocean	0	0	0	0	0	9	0	0		9	65 71
Sand	0	0	0	0	0	0	14	0		14	100 00
Clay	0	0	0	0	0	0	0	10	222	10	100 00
col total	109	67	68	31	69	9	15	10		378	58 73
producer acc	38 53	52 24	33 82	74 19	95 65	100 00	93 33	100 00			Overall Acc

25 NM 1M SEED 15 CULTURAL RAW DATA

	Asphalt	Concrete	Roof-grey	Roof-brown	Rip rap	diagonal	row total	users acc
Asphalt	36	1	0	0	2		39	92 31
Concrete	0	13	0	0	0		13	100 00
Roof-grey	0	1	3	0	0		4	75 00
Roof-brown	1	0	0	7	0		8	87 50
Rip rap	12	2	5	1	11	70	31	35 48
col total	49	17	8	8	13		95	73 68
producer acc	73 47	76 47	37 50	87 50	84 62			Overall Acc

25NM 1M SEED 25 NATURAL AND CULTURAL

RAW DATA

	Oak holly	Mixed	Loblolly	Dune grass	Maint grass	Ocean	Sand	Clay	Asphalt	Concrete	Roof-grey	Roof-brown	Rip rap	diagonal	row total	users acc
Oak holly	41	26	7	2	1	0	0	0	0	0	1	0	0		78	52.56
Mixed	30	27	25	1	0	0	0	0	0	0	0	0	0		83	32.53
Loblolly	29	8	30	0	0	0	0	0	0	0	0	0	0		67	44.78
Dune grass	4	4	3	25	3	0	0	0	0	0	0	0	0		39	64.10
Maint grass	5	2	2	4	66	0	1	0	0	1	0	1	0		83	44.78
Ocean	0	0	0	0	0	9	0	0	0	0	0	0	0		9	64.10
Sand	0	0	0	0	0	0	15	0	0	1	0	0	0		16	93.75
Clay	0	0	0	0	0	0	0	10	0	0	0	0	0		10	100.00
Asphall	0	0	1	2	5	6	5	0	42	2	1	0	7		71	59.15
Concrete	0	0	0	0	0	0	1	0	0	17	0	0	0		18	94.44
Roof-grey	0	0	0	0	0	4	0	0	1	0	7	0	1		13	53.85
Roof-brown	0	0	1	0	0	1	0	0	1	0	0	8	0		11	72.73
Rip rap	0	0	0	0	0	13	1	0	6	0	0	0	5	302	25	20.00
col. total	109	67	69	34	75	33	23	10	50	21	10	9	13		523	57.74
producer acc	37.61	40.30	43.48	73.53	88.00	27.27	65.22	100.00	84.00	80.95	70.00	88.89	38.46			Overall Acc

25NM 1M SEED25 NATURAL

RAW DATA

	Oak holly	Mixed	Loblolly	Dune grass	Maint grass	Ocean	Sand	Clay	diagonal	row total	users acc
Oak holly	41	26	7	2	1	0	0	0		77	52.56
Mixed	30	27	25	1	0	0	0	0		83	32.53
Loblolly	29	8	30	0	0	0	0	0		67	44.78
Dune grass	4	4	3	25	3	0	0	0		39	64.10
Maint grass	5	2	2	4	66	0	1	0		80	44.78
Ocean	0	0	0	0	0	9	0	0		9	64.10
Sand	0	0	0	0	0	0	15	0		15	100.00
Clay	0	0	0	0	0	0	0	10	223	10	100.00
col. total	109	67	67	32	70	9	16	10		380	58.68
producer acc	37.61	40.30	44.78	78.13	94.29	100.00	93.75	100.00			Overall Acc

25nm 1m seed25 cultural

RAW DATA

	Asphalt	Concrete	Roof-grey	Roof-brown	Rip rap	diagonal	row total	users acc
Asphall	42	2	1	0	7		52	80.77
Concrete	0	17	0	0	0		17	100.00
Roof-grey	1	0	7	0	1		9	77.78
Roof-brown	1	0	0	8	0		9	88.89
Rip rap	6	0	0	0	5	79	11	45.45
col. total	50	19	8	8	13		98	80.61
producer acc	84.00	89.47	87.50	100.00	38.46			Overall Acc

25NM 1M SEED2 NATURAL AND CULTURAL
RAW DATA

	Oak holly	Mixed	Loblolly	Dune grass	Maint grass	Ocean	Sand	Clay	Asphalt	Concrete	Roof-grey	Roof-brown	Rip rap	diagonal	row total	users acc
Oak holly	49	29	16	4	1	6	0	0	0	0	0	0	0		105	46 67
Mixed	38	31	31	1	0	0	0	0	0	0	0	0	0		101	30 69
Loblolly	10	3	15	0	0	0	0	0	0	0	0	0	0		28	53 57
Dune grass	3	1	2	15	4	0	0	0	0	0	0	0	0		25	60 00
Maint grass	8	2	2	6	66	0	2	0	0	1	1	1	0		89	53 57
Ocean	0	0	0	0	0	4	0	0	0	0	0	0	0		4	60 00
Sand	0	0	0	0	1	0	15	0	1	3	0	0	0		20	75 00
Clay	0	0	0	0	0	0	0	10	0	0	0	0	0		10	100 00
Asphalt	0	0	0	0	1	7	1	0	26	1	0	2	0		38	68 42
Concrete	0	0	0	0	0	0	1	0	0	3	0	0	0		4	75 00
Roof-grey	0	0	0	0	0	0	0	0	0	1	2	0	0		3	66 67
Roof-brown	0	0	1	0	0	0	0	0	0	0	0	6	0		7	85 71
Rip rap	1	1	2	8	2	16	4	0	23	12	7	0	13	255	89	14 61
col total	109	67	69	34	75	33	23	10	50	21	10	9	13		523	48 76
producer acc	44 95	48 27	21 74	44 12	88 00	12 12	65 22	100 00	52 00	14 29	20 00	66 67	100 00			Overall Acc

25NM 1M SEED2 NATURAL
RAW DATA

	Oak holly	Mixed	Loblolly	Dune grass	Maint grass	Ocean	Sand	Clay	diagonal	row total	users acc
Oak holly	49	29	16	4	1	6	0	0		105	46 67
Mixed	38	31	31	1	0	0	0	0		101	30 69
Loblolly	10	3	15	0	0	0	0	0		28	53 57
Dune grass	3	1	2	15	4	0	0	0		25	60 00
Maint grass	8	2	2	6	66	0	2	0		86	53 57
Ocean	0	0	0	0	0	4	0	0		4	60 00
Sand	0	0	0	0	1	0	15	0		16	93 75
Clay	0	0	0	0	0	0	0	10		10	100 00
col total	108	66	66	26	72	10	17	10	205	375	54 67
producer acc	45 37	46 97	22 73	57 69	91 67	40 00	88 24	100 00			Overall Acc

25NM 1M SEED2 CULTURAL
RAW DATA

	Asphalt	Concrete	Roof-grey	Roof-brown	Rip rap	diagonal	row total	users acc
Asphalt	26	1	0	2	0		29	89 66
Concrete	0	3	0	0	0		3	100 00
Roof-grey	0	1	2	0	0		3	66 67
Roof-brown	0	0	0	6	0		6	100 00
Rip rap	23	12	7	0	13	50	55	23 64
col total	49	17	9	8	13		96	52 08
producer acc	53 06	17 65	22 22	75 00	100 00			Overall Acc

25NM 1M SEEDS NATURAL AND CULTURAL RAW DATA

	Oak holly	Mixed	Lobolly	Dune grass	Maint grass	Ocean	Sand	Clay	Asphalt	Concrete	Roof-grey	Roof-brown	Rip rap	diagonal	row total	users acc
Oak holly	51	25	22		5										104	49.04
Mixed	48	35	39												123	28.48
Lobolly	6	2	4												12	33.33
Dune grass	1	1	3	21											28	75.00
Maint grass	3	4	1	7	66		11					1			89	75.00
Ocean						11									11	100.00
Sand						11	9								9	100.00
Clay								10							10	100.00
Asphalt							4		39	2		5	5		62	62.90
Concrete							2			13		3			15	86.67
Roof-grey							3		3	4	5	3	1		21	23.81
Roof-brown				1			1					8			9	88.89
Rip rap					3		4		6	1	3		7		30	23.33
col total	109	67	69	34	75	33	23	10	50	21	10	9	13	279	523	
producer acc	46.79	52.24	5.80	61.76	88.00	33.33	39.13	100.00	78.00	61.90	50.00	88.89	53.85			Overall Acc 53.15

25NM 1M SEED 5 NATURAL RAW DATA

	Oak holly	Mixed	Lobolly	Dune grass	Maint grass	Ocean	Sand	Clay	diagonal	row total	users acc
Oak holly	51	25	22		5					104	49.04
Mixed	48	35	39							122	28.69
Lobolly	6	2	4							12	33.33
Dune grass	1	1	3	21						27	77.78
Maint grass	3	4		7	66		11			84	77.78
Ocean						11				11	100.00
Sand							9			9	100.00
Clay								10		10	100.00
col total	109	67	68	33	71	11	10	10	207	379	
producer acc	46.79	52.24	5.88	63.64	92.96	100.00	90.00	100.00			Overall Acc 54.62

25NM 1M SEED5 CULTURAL RAW DATA

	Asphalt	Concrete	Roof-grey	Roof-brown	Rip rap	diagonal	row total	users acc
Asphalt	39	1			5		45	86.67
Concrete		13					13	100.00
Roof-grey	3	4	5		1		13	38.46
Roof-brown				8			8	100.00
Rip rap	6	1	3		7		17	41.18
col total	48	19	8	8	13	72	96	
producer acc	81.25	68.42	62.50	100.00	53.85			Overall Acc 75.00

25NM 4M POINT NATURAL AND CULTURAL
RAW DATA-25-4-point

	Oak holly	Mixed	Loblolly	Dune grass	Maint grass	Ocean	Sand	Clay	Asphalt	Concrete	Roof-grey	Roof-brown	Rip rap	diagonal	row total	users acc
Oak holly	32	18	14	1	1	0	0	0	0	0	0	0	0		66	48 48
Mixed	14	10	6	0	0	0	0	0	0	0	0	0	0		30	33 33
Loblolly	25	11	20	1	0	0	0	0	0	0	1	0	0		58	34 48
Dune grass	9	6	14	19	2	0	0	0	0	0	0	0	0		50	38 00
Maint grass	29	22	13	5	65	0	1	0	0	1	1	0	0		137	34 48
Ocean	0	0	0	0	0	3	0	0	0	0	0	0	0		3	38 00
Sand	0	0	0	0	0	0	0	0	0	0	0	0	0		0	#DIV/0!
Clay	0	0	0	0	0	0	0	10	0	0	0	0	0		10	100 00
Asphalt	0	0	1	0	0	0	9	0	27	2	0	5	5		49	55 10
Concrete	0	0	0	0	0	0	1	0	0	8	0	0	0		9	88 89
Roof-grey	0	0	1	8	7	30	11	0	20	10	8	1	8		104	7 69
Roof-brown	0	0	0	0	0	0	0	0	0	0	0	3	0		3	100 00
Rip rap	0	0	0	0	0	0	1	0	3	0	0	0	0		4	0 00
														205		
col total	109	67	69	34	75	33	23	10	50	21	10	9	13		523	39 20
producer acc	29 36	14 93	28 99	55 88	86 67	9 09	0 00	100 00	54 00	38 10	80 00	33 33	0 00			Overall Acc

25NM 4M POINT NATURAL
RAW DATA

	Oak holly	Mixed	Loblolly	Dune grass	Maint grass	Ocean	Sand	Clay	diagonal	row total	users acc
Oak holly	32	18	14	1	1	0	0	0		66	48 48
Mixed	14	10	6	0	0	0	0	0		30	33 33
Loblolly	25	11	20	1	0	0	0	0		57	35 09
Dune grass	9	6	14	19	2	0	0	0		50	38 00
Maint grass	29	22	13	5	65	0	1	0		135	35 09
Ocean	0	0	0	0	0	3	0	0		3	38 00
Sand	0	0	0	0	0	0	0	0		0	#DIV/0!
Clay	0	0	0	0	0	0	0	10		10	100 00
									159		
col total	109	67	67	26	68	3	1	10		351	45 30
producer acc	29 36	14 93	29 85	73 08	95 59	100 00	0 00	100 00			Overall Acc

25NM 4M POINT CULTURAL
RAW DATA

	Asphalt	Concrete	Roof-grey	Roof-brown	Rip rap	diagonal	row total	users acc
Asphalt	27	2	0	5	5		39	69 23
Concrete	0	8	0	0	0		8	100 00
Roof-grey	20	10	8	1	8		47	17 02
Roof-brown	0	0	0	3	0		3	100 00
Rip rap	3	0	0	0	0		3	0 00
						46		
col total	50	20	8	9	13		100	46 00
producer acc	54 00	40 00	100 00	33 33	0 00			Overall Acc

25MM 4M POLYGON NATURAL AND CULTURAL RAW DATA

	Oak holly	Mixed	Lobolly	Dune grass	Maint grass	Ocean	Sand	Clay	Asphalt	Concrete	Roof-grey	Roof-brown	Rip rap	diagonal	row total	users acc
Oak holly	55	19	6	0	0	0	0	0	0	0	0	0	0		80	68 75
Mixed	17	23	13	0	0	0	0	0	0	0	0	0	0		54	42 59
Lobolly	30	22	46	0	1	0	0	0	0	0	0	0	0		99	46 46
Dune grass	3	2	2	28	12	0	0	0	0	0	0	0	0		51	54 90
Maint grass	2	1	0	0	58	8	2	0	0	0	0	0	0		67	46 46
Ocean	0	0	0	0	0	8	0	10	0	0	0	0	0		8	54 90
Sand	0	0	0	0	0	1	14	0	2	0	1	0	0		18	87 50
Clay	0	0	1	2	3	2	0	10	0	0	0	0	0		10	100 00
Asphalt	0	0	0	0	1	3	3	0	42	1	17	2	5		58	72 41
Concrete	2	0	1	0	0	0	0	0	0	17	0	0	0		20	85 00
Roof-grey	0	0	0	1	0	1	0	0	2	0	8	8	0		22	36 36
Roof-brown	0	0	0	0	0	0	0	0	0	0	0	7	0		7	100 00
Rip rap	0	0	0	1	0	0	1	0	4	0	0	0	7		31	22 58
col total	109	67	69	34	75	33	23	10	50	21	10	9	13	323	523	61 76
producer acc	50 46	34 33	66 67	82 35	77 33	24 24	60 87	100 00	84 00	80 95	80 00	77 78	53 85			Overall Acc

25MM 4M POLYGON NATURAL RAW DATA

	Oak holly	Mixed	Lobolly	Dune grass	Maint grass	Ocean	Sand	Clay	diagonal	row total	users acc
Oak holly	55	19	6	0	0	0	0	0		80	68 75
Mixed	17	23	13	0	0	0	0	0		54	42 59
Lobolly	30	22	46	1	0	0	0	0		99	46 46
Dune grass	3	2	2	28	12	0	0	0		48	58 33
Maint grass	2	1	0	0	58	0	1	2		64	58 33
Ocean	0	0	0	0	0	8	0	8		8	93 33
Sand	0	0	0	0	1	0	14	0		15	100 00
Clay	0	0	0	0	0	1	0	10		10	
col total	107	67	67	30	71	9	17	10	242	378	64 02
producer acc	51 40	34 33	68 66	93 33	81 69	88 89	82 35	100 00			Overall Acc

25MM 4M POLYGON CULTURAL RAW DATA

	Asphalt	Concrete	Roof-grey	Roof-brown	Rip rap	diagonal	row total	users acc
Asphalt	42	1	2	0	5		50	84 00
Concrete	0	17	0	0	0		17	100 00
Roof-grey	2	1	8	0	0		11	72 73
Roof-brown	0	0	0	7	0		7	100 00
Rip rap	4	0	0	0	7		11	63 64
col total	48	19	10	7	12	81	96	84 38
producer acc	87 50	89 47	80 00	100 00	58 33			Overall Acc

25NM 4M SEED15 NATURAL AND CULTURAL RAW DATA

	Oak holly	Mixed	Lobiolly	Dune grass	Maint grass	Ocean	Sand	Clay	Asphalt	Concrete	Roof-grey	Roof-brown	Rip rap	diagonal	row total	users acc
Oak holly	60	24	13											0	98	61.22
Mixed	9	19	11			1								0	39	48.72
Lobiolly	33	19	41											0	94	43.62
Dune grass	2	2	1	28										0	38	73.68
Maint grass	4	3		3	65				7			1		2	90	43.62
Ocean						15	3							0	15	73.68
Sand						1	13							-	17	76.47
Clay		1			4			10						0	10	100.00
Asphalt				3	1	14	6		42	16				4	83	50.60
Concrete											5			0	18	88.89
Roof-grey										1				0	-	100.00
Roof-brown												8		0	8	100.00
Rip rap					3				1	1			6	6	12	50.00
col total	109	67	69	34	75	33	23	10	50	21	10	9	13	324	523	61.95
producer acc	55.05	28.36	59.42	82.35	86.67	45.45	56.52	100.00	84.00	76.19	10.00	88.89	46.15			Overall Acc

25NM 4M SEED15 NATURAL RAW DATA

	Oak holly	Mixed	Lobiolly	Dune grass	Maint grass	Ocean	Sand	Clay	diagonal	row total	users acc
Oak holly	60	24	13		1			0		98	61.22
Mixed	9	19	11			0		0		39	48.72
Lobiolly	33	19	41				0	0		93	44.09
Dune grass	2	2	1	28	4	0	0	3		37	75.68
Maint grass	4	3		3	65	15	3	0		78	44.09
Ocean						15		13		15	75.68
Sand						1	13	0		14	92.86
Clay		0	0	0	0			10		10	100.00
col total	108	67	66	31	70	16	16	10	251	384	65.36
producer acc	55.56	28.36	62.12	90.32	92.86	93.75	81.25	100.00			Overall Acc

25NM 4M SEED15 CULTURAL RAW DATA

	Asphalt	Concrete	Roof-grey	Roof-brown	Rip rap	diagonal	row total	users acc
Asphalt	42	1	5		4		52	80.77
Concrete	0	18	1	0	0		17	94.12
Roof-grey	0	0		8	0		1	100.00
Roof-brown	0	0	0	0	0		8	100.00
Rip rap	1	1	0	0	6		8	75.00
col total	43	18	7	8	10	73	86	84.88
producer acc	97.67	88.89	14.29	100.00	60.00			Overall Acc

25NM 4M SEED25 NATURAL AND CULTURAL
RAW DATA

	Oak holly	Mixed	Loblolly	Dune grass	Maint grass	Ocean	Sand	Clay	Asphalt	Concrete	Roof-grey	Roof-brown	Rip rap	diagonal	row total	users acc
Oak holly	38	6	3	0	1	0	0	0	0	0	1	0	0		49	77 55
Mixed	13	20	8	1	0	0	0	0	0	0	0	0	0		42	47 62
Loblolly	48	36	53	0	1	0	0	0	0	0	0	0	0		138	38 41
Dune grass	5	2	2	26	3	0	0	0	0	0	0	0	0		38	68 42
Maint grass	3	2	0	3	66	0	3	0	4	2	1	1	1		86	38 41
Ocean	0	0	0	0	0	16	0	0	0	0	0	0	0		16	68 42
Sand	0	0	0	0	0	0	13	0	0	1	0	0	0		14	92 86
Clay	0	0	0	0	0	0	0	10	0	0	0	0	0		10	100 00
Asphalt	2	1	3	2	3	9	6	0	39	1	3	0	4		73	53 42
Concrete	0	0	0	0	1	0	0	0	0	14	0	0	0		15	93 33
Roof-grey	0	0	0	0	0	8	0	0	2	1	5	0	0		16	31 25
Roof-brown	0	0	0	0	0	0	0	0	0	0	0	8	0		8	100 00
Rip rap	0	0	0	2	0	0	1	0	4	2	0	0	8	316	17	47 06
col total	109	67	69	34	75	33	23	10	49	21	10	9	13		522	60 54
producer acc	34 86	29 85	76 81	76 47	88 00	48 48	56 52	100 00	79 59	66 67	50 00	88 89	61 54			Overall Acc

25NM 4M SEED25 NATURAL
RAW DATA

	Oak holly	Mixed	Loblolly	Dune grass	Maint grass	Ocean	Sand	Clay	diagonal	row total	users acc
Oak holly	38	6	3	0	1	0	0	0		48	79 17
Mixed	13	20	8	1	0	0	0	0		42	47 62
Loblolly	48	36	53	0	1	0	0	0		138	38 41
Dune grass	5	2	2	26	3	0	0	0		38	68 42
Maint grass	3	2	0	3	66	0	3	0		77	38 41
Ocean	0	0	0	0	0	16	0	0		16	68 42
Sand	0	0	0	0	0	0	13	0		13	100 00
Clay	0	0	0	0	0	0	0	10	242	10	100 00
col total	107	66	66	30	71	16	16	10		382	63 35
producer acc	35 51	30 30	80 30	86 67	92 96	100 00	81 25	100 00			Overall Acc

25NM 4M SEED25 CULTURAL
RAW DATA

	Asphalt	Concrete	Roof-grey	Roof-brown	Rip rap	diagonal	row total	users acc
Asphalt	39	1	3	0	4		47	82 98
Concrete	0	14	0	0	0		14	100 00
Roof-grey	2	1	5	0	0		8	62 50
Roof-brown	0	0	0	8	0		8	100 00
Rip rap	4	2	0	0	8	74	14	57 14
col total	45	18	8	8	12		91	81 32
producer acc	86 67	77 78	62 50	100 00	66 67			Overall Acc

25NM 4M SEED2 NATURAL AND CULTURAL
RAW DATA

	Oak holly	Mixed	Loblolly	Dune grass	Maint grass	Ocean	Sand	Clay	Asphalt	Concrete	Roof-grey	Roof-brown	Rip rap	diagonal	row total		users acc
Oak holly	0	0	0	0	0	0	0	0	0	0	0	0	0		0		#DIV/0!
Mixed	26	14	3	0	0	0	0	0	0	0	0	0	0		43		32 56
Loblolly	61	43	64	1	1	0	0	0	0	0	0	0	0		170		37 65
Dune grass	0	0	0	6	0	0	0	0	0	0	0	0	0		6		100 00
Maint grass	22	10	0	19	71	0	3	0	4	1	0	0	2		132		37 65
Ocean	0	0	0	0	0	9	0	0	0	0	0	0	0		9		100 00
Sand	0	0	0	0	0	0	10	0	0	6	0	0	0		16		62 50
Clay	0	0	0	0	0	0	0	10	0	0	0	0	0		10		100 00
Asphalt	0	0	0	7	0	0	6	0	27	1	0	0	5		46		58 70
Concrete	0	0	0	0	0	0	0	0	0	3	0	0	0		3		100 00
Roof-grey	0	0	1	1	2	23	3	0	5	10	9	0	3		57		15 79
Roof-brown	0	0	0	0	0	0	0	0	0	0	0	8	0		8		100 00
Rip rap	0	0	1	0	1	1	0	0	14	0	1	1	3	234	22		13 64
col total	109	67	69	34	75	33	22	10	50	21	10	9	13		522		44 83
producer acc	0 00	20 90	92 75	17 65	94 67	27 27	45 45	100 00	54 00	14 29	90 00	88 89	23 08				Overall Acc

25NM 4M SEED2 NATURAL
RAW DATA

	Oak holly	Mixed	Loblolly	Dune grass	Maint grass	Ocean	Sand	Clay	diagonal	row total	users acc
Oak holly	0	0	0	0	0	0	0	0		0	#DIV/0!
Mixed	26	14	3	0	0	0	0	0		43	32 56
Loblolly	61	43	64	1	1	0	0	0		170	37 65
Dune grass	0	0	0	6	0	0	0	0		6	100 00
Maint grass	22	10	0	19	71	0	3	0		125	37 65
Ocean	0	0	0	0	0	9	0	0		9	100 00
Sand	0	0	0	0	0	0	10	0		10	100 00
Clay	0	0	0	0	0	0	0	10	184	10	100 00
col total	109	67	67	26	72	9	13	10		373	49 33
producer acc	0 00	20 90	95 52	23 08	98 61	100 00	76 92	100 00			Overall Acc

25NM 4M SEED2 CULTURAL
RAW DATA

	Asphalt	Concrete	Roof-grey	Roof-brown	Rip rap	diagonal	row total	users acc
Asphalt	27	1	0	0	5		33	81 82
Concrete	0	3	0	0	0		3	100 00
Roof-grey	5	10	9	0	3		27	33 33
Roof-brown	0	0	0	8	0		8	100 00
Rip rap	14	0	1	1	3	50	19	15 79
col total	46	14	10	9	11		90	55 56
producer acc	58 70	21 43	90 00	88 89	27 27			Overall Acc

25NM 4M SEED5 NATURAL AND CULTURAL
RAW DATA

	Oak holly	Mixed	Loblolly	Dune grass	Maint grass	Ocean	Sand	Clay	Asphalt	Concrete	Roof-grey	Roof-brown	Rip rap	diagonal	row total	users acc
Oak holly	32	10	8	2	3	0	0	0	0	0	2	0	0		57	56 14
Mixed	35	42	26	1	0	0	0	0	0	0	0	0	0		104	40 38
Loblolly	34	10	33	0	0	0	0	0	0	0	0	0	0		77	42 86
Dune grass	1	0	1	16	1	0	0	0	0	0	0	0	0		19	84 21
Maint grass	7	5	0	5	67	0	3	0	6	2	2	1	2		100	42 86
Ocean	0	0	0	0	0	10	0	0	0	0	0	0	0		10	84 21
Sand	0	0	0	0	0	0	0	0	0	0	0	0	0		0	#DIV/0!
Clay	0	0	0	0	0	0	0	10	0	0	0	0	0		10	100 00
Asphalt	0	0	0	1	0	22	6	0	30	2	4	0	11		76	39 47
Concrete	0	0	0	0	1	0	10	0	0	16	0	0	0		27	59 26
Roof-grey	0	0	0	0	0	1	3	0	0	0	1	0	0		5	20 00
Roof-brown	0	0	0	0	0	0	0	0	0	0	0	8	0		8	100 00
Rip rap	0	0	1	9	3	0	0	0	13	1	1	0	0	265	28	0 00
col total	109	67	69	34	75	33	22	10	49	21	10	9	13		521	50 86
producer acc	29 36	62 69	47 83	47 06	89 33	30 30	0 00	100 00	61 22	76 19	10 00	88 89	0 00			Overall Acc

25NM 4M SEED 5 NATURAL
RAW DATA

	Oak holly	Mixed	Loblolly	Dune grass	Maint grass	Ocean	Sand	Clay	diagonal	row total	users acc
Oak holly	32	10	8	2	3	0	0	0		55	58 18
Mixed	35	42	26	1	0	0	0	0		104	40 38
Loblolly	34	10	33	0	0	0	0	0		77	42 86
Dune grass	1	0	1	16	1	0	0	0		19	84 21
Maint grass	7	5	0	5	67	0	3	0		87	42 86
Ocean	0	0	0	0	0	10	0	0		10	84 21
Sand	0	0	0	0	0	0	0	0		0	#DIV/0!
Clay	0	0	0	0	0	0	0	10	210	10	100 00
col total	109	67	68	24	71	10	3	10		362	58 01
producer acc	29 36	62 69	48 53	66 67	94 37	100 00	0 00	100 00			Overall Acc

25NM 4M SEED 5 CULTURAL
RAW DATA

	Asphalt	Concrete	Roof-grey	Roof-brown	Rip rap	diagonal	row total	users acc
Asphalt	30	2	4	0	11		47	63 83
Concrete	0	16	0	0	0		16	100 00
Roof-grey	0	0	1	0	0		1	100 00
Roof-brown	0	0	0	8	0		8	100 00
Rip rap	13	1	1	0	0	55	15	0 00
col total	43	19	6	8	11		87	63 22
producer acc	69 77	84 21	16 67	100 00	0 00			Overall Acc

70nm 1m point Natural and cultural
RAW DATA-70-1-point

	Oak holly	Mixed	Loblolly	Dune grass	Maint grass	Ocean	Sand	Clay	Asphalt	Concrete	Roof-grey	Roof-brown	Rip rap	diagonal	row total	users acc
Oak holly	8	4	3	10	3	0	0	0	0	0	0	0	0		28	28 57
Mixed	81	52	54	9	20	0	0	0	0	2	0	0	0		218	23 85
Loblolly	13	7	9	0	0	0	0	0	0	0	0	0	0		29	31 03
Dune grass	0	0	0	4	1	0	0	0	1	0	0	0	0		6	66 67
Maint grass	7	3	1	6	36	0	2	0	1	0	1	2	1		60	31 03
Ocean	0	0	0	0	0	10	0	0	0	0	0	0	0		10	66 67
Sand	0	0	1	1	13	1	10	1	1	4	0	0	0		32	31 25
Clay	0	0	0	0	0	0	0	9	0	0	0	0	0		9	100 00
Asphalt	0	1	1	1	1	1	0	0	29	1	4	7	6		52	55 77
Concrete	0	0	0	0	0	0	0	0	0	8	0	0	0		8	100 00
Roof-grey	0	0	0	1	1	8	9	0	8	5	3	0	1		36	8 33
Roof-brown	0	0	0	1	0	0	0	0	0	0	0	0	0		1	0 00
Rip rap	0	0	0	1	0	13	2	0	10	1	2	0	5	183	34	14 71
col total	109	67	69	34	75	33	23	10	50	21	10	9	13		523	34 99
producer acc	7 34	77 61	13 04	11 76	48 00	30 30	43 48	90 00	58 00	38 10	30 00	0 00	38 46			Overall Acc

70nm 1m point Natural
RAW DATA

	Oak holly	Mixed	Loblolly	Dune grass	Maint grass	Ocean	Sand	Clay	diagonal	row total	users acc
Oak holly	8	4	3	10	3	0	0	0		28	28 57
Mixed	81	52	54	9	20	0	0	0		216	24 07
Loblolly	13	7	9	0	0	0	0	0		29	31 03
Dune grass	0	0	0	4	1	0	0	0		5	80 00
Maint grass	7	3	1	6	36	0	2	0		55	31 03
Ocean	0	0	0	0	0	10	0	0		10	80 00
Sand	0	0	1	1	13	1	10	1		27	37 04
Clay	0	0	0	0	0	0	0	9		9	100 00
col total	109	66	68	30	73	11	12	10	138	379	36 41
producer acc	7 34	78 79	13 24	13 33	49 32	90 91	83 33	90 00			Overall Acc

70nm 1m point cultural
RAW DATA

	Asphalt	Concrete	Roof-grey	Roof-brown	Rip rap	diagonal	row total	users acc
Asphalt	29	1	4	7	6		47	61 70
Concrete	0	8	0	0	0		8	100 00
Roof-grey	8	5	3	0	1		17	17 65
Roof-brown	0	0	0	0	0		0	#DIV/0!
Rip rap	10	1	2	0	5	45	18	27 78
col total	47	15	9	7	12		90	50 00
producer acc	61 70	53 33	33 33	0 00	41 67			Overall Acc

70NM 1M POLYGON NATURAL AND CULTURAL
RAW DATA-70-1-poly

	Oak holly	Mixed	Loblolly	Dune grass	Maint grass	Ocean	Sand	Clay	Asphalt	Concrete	Roof-grey	Roof-brown	Rip rap	diagonal	row total	users acc
Oak holly	41	17	10	0	0	0	0	0	0	0	0	0	0		68	60 29
Mixed	37	24	14	0	2	0	0	0	0	0	0	2	0		79	30 38
Loblolly	26	23	39	1	1	0	0	0	0	0	0	0	0		90	43 33
Dune grass	4	1	4	27	15	0	0	0	2	0	0	0	0		53	50 94
Maint grass	1	1	1	0	52	0	3	0	2	1	1	0	0		62	43 33
Ocean	0	0	0	0	0	9	0	0	0	0	0	0	0		9	50 94
Sand	0	0	0	0	0	1	15	0	0	3	1	0	1		21	71 43
Clay	0	0	0	0	0	0	0	10	0	0	0	0	0		10	100 00
Asphalt	0	0	0	3	1	1	1	0	35	1	3	0	10		55	83 64
Concrete	0	0	0	0	0	0	1	0	0	11	0	0	0		12	91 67
Roof-grey	0	1	1	1	4	16	3	0	1	4	4	0	1		36	11 11
Roof-brown	0	0	0	0	0	0	0	0	0	0	0	7	0		7	100 00
Rip rap	0	0	0	2	0	6	0	0	10	1	1	0	1	275	21	4 76
col total	109	67	69	34	75	33	23	10	50	21	10	9	13		523	52 58
producer acc	37 61	35 82	56 52	79 41	69 33	27 27	65 22	100 00	70 00	52 38	40 00	77 78	7 69			Overall Acc

70NM 1M POLYGON NATURAL
RAW DATA

	Oak holly	Mixed	Loblolly	Dune grass	Maint grass	Ocean	Sand	Clay	diagonal	row total	users acc
Oak holly	41	17	10	0	0	0	0	0		68	60 29
Mixed	37	24	14	0	2	0	0	0		77	31 17
Loblolly	26	23	39	1	1	0	0	0		90	43 33
Dune grass	4	1	4	27	15	0	0	0		51	52 94
Maint grass	1	1	1	0	52	0	3	0		58	43 33
Ocean	0	0	0	0	0	9	0	0		9	52 94
Sand	0	0	0	0	0	1	15	0		16	93 75
Clay	0	0	0	0	0	0	0	10	217	10	100 00
col total	109	66	68	28	70	10	18	10		379	57 26
producer acc	37 61	36 36	57 35	96 43	74 29	90 00	83 33	100 00			Overall Acc

70NM 1M POLYGON CULTURAL
RAW DATA

	Asphalt	Concrete	Roof-grey	Roof-brown	Rip rap	diagonal	row total	users acc
Asphalt	35	1	3	0	10		49	71 43
Concrete	0	11	0	0	0		11	100 00
Roof-grey	1	4	4	0	1		10	40 00
Roof-brown	0	0	0	7	0		7	100 00
Rip rap	10	1	1	0	1	58	13	7 69
col total	46	17	8	7	12		90	64 44
producer acc	76 09	64 71	50 00	100 00	8 33			Overall Acc

70NM 1M SEED 15 NATURAL AND CULTURAL

RAW DATA

	Oak holly	Mixed	Lobolly	Dune grass	Maint grass	Ocean	Sand	Clay	Asphalt	Concrete	Roof-grey	Roof-brown	Rip rap	diagonal	row total	users acc
Oak holly	58	26	22	3											110	52 73
Mixed	24	21	29	3											74	28 38
Lobolly	21	15	14	1											56	25 00
Dune grass	5	2	2	22											35	62 86
Maint grass	1	3	1	3	65	10	3		4						63	82 86
Ocean						10									10	80 00
Sand							8								10	100 00
Clay								10					1		10	70 37
Asphalt				2		2			38		6				54	100 00
Concrete										12					12	8 70
Roof-grey						7	9			4	2	2			23	72 73
Roof-brown												8			11	25 71
Rip rap	1			3	2		13		5				9		35	
col total	109	67	69	34	75	33	23	10	50	21	10	9	13	277	523	
producer acc	53 21	31 34	20 29	64 71	86 67	30 30	34 78	100 00	76 00	57 14	20 00	88 89	69 23			Overall Acc 52 96

70NM 1M SEED15 NATURAL

RAW DATA

	Oak holly	Mixed	Lobolly	Dune grass	Maint grass	Ocean	Sand	Clay	diagonal	row total	users acc
Oak holly	58	26	22	3	1					110	52 73
Mixed	24	21	29							74	28 38
Lobolly	21	15	14	1	2					53	26 42
Dune grass	5	2	2	22	4					35	62 86
Maint grass	1	3	1	3	65		3			76	85 53
Ocean						10				10	100 00
Sand							8			9	88 89
Clay								10		10	100 00
col total	109	67	68	29	72	11	11	10	208	377	
producer acc	53 21	31 34	20 59	75 86	90 28	90 91	72 73	100 00			Overall Acc 55 17

70NM 1M SEED15 CULTURAL

RAW DATA

	Asphalt	Concrete	Roof-grey	Roof-brown	Rip rap	diagonal	row total	users acc
Asphalt	38	0	6	0	4		48	79 17
Concrete	0	12	0	0	0		12	100 00
Roof-grey	1	4	2	0	0		7	28 57
Roof-brown	2	1	0	8	0		11	72 73
Rip rap	5	0	0	0	9		14	64 29
col total	46	17	8	8	13	69	92	
producer acc	82 61	70 59	25 00	100 00	69 23			Overall Acc 75 00

70NM 1M SEED25 NATURAL AND CULTURAL — RAW DATA

	Oak holly	Mixed	Lobolly	Dune grass	Maint grass	Ocean	Sand	Clay	Asphalt	Concrete	Roof-grey	Roof-brown	Rip rap	diagonal	row total	users acc
Oak holly	42	19	10	0	1	0	0	0	0	0	0	0	0		73	57.53
Mixed	31	23	31	1	0	0	0	0	0	0	0	0	1		87	26.44
Lobolly	28	17	23	23	0	0	0	0	0	0	0	0	0		69	33.33
Dune grass	6	3	3	4	4	0	0	0	0	0	0	0	0		39	58.97
Maint grass	2	5	3	1	67	9	3	0	2	0	0	0	0		90	58.97
Ocean	0	0	0	0	0	9	11	0	0	0	0	0	0		9	100.00
Sand	0	0	0	3	0	15	11	10	0	0	0	0	0		15	73.33
Clay	0	0	1	0	0	0	0	10	35	4	1	1	0		10	100.00
Asphalt	0	0	0	0	0	0	0	0	35	11	1	0	0		69	50.72
Concrete	0	0	0	0	0	8	3	0	0	11	4	1	0		15	73.33
Roof-grey	0	0	0	0	0	0	0	0	2	2	2	2	0		18	11.11
Roof-brown	0	0	0	0	0	0	0	0	9	0	0	7	7		9	77.78
Rip rap	0	1	0	2	2	3	3	0	0	0	0	0	4		20	20.00
col total	109	67	69	34	75	33	23	10	50	21	10	9	13	267	523	51.05 Overall Acc
producer acc	38.53	34.33	33.33	67.65	89.33	27.27	47.83	100.00	70.00	52.38	20.00	77.78	30.77			

70NM 1M SEED25 NATURAL — RAW DATA

	Oak holly	Mixed	Lobolly	Dune grass	Maint grass	Ocean	Sand	Clay	diagonal	row total	users acc
Oak holly	42	19	10	0	1	0	0	0		73	57.53
Mixed	31	23	31	1	0	0	0	0		85	27.06
Lobolly	28	17	23	23	0	0	0	0		69	33.33
Dune grass	6	3	3	4	4	0	0	0		39	58.97
Maint grass	2	5	3	1	67	9	3	0		82	58.97
Ocean	0	0	0	0	0	9	9	0		9	91.67
Sand	0	0	0	0	0	1	11	0		12	100.00
Clay	0	0	0	0	0	0	0	10		10	
col total	109	67	68	29	72	10	14	10	208	379	54.88 Overall Acc
producer acc	38.53	34.33	33.82	79.31	93.06	90.00	78.57	100.00			

70NM 1M SEED25 CULTURAL — RAW DATA

	Asphalt	Concrete	Roof-grey	Roof-brown	Rip rap	diagonal	row total	users acc
Asphalt	35	1	5	8	0		49	71.43
Concrete	0	11	1	0	0		12	91.67
Roof-grey	1	1	2	0	0		7	28.57
Roof-brown	2	0	0	7	0		9	77.78
Rip rap	9	0	0	0	4		13	30.77
col total	47	16	8	7	12	59	90	65.56 Overall Acc
producer acc	74.47	68.75	25.00	100.00	33.33			

70NM 1M SEED2 NATURAL AND CULTURAL — RAW DATA

	Oak holly	Mixed	Lobolly	Dune grass	Maint grass	Ocean	Sand	Clay	Asphalt	Concrete	Roof-grey	Roof-brown	Rip rap	diagonal	row total	users acc
Oak holly	4	2													9	44 44
Mixed	85	54	56	8	5										209	25 84
Lobolly	17	9	8		4										40	20 00
Dune grass	2	2	1	16	2										21	76 19
Maint grass					59	11			2						73	20 00
Ocean						11	1								11	76 19
Sand							7								12	58 33
Clay								10							10	100 00
Asphalt	1								29	3	1				50	58 00
Concrete										7		5			7	100 00
Roof-grey							5			2	4		5		18	22 22
Roof-brown										2		3			3	100 00
Rip rap					4	7	7		19	5			7		60	11 67
col total	109	67	69	34	75	33	23	10	50	21	10	9	13	219	523	
producer acc	3 67	80 60	11 59	47 06	78 67	33 33	30 43	100 00	58 00	33 33	40 00	33 33	53 85			Overall Acc 41 87

70NM 1M SEED2 NATURAL — RAW DATA

	Oak holly	Mixed	Lobolly	Dune grass	Maint grass	Ocean	Sand	Clay	diagonal	row total	users acc
Oak holly	4	2	1	2						9	44 44
Mixed	85	54	56	8	5					208	25 96
Lobolly	17	9	8		4					38	21 05
Dune grass	2	2	1	16						21	76 19
Maint grass				4	59		4			70	84 29
Ocean						11				11	91 67
Sand						1	7			8	87 50
Clay								10		10	100 00
col total	108	67	67	30	70	12	11	10	169	375	
producer acc	3 70	80 60	11 94	53 33	84 29	91 67	63 64	100 00			Overall Acc 45 07

70NM 1M SEED2 CULTURAL — RAW DATA

	Asphalt	Concrete	Roof-grey	Roof-brown	Rip rap	diagonal	row total	users acc
Asphalt	29	2	4	5	5		45	64 44
Concrete		7					7	100 00
Roof-grey		2	4				6	66 67
Roof-brown				3			3	100 00
Rip rap	19	5	1		7		32	21 88
col total	48	16	9	8	12	50	93	
producer acc	60 42	43 75	44 44	37 50	58 33			Overall Acc 53 76

70MM 1M SEEDS NATURAL AND CULTURAL
RAW DATA

	Oak holly	Mixed	Lobolly	Dune grass	Maint grass	Ocean	Sand	Clay	Asphalt	Concrete	Roof-grey	Roof-brown	Rip rap	diagonal	row total	users acc
Oak holly	19	13	8	0	0	0	0	0	0	0	0	0	0		40	47.50
Mixed	73	38	50	2	1	0	0	0	0	0	0	0	0		164	23.17
Lobolly	4	9	6	0	2	0	0	0	0	0	0	0	0		21	28.57
Dune grass	3	0	2	21	0	0	0	0	0	0	0	0	0		26	80.77
Maint grass	10	7	3	11	68	0	0	0	0	0	0	0	0		103	28.57
Ocean	0	0	0	0	0	10	0	0	0	0	0	0	0		10	100.00
Sand	0	0	0	0	0	0	5	0	0	0	0	0	0		9	55.56
Clay	0	0	0	0	0	0	0	10	0	0	0	0	0		10	100.00
Asphalt	0	0	0	0	0	0	0	0	35	2	0	0	2		46	76.09
Concrete	0	0	0	0	0	0	0	0	0	8	0	0	0		8	100.00
Roof-grey	0	0	0	0	0	0	0	0	4	8	4	0	3		45	8.89
Roof-brown	0	0	0	0	0	0	0	0	0	0	0	6	0		6	100.00
Rip rap	0	0	0	0	0	0	0	0	9	0	1	0	7		35	20.00
col total	109	67	69	34	75	33	23	10	50	21	10	9	13	237	523	
producer acc	17.43	56.72	8.70	61.76	90.67	30.30	21.74	100.00	70.00	38.10	40.00	66.67	53.85			45.32 Overall Acc

70MM 1M SEEDS NATURAL
RAW DATA

	Oak holly	Mixed	Lobolly	Dune grass	Maint grass	Ocean	Sand	Clay	diagonal	row total	users acc
Oak holly	19	13	8	0	0	0	0	0		40	47.50
Mixed	73	38	50	2	1	0	0	0		164	23.17
Lobolly	4	9	6	0	0	0	0	0		19	31.58
Dune grass	3	0	3	21	0	0	0	0		26	80.77
Maint grass	10	7	0	7	68	0	5	0		98	31.58
Ocean	0	0	0	0	0	10	0	0		10	80.77
Sand	0	0	0	0	0	1	0	0		6	83.33
Clay	0	0	0	0	0	0	0	10		10	100.00
col total	109	67	67	30	71	11	8	10	177	373	
producer acc	17.43	56.72	8.96	70.00	95.77	90.91	62.50	100.00			47.45 Overall Acc

70MM 1M SEEDS CULTURAL
RAW DATA

	Asphalt	Concrete	Roof-grey	Roof-brown	Rip rap	diagonal	row total	users acc
Asphalt	35	1	3	2	2		43	81.40
Concrete	0	8	0	0	0		8	100.00
Roof-grey	4	8	4	0	3		19	21.05
Roof-brown	0	0	0	6	0		6	100.00
Rip rap	9	0	1	0	7		17	41.18
col total	48	17	8	8	12	60	93	
producer acc	72.92	47.06	50.00	75.00	58.33			64.52 Overall Acc

70NM 4M POINT NATURAL AND CULTURAL
RAW DATA-70-4-point

	Oak holly	Mixed	Loblolly	Dune grass	Maint grass	Ocean	Sand	Clay	Asphalt	Concrete	Roof-grey	Roof-brown	Rip rap	diagonal	row total	users acc
Oak holly	59	20	41	12	3	0	0	0	0	0	0	0	0		135	43 70
Mixed	16	22	7	2	0	0	0	0	0	0	0	0	0		47	46 81
Loblolly	9	11	5	0	1	0	0	0	0	0	0	0	0		26	19 23
Dune grass	0	0	0	4	0	0	0	0	0	0	0	0	0		4	100 00
Maint grass	24	14	13	9	65	0	3	0	3	1	1	0	0		133	19 23
Ocean	0	0	0	0	0	5	0	0	0	0	0	0	0		5	100 00
Sand	0	0	0	0	0	0	1	0	0	0	0	0	0		1	100 00
Clay	0	0	0	0	0	0	0	9	0	0	0	0	0		9	100 00
Asphalt	0	0	0	0	0	0	0	0	4	0	0	0	1		5	80 00
Concrete	0	0	0	0	0	0	0	0	0	5	0	0	0		5	100 00
Roof-grey	0	0	0	2	4	23	19	1	22	14	6	1	8		100	6 00
Roof-brown	1	0	2	3	1	0	0	0	2	1	2	8	0		20	40 00
Rip rap	0	0	1	2	1	5	0	0	19	0	1	0	4		33	12 12
														197		
col total	109	67	69	34	75	33	23	10	50	21	10	9	13		523	37 67
producer acc	54 13	32 84	7 25	11 76	86 67	15 15	4 35	90 00	8 00	23 81	60 00	88 89	30 77			Overall Acc

70NM 4M POINT NATURAL
RAW DATA

	Oak holly	Mixed	Loblolly	Dune grass	Maint grass	Ocean	Sand	Clay	diagonal	row total	users acc
Oak holly	59	20	41	12	3	0	0	0		135	43 70
Mixed	16	22	7	2	0	0	0	0		47	46 81
Loblolly	9	11	5	0	1	0	0	0		26	19 23
Dune grass	0	0	0	4	0	0	0	0		4	100 00
Maint grass	24	14	13	9	65	0	3	0		128	19 23
Ocean	0	0	0	0	0	5	0	0		5	100 00
Sand	0	0	0	0	0	0	1	0		1	100 00
Clay	0	0	0	0	0	0	0	9		9	100 00
									170		
col total	108	67	66	27	69	5	4	9		355	47 89
producer acc	54 63	32 84	7 58	14 81	94 20	100 00	25 00	100 00			Overall Acc

70NM 4M POINT CULTURAL
RAW DATA

	Asphalt	Concrete	Roof-grey	Roof-brown	Rip rap	diagonal	row total	users acc
Asphalt	4	0	0	0	1		5	80 00
Concrete	0	5	0	0	0		5	100 00
Roof-grey	22	14	6	1	8		51	11 76
Roof-brown	2	1	2	8	0		13	61 54
Rip rap	19	0	1	0	4		24	16 67
						27		
col total	47	20	9	9	13		98	27 55
producer acc	8 51	25 00	66 67	88 89	30 77			Overall Acc

70NM 4M POLYGON NATURAL AND CULTURAL
RAW DATA-70-4-poly

	Oak holly	Mixed	Loblolly	Dune grass	Maint grass	Ocean	Sand	Clay	Asphalt	Concrete	Roof-grey	Roof-brown	Rip rap	diagonal	row total	users acc
Oak holly	49	21	4	0	0	0	0	0	0	0	0	0	0		74	66 22
Mixed	32	31	15	2	1	0	0	0	0	0	0	0	0		81	38 27
Loblolly	23	9	46	0	0	0	0	0	0	0	0	0	0		78	58 97
Dune grass	5	3	2	28	18	0	0	0	7	1	1	2	1		68	41 18
Maint grass	0	3	1	0	51	0	3	0	2	1	0	0	0		61	58 97
Ocean	0	0	0	0	0	5	0	0	0	0	0	0	0		5	41 18
Sand	0	0	0	0	0	1	13	0	0	4	0	0	2		20	65 00
Clay	0	0	0	0	0	0	0	10	0	0	0	0	0		10	100 00
Asphalt	0	0	1	3	1	2	3	0	22	0	0	0	7		39	56 41
Concrete	0	0	0	0	0	0	0	0	0	13	0	0	0		13	100 00
Roof-grey	0	0	0	1	4	25	1	0	7	2	8	1	0		49	16 33
Roof-brown	0	0	0	0	0	0	0	0	0	0	0	6	0		6	100 00
Rip rap	0	0	0	0	0	0	3	0	12	0	1	0	3	285	19	15 79
col total	109	67	69	34	75	33	23	10	50	21	10	9	13		523	54 49
producer acc	44 95	46 27	66 67	82 35	68 00	15 15	56 52	100 00	44 00	61 90	80 00	66 67	23 08			Overall Acc

70NM 4M POLYGON NATURAL
RAW DATA

	Oak holly	Mixed	Loblolly	Dune grass	Maint grass	Ocean	Sand	Clay	diagonal	row total	users acc
Oak holly	49	21	4	0	0	0	0	0		74	66 22
Mixed	32	31	15	2	1	0	0	0		81	38 27
Loblolly	23	9	46	0	0	0	0	0		78	58 97
Dune grass	5	3	2	28	18	0	0	0		56	50 00
Maint grass	0	3	1	0	51	0	3	0		58	58 97
Ocean	0	0	0	0	0	5	0	0		5	50 00
Sand	0	0	0	0	0	1	13	0		14	92 86
Clay	0	0	0	0	0	0	0	10	233	10	100 00
col total	109	67	68	30	70	6	16	10		376	61 97
producer acc	44 95	46 27	67 65	93 33	72 86	83 33	81 25	100 00			Overall Acc

70NM 4M POLYGON CULTURAL
RAW DATA

	Asphalt	Concrete	Roof-grey	Roof-brown	Rip rap	diagonal	row total	users acc
Asphalt	22	0	0	0	7		29	75 86
Concrete	0	13	0	0	0		13	100 00
Roof-grey	7	2	8	1	0		18	44 44
Roof-brown	0	0	0	6	0		6	100 00
Rip rap	12	0	1	0	3	52	16	18 75
col total	41	15	9	7	10		82	63 41
producer acc	53 66	86 67	88 89	85 71	30 00			Overall Acc

70NM 4M SEED 16 NATURAL AND CULTURAL RAW DATA

	Oak holly	Mixed	Lobolly	Dune grass	Maint grass	Ocean	Sand	Clay	Asphalt	Concrete	Roof-grey	Roof-brown	Rip rap	diagonal	row total	users acc
Oak holly	61	22	11												94	64.89
Mixed	27	28	18	10	21				11	3	3	1			130	21.54
Lobolly	20	18	38												74	51.35
Dune grass	1	1		21											23	91.30
Maint grass					52		3								62	51.35
Ocean						11									11	91.30
Sand				2			10	9		2	1				15	66.67
Clay								9							9	100.00
Asphalt									35		1				56	62.50
Concrete										11					13	84.62
Roof-grey											3				20	15.00
Roof-brown												8			8	100.00
Rip rap									3				4		8	50.00
col total	109	67	69	34	75	33	23	10	50	21	10	9	13	291	523	55.64 Overall Acc
producer acc	55.96	41.79	55.07	61.76	69.33	33.33	43.48	90.00	70.00	52.38	30.00	88.89	30.77			

70NM 4M SEED15 NATURAL RAW DATA

	Oak holly	Mixed	Lobolly	Dune grass	Maint grass	Ocean	Sand	Clay	diagonal	row total	users acc
Oak holly	61	22	11							94	64.89
Mixed	27	28	18	10	21		3	3		110	25.45
Lobolly	20	18	38							74	51.35
Dune grass	1	1		21						23	91.30
Maint grass				1	52		3			59	51.35
Ocean						11				11	91.30
Sand							10	1		11	91.30
Clay								9		9	100.00
col total	109	67	68	32	74	15	16	10	230	391	58.82 Overall Acc
producer acc	55.96	41.79	55.88	65.63	70.27	73.33	62.50	90.00			

70NM 4M SEED15 CULTURAL RAW DATA

	Asphalt	Concrete	Roof-grey	Roof-brown	Rip rap	diagonal	row total	users acc
Asphalt	35	2			6		43	81.40
Concrete		11					11	100.00
Roof-grey		1	3	3			7	42.86
Roof-brown				8			8	100.00
Rip rap	3				4		7	57.14
col total	38	15	5	8	10	61	76	80.26 Overall Acc
producer acc	92.11	73.33	60.00	100.00	40.00			

70NM 4M SEED 25 NATURAL AND CULTURAL
RAW DATA

	Oak holly	Mixed	Lobolly	Dune grass	Maint grass	Ocean	Sand	Clay	Asphalt	Concrete	Roof-grey	Roof-brown	Rip rap	diagonal	row total	users acc
Oak holly	56	20	5	0	1	0	0	0	0	0	0	0	0		82	68 29
Mixed	18	22	14	1	0	0	0	0	0	0	0	0	0		55	40 00
Lobolly	23	16	46	0	0	0	0	0	0	0	0	0	0		85	54 12
Dune grass	10	5	1	25	5	0	0	0	0	0	0	0	0		49	51 02
Maint grass	1	4	2	4	62	1	0	0	2	0	0	0	0		81	76 54
Ocean	0	0	0	0	0	14	0	0	0	0	0	0	0		14	51 02
Sand	0	0	0	0	0	3	13	0	0	0	0	0	0		18	72 22
Clay	0	0	0	0	0	0	0	10	0	0	0	0	0		10	100 00
Asphalt	0	0	0	0	0	0	0	0	39	14	0	0	0		80	48 75
Concrete	0	0	0	0	0	0	0	0	0	14	2	0	0		16	87 50
Roof-grey	0	0	0	0	0	0	0	0	0	0	3	3	0		8	37 50
Roof-brown	0	0	0	0	0	0	0	0	1	0	0	8	0		10	80 00
Rip rap	0	0	0	2	0	0	0	0	7	0	0	0	4		15	26 67
col total	109	67	69	34	75	33	23	10	50	21	10	9	13	318	523	60 42
producer acc	51 38	32 84	66 67	73 53	82 67	42 42	56 52	100 00	78 00	66 67	30 00	88 89	30 77			Overall Acc

70NM 4M SEED 25 NATURAL
RAW DATA

	Oak holly	Mixed	Lobolly	Dune grass	Maint grass	Ocean	Sand	Clay	diagonal	row total	users acc
Oak holly	56	20	5	0	1	0	0	0		82	68 29
Mixed	18	22	14	1	0	0	0	0		55	40 00
Lobolly	23	16	46	0	0	0	0	0		85	54 12
Dune grass	10	5	1	25	5	0	0	0		46	54 35
Maint grass	1	4	2	4	62	1	1	0		76	81 58
Ocean	0	0	0	0	0	14	0	0		14	100 00
Sand	0	0	0	0	0	0	13	0		14	92 86
Clay	0	0	0	0	0	0	0	10		10	100 00
col total	108	67	68	30	68	15	16	10	248	382	64 92
producer acc	51 85	32 84	67 65	83 33	91 18	93 33	81 25	100 00			Overall Acc

70NM 4M SEED25 CULTURAL
RAW DATA

	Asphalt	Concrete	Roof-grey	Roof-brown	Rip rap	diagonal	row total	users acc
Asphalt	39	4	3	0	5		51	76 47
Concrete	0	14	0	0	0		14	100 00
Roof-grey	0	0	3	0	2		5	60 00
Roof-brown	2	0	0	8	0		10	80 00
Rip rap	5	0	1	0	4		11	36 36
col total	46	18	7	8	12	68	91	74 73
producer acc	84 78	77 78	42 86	100 00	33 33			Overall Acc

70NM 4M SEED2 NATURAL AND CULTURAL
RAW DATA

	Oak holly	Mixed	Loblolly	Dune grass	Maint grass	Ocean	Sand	Clay	Asphalt	Concrete	Roof-grey	Roof-brown	Rip rap	diagonal	row total	users acc
Oak holly	38	7	16	7	1	0	0	0	0	0	0	0	0		69	55 07
Mixed	11	12	3	0	0	0	0	0	0	0	0	0	0		26	46 15
Loblolly	40	31	44	0	2	0	0	0	0	0	0	0	0		117	37 61
Dune grass	0	0	0	1	0	0	0	0	0	0	0	0	0		1	100 00
Maint grass	20	16	4	21	70	0	5	1	8	1	1	1	1		149	37 61
Ocean	0	0	0	0	0	9	0	0	0	0	0	0	0		9	100 00
Sand	0	0	0	0	0	0	3	0	0	1	0	0	0		4	75 00
Clay	0	0	0	0	0	0	0	9	0	1	0	0	0		9	100 00
Asphalt	0	1	2	1	0	0	0	0	17	1	1	0	1		24	70 83
Concrete	0	0	0	0	1	0	0	0	0	8	0	0	0		9	88 89
Roof-grey	0	0	0	2	1	24	15	0	25	10	8	0	11		96	8 33
Roof-brown	0	0	0	2	0	0	0	0	0	0	0	8	0		10	80 00
Rip rap	0	0	0	0	0	0	0	0	0	0	0	0	0		0	#DIV/0!
														227		
col total	109	67	69	34	75	33	23	10	50	21	10	9	13		523	43 40
producer acc	34 86	17 91	63 77	2 94	93 33	27 27	13 04	90 00	34 00	38 10	80 00	88 89	0 00			Overall Acc

70NM 4M SEED2 NATURAL
RAW DATA

	Oak holly	Mixed	Loblolly	Dune grass	Maint grass	Ocean	Sand	Clay	diagonal	row total	users acc
Oak holly	38	7	16	7	1	0	0	0		69	55 07
Mixed	11	12	3	0	0	0	0	0		26	46 15
Loblolly	40	31	44	0	2	0	0	0		117	37 61
Dune grass	0	0	0	1	0	0	0	0		1	100 00
Maint grass	20	16	4	21	70	0	5	1		137	37 61
Ocean	0	0	0	0	0	9	0	0		9	100 00
Sand	0	0	0	0	0	0	3	0		3	100 00
Clay	0	0	0	0	0	0	0	9		9	100 00
									186		
col total	109	66	67	29	73	9	8	10		371	50 13
producer acc	34 86	18 18	65 67	3 45	95 89	100 00	37 50	90 00			Overall Acc

70NM 4M SEED2 CULTURAL
RAW DATA

	Asphalt	Concrete	Roof-grey	Roof-brown	Rip rap	diagonal	row total	users acc
Asphalt	17	1	1	0	1		20	85 00
Concrete	0	8	0	0	0		8	100 00
Roof-grey	25	10	8	0	11		54	14 81
Roof-brown	0	0	0	8	0		8	100 00
Rip rap	0	0	0	0	0		0	#DIV/0!
						41		
col total	42	19	9	8	12		90	45 56
producer acc	40 48	42 11	88 89	100 00	0 00			Overall Acc

70NM 4M SEED5 NATURAL AND CULTURAL
RAW DATA

	Oak holly	Mixed	Loblolly	Dune grass	Maint grass	Ocean	Sand	Clay	Asphalt	Concrete	Roof-grey	Roof-brown	Rip rap	diagonal	row total	users acc
Oak holly	58	14	23	10	2	0	0	0	0	0	0	0	0		107	54 21
Mixed	43	47	33	2	0	0	0	0	0	0	0	0	0		125	37 60
Loblolly	3	2	10	0	0	0	0	0	0	0	0	0	0		15	66 67
Dune grass	0	0	0	13	1	0	0	0	0	0	0	1	0		15	86 67
Maint grass	5	4	3	6	68	0	4	1	7	2	1	1	1		103	66 67
Ocean	0	0	0	0	0	10	0	0	0	0	0	0	0		10	86 67
Sand	0	0	0	0	0	0	2	0	0	0	0	0	0		2	100 00
Clay	0	0	0	0	0	0	0	9	0	0	0	0	0		9	100 00
Asphalt	0	0	0	0	0	0	0	0	14	1	0	0	0		15	93 33
Concrete	0	0	0	0	1	0	0	0	0	9	0	0	0		10	90 00
Roof-grey	0	0	0	3	3	23	17	0	27	9	8	0	12		102	7 84
Roof-brown	0	0	0	0	0	0	0	0	1	0	0	8	0		9	88 89
Rip rap	0	0	0	0	0	0	0	0	1	0	0	0	0		1	0 00
														256		
col total	109	67	69	34	75	33	23	10	50	21	10	9	13		523	48 95
producer acc	53 21	70 15	14 49	38 24	90 67	30 30	8 70	90 00	28 00	42 86	80 00	88 89	0 00			Overall Acc

70NM 4M SEED5 NATURAL
RAW DATA

	Oak holly	Mixed	Loblolly	Dune grass	Maint grass	Ocean	Sand	Clay	diagonal	row total	users acc
Oak holly	58	14	23	10	2	0	0	0		107	54 21
Mixed	43	47	33	2	0	0	0	0		125	37 60
Loblolly	3	2	10	0	0	0	0	0		15	66 67
Dune grass	0	0	0	13	1	0	0	0		14	92 86
Maint grass	5	4	3	6	68	0	4	1		91	66 67
Ocean	0	0	0	0	0	10	0	0		10	92 86
Sand	0	0	0	0	0	0	2	0		2	100 00
Clay	0	0	0	0	0	0	0	9		9	100 00
									217		
col total	109	67	69	31	71	10	6	10		373	58 18
producer acc	53 21	70 15	14 49	41 94	95 77	100 00	33 33	90 00			Overall Acc

70NM 4M SEED5 CULTURAL
RAW DATA

	Asphalt	Concrete	Roof-grey	Roof-brown	Rip rap	diagonal	row total	users acc
Asphalt	14	1	0	0	0		15	93 33
Concrete	0	9	0	0	0		9	100 00
Roof-grey	27	9	8	0	12		56	14 29
Roof-brown	1	0	0	8	0		9	88 89
Rip rap	1	0	0	0	0		1	0 00
						39		
col total	43	19	8	8	12		90	43 33
producer acc	32 56	47 37	100 00	100 00	0 00			Overall Acc

VITA

KEVIN RICHARD SLOCUM

Born in Washington, D.C., 26 March 1957. Graduated from Springbrook High School, Silver Spring, Maryland in 1975. Earned Bachelor of Science in Geography from James Madison University, Harrisonburg, Virginia in 1979. Completed requirements for Masters of Applied Geography with environmental focus from Southwest Texas State University, San Marcos, Texas, in 1990. Entered the doctoral program in the College of William and Mary, School of Marine Science, Department of Coastal and Ocean Policy in Fall 1999. Originally employed by the National Imagery and Mapping Agency (formerly the Defense Mapping Agency) as a cartographer from 1979 until 1989, responsible for compilation and technical management of standard and non-standard topographic and hydrographic maps. Served as United States liaison to Latin America directing international nautical chart development between 1987 and 1989. Presently employed as a senior research scientist at the US Army Topographic Engineering Center since 1990 addressing tactical military and environmental data generation and modeling requirements. Research projects have included exploitation of geo-spatial technologies including remote sensing, spatial statistics, geographic information systems, and global positioning systems with specific projects for which I am, or have been, principle investigator including: assessment of DEM accuracy under forest canopy; remote habitat assessment for red-cockaded woodpeckers; model sensitivity to missing terrain data; reliability of imagery classifications; remote vegetation classification; and, empirical and heuristic inference of soil properties data. The following citations reference my most recent professional and academic endeavors:

1. Oliver, M.A., Shine, J., **Slocum, K.** Using the variogram to explore imagery of two different spatial resolutions, *International Journal of Remote Sensing*, in press.

2. **Slocum, K.**, Perry, J., Anderson, J., Campbell, M., and Fischer, R., Vegetation association with elevation, soil type, and soil compaction at Parramore Island, Virginia, presently in draft form.

3. **Slocum, K.**, Jarrett, J., Fischer, R. Anderson, J.E., and Perry, J.E. An assessment of spatial and spectral resolutions used in coastal zone landscape characterization, presently in draft form.

4. **Slocum, K.**, Perry, J.E., Oliver, M.A., Krause, P.F. Remote identification of biomass differences in *Phragmites australis* stands from high-resolution spectral imagery, presently in draft.

5. **Slocum, K.** and Jarrett, J., Perry, J.E., Oliver, M.A., Krause, P.F. Prototype ecology-based models for correcting imagery-derived vegetation classification errors, presently in draft.

6. Fisher, R., Campbell, M., Anderson, J., and **Slocum, K.**, 2001. Barrier island vegetation classification using digital multispectral video, submitted for publication.

7. Oliver, M.A., Bosch, E., and **Slocum, K.**, 2000. Wavelets and kriging for filtering and data reconstruction, refereed Proceedings of the 6th International Geostatistics Congress, Capetown, South Africa.

8. Oliver, M.A., Webster, R., and **Slocum, K.**, 2000. Filtering SPOT imagery by kriging analysis, *International Journal of Remote Sensing*, 21 (4): 735-752.

9. **Slocum, K.**, Wakefield, G., Fischer,R., and Campbell, M., 1999.
Application of digital multispectral imagery to littoral zone soil and
elevation modeling. In Proceedings, 4th Annual Airborne Remote Sensing Conference,
Ontario, Canada.

10. Watts, J., Jarrett, J., Wakefield, G., **Slocum, K.**, Precht, F., and
Fels, J., 1999. Rule-based vegetation classification: The integration of
predictive modeling and digital image processing. In Proceedings, GeoComp 4th
International Conference, Fredricksburg, VA.

11. Fischer, R.L., **Slocum, K.**, Campbell, M.V., Anderson, J.E., Perry,
J., 1999. Application of Digital Multspectral Imagery to Littoral Zone
Monitoring. In Proceedings, 17th Biennial Conference on Videography and Color
Photography in Resource Assessment, May 5-7, Reno, NV.

12. **Slocum, K.**, Fisher, R., Campbell, M., Anderson, J., and Perry, J.,
1998. The use of digital multispectral video for coastal zone
characterization. In Proceedings, 16th International Conference of the
Coastal Society, Williamsburg, VA.

13. Fisher, R., **Slocum, K.**, Anderson, J.E., Perry, J.E., 1998. Use
of digital multispectral video for littoral zone applications. In Proceedings, 21st Army
Science Conference, Norfolk, VA.

14. Campbell, M., **Slocum, K.**, Jarrett, J., and Puffenberger, H., 1998.
Vegetation feature extraction using airborne multispectral imagery,
In Proceedings, Society of Photogrammetry and Remote Sensing Conference.

15. U.S. Army Topographic Engineering Center, 1996. Vegetation Mapping.
Final Report to the Government Applications Task Force Program Office.

16. Campbell, M., and **Slocum, K.**, 1996. Efficient Extraction of Vegetation Attributes from High Resolution Multispectral Imagery. In Proceedings, EcoInforma '96, Lake Buena Vista, FL.

17. U.S. Army Topographic Engineering Center and Construction Engineering Research Laboratory, 1995. Hyperspectral data identification of red-cockaded woodpecker habitat. Final Report to the Legacy Office of the Army Environmental Center.

18. **Slocum, K.**, Getlein, S., and Anderson, J., 1995. Integrated vegetation data collection. Department of Defense Environmental Technology Workshop Proceedings, Hershey, PA.

19. Getlein, S., **Slocum, K.**, and Anderson, J., 1995. Off-the-shelf and in the field: Innovative technologies for natural resource management. Department of Defense Environmental Technology Workshop Proceedings, Hershey, PA.

20. U.S. Army Topographic Engineering Center, New Mexico State University, US Agricultural Research Service, and EnviroTech Associates, 1994. Information support for environmental management: Legacy data capture and data assessment phase. Final Report to the Strategic Environmental Research and Development Program Office.

21. **Slocum, K.**, 1993. Selection of Climate Station Data Using Clustering and Triangulated Irregular Network Techniques, U.S. Army Topographic Engineering Report, TEC-0041.

22. **Slocum, K.**, 1993. Conifer Tree Influence on Digital Terrain Elevation Data: A Case Study at Dulles International Airport, U.S. Army Topographic Engineering Report, TEC-0038.